

**Proteins and protein/surfactant mixtures
at interfaces in motion**

F.J.G. Boerboom

Promotoren: Dr. A. Prins
emeritus hoogleraar fysika en fysische chemie van
levensmiddelen met bijzondere aandacht voor de zuivel.

Dr. M.A. Cohen Stuart
hoogleraar in de fysische chemie
met bijzondere aandacht voor de kolloïdchemie

PN08201, 2826

**Proteins and protein/surfactant mixtures
at interfaces in motion**

F.J.G. Boerboom

Proefschrift

ter verkrijging van de graad van doctor
op gezag van de rector magnificus
van Wageningen Universiteit
dr. ir. L. Speelman
in het openbaar te verdedigen
op dinsdag 5 september 2000
des namiddags te 13:30 in de Aula

wn 981031

BIJLAGE
LANDBOUWUNIVERSITEIT
WAGENINGEN

ISBN 90-5808-281-4

Cover: Frank Boerboom

Stellingen

1. Een hoge weerstand van vloeistofoppervlakken tegen vervorming in shear werkt bij het opkloppen van waterige eiwit oplossingen de vorming van kleine bellen in de hand. (dit proefschrift)
2. De tijdsafhankelijkheid van de oppervlaktespanning van waterige eiwitoplossingen wordt bepaald door het transport naar en de ontvouwing van de eiwitten aan het grensvlak. (dit proefschrift)
3. Het succes van eiwithydrolysaten als hulpstof bij het maken van waterig schuim is te danken aan hun relatief lage molekuulgewicht en de afwezigheid van een stabiele secundaire en tertiare structuur Verder speelt de preferentiële adsorptie van eiwitmoleculen met een hoog molekuulgewicht een rol bij het stabiliseren van schuim. (dit proefschrift)
4. De honorering van promovendi is sterk afhankelijk van het aanbod op de arbeidsmarkt van jonge academici. Dit leidt ertoe dat de beste promovendi gemiddeld het slechtst betaald krijgen.
5. Auto's in Nederland zijn heilige melkkoeien.
6. Het is paradoxaal te noemen dat iedereen het rustiger aan schijnt te willen doen maar dat je in deze maatschappij niet meetelt als je het niet druk hebt.
7. De rode golf op de ringweg in Groningen die slechts te ontwijken is door dertig kilometer harder te rijden dan is toegestaan is een bijzondere vorm van rekeningrijden.
8. Het solistische karakter van veel AIO posities is niet bevorderlijk voor het vervullen van een vervolgfunctie.
9. De vergrijzing in de wetenschappelijke wereld in Nederland veroorzaakt de vernietiging van menselijk kapitaal.
10. Vergeetachtigheid is een onbewuste maar zeer effectieve remedie tegen stress.
11. De publieke discussie ten aanzien van genetische manipulatie wordt sterk vertroebeld door verhalen met een hoog Frankenstein gehalte die door pressiegroepen worden gebruikt om aandacht te trekken.
12. Wijsheid is het omzetten van juist geselecteerde feiten naar relevante kennis.
13. Hoe verder men van het Groene Hart afwoont hoe minder groen het er lijkt.

Stellingen behorende bij het proefschrift:

Proteins and protein/surfactant mixtures at interfaces in motion

F.J.G. Boerboom 5 september 2000

voor mijn ouders

1.1 INTRODUCTION	1
1.2 SURFACE PROPERTIES	3
1.2.1. Adsorption behaviour of low molecular surfactants	3
1.2.2 Adsorption behaviour of proteins	4
1.2.3 Adsorption of Mixtures of Surfactants and Proteins	8
1.2.4 Surface behaviour under dynamic conditions	9
1.2.4.1 Transport to and from the surface	10
1.2.5 Methods and techniques for determining dynamic surface properties	14
1.2.5.1 Viscoelasticity of adsorbed layers	15
1.2.5.2 Surface properties in continuous deformation	17
1.3 MECHANICAL PROPERTIES OF ADSORBED SURFACE LAYERS	18
1.3.1 Homogeneous deformations of surfaces	20
1.3.2 Deformations caused by viscous drag	22
1.4 FOAM CREATION AND FOAM STABILITY	23
1.4.1 Creation of foams	24
1.4.2 Foam stability	27
1.4.2.1 Drainage	27
1.4.2.2 Disproportionation	28
1.4.2.3 Coalescence	29
1.4.2.4 Spreading particles and hydrophobic particles	30
1.5 MECHANICAL ASPECTS OF SUB-PROCESSES OCCURRING IN FOAMS	31
1.6 AIM OF THIS THESIS	33
1.6.1 Contents of this thesis	35
2.1 ABSTRACT	37
2.2 INTRODUCTION	38

2.3 THEORY	38
2.3.1 Unfolding of adsorbed proteins	40
2.3.2 Transport to the surface	42
2.3.3 Mass balances	44
2.3.4 Surface Tension	47
2.3.5 Mechanical properties	50
2.3.6 The influence of transport: the surface Fourier number	52
2.3.7 Methods of calculation of the parameters of the model	53
2.4 RESULTS AND DISCUSSION.	56
2.4.1 Model calculations: effect of diffusion coefficient and unfolding parameters.	59
2.4.2 Comparison between Tween 20 and SDS	61
2.4.2 Comparison between β -casein and β -lactoglobulin	66
2.5 CONCLUSIONS	69
Appendix 2.1	70
Appendix 2.2 Constants used in the calculations	71
3.1 ABSTRACT	72
3.2 INTRODUCTION	73
3.3 THEORY FOR THE FALLING FILM	74
3.3.1 Overflowing cylinder	74
3.3.2 General Properties	75
3.3.3 Generalized flow profiles	81
3.3.4 The height and the form of the meniscus	86
3.3.5 Correlation between falling height and shear stress at the surface of the falling film	89
3.3.6 Dynamic surface properties	98

3.4 MATERIALS AND METHODS	99
3.4.1 Materials	99
3.4.2 Methods	99
3.5 RESULTS AND DISCUSSION	102
3.5.1 Mechanical Characteristics of adsorbed protein layers	102
3.5.1.1 The relation between deformation and viscous stress at the top surface	103
3.5.1.2 Mechanical Properties of the Falling Film	108
3.5.2 Surface Properties of proteins	113
3.5.2.1 Surface properties of proteins: Experiments	113
3.5.2.2 Surface properties of proteins: comparison to the model	122
3.5.3 Relation between mechanical properties and surface properties	124
3.5.3.1 Applicability to foaming behaviour	125
3.6 CONCLUSIONS	126
4.1 ABSTRACT	129
4.2 INTRODUCTION	129
4.2.1 Scope of this chapter	130
4.2.2 Model	131
4.2.3 Literature	131
4.3 MODEL OF BINARY ADSORPTION AT EXPANDING SURFACES UNDER STEADY STATE DILATION	133
4.3.1 Adsorption kinetics	133
4.3.2 Influence of micelles	135
4.3.3 The surface tension	136
4.3.4. The surface tension gradient	138
4.3.5 The surface Fourier number	138

4.4 MATERIALS AND METHODS	139
4.4.1 Materials	139
4.4.2 Calculations	139
4.4.3 Overflowing cylinder technique.	140
4.5 RESULTS AND DISCUSSION	140
4.5.1 General trends of calculations	141
4.5.1.1 Calculated Surface Concentration	141
4.5.1.2 Calculated Surface Tension	144
4.5.1.3. Calculated Relative rate of expansion	146
4.5.1.4 Calculated Surface Fourier number	147
4.5.2 Influence of intricacies	149
4.5.3 Experiments	151
4.6 CONCLUSIONS	156
Appendix 4.1	157
5.1 ABSTRACT	158
5.2 INTRODUCTION	159
5.2.1 Foam Production	161
5.2.2 Drainage of foams	162
5.3 MATERIALS AND METHODS	164
5.3.1 Materials	164
5.3.2 Methods	165
5.4 RESULTS AND DISCUSSION	165
5.4.1 Foam Formation	165
5.4.2 Drainage behaviour	172
5.5 CONCLUSIONS	177
APPENDIX 5.1 LIST OF SYMBOLS	179

6.1 INTRODUCTION	180
6.2 IMPORTANT FINDINGS	180
6.2.1 Foaming properties	181
6.2.2 Mechanical properties of surfaces	182
6.2.3 Influence of transport and unfolding for dynamic surface properties	183
6.3 SIGNIFICANCE FOR PRACTICAL SITUATIONS	185
6.3.1 Resistance to creaming and drainage of foams	186
6.3.2 Bubble break up by viscous forces	187
6.4 FOAMING PROPERTIES OF PROTEIN HYDROLYSATES	190
SUMMARY	192
Unfolding behaviour of proteins at interfaces	194
Foam formation and foam stability	197
SAMENVATTING	199
Ontvouwingsgedrag van eiwitten aan grensvlakken	202
Schuimvorming en schuimstabiliteit	204
REFERENCES	206

Chapter 1

General Introduction

1.1 Introduction

Dispersions are substances in which one phase, liquid, gas or solid, is finely distributed in another phase. In this thesis we will mainly consider just one type of dispersion: foams. Foams are dispersions in which gas is distributed into a liquid or a solid phase. Here we will restrict ourselves to systems in which gas is dispersed in a liquid phase.

Anyone who has ever tried to produce a foam from a pure substance like water must have observed that these are unstable. The gas dispersed in the liquid in the form of bubbles rises quickly and merges during the rise with other bubbles and eventually disappears into the surrounding air.

Immediate disappearance of the foam can be prevented by adding surface active molecules. These molecules tend to accumulate at the interface between liquid and gas. An example of such surface active materials are soaps. These substances are amphiphilic which means that they have a polar and an apolar part in the molecule. Amphiphilic substances lower the surface tension (γ) which is a measure of the tendency of the surface to contract. When the surface tension is lowered, the tendency of the surface to contract becomes lower. The surface tension has the dimension N m^{-1} , a force per unit length or, Jm^{-2} an energy per unit area. An increased amount of surface active material per unit area causes a decrease in surface tension. In general it is observed that a lower surface tension facilitates the creation of foams. However if the bubbles still would have the tendency to merge then the foam would disappear quickly. So surface active materials that are able to stabilise foams have to meet another condition which is that they need to stabilise the bubbles against the tendency to merge.

Stability can be achieved if adsorbed layers repel each other. The repulsion takes the form of a force per unit area, which is called the disjoining pressure. This pressure can be caused by several interactions between the adsorbed layers such as steric or electrostatic interactions. When surface active materials are not able to create enough disjoining pressure such as alcohols (¹) indeed the foams collapse quickly.

There are different types of surface active substances with different characteristic properties in the creation and in breakdown properties of foams. It would be interesting to have some idea about the relation between the molecular properties and performance of a surfactant with respect to foaming properties. Among others, the trend in the food industry to produce foods which are designed on the basis of functionality of their constituents makes this desirable.

The reason that it is difficult to predict the properties of surface active species is that both the formation and the breakdown of foams are very intricate processes in which surface properties and hydrodynamics go hand in hand and. This makes that foaming properties are scientifically not well understood.

The research described in this thesis was aimed at finding static and dynamic properties that play a role in foaming behaviour of solutions of various surface active species. The class of surfactants which has received most of the attention in this thesis are proteins. Also low molecular surfactants were studied however in order to compare the behaviour of these substances. In order to study the interactions at the surface also mixtures of proteins and low molecular surfactants were studied.

Since we are not able to formulate a direct link between molecular structure and foaming properties the strategy used in this thesis was to first correlate molecular properties to surface properties. Next these surface properties can be related to mechanical properties of adsorbed layers. These mechanical properties were subsequently be used to explain certain aspects of foaming characteristics.

1.2 Surface properties

Surface properties are responsible for the ability of a surface active substance to create and stabilise foams. In this thesis we will mainly concentrate on how the surface active material adsorbed to the surface enables the creation and stabilisation of foams. As most sub-processes in foams are determined by time dependent processes, we will concentrate on these. Surface properties considered are the surface concentration Γ defined as the excess amount of adsorbed material per unit area and the surface tension γ defined as the free energy per unit area, Lyklema (²).

In non equilibrium circumstances both surface concentration and surface tension can be considered to be a function of time and place on a surface. Since surface active material needs to be transported to a surface it takes time before the surface has reached equilibrium with respect to surface concentration. Moreover macromolecular surfactants may need to unfold before a significant decrease in surface tension takes place which is another reason for this time dependence. Due to redistribution of surface active material over the surface, the surface concentration of the surface active species may not be uniform over the whole surface which causes the surface tension to differ over the surface as well. In the following paragraphs first the equilibrium properties of surfaces will be discussed. After that we will pay attention to non equilibrium properties of surfaces.

1.2.1. Adsorption behaviour of low molecular surfactants

The adsorption behaviour of low molecular surfactants is well documented in literature Chang and Frances (³), Lucassen-Reijnders (⁴). Essentially two types of equations are needed to describe the behaviour of low molecular surfactants at air/water interfaces in equilibrium: (i) The relation between bulk concentration and surface concentration called the adsorption isotherm and (ii) the relation between the surface concentration and surface tension, the equation of state. The most commonly used adsorption isotherm is the Langmuir isotherm, which reads for dilute solutions:

$$\Gamma = \Gamma_m \frac{K_l c}{1 + K_l c}$$

Equation 1. 1

In this equation, Γ is the surface concentration. Γ_m and K_l are constants indicating respectively the maximum surface concentration of surfactant and the Langmuir constant which are characteristic for the adsorption behaviour of a certain species. The c in the equation means the bulk concentration. The relation between surface tension and surface concentration can be described by the Gibbs adsorption equation:

$$\Gamma = -\frac{1}{RT} \left(\frac{\partial \gamma}{\partial \ln c} \right)_T$$

Equation 1. 2

In this equation, Γ is the surface concentration of the surfactant, R and T are respectively the gas constant and the absolute temperature. $\left(\frac{\partial \gamma}{\partial \ln c} \right)_T$ indicates the partial derivative of surface tension with respect to the natural logarithm of concentration at constant temperature. In case the concentrations are not equal to the activity of the surfactant, the activity instead of the concentration must be used in both equations. This is very important in the case of low molecular surfactants since these substances aggregate in the form of micelles, causing the activity to be significantly lower than the bulk concentration. The Gibbs equation indicates that the surface tension is a function of surface concentration and concentration in the bulk phase. Equations 1.1 and 1.2 are only valid for low molecular surfactants however. In the case of macromolecules, both the Langmuir equation and the Gibbs equation do not hold anymore De Feyter et al.⁽⁵⁾.

1.2.2 Adsorption behaviour of proteins

A large number of authors studied the adsorption of proteins at air water surfaces in static conditions. Equilibrium adsorption isotherms (i.e. relations between surface tension and surface concentration) of different proteins were studied by Benjamins et al.

(⁶), Graham and Phillips (⁷), De Feijter and Benjamins (⁸), Hunter et al. (⁹, ¹⁰). These studies investigated the surface concentration of proteins in relation to the surface tension of these systems in equilibrium. From these studies it appears that proteins like most polymers, exhibit a high affinity behaviour. The surface concentration of proteins in equilibrium with the bulk phase is high even at very low bulk concentrations. Figure 1.1 shows a typical example of the relation between surface tension and bulk concentration for a protein and a surfactant.

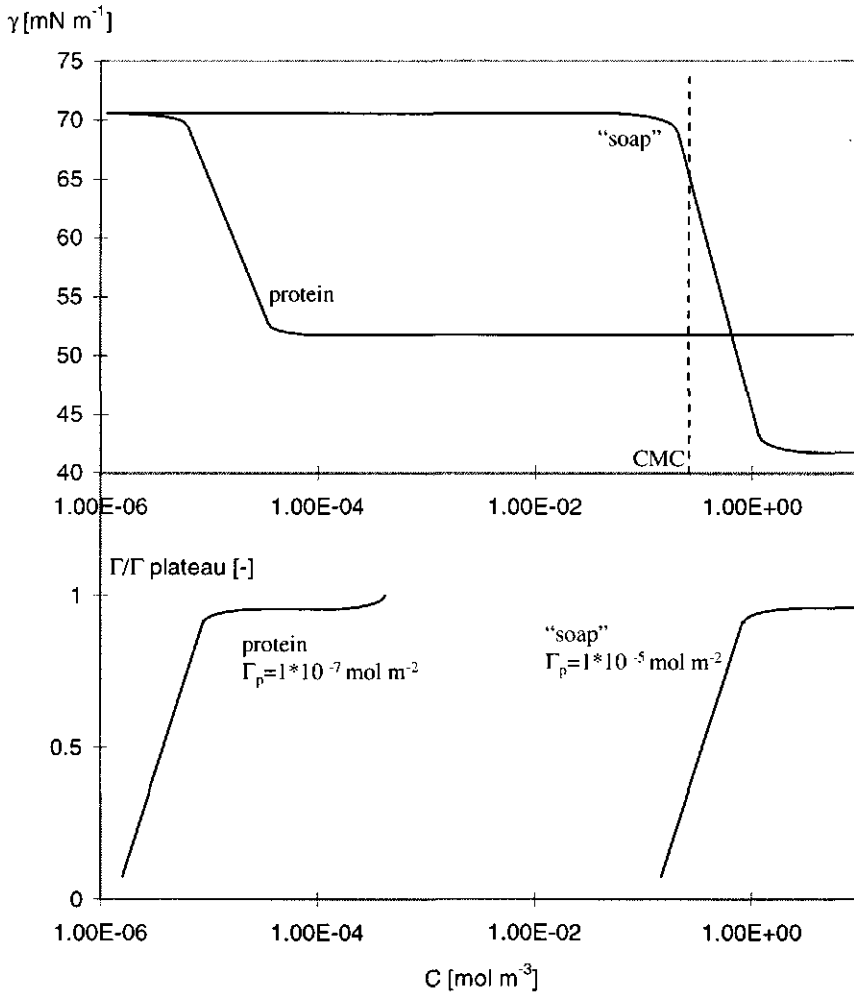


Figure 1.1 Relation between bulk concentration and surface tension and surface concentration after Walstra (¹¹)

From this relation we can see that proteins have a high surface concentration even at relatively low bulk concentrations. Generally an S shaped relation is found between the surface pressure and the surface concentration (figure 1.2)

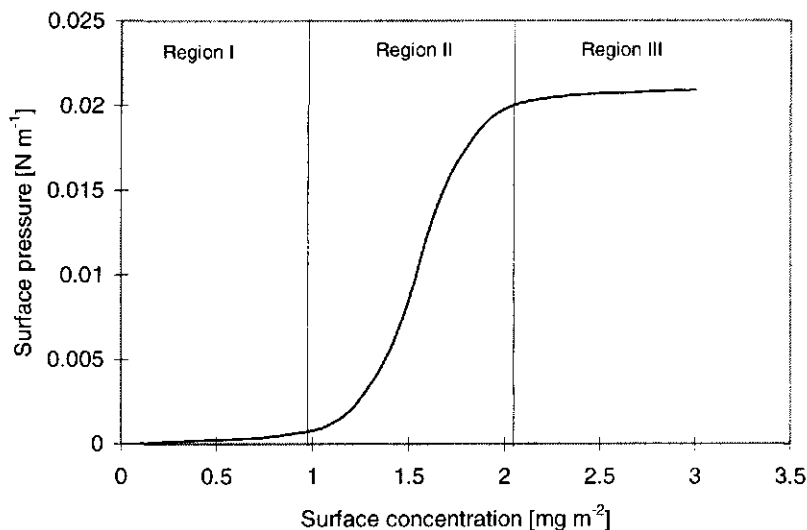


Figure 1. 2 Relation between surface pressure and surface concentration for an arbitrary protein.

This S curve consists of three distinctly different regions marked with roman numbers I, II and III. When the surface pressure (which is the surface tension of the pure solvent minus the actual surface tension) is below 1 mN m^{-1} a dilute region can be found. The adsorbed molecules act as a two dimensional gas. In the region in which the surface pressure is between 1 and around 20 mN m^{-1} the surface pressure rises steeply with the surface concentration. There is no general consensus yet as to the exact reason for this behaviour. General homopolymer theories are not able to predict such a behaviour because the interactions between the different groups in proteins are too diverse to fit into practically applicable theories. Norde (¹²). De Feyter and Benjamins (¹³) and van Aken (¹⁴) use deformable particle models to explain this behaviour. In these types of models interactions between the proteins are summed up into one or more interaction parameters. Also scaling is used to explain the shape of the dependence of surface pressure on surface concentration Douillard et. al. (¹⁵, ¹⁶). In the third region the surface pressure increases less steeply with surface concentration, in this region it is thought that trains and loops are formed which contribute only very weakly to the surface tension .

Recently, more detailed information became available on density profiles of adsorbed layers by means of neutron reflectometry Eaglesham et al. (¹⁷), Atkinson et al. (¹⁸, ¹⁹). These studies indicated that the density profiles of adsorbed protein layers normal to the surface consist of a dense layer (protein fraction around 0.8) of a few nanometers thick close to the surface and a distal region in the order of tens of nanometers thick with a protein fraction in the order of 0.1 to 0.2. These experiments seemed to confirm self consistent field calculations carried out on β -casein look-alikes, taking in account electrostatic and hydrophobic interactions Leermakers et al. (²⁰). However more accurate measurements with the same technique suggest that a parabola would describe the density profile better than a step function (²¹). Another method of establishing the conformation of adsorbed protein molecules has been described by Leaver and Dalglish (²²). They studied the susceptibility of β -casein to hydrolysis by trypsin. It was shown for β -casein that the bonds between the 25th to 28th amino acid from the N terminus were most susceptible to hydrolysis, which shows that this part of the chain will be farthest from the surface. This technique enables us to obtain a general idea of the conformation of adsorbed proteins.

Norde and Favier (²³) demonstrate that adsorption of BSA onto silica particles leads to a decrease in secondary structure which does not recover completely on desorption by means of circular dichroism. With lysozyme however no significant change in the molecular structure was observed on adsorption.

Another technique which may provide more information of the spatial structure of adsorbed molecules over the surface is atomic force microscopy of adsorbed layers transferred to mica plates. This may enable to quantify aggregation of proteins into network structures at oil/water or possibly air/water interfaces Gunning et al. (²⁴).

1.2.3 Adsorption of Mixtures of Surfactants and Proteins

Apart from the adsorption of single species also the adsorption of mixtures is interesting for two reasons. First the surface active species applied in practice generally are not pure systems but consist of more than just one type of surfactant. Second, in processing sometimes more than just one type of surfactant is applied deliberately during several

processing steps to be able to obtain the desired product. De Feijter et al. ⁽²⁵⁾ studied the displacement of proteins by surfactants at the oil/water and air/water interface. They introduced a model in which the exchange of proteins and surfactants is described. From this model they conclude that in static conditions low molecular surfactants adsorb preferentially due to their higher energy of adsorption per unit area both at air/water and oil/water interfaces.

It was found that complications may occur in the behaviour of binary mixtures of surface active species. Coke et al. ⁽²⁶⁾ demonstrated that β -lactoglobulin and Tween 20 aggregate in solution. Both the complex and the individual species are observed to adsorb at the surface. Clark et al. ⁽²⁷⁾ demonstrated that purified β -lactoglobulin may contain low molecular surfactants which may disrupt the interactions between the protein molecules adsorbed at the surface which may lead to misinterpretations in the behaviour of β -lactoglobulin.

1.2.4 Surface behaviour under dynamic conditions

When surfaces are deformed for instance by expansion or compression the adsorbed layers are also deformed which means that they are no longer in equilibrium with the bulk liquid. Deformation causes rearrangements to take place in the adsorbed layer and causes net transport to and from the bulk phase. In this following section we will discuss the transport and rearrangement mechanisms that determine the dynamic surface behaviour. Second we will discuss several techniques by which information can be obtained on these surface properties.

Molecular rearrangements at the surface can occur due to phase behaviour at surfaces such as the creation of lamellar gel phases at oil/water- and air/water surfaces by means of substances like Glycerol Lacto Palmitate (GLP). These glycerides can form micro crystalline phases at the surface which cause very rigid surface layers Westerbeek and Prins ⁽²⁸⁾. Rearrangements of proteins due to adsorption at solid or liquid surfaces have been reported by Norde and Favier ⁽²²⁾ and Norde and Kleijn ⁽¹¹⁾. They demonstrated that adsorption of some proteins leads to loss of secondary structure. In that case the

behaviour of unfolded protein molecules with respect to desorption differs considerably from the behaviour of native proteins at interfaces.

Clark et al. (²⁹) reported that BSA exhibits irreversible conformation changes after foaming which means that proteins change their conformation to such a degree that partial denaturation takes place. This behaviour can also be ascribed to loss of secondary structure, Norde and Favier (²²). Also reactions at the surface may be responsible for time dependent behaviour of surface. For instance cystine residues in proteins are suspected to form intra- and intermolecular covalent bonds in protein layers resulting in a high resistance to deformation Clark et al. (³⁰).

1.2.4.1 Transport to and from the surface

When a surface active species is present in the bulk phase, the molecules will tend to accumulate at the surface. The transport to the surface can be considered to take place for instance by diffusion (Brownian motion) of molecules. The purely diffusive flux to interfaces was described by Ward and Torday (³¹). For a bare surface they find this flux to be:

$$J = c_b \left(\frac{D}{\pi t} \right)^{\frac{1}{2}}$$

Equation 1.3

In this equation J is the flux, c_b is the bulk concentration and t is time.

In order to use the relationship between γ , Γ and c_b in equilibrium for a surface that is not in equilibrium, the concept "sub-surface concentration" is introduced. It is assumed that even under non-equilibrium conditions there is "equilibrium" between γ and Γ and c_s (c_s is subsurface concentration). This subsurface layer is assumed to be present within a distance of molecular dimension from the surface. The difference between c_b and c_s is the driving force for the diffusional transport of surfactant to or from the surface which is not in equilibrium. When the surface expands continuously Van Voorst Vader et al. (³²) demonstrated that in case of a steady state, the surface dilution of the adsorbed material

just compensates the transport to the surface. Hence the flux to the surface in this case of convective diffusion is given by:

$$J = D \left(\frac{\delta c}{\delta z} \right)_{z=0} = \Gamma \left(\frac{d \ln A}{dt} \right)$$

Equation 1. 4

In this equation D means the diffusion coefficient, $\left(\frac{\delta c}{\delta z} \right)_{z=0}$ means the first partial derivative of the concentration with respect to the distance normal to the surface taken at the surface, Γ means the surface concentration and $\frac{d \ln A}{dt}$ is the relative rate of expansion. Combining equations 1.3 and 1.4 leads to the following expression of the flux:

$$J = (c_b - c_s) \sqrt{\frac{2 \left(\frac{d \ln A}{dt} \right) D}{\pi}} = \Gamma \left(\frac{d \ln A}{dt} \right)$$

Equation 1. 5

The lowering of surface tension due to the adsorption of surface active material strongly depends on type of the species adsorbed to the surface. We will discuss the relations between the surface concentration and the surface tension of low molecular surfactants and proteins.

In literature numerous studies were described on the adsorption at the air/water interface. In comparison desorption has received considerably less attention. Desorption is a relaxation mechanism that can be of vital importance for disproportionation (1.4.2.2.) or the generation of a surface tension gradient (1.3.2.) however. When a soluble low

molecular surfactant desorbs from a compressed surface the discharge of molecules from the adsorbed layer is rapid in comparison to the diffusion away from the surface. In the case also convection takes place the rate of discharge from a surface at equal circumstances is not dependent on time but on the thickness of the stagnant layer δ , the concentration difference between the stagnant layer and the bulk ($c_s - c_b$) and the diffusion constant D , MacRitchie (³³). In that case the rate of transport is given by:

$$J = \frac{D(c_s - c_b)}{\delta}$$

Equation 1. 6

Here, δ depends on the particular flow pattern. Unlike low molecular surfactants, the desorption kinetics of substances like proteins are much slower than the adsorption kinetics. The resistance to desorption of proteins were found to be extremely high by MacRitchie (³³). Compression of the adsorbed layer for BSA beyond surface pressures of 30 mN m^{-1} leads to collapse phenomena in which the occupied area per molecule decreases significantly to only fractions of the original area. In that case compression leads to very thick protein layers. Figure 1.3 depicts the decrease in surface area in time due to compression of the surface at equal surface tension, Mac Ritchie (³⁴).

MacRitchie (³⁵) determined that the resistance to desorption due to the interfacial interactions of BSA is four orders of magnitude larger than the resistance to diffusion.

Van Kalsbeek (³⁶) reports on the generation of insoluble protein layers with β -

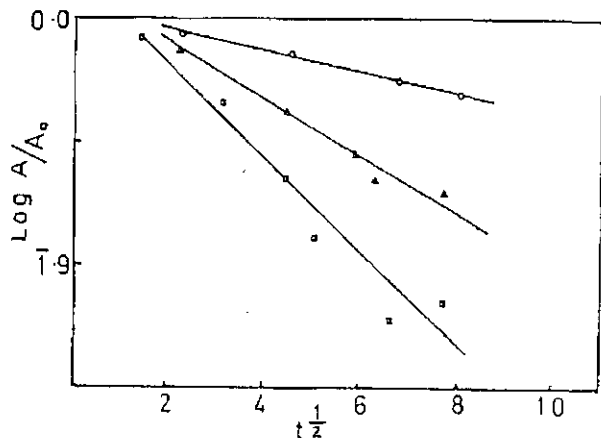


Figure 1.3 Relative surface area as a function of the square root of time after initial compression of adsorbed layers of β -lactoglobulin to different surface pressures, $\pi = 10 \text{ mN m}^{-1}$: \circ $\pi = 20 \text{ mN m}^{-1}$: Δ $\pi = 30 \text{ mN m}^{-1}$: \square MacRitchie (³⁵).

lactoglobulin when bubbles dissolve in the disproportionation process. Apparently the generation of a collapsed monolayer does not lead to a significant decrease in the dissolution rate of a bubble. This leads to the speculation whether these layers may be regarded as macroscopic or that these layers should be regarded as concentrated bulk layers (skins). Fisher et al. (³⁷) found that the coalescence probability of emulsion droplets stabilised by lysozyme is lowered significantly if the droplet surface area is decreased by a factor 2.3. They ascribe this to surface coagulation of the protein. This indicates that desorption properties may have a significant effect on foaming and emulsification.

In the case of mixed monolayers of DPPC and β -lactoglobulin it has been observed that the β -lactoglobulin molecules are displaced preferentially when the surface is subjected to compression, MacRitchie (³⁸). This indicates that there may be a considerable

influence of a second surface active species on the behaviour of adsorbed protein layers. The same has essentially been found for surfaces in equilibrium.

1.2.5 Methods and techniques for determining dynamic surface properties

There are several methods by which the dynamic surface behaviour can be studied. Depending on the information that is needed, a technique can be chosen that matches the practical conditions as closely as possible.

Viscoelasticity of adsorbed layers can be studied by subjecting surfaces to a sinusoidal deformation and measuring the response of the surface in terms of surface tension or resistance to shear forces analogous to bulk rheological techniques. This can be done both in shear, van Voorst Vader et al. (³⁹), Krägel et al (⁴⁰, ⁴¹) and in dilation, Graham and Phillips (⁴²), Kokelaar et al. (⁴³). These experiments are meant to quantify the total resistance to deformation of adsorbed layers close to equilibrium by means of shear or dilational moduli and quantify the relaxation behaviour in terms of a loss angle.

Other methods subject the surface to continuous deformation either in shear or dilation. An interesting method that measures surface properties in continuous steady state dilation is the overflowing cylinder method Bergink (⁴⁴), Joos (⁴⁵). In this device the surface tension can be measured in relation to the relative rate of expansion. Another technique is described by Rillaerts and Joos (⁴⁶) in which the surface is expanded continuously by means of pulling a strip from the surface. These devices provide information on transport and possibly unfolding of polymers at the surface. Dickinson (⁴⁷) reports on a device which measures an apparent surface shear viscosity by means of shearing of a surface layer. The apparent surface shear viscosity is an indication of interactions between adsorbed molecules which are formed during deformation of the surface. More recently developed techniques measure the response in terms of pressure of a bubble created from a capillary to an increase of volume of the bubble in a sinusoidal or continuous fashion (⁴⁸). In table 1.1 the different measuring techniques have been classified according to the type of deformation and type of information that can be obtained.

Determined properties	Sinusoidal (close to equilibrium)	Continuous (steady state, far from equilibrium)
Shear	references: ^{39, 40, 41} parameters: frequency, amplitude measured properties: $ G , G', G'', \tan \delta$	reference: ⁴⁷ parameter: shear rate measured property: η_s^c
Dilation	references: ^{42, 43} parameters: frequency, amplitude measured properties: $ E , E', E'', \tan \delta$	references: ^{44, 45, 46} parameter: relative expansion rate measured property: η_s^d

Table 1. 1 Measurable properties of homogeneous surfaces.

1.2.5.1 Viscoelasticity of adsorbed layers

In contrast to surface properties of substances under continuous dilation, viscoelasticity of surface active substances has been studied rather extensively. In general, adsorbed layers of low molecular surfactants have small dilational- and shear moduli accompanied by high loss angles when surfaces are deformed with frequencies around 0.01 to 10 Hz., Murray and Dickinson (⁴⁹). When surfaces occupied with low molecular surfactants are deformed with frequencies in the range of 100 to 1000 Hz, the dilational moduli are much larger (⁵⁰), (⁵¹) This increase in the dilational modulus shows that the relaxation mechanisms probed depends on the time scales of the measurements. This can be compared well to bulk properties in which we distinguish between a glass, a rubber and a viscoelastic material. Apparently the frequencies between 100 to 1000 Hz are in a region comparable to the "rubber regime" while viscoelasticity of the surface can be found in the area between 0.01 and 10 Hz. This shift from a rubbery region to a viscoelastic region does not occur if the exchange between the surface and the bulk phase is inhibited due to insolubility of the surfactant in the bulk phase or phase transitions at

the surface. Especially the dilational modulus at lower frequencies remains high in such cases due to the absence of relaxation phenomena such as diffusion from the surface⁽⁵²⁾.

Adsorbed protein layers generally have a substantial resistance to deformation both in shear and in dilation. In shear substantial differences were detected between proteins. Generally proteins with a large conformational stability have a high shear modulus. The presence of high shear moduli are ascribed to lateral interactions between the molecules in the surface due to interactions between the protein molecules in network like structures, Benjamins and van Voorst Vader⁽³⁹⁾. From these experiments it is possible to obtain relaxation times of these adsorbed layers to deformations in shear, which provides information on the type of rearrangement processes.

In dilation the resistance to deformation is also relatively high for proteins. Graham and Phillips⁽⁴²⁾, Williams and Prins⁽⁵³⁾ Serrien et. al.⁽⁵⁴⁾, Murray and Dickinson⁽⁴⁹⁾. A distinct dependence on the frequency of deformation can be detected in the range of frequencies between $1 \cdot 10^{-4}$ and $1 \cdot 10^{-2}$ hz for β -lactoglobulin, Murray and Dickinson⁽⁴⁹⁾. This tells us that the time scale of rearrangements in the adsorbed layers as a consequence of a dilational deformation is between 10^4 to 10^2 seconds. Also in dilation a distinct positive relation can be detected between the conformational stability and the modulus for proteins Benjamins et al⁽³⁹⁾. Also a distinct optimum is observed in the dilational modulus at certain surface tensions. This indicates that at certain surface tensions, the surface tension is more susceptible to variations in relative surface area. This can assumed to be caused by the shape of the adsorption isotherm, in the region the surface tension is most susceptible to variations in surface concentration the maximum in the modulus is attained.

For low molecular surfactants, these time scales for rearrangements generally range between 10^{-2} to 10^{+3} seconds according to Lucassen-Reynders⁽⁵¹⁾. Going back to the analogy to bulk properties we may assume that there is a shift to a longer relaxation time

with proteins compared to low molecular surfactants hence the shift from the rubber plateau to the visco-elastic region takes place at longer relaxation times.

Murray and Dickinson (⁴⁹), Chen et al. (⁵⁵), Chen and Dickinson (⁵⁶) Krägel et al. (⁵⁷) describe the viscoelasticity of mixtures of proteins and surfactants and mixtures of proteins. These studies showed that the desorption of proteins by low molecular surfactants has a significant influence on the visco-elastic properties of the surface. Even when a relatively small amount of low molecular surfactants has been adsorbed, the resistance to shear and dilation decreases significantly resulting in a surface which exhibits a predominantly surfactant like behaviour. The dilational behaviour may be explained by relaxation of the surface due to a more rapid exchange of molecules between the bulk and the surface of low molecular surfactants. As we mentioned before, this process is much faster in the presence of low molecular surfactants than in the presence of proteins. The decrease in the surface shear moduli may be explained by the disruption of the intermolecular interactions of the proteins. This last hypothesis is supported by Wilde and Clark (⁵⁸) and Clark et al. (⁵⁹) who determined the mobility of molecules adsorbed at the surface as a function of Tween 20 concentration by FRAP (Fluorescence Recovery After Photobleaching) experiments. They found that the mobility of β -lactoglobulin at the air/water and oil/water surface increased considerably when Tween 20 was added to the bulk phase. This supports the idea that β -lactoglobulin is able to form intermolecular bonds which can be disrupted by the presence of Tween 20 in the adsorbed layer.

1.2.5.2 Surface properties in continuous deformation

In the case of the adsorption of most low molecular surfactants, the transport to and from the surface are the only mechanisms that determine the surface properties under dynamic circumstances when surfaces are subjected to expansion or compression. The transport to the surface was discussed in section 1.2.5. Van Voorst Vader et al. (³²) studied the adsorption of low molecular surfactants in a Langmuir trough at constant relative rates of expansion. They derived the relations between the bulk concentration, the relative expansion rate and the surface tension. It was concluded that the transport to expanding

liquid surfaces could be described by convective diffusion. Bergink et. al. (⁶⁰, ⁶¹) studied the adsorption of low molecular surfactants at continuously expanding liquid surfaces in an overflowing cylinder and came to the same conclusion.

Van Aken and Merks (⁶²) studied the adsorption of proteins to slowly dilating surfaces. They observed that the sensitivity of the surface tension to variations in the relative rate of expansion of adsorbed protein was very high, both in compression and in dilation, even at very low relative deformation rates. In compression they found irregularities in the surface tension measured, which could be ascribed to the adsorbed layer becoming insoluble (skin formation). Serrien et al (⁵⁴) studied the unfolding rate of BSA at expanding surfaces. This unfolding rate was calculated from surface tension data. Assuming first order kinetics for the unfolding of the molecules at the surface, a first order constant could be fitted to surface tension data. The order of magnitude found for the first order constant was in the order of $1 \cdot 10^{-2} \text{ s}^{-1}$. In literature however little information on the time scales of the unfolding of protein molecules at surfaces is available. This is most probably due to the difficult experimental accessibility of such data.

Murray and Dickinson (⁴⁹), Chen and Dickinson (⁶³), Dickinson et. al. (⁶⁴) described shear measurements on adsorbed protein layers under constant deformation rates of the surface. The resistance to deformations in shear, expressed in the apparent surface shear viscosity depended strongly on time, which is ascribed to the time needed for the proteins to create a network structure in the adsorbed layer. The apparent surface shear viscosity differed 4 orders of magnitude between the different proteins indicating that the capability of forming network structures in time also differs considerably.

1.3 Mechanical properties of adsorbed surface layers

In the previous sections we discussed the surface properties in relation to molecular properties of different species. An important issue in this thesis is to find out what relations exist between surface properties and foaming properties. In order to obtain a better understanding of foaming behaviour in terms of foamability and foam stability, it

has to be realised that the relations between force and deformation of surfaces play an important role. In order to reach mechanical equilibrium certain relations need to be satisfied between the motion of the surface, the surface properties and the forces applied to the surface. To establish these relations we will need to know how surfaces react to forces.

Generally deformation of a surface can be caused either by a force exerted parallel (viscous drag) or a force exerted normal (pressure) to the surface of a bubble. This gives rise to respectively a heterogeneous or homogeneous deformation over the surface. This is illustrated in the following picture of a bubble deformed by a parallel and a normal

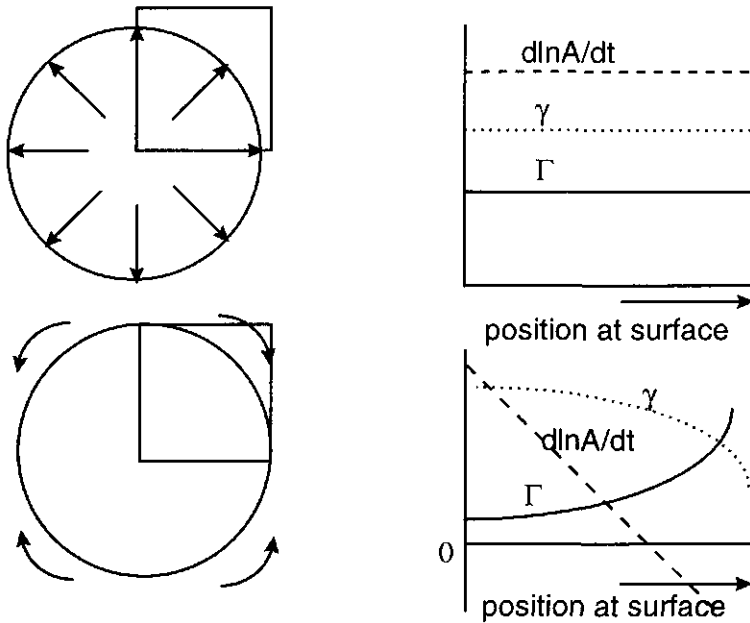


Figure 1. 4 Highly schematic representation of a bubble deformed by a force normal and parallel to the surface and the variation of a number of relevant parameters over a characteristic part of a surface of a bubble.

force.

In the schematic graphs on the right of the diagram, the parameters surface tension, surface concentration and relative rate of expansion and compression have been indicated as well. When the surface is deformed by a normal force, all parameters remain uniform over the bubble. In the situation the surface is deformed by forces parallel to the surface all surface properties change over the surface of the bubble.

1.3.1 Homogeneous deformations of surfaces

In the situation a surface is deformed uniformly, for instance when pressure fluctuations are applied to a bubble or during the disproportionation process, there should be a mechanical balance between the pressure which is inside the bubble and the pressure in the surrounding medium. There are two contributions to the pressure in the bubble: one is due to Boyle's law that says that pressure times volume is a constant, the other contribution originates from Laplace's law given in equation 1.7.

$$\Delta p = \frac{2\gamma}{r}$$

Equation 1.7

In this equation Δp is the difference between pressure in the bubble and the pressure of the surrounding medium, γ is the surface tension and r is the bubble radius. When a bubble grows or shrinks due to disproportionation in a continuous process (steady state) the surface properties are determined by the surface dilational viscosity as given in equation 1.8.

$$\eta_s^d = \frac{\gamma_{dyn} - \gamma_{eq}}{\left[\frac{d \ln A}{dt} \right]}$$

Equation 1.8

in this equation η_s^d is the surface dilational viscosity, γ_{dyn} and γ_{eq} mean the surface tensions in dynamic and equilibrium conditions respectively and $d \ln A / dt$ means the relative rate of expansion or compression. This parameter describes the response of surface tension to the relative rate of expansion or compression and its value depends

strongly on the time scale. The parameter η_s^d compares two situations, the reference point is taken to be the surface tension in equilibrium which is compared to a situation far from equilibrium. There can be a significant difference in magnitude between surface dilational viscosities in compression and expansion because the relaxation in compression involves desorption from the surface while in expansion this parameter is determined by adsorption. The rates at which these processes occur may be orders of magnitude different especially in the case the molecules interact at the surface (⁶⁵). Generally the dependence of the surface dilational viscosity on time scale can be assumed to be given by a power law Prins (⁶⁶).

$$\eta_s^d = n \left(\frac{d \ln A}{dt} \right)^m$$

Equation 1. 9

In this equation n Represents the magnitude of the surface dilational viscosity at a relative rate of expansion or compression of 1 s^{-1} and m indicates the influence of the time scale. In most cases we find that m is around -1. This means that in general the surface dilational viscosity decreases with increasing relative expansion or compression rate.

When viscoelasticity plays a role, the resistance to deformation of a surface can be assumed to consist of an elastic and a viscous part. The total resistance to deformation is expressed in the complex modulus E . Equation 1. 10 relates the elastic and viscous part to each other.

$$E = E_d + i\omega\eta_d$$

Equation 1. 10

In this equation E is the dilational modulus: E_d is the elastic part and $i\omega\eta_d$ is the viscous part. i Is the imaginary number ($i^2 = -1$), ω is the angular frequency and η_d is the dilational viscosity. Another parameter which is relevant is $\tan \delta$ which is the ratio between $\omega\eta_d$ and E_d . A small $\tan \delta$ indicates that the surface behaves predominantly elastic which means “more solid like”.

Lucassen-Reynders⁽⁴⁾ defined a condition given in Equation 1. 11 for the inhibition of disproportionation of a completely elastic surface in the case of a Laplace pressure difference between bubbles. If the following condition is true the dilation of the surface is stopped completely.

$$E' \geq \frac{1}{2} \gamma$$

Equation 1. 11

If the viscous part of the dilational modulus: $\omega\eta_d$ is finite however, disproportionation will take place.

1.3.2 Deformations caused by viscous drag

When a liquid flows parallel to a deformable or liquid surface in the presence of surface active material a redistribution of surface active material takes place. This leads to a surface tension gradient which is equal to the viscous stress. Hence at every point at the surface Equation 1. 12 applies⁽⁶⁷⁾:

$$\eta \left(\frac{dv_x}{dz} \right)_{(z=0)} = - \frac{d\gamma}{dx}$$

Equation 1. 12

In this equation η is the viscosity of the bulk phase, the differential indicates the velocity gradient normal to the surface, and $d\gamma/dx$ indicates the surface tension gradient along the surface. The equation merely tells us that mechanical equilibrium is reached when the surface tension gradient is equal to the viscous drag exerted by the liquid to the surface. Figure 1.5 illustrates that this can work in two different ways, because both the viscous drag and the surface tension gradient may cause the motion of the surface.

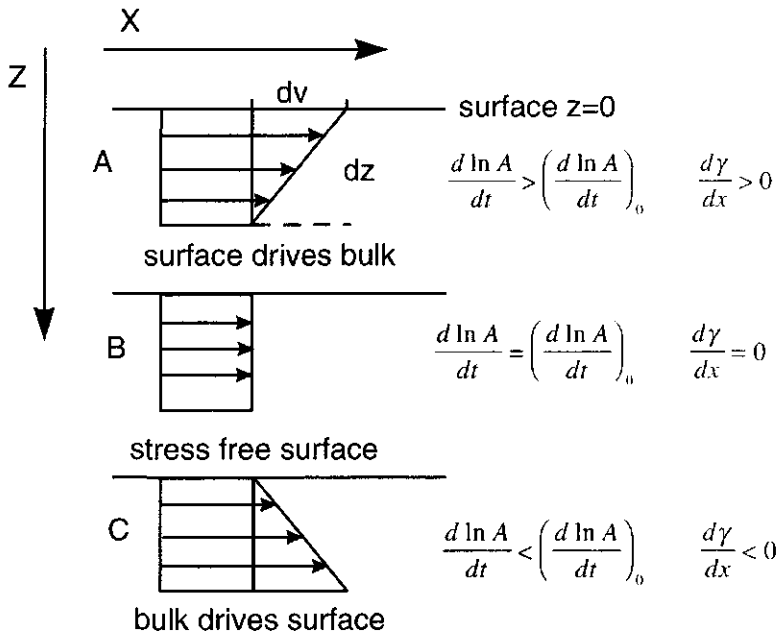


Figure 1. 5 Relation between viscous stress and relative rate of expansion of the surface under three different conditions.

When the surface tension gradient is the cause of the deformation (case A), the surface essentially drags the liquid below it because of the motion of the surface. In case B, both the surface tension gradient and the velocity gradient vanish. Note that the velocity as well as $\frac{d \ln A}{dt}$ still can have a finite value in this case. This happens e.g. in the overflowing cylinder in the presence of pure liquids.

In situation C the bulk liquid causes the motion of the surface thereby creating a surface tension gradient.

1.4 Foam creation and foam stability

Many authors from various disciplines studied the factors that affect the formation, stability and breakdown of foams. They demonstrated that both creation of foams and stability of foams are processes in which several surface properties are relevant. The difficulty in understanding the field of foam creation and stability lies in quantifying the

influence of all the sub-processes involved. Moreover this is complicated by the mutual dependence of the various sub-processes. In this section we will discuss several aspects of the creation and stability of foams.

1.4.1 Creation of foams

Foams can be created by means of wide number of methods such as whipping, stirring, sparging and heterogeneous and homogeneous nucleation in a liquid supersaturated with gas. The result of all these methods is the same, namely the creation of a more or less fine distribution of gas into a liquid. The mechanisms however by which these foams are created differ quite considerably. With sparging the area is enlarged due to pumping of gas through an orifice in contact with the liquid. A bubble is literally pumped up and is released from the orifice due to the buoyancy of the bubble or by viscous drag or inertial effects. During whipping and stirring large bubbles are broken up into smaller bubbles. Break-up occurs due to viscous forces when the flow is laminar and due to pressure gradients when the flow is turbulent. With heterogeneous and homogeneous nucleation bubbles are created because the liquid is supersaturated with gas. With heterogeneous nucleation bubbles form at so called active sites which consist of gas pockets. Because of gas diffusion, the bubbles grow and detach from the nucleus as a consequence of gravity and a new bubble is created. With homogeneous nucleation the bubbles are created at very high super-saturations, and are formed spontaneously in the liquid. This thesis will concentrate on the creation of foams by whipping since it a widespread technique by which foams are created in practice.

The type of foam depends strongly on the conditions under which the foam is created. The most important aspects are the flow properties (laminar or turbulent) around the bubbles created by the stirring action and also the type of surface active species. This will result in a foam with certain characteristic properties with respect to bubble size and the gas fraction in the foam.

When break-up of bubbles in laminar flow is considered, an important parameter is the Weber number which is defined as follows:

$$We = \frac{dv_x}{dz} \frac{\eta_c r}{\gamma}$$

Equation 1.13

In this equation $\frac{dv_x}{dz}$ means the velocity gradient normal to the surface, η_c means the viscosity of the continuous phase, r is the radius of the bubble and γ is the surface tension in equilibrium, Walstra (⁶⁸). Hence the Weber number is the ratio of the external stress over the Laplace pressure. In the case of emulsions, there are relations between the Weber number at which a droplet becomes unstable and the viscosity ratio between the disperse and the continuous phase for different flow types. Generally in air/water systems (viscosity ratio 10^{-3}) in simple shear flow the critical Weber number is around 10. In figure 1.6 the relation between the viscosity ratio (the ratio of the viscosity of the disperse and continuous phase) and the critical Weber number has been given. Williams et al. (⁶⁹) found a distinct dependence of the critical Weber number in simple shear flow in the break up of oil droplets on the concentration of β -lactoglobulin. At low concentrations of this protein (below 10^{-2} g/l) and at all concentrations of the protein β -casein, the critical Weber number has the theoretical value indicated in figure 1.6.

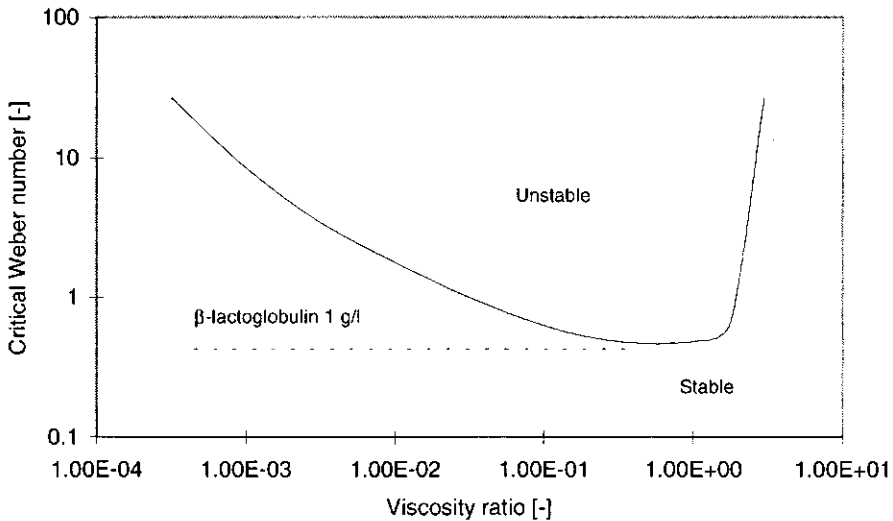


Figure 1.6 Relation between the critical Weber number and the viscosity ratio in "normal" situations solid line and in the case of β -lactoglobulin 1 g l⁻¹ dotted line ⁽⁶⁹⁾.

At high concentrations of β -lactoglobulin however, the critical Weber number remained at a constant value of 0.47 at viscosity ratios between 10^{-4} to 10^1 . This phenomenon was ascribed to the generation of a network structure at the surface which facilitates bubble break-up. This may be caused by a high rigidity of the surface, causing the break up to occur at lower velocity gradients. This indicates that the surface properties may influence the transfer of stress to the surface by viscous forces. Hence not only the intensity of the flow around the bubble determines the break-up, but also the surface properties.

Another indication of the influence of surfactant action on the bubble break-up behaviour has been shown by De Bruijn ⁽⁷⁰⁾. It is demonstrated that in simple shear flow, tip-streaming can occur under subcritical conditions of shear rate at intermediate levels of surfactants. The tip-streaming is ascribed to the accumulation of surfactant to the tips of the bubbles, causing very low surface tensions and consequently very low Laplace pressures, resulting in the break off of small bubbles. The cause of this process is attributed to small amounts of impurities in the surfactant.

Also the type of equipment may have a significant effect on the result of foaming or emulsification tests. Walstra and Smulders demonstrate that different types of emulsification equipment produce emulsions with different mean bubble sizes at comparable levels of energy dissipation. This indicates that it is very difficult to compare different types of foaming and emulsification equipment.

Taisne and Walstra ⁽⁷¹⁾ studied the recoalescence during the production of emulsions by means of an elegant method. It was found that there is an equilibrium between break-up and coalescence of emulsion droplets during emulsification.

Prins ⁽⁷²⁾ studied the creation of foams by a rotating wire cage from solutions of a non-ionic surfactant in relation to the surface properties. An optimum in the creation of the foam was observed which was ascribed to an increase in coalescence during foam formation. By means of a simple consideration in which the relative rate of expansion of surfaces in the foam were related to dynamic surface properties of the species he was able to reconcile the relative rate of expansion in the foam to that at a free surface in expansion. These observations mean that not only the creation of the dispersion is important but that also instability may be relevant during the formation of the dispersion.

1.4.2 Foam stability

In this section three different mechanisms influencing foam stability: drainage, disproportionation and coalescence will be discussed.

1.4.2.1 Drainage

When a foam is created, the difference in density between the dispersed phase (the gas) and the continuous phase (the liquid) will cause the rise of bubbles. This process is called creaming. The velocity of bubble rise depends on the type of flow around the bubble, the density of the continuous phase, the viscosity of the liquid and the density difference between the continuous phase and the disperse phase. Also the kind of surfactant used to stabilise the bubbles in the liquid is important Zuidberg ⁽⁷³⁾. It could be concluded that bubbles with rigid surfaces cream up to a factor 2 slower than bubbles with a mobile surface.

A phenomenon closely related to creaming is drainage, which is the flow of liquid out of the foam under the action of gravity, which causes the foam films and Plateau borders to become thinner. The drainage process essentially depends on the same flow properties and surfactant characteristics which determine creaming. Drainage of foams can be considered to be influenced by two separate processes taking place at the same time. Liquid flow through the films into the plateau borders and liquid flow through the plateau borders into the bulk phase underneath. Several factors related to surface properties, bubble size distribution and composition were studied in literature. Malhotra and Wasan (⁷⁴), Narsimhan (⁷⁵), Bhakta and Ruckenstein (⁷⁶) present models which describe drainage of foams as percolation through a network in which the volume fraction of liquid varies with time. Chesters (⁷⁷) studied the drainage from films between bubbles on which a force is applied. Three types of surfaces are distinguished. These are described as: mobile, partially mobile and immobile. These types of surfaces in this order cause a decrease in the rate of drainage.

Also several studies have been carried out on single films. In single films, the balance between the suction of the plateau borders, the disjoining pressure and the film elasticity can be determined in a more straightforward way Kruglyakov et. al. (⁷⁸), Baets and Stein (⁷⁹), Prins et. al. (⁸⁰) Aronson et. al. (⁸¹). The results of the studies on single films and drainage of macroscopic foams do not match very well however. Probably this can be ascribed to the fact that the dimensions of films in foams and static films are not comparable, moreover the plateau border drainage which is absent in single films has a substantial influence in foams. In addition, marginal regeneration, a process which promotes drainage, occurs in single films does not occur in foams.

1.4.2.2 Disproportionation

Disproportionation is the process of net transport of gas from small bubbles to larger bubbles. This process is caused by the higher Laplace pressure in small bubbles as shown in equation 1.6. The higher Laplace pressure around a small bubble causes the bulk concentration of gas to be higher than around a bigger bubble. Consequently a net transport of gas by diffusion from small bubbles to bigger bubbles takes place. This

causes smaller bubbles to become smaller and disappear eventually. This leads to a coarser foam. This sub-process is inhibited by surfactants because the surface tension decreases if a surface is compressed and increases if a bubble expands. The compression of the surface causes the surface tension to decrease, which causes a decrease in the Laplace pressure. This makes the disproportionation to proceed more slowly. Ronteltap⁽⁸²⁾, Ronteltap et. al.^{(83), (84)} concluded that the rate of disproportionation depends on the surface dilational viscosity in compression. If this parameter has a high value, a small relative rate of compression gives a high decrease in surface tension, which inhibits the rate of disproportionation. By means of this parameter the rate of disproportionation of beer foam could be explained.

In addition it was found that the rate of disproportionation was also determined by the solubility of the gas in the liquid phase. If this was high, disproportionation was found to more rapid as well since the rate of transport from one bubble to the other is increased. Monsalve and Schechter⁽⁸⁵⁾ described the relation between the bubble size, the drainage and the disproportionation of foams. It was concluded that disproportionation and drainage both resulted in decrease in surface area in the foam, which can be described by means of two exponential terms, corresponding to the drainage and the disproportionation process.

At purely elastic surfaces, disproportionation can be stopped if the modulus is larger than half the surface tension Lucassen-Reynders⁽⁵¹⁾ as described in section 1.3.1. At a visco-elastic surface the rate of disproportionation will be determined by the rate of surface relaxation.

1.4.2.3 Coalescence

Coalescence is the merge of bubbles because of a breaking of the film between them. It is a stochastic process, which means that the breaking of a certain film is depends on chance. Generally the coalescence process needs instabilities such as waves in the surface of the film which cause the film to become thin and this can be the introduction to film breaking. In thin films coalescence can be opposed by a disjoining pressure. The

disjoining pressure is the pressure in a thin film which is caused by the repulsion of the adsorbed layers at both surfaces. This repulsion may be due to electrostatic or steric interactions between adsorbed molecules Walstra (⁸⁶) Tadros and Vincent (⁸⁷). These repulsive forces generally work over length scales which are in the order of nanometers which means that the disjoining pressure is effective only for very thin films.

The resistance to coalescence in stirred suspensions of bubbles or drops due to the presence of surface active species, is generally ascribed to the Gibbs Marangoni Effect. The impact of bubbles causes a liquid flow parallel to the surface locally dilating the surface. If the bubbles are too close to each other the film becomes too thin to supply the surface with enough surface active material. This causes a local increase in surface tension which gives rise to a surface tension gradient. This surface tension gradient causes the motion of the surface to slow down and slows down the dilation of the film. In this case the rate of flow of liquid from the space in between the bubbles is decisive for the moment of coalescence.

Coalescence of bouncing bubbles also can be strongly inhibited if the molecules in the film surface are able to interact laterally, for instance in the presence of various proteins. There local dilation of the surface is strongly opposed. In that case also strong repulsive interactions between the adsorbed layers are observed due to both steric and electrostatic interactions between the adsorbed proteins. This results in relatively thick films. Clark et al. (⁸⁸).Coke et. al.(²⁵) demonstrate that the addition of a surfactant to a protein solution leads to a lower rigidity of a film which manifests itself in a increased lateral diffusion of the adsorbed species and in a decreased stability of the films.

1.4.2.4 Spreading particles and hydrophobic particles

If either spreading, or hydrophobic particles are present in foams, they may seriously affect foam stability. When hydrophobic particles are present in an aqueous film these can promote coalescence when both ends of the particles protrude through the film. Since the contact angle of the liquid with the particle is large it causes the liquid to recede from the particle and causes film rupture.

Bisperink⁽⁸⁹⁾ and Prins⁽⁹⁰⁾ studied the influence of spreading particles on the stability of thin liquid films. It was concluded that when spreading particles are present in the liquid two parameters determine if the particle will spread at the surface. The first parameter determines if the particle can penetrate the film surface, the second parameter determines if the particle will start spreading at the surface. If such a particle is present at the surface of a thin film the spreading surfactant will drag liquid away from the particle which will cause the film to become thinner and eventually break. The criterion for a bubble to be susceptible to this spreading mechanism depends on the size of the bubble, the thickness of the film and the type of surface active species at the surface of the film and in the spreading particle. However if the bubble surface area is too small, the spreading cannot proceed far enough due to the limitation in the area of the surface over which it can spread. Finally the surfactant adsorbed to the surface also determines the spreading of the surfactant. This is because the surfactant already adsorbed to the surface will inhibit the spreading of the surface active species from the particle since the tendency to spread over the surface is lower due to the lower surface tension at the surface of the film.

1.5 Mechanical aspects of sub-processes occurring in foams

One characteristic property of these sub-processes causing instability in foams is that in all of them the bubble surface is deformed in a certain characteristic way. In order to cause this deformation, a certain force needs to be imposed on the adsorbed layer. This force can be applied parallel to the surface which happens during drainage. The force can also be applied normal to the surface when a pressure difference causes a deformation as in the case of disproportionation. The way this force is applied to the surface makes a distinct difference in the way a surface reacts to the deformation and which surface properties play a role.

Another important factor is the time scale of deformation of the surface. During creation of foams, the deformation rates of the surface are relatively high, while during the initial stages of disproportionation, the deformation rate is low. At low deformation rates, slow

relaxation processes have a much larger influence on the surface behaviour. The two main relaxation processes which affect the surface behaviour are: The transport of surface active material from the bulk to the surface and vice versa, and conformation changes of the molecules, which play a role with polymers such as proteins.

In table 1.1 the most important sub-processes in foams are listed. This table shows the types of deformation and the approximate time scales over which the different sub processes take place. The cause of the deformation in the sub-process has been indicated as well as the effect the deformation causes in the surface. This table clearly shows that the creation and stability of foams depend on sub-processes which take place over different time scales and are affected by different surface properties. Bubble break-up in turbulent flow, disproportionation and coalescence of static foam films are sub-processes which are caused by forces which work normal to the surface. Bubble break-up in laminar flow, creaming and drainage, coalescence during stirring and spreading, however, are sub-processes which depend on forces which work parallel to the surface.

In this thesis we will pay attention to deformations parallel to the surface because this is where the need for investigation lies whereas abundant information is available on uniform deformations of the surface.

Sub-Process	Direction of force (stress)	Time Scale [s]	Cause Sub-process	Effect (response)
Bubble break-up Turbulent	Normal	10^{-4} to 10^{-2}	Pressure difference	Laplace pressure
Bubble break-up Laminar	Parallel	10^{-3} to 1	Viscous Flow	Surface tension gradient
Creaming and Drainage	Parallel	10^{-1} to 10^1	Viscous Flow	Surface tension gradient
Disproportionation	Normal	10^{-3} to 10^3	Laplace Pressure	Dilational Modulus
Coalescence (static)	Normal		Drainage, Waves.	Disjoining pressure
Coalescence (dynamic)	Parallel	10^{-4} to 1	Bouncing	Viscous Flow
Spreading	Parallel	10^{-2} to 1	Surface tension gradient	Viscous Flow

Table 1. 2 Classification of sub-processes occurring in foams

1.6 Aim of this thesis

The work on this thesis resulted from a direct question from industry about the possibility of obtaining a working knowledge on the performance of protein hydrolysates as a foaming agent in relation to their composition in terms of molecular weight distribution. Since the direct translation from the molecular composition to foaming properties was considered not feasible a distinction was made into four levels of information which needed to be investigated and related to each other in order to come to a satisfactory answer.

1: On the molecular level molecules interact in bulk and on the surface and cause certain surface properties which are measurable by means of different techniques depending on

the information required. 2: These surface properties in turn are responsible for the mechanical properties of surface layers over various time scales. 3: This correlates with time scales of the different mechanisms playing a role in the creation and stability of foams. 4: In turn the mechanical properties also need to be translated into foaming properties relevant for our industrial counterparts. Since this scope was too wide to cover completely, choices were made to tackle only a number of aspects we considered to be most relevant considering the gaps in our understanding.

In the translation of molecular properties to surface properties of proteins it was considered that the transport from bulk to the surface and vice versa and the unfolding and refolding of protein molecules at the surface were ultimately responsible for the surface behaviour of proteins. Since various time scales play a role during foaming we chose to cover a wide range of time scales and study the influence of transport and unfolding of proteins. Our main aim was to be able to separate these two processes from each other and achieve an understanding of the time scales involved in both processes depending on the type of protein and other circumstances. Different types of model proteins differing in physical stability (globular, random coil) were considered. In addition we chose to study this behaviour for mixtures of proteins and surfactants since these systems are relevant for the industrial practice and might be related to the behaviour of protein hydrolysates. The effect of the presence of surfactants on the unfolding behaviour of proteins was unknown especially under dynamic conditions. Studying the transport and unfolding for these systems would indicate whether the substances adsorbed to the surface would mutually influence each other.

Another gap in our knowledge was, in our opinion, the absence of information dealing with the response of surfaces to viscous forces. These forces may play a significant role in foaming but had not been studied in a systematic way. Hence we chose to use the overflowing cylinder technique in a special way to provide information on mechanical properties of surfaces of various systems deformed by forces acting parallel to the surface.

In order to translate mechanical properties to foaming properties, foam generation and drainage behaviour of a number of systems was considered. We chose to study systems of which the mechanical properties of the surface differed considerably and concentrated on obtaining an answer on which surface properties at what time scales are relevant for break-up of bubbles and drainage. These sub-processes were chosen because they were suspected to be influenced by the resistance to deformation to forces acting parallel to the surface.

1.6.1 Contents of this thesis

In chapter 2 a model will be presented in which transport to the surface and unfolding properties of proteins at the surface are related to mechanical properties of the surface. This is necessary to interpret the behaviour of proteins at expanding air/water surfaces in the overflowing cylinder. A model will make the interpretation of data on adsorption of proteins at expanding interfaces possible. The understanding of the separate contributions of unfolding and transport to expanding surfaces is the main goal of this model.

In chapter 3 the model will be used to interpret measurements of surface tension, surface concentration and relative rate of expansion of expanding surfaces in the overflowing cylinder. The unfolding behaviour of diverse types of proteins will also be investigated. In addition, a new technique will be presented which enables the measurement of surface tension gradients generated at air/water surfaces. These measurements will be used to quantify the resistance to deformation to forces applied parallel to the surface.

In chapter 4 the model of chapter 2 will be adapted for binary mixtures of low molecular surfactants and proteins adsorbing simultaneously at expanding air/water surfaces. Several aspects of the adsorption and mechanical behaviour of air/water surfaces of binary surfactant mixtures will be covered. The extended model will be compared to experimental data obtained by means of the techniques described in chapter 3.

In chapter 5 aspects of foaming behaviour of a number of different systems studied in this thesis will be treated. In this chapter we will concentrate on the measurement of the bubble size distribution and the drainage behaviour of diverse systems as a function of the foaming conditions. These will be compared to measurements and the models presented in the previous chapters.

In chapter 6 the main conclusions obtained in the previous chapters will be put into perspective by describing how the methods developed can be used in practice. Also the implications of the information provided in the thesis are put forward.

Chapter 2

Modelling the surface behaviour of surfactants and proteins at expanding surfaces and application to the overflowing cylinder technique

2.1 Abstract

An essential aspect of the approach of this thesis is to quantify the separate effects of transport and unfolding of proteins at air water interfaces on dynamic surface behaviour. The starting point of this chapter is that dynamic behaviour of proteins at surfaces cannot be understood by transport to the surface only but unfolding needs to be taken into account as well. In this chapter a simple model is presented which can enhance our understanding of the contribution of both processes. The model is designed to understand experimental results obtained at expanding interfaces in the overflowing cylinder by introducing the characteristic time scales for transport and unfolding. Although the model has been created specifically for proteins, it can be adapted to describe the behaviour of low molecular weight surfactants as well.

Results obtained by calculations performed by the model indicate that it is possible to describe the dynamic behaviour of protein molecules at expanding surfaces in the overflowing cylinder by transport and unfolding of proteins at the surface.

In order to make the link to the overflowing cylinder, the relation between the surface tension gradient and the relative rate of expansion described by Bergink-Martens (¹) was brought in the model which enables to calculate the maximum relative rate of expansion that can be generated in the overflowing cylinder. Here the random coil β -casein and the globular β -lactoglobulin were compared. β -Lactoglobulin which unfolds slower than β -casein can be observed to create lower surface tension gradients and lower relative expansion rates in comparison to β -casein. Also the sensitivity of surface tension to the relative rate of expansion is much higher for β -lactoglobulin.

2.2 Introduction

In this chapter a model will be created in which semi-empirical parameters describing the molecular properties of protein molecules can be translated into surface- and mechanical properties of the surface. This model considers the dynamic properties of surfaces in continuous steady state dilation far from equilibrium. The conditions are chosen to match the overflowing cylinder technique and contribute to explain the effects of unfolding behaviour of proteins on surface properties.

The hypothesis behind the description of the behaviour of adsorbed protein molecules, assumes that two processes are important in the surface active behaviour in dynamic situations. 1: Transport to the surface by means of convective diffusion. 2: Molecular rearrangements of proteins adsorbed at the surface. These processes both have a characteristic time scale. These time scales combined, determine the resulting dynamic surface properties.

Measurements of surface concentration (adsorption), relative rate of expansion and surface tension of radially expanding surfaces were performed in an overflowing cylinder by means of ellipsometry, laser Doppler anemometry and the Wilhelmy plate technique respectively. These measurements are described in chapter 3. The results were used to assess the parameters of the model relating molecular properties to dynamic surface properties. The theory and the adjustable parameters in the model were validated with the results from the measurements.

When the parameters describing the unfolding and the transport to the surface are established they can be used to quantify the relative rate of expansion that can be generated at the overflowing cylinder surface. This enables us to calculate the surface tension gradient that can be generated at the surface of the overflowing cylinder.

2.3 Theory

In order to create the model three simplifying assumptions need to be made. We discuss these below. First three considerations underlying the model will be defined. Subsequently we describe the model.

(1): First of all the unfolding of proteins is simplified considerably. Here the hypothesis of Serrien et al.⁽²⁾ will be used. This hypothesis states that adsorbed proteins can occur in two extreme states; native and unfolded. The transition between

these two states occurs by means of first order kinetics. The unfolded and native molecules are assumed to occupy a different area at the surface. The total area occupied by proteins inhibits the adsorption of additional protein molecules due to the space the molecules occupy as the surface.

This simplification can be motivated as follows: Since the averaging takes place over a large number of molecules, the fraction of unfolded molecules serves as a “mean conformation”. Since we will use this parameter to calculate the surface tension which is a parameter that depends on the number of protein segments adsorbed to the surface, the extrapolation to a mean conformation is justifiable.

(2): In the model of Serrien et al. ⁽²⁾, unfolded molecules cannot desorb, in contrast to native molecules. This is a consequence of the fact that when proteins are in a totally unfolded conformation, the desorption is highly improbable. However, in the situation that only very few amino acid segments are adsorbed, the chance of desorption is much higher.

(3): since there are only two extreme states in which the molecule can exist in the model, the ratio of the two populations and the total adsorbed amount together determines the surface tension. As limiting values for the surface tension we adopt: the surface tension due to hard disk interactions for native molecules on one hand and the surface tension for a layer consisting of unfolded molecules only on the other hand. In first approximation the surface tension of a mixture of these is calculated as a weighted mean of these two limiting surface tensions.

Now these simplifications are made, the surface concentration of native and unfolded proteins can be calculated at an expanding surface if we know the velocity of the surface at each point. In order to match the situation in the overflowing cylinder the corresponding velocity profile needs to be taken. The velocity of the surface at the overflowing cylinder was determined at various distances to the centre at different relative expansion rates in preliminary experiments by among others Bergink et al. ⁽²⁾. From these experiments the variation of the relative rate of expansion of the surface was calculated and applied in this model. With this variation in the relative rate of expansion the velocity profile in the overflowing cylinder was accounted for. Now we can calculate the surface tension as a function of the distance to the centre so the surface tension gradient is known.

Bergink ⁽²⁾ has shown that there is a characteristic relation between the stress at the surface of the overflowing cylinder and the relative rate of expansion of the surface. Hence the maximum relative rate of expansion generated by the overflowing cylinder can be calculated numerically by varying the relative rate of expansion in the model until agreement is found between the model and the theory

The following paragraphs presents the mathematical translation of the physical considerations underlying the model.

2.3.1 Unfolding of adsorbed proteins

In figure 2.1 a schematic representation of the model of unfolding of proteins at interfaces is shown.

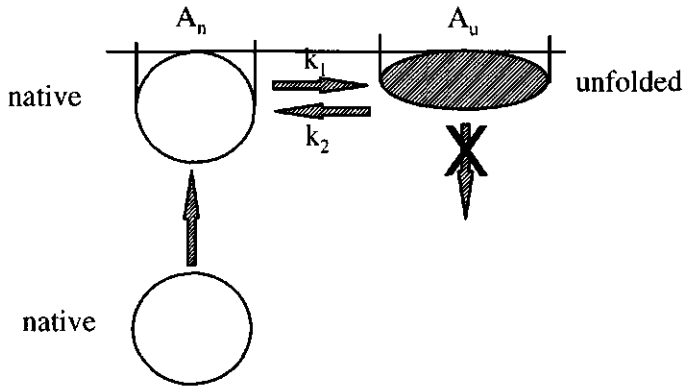


Figure 2. 1: Schematic representation of the unfolding of protein molecules.

This has been presented by Serrien et. al. ⁽²⁾. In the model presented there, it can be seen that first proteins adhere to the surface in a native conformation, after which, these proteins may unfold to an unfolded conformation. The rate of unfolding is determined by a first order rate constant k_1 . The transition back from an unfolded to a native molecule is also possible. This process is assumed to be determined also by a first order rate constant k_2 . The molecules cannot desorb from the surface in this unfolded conformation. Also the direct transition of a native molecule in bulk to an unfolded molecule in the surface is assumed to be impossible.

In addition to the model of Serrien ⁽¹⁾, another intricacy has been assumed in the model presented here. This is the area the molecules occupy in the surface: It has

been assumed that as a consequence of the unfolding of the molecules the geometrical occupied area at the surface changes. This area is defined as the area not accessible for adsorption of other protein molecules due to the fact that the surface is already occupied.

The rate constants k_1 and k_2 and the time molecules have available for unfolding, now determine the distribution of the molecules over the native and unfolded conformation. The cross sectional areas A_n and A_u respectively determine the areas these molecules occupy in the surface. Essentially, k_1 , k_2 , A_n , and A_u are the parameters which determine the unfolding behaviour of the proteins at the surface. The aim of the model is to predict these, by matching the constants to data obtained from characteristic measurements of relations between relative rate of expansion, surface concentration and surface tension.

Considering the consequences of this model we can infer that in the case k_2 has a finite value the model will not reach the equilibrium state since we assume that still a fraction of the molecules is in a native state. Hence the limit for $t \Rightarrow \infty$ so the relative expansion rate ($\frac{d \ln A}{dt}$) = 0 does not give the equilibrium value for the surface tension. This could be considered to be a drawback of the model. However in this model we only consider the initial phase of the adsorption process, taking place over time scales in between 0.1 to 100 seconds. Damadoran and Song⁽³⁾ for instance observed that the change in surface tension of proteins proceeds over time scales in the order of hours. Hence it may very well be that after this initial phase the model suggested here does not apply.

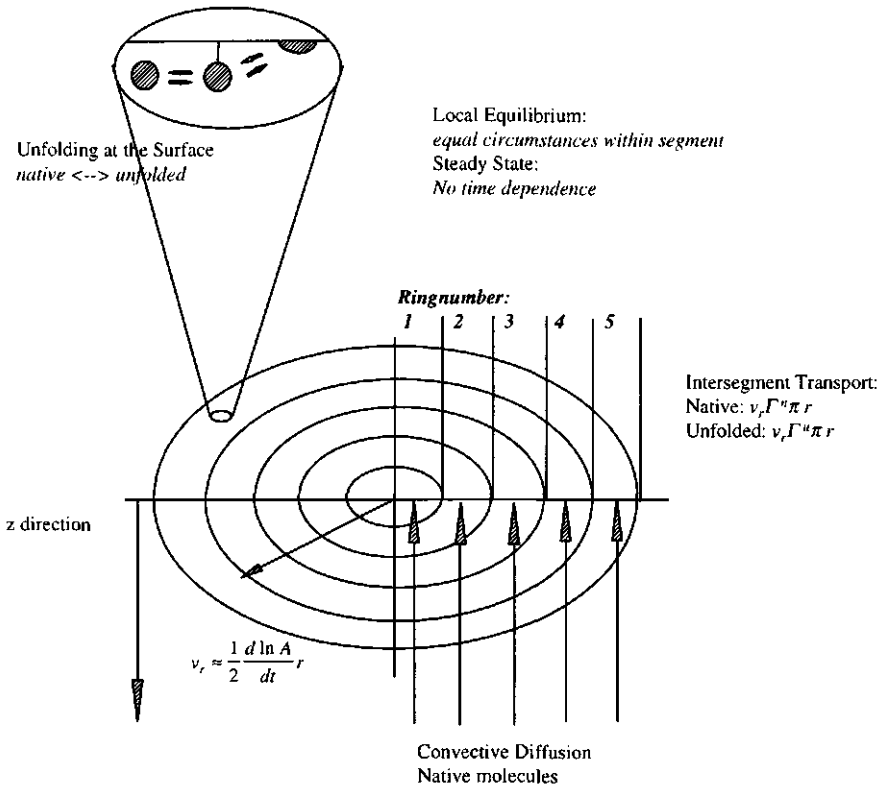


Figure 2. 2 Schematic representation of the model for the unfolding of proteins.

2.3.2 Transport to the surface

In figure 2.2 a schematic representation of the model has been given. In this figure the underlying considerations concerning the transport have been given. Some preliminary calculations and the results obtained by Bergink et. al.^(1,4) have indicated that in the case of a radially expanding surface in a steady state, the transport to the surface can be described best by convective diffusion Van Voorst Vader,⁽⁵⁾. In the solution, the basic continuity equation for the steady state ($dc/dt=0$) is:

$$D \frac{\delta^2 c}{\delta z^2} = V_z \frac{\delta c}{\delta z}$$

Equation 2. 1: Continuity equation for an expanding surface

In this equation D is the diffusion constant, c is the concentration in bulk and z is the co-ordinate perpendicular to the surface. From this the concentration gradient $(dc/dz)_{z=0}$ and the flux Φ towards the surface $D(dc/dz)_{z=0}$ is found to be:

$$D(c_b - c_s) \left(\frac{2 \frac{d \ln A}{dt}}{\pi D} \right)^{\frac{1}{2}}, \text{ where } c_s \text{ and } c_b, \text{ respectively mean subsurface concentration}$$

and bulk concentration, and $\frac{d \ln A}{dt}$ means the relative rate of expansion of the

surface $\frac{d \ln A}{dt}$. At the expanding surface, the mass balance is given by

$$D \left(\frac{dc}{dz} \right)_{z=0} - \Gamma \left(\frac{d \ln A}{dt} \right) = 0, \text{ hence in steady state we have:}$$

$$\Phi = D \left(\frac{\delta c}{\delta z} \right)_{z=0} = \Gamma \cdot \frac{d \ln A}{dt}$$

Equation 2. 2 Flux to an expanding surface.

Here, Γ means surface concentration which can be expressed in D , $\frac{d \ln A}{dt}$, c_b and the

unknown c_s . In order to proceed, the value of c_s needs to be determined. Often local

equilibrium is assumed, which implies that the function $\Gamma(\overline{c_s})$ corresponds to the

(equilibrium) isotherm; by inversion one then obtains $\overline{c_s}(\Gamma)$. However, as we

consider unfolding, such an isotherm is not uniquely defined. We therefore postulate

that $\frac{c_s}{c_b}$ equals the fraction of occupied surface area which comes down to

introducing an inhibitory parameter for adsorption of proteins to solid surfaces to

account for the presence of other molecules already adsorbed. Eliminating c_s one

obtains:

$$\Phi = \Phi_0 \left(\frac{\Gamma_{\max} - A_n \Gamma^n - A_n \Gamma^u}{\Gamma_{\max}} \right) \text{ and } \Phi_0 = c_b D \sqrt{\frac{2 \left(\frac{d \ln A}{dt} \right)}{\pi D}}$$

Equation 2. 3 Inhibitory parameter

In this equation A_n and A_u respectively mean the dimensionless surface areas of the native and unfolded conformation. The superscripts for Γ , n and u indicate the native and unfolded state of the protein respectively. A_n and A_u are not independent variables because they are linked by means of Γ_{\max} . Hence if the maximum surface concentration in equilibrium is taken to be Γ_{\max} , A_u is equal to 1 (in that case

$$A_u \equiv \frac{\Gamma_{\max}^u}{\Gamma_{\max}^n} \text{ and } A_n \equiv \frac{\Gamma_{\max}^n}{\Gamma_{\max}^u}.$$

2.3.3 Mass balances

The basic equations for mass transport to the surface and discharge from the surface have been defined now in equations 2.1 to 2.3. These equations can be applied to the mass balances by which the radially expanding surface is described. The schematic drawing in figure 2.2 summarises the different contributions of transport and unfolding in and to the surface.

Here we adopt a finite element method: The radially expanding surface is divided into concentric rings of equal width. Over each concentric ring, the surface concentration, the fraction of unfolded molecules and the surface tension is considered to be single valued and constant. (steady state).

For each concentric ring it is possible to calculate the fraction of unfolded molecules, and the surface concentration by solving two mass balances over each ring. These mass balances describe the balance between the supply and discharge of native and unfolded proteins to and from the surface.

In figure 2.3 and 2.4 the mass balances underlying the model are explained for native and unfolded molecules respectively. In these figures it can be seen that the mass balance of native molecules over each concentric ring can be described by means of five contributions:

1. adsorption to the surface from the bulk solution
2. transport from the previous ring
3. discharge to the next ring
4. unfolding: transfer from a native to an unfolded conformation
5. refolding: transfer from an unfolded state to a native state

Hence we arrive at the following expression for the mass balance of native molecules:

$$\underbrace{\pi(r_n^2 - r_{n-1}^2)\Phi}_A + \underbrace{\pi r_{n-1}^2 \frac{d \ln A}{dt}}_B \Gamma_{n-1}^u - \underbrace{\pi r_n^2 \frac{d \ln A}{dt}}_C \Gamma_n^u - \underbrace{\pi(r_n^2 - r_{n-1}^2)k_1 \Gamma_n^u}_D + \underbrace{\pi(r_n^2 - r_{n-1}^2)k_2 \Gamma_n^u}_E = 0$$

Equation 2. 4: Mass balance for native molecules at a surface element (Symbols correspond to those in figure 2.3).

Here Φ means the net flux to the surface, which is considered to consist only of native molecules. The superscript u means that it applies to proteins in the unfolded conformation. The k_1 and k_2 are the rate constants for the transitions in conformation from native to unfolded and vice versa respectively. Here the subscripts n and $n-1$ for Γ indicates the ringnumber, this parameter refers to. So $n-1$ means the segment previous to ring n which is considered at that moment, closer to the stagnation point, (see figure 2.2).

Mass balance Native Molecules

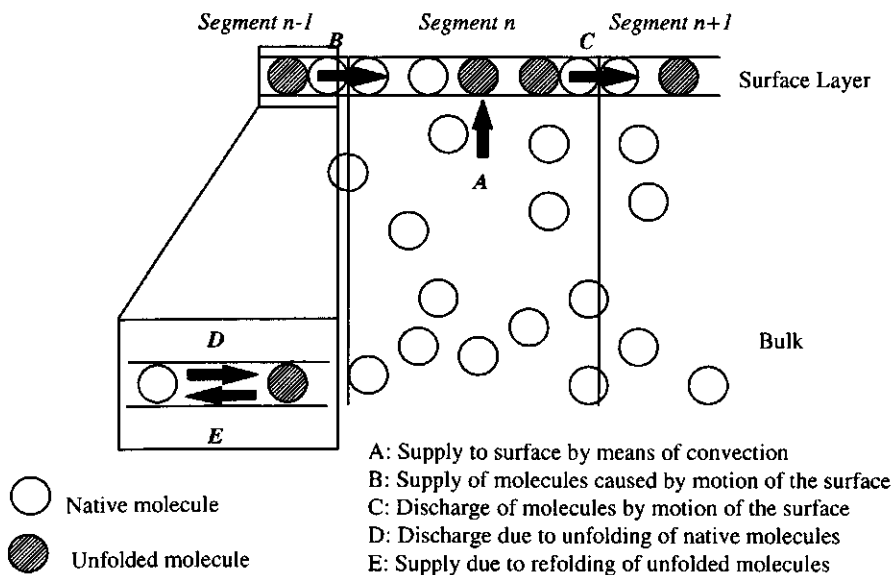


Figure 2. 3: Schematic representation of mass balance of native molecules of ring n .

In figure 2.3 A represents the net flux of native molecules to the surface, which is the first term $\pi(r_{n-1}^2 - r_n^2)\Phi$ in equation 2.5. The second and third contribution in the equation are represented by respectively B and C in figure 2.3. The fourth and fifth term are represented by D and E in this figure.

For the unfolded molecules the mass balance can be written as follows:

$$\underbrace{\pi r_{n-1}^2 \frac{d \ln A}{dt}}_A \Gamma_{n-1}^u - \underbrace{\pi r_n^2 \frac{d \ln A}{dt}}_B \Gamma_n^u + \underbrace{\pi(r_n^2 - r_{n-1}^2)k_1}_{C} \Gamma_n^u - \underbrace{\pi(r_n^2 - r_{n-1}^2)k_2}_{D} \Gamma_n^u = 0$$

Equation 2. 5: Mass balance of unfolded proteins at a surface element (symbols correspond to those in figure 2.5).

The notations used in this balance are the same as the notation used in equation 2.4.

In figure 2.4 this mass balance is indicated schematically. The first and second

Mass balance Unfolded Molecules

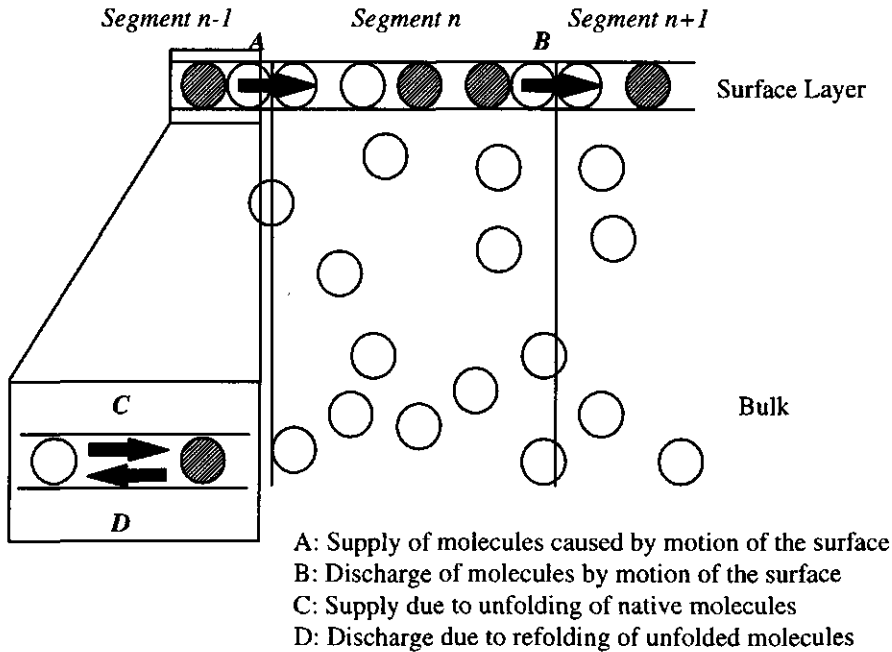


Figure 2. 4: Schematic representation of mass balance of unfolded molecules for ring n.

contribution are represented by respectively A and B. The third and fourth contribution are represented by respectively C and D.

These equations can simply be solved by combining equations 2.4, 2.5 and 2.6 to obtain a lengthy but simple expression for Γ_n^u given in appendix 2.1. From the

equations given there, the adsorbed amount of unfolded and native molecules for ring n can be calculated.

2.3.4 Surface Tension

From the equations described in the previous paragraphs, the surface concentration of native and unfolded molecules can be calculated. In order to calculate surface tension a relation between surface concentration and fraction of unfolded proteins needs to be known. From theoretical considerations it is known that the surface pressure π , (which is the difference between the surface tension of the pure solvent γ_0 and the surface tension which is measured γ), can be considered to consist of two contributions. An ideal gas contribution $\pi = \gamma_0 - \gamma = kT\Gamma$, in which k is the Boltzmann constant, T is the absolute temperature and Γ is the surface concentration in moles per square meter. The second contribution is due to interaction of the adsorbed molecules at the surface. This is considered to be a function of the fraction of the surface occupied by the adsorbed molecules. The ideal gas contribution is negligible in the case of proteins because of their high molecular weight. Therefore it is assumed that the second contribution totally determines the surface tension. When protein molecules interact as hard disks, de Helfand (⁶) demonstrated that the surface pressure can be predicted by the Helfand equation:

$$\pi = \frac{kT\Gamma^n}{(1-\Omega)^2}$$

Equation 2. 6: Helfand equation

Here Ω is the fraction of occupied area by native molecules $\frac{\Gamma^n}{\Gamma_{\max}^n}$. We will assume that molecules in their native conformation behave like hard particles, which satisfy the Helfand equation. When proteins unfold the interaction between the particles changes from "hard disk behaviour" to the behaviour of "compressible particles" however. Since we have no better alternative we will use experimentally obtained data of the equation of state to describe the unfolded conformation. In order to mathematically describe these data we adopt the model developed by van Aken (⁷) for various proteins. Van Aken used the Helfand equation and assumed that the area occupied by a molecule at the surface (which is $\Gamma\Omega$, the surface concentration

multiplied by the area occupied by a single molecule) depends on the elastic compressibility β of a molecule, an unfolding parameter α and the area occupied by a completely unfolded molecule Ω_0 . The equation describing the area Ω occupied by the adsorbed molecules is the following:

$$\Omega = \alpha \Omega_0 \text{Exp}(-\beta\pi)$$

Equation 2. 7: Occupied area per protein molecule.

In this equation α is determined by two fit parameters π^* and Ω^* given in the following equation.

$$\frac{1-\alpha}{\alpha} = \exp\left(\frac{(\pi_c - \pi^*)\Omega^*}{kT}\right)$$

Equation 2. 8

From this equation it follows that the unfolding of the protein depends on the surface tension and the two parameters.

Van Aken was able to fit the equation of state several well known proteins. In figure 2.5 the equations of state for β -casein have been given assuming the hard particle model and equation of state in equilibrium. The values used to calculate these curves are given in appendix 2.2.

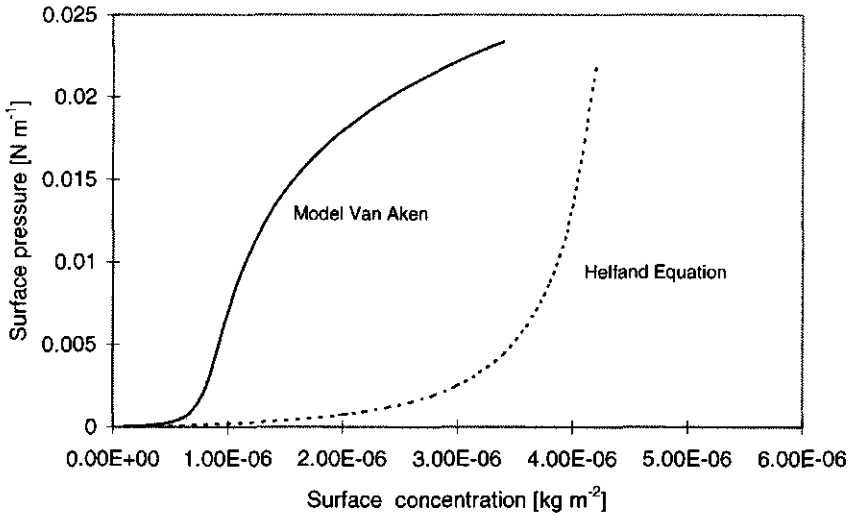


Figure 2.5 Relations between surface pressure and surface concentration for β -casein assuming hard disc interaction (Helfand equation) or soft disc interaction (Model van Aken).

The surface pressure of an adsorbed layer of proteins under dynamic conditions $\pi_{\Gamma_{dyn}}$ in a partially unfolded state is assumed to be a linear combination of these surface pressures as given in equation 2.9.

$$\pi_{\Gamma_{dyn}} = \pi_{\Gamma_{helf}} + \frac{\Gamma^u}{\Gamma} (\pi_{\Gamma_{SS}} - \pi_{\Gamma_{helf}})$$

Equation 2.9: Surface pressure

Here $\pi_{\Gamma_{helf}}$ means the surface pressure of hard particles at surface concentration Γ (the total surface concentration), $\pi_{\Gamma_{SS}}$ means the surface pressure at surface concentration in equilibrium. A linear combination of the surface pressures is not very elegant from a physical point of view. Physically it would be better to calculate the surface pressure by calculating the area occupied by each species at the surface at which the surface pressures become equal for both relations between surface pressure and surface concentration. This linear combination was chosen for reasons of simplicity however and is defensible by considering figure 2.6. There it can be seen that the Helfand equation only plays a role of significance when both the fraction of unfolded molecules is very small (low Γ^u) and the surface concentration is high (high Γ). This is the only condition in which the surface tension decrease is mostly caused

by the native molecules. Otherwise the contribution of hard disk behaviour is generally negligible. In other words the different adsorption isotherms contribute to the total adsorption behaviour at different time scales and concentrations so there is hardly a combined effect. In that case a linear combination is justifiable.

2.3.5 Mechanical properties

For the radially expanding surface at the top of an overflowing clinder, the mechanical properties dictate a relation between the relative rate of expansion, surface tension gradient and the velocity gradient at a surface. In this section these relations are described.

As the surface tension is known now at n different places at the surface, the surface tension gradient over subsequent rings can be calculated also by using the following simple equation:

$$\frac{d\gamma}{dr} = \frac{\gamma_{n-1} - \gamma_n}{\Delta r}$$

Equation 2. 10: Surface tension gradient over subsequent rings.

Here the subscripts n and n-1 indicate the ringnumber of which the surface tension is considered, Δr means the width of one ring. From hydrodynamic theory it can be deduced that since the surface is a free surface, all stresses must cancel. This implies that the relation between surface tension gradient and velocity gradient in the bulk liquid close to the surface can be written as follows:

$$\frac{d\gamma}{dr} = -\eta_b \left(\frac{\delta v_r}{\delta z} \right)_{z=0}$$

Equation 2. 11: Relation between surface tension gradient and the velocity gradient below the surface.

Here η_b means the bulk viscosity of the solution.

Up to now $\frac{d \ln A}{dt}$ has been considered to be a parameter which could be varied at will. However, in the case of the overflowing cylinder there is a relationship between the stress imposed on a surface and the relative rate of expansion which is the response of the system to this stress. In the paper by Bergink et. al. (8) an equation is derived which describes the relation between this stress and the relative rate of

expansion for the overflowing cylinder in the case that the surface is propelled by a surface tension gradient. This results in the relation between the velocity gradient and

$\frac{d \ln A}{dt}$ in equation 2.12.

$$\frac{1}{\eta_b} \frac{d\gamma}{dr} = \left(\frac{dv_r}{dz} \right)_{z=0} = 0.415r \left(\frac{d \ln A}{dt} - \left[\frac{d \ln A}{dt} \right]_0 \right)^{\frac{3}{2}} \sqrt{\frac{\rho}{\eta_b}}$$

Equation 2.12 relation between the surface tension gradient, the velocity gradient and the relative expansion rate.

Here r is the distance to the centre of the surface, ρ and η are respectively the density and the bulk viscosity and $\left[\frac{d \ln A}{dt} \right]_0$ is the relative rate of expansion of a pure water surface. Now only certain combinations of surface tension, surface tension gradient, and relative rate of expansion are possible for a certain situation at the surface of an overflowing cylinder. Bergink-Martens (¹) determined the relations between the mean surface tension gradient calculated from the centre to 1.5 cm from the centre for different solutions of Teepol (a nonionic soap) and other surface active species. A relationship between the surface tension gradient and the relative expansion rate as shown in figure 2.6 was found. Hence in the overflowing cylinder, a certain mean surface tension gradient generates a certain relative rate of expansion.

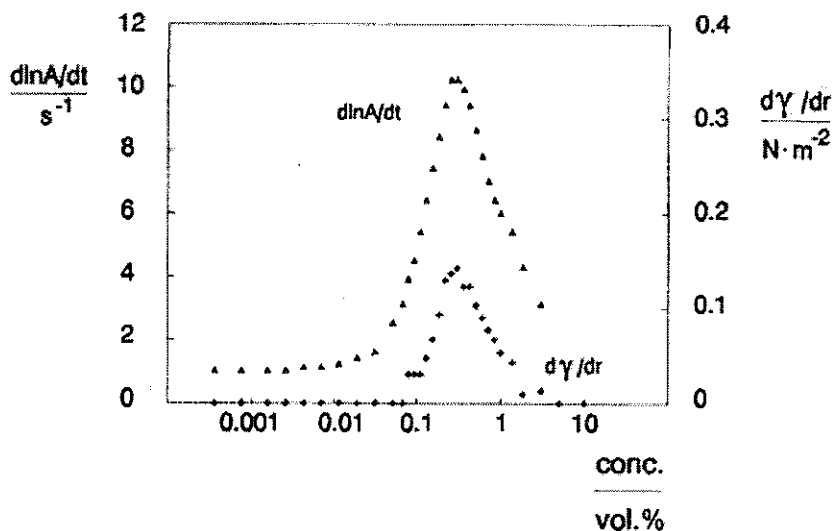


Figure 2. 6 The relation between the relative expansion rate and the surface tension gradient for different volume fractions of Teepol, an industrial type surfactant.

2.3.6 The influence of transport: the surface Fourier number

For both proteins and low molecular surfactants transport of molecules to the surface play an important role in the actual lowering of surface tension and probably also in the generation of a surface tension gradient. In order to establish if the transport of molecules to the surface plays a role of significance in the surface properties we need to assess if the transport is limiting for the surface concentration. In order to obtain this information we re-introduce the surface Fourier number introduced by Prins (⁹). Prins defined the surface Fourier number as:

$$Fo_s \equiv \frac{c_b^2 \pi D}{\Gamma^2 \left(\frac{d \ln A}{dt} \right)}$$

Equation 2. 13 The surface Fourier number, Prins (¹⁰).

In this equation which is based on the transfer from bulk to the surface by means of diffusion (penetration theory), c_b means bulk concentration, D is the diffusion

coefficient, Γ is surface concentration and $\frac{d \ln A}{dt}$ is the relative rate of expansion.

The surface Fourier number gives the ratio between the supply time for diffusive transport and the discharge time due to the expansion of the surface. In the case this number is around 1, every molecule transported to the surface indeed adsorbs. A higher number indicates that the transport to the surface is so high that only a fraction of the molecules transported to the surface indeed adsorbs. Hence in this case not the transport but the adsorption to the surface is limiting, the surface Fourier number increases above 1.

However we are more interested in the ratio between the fluxes than in the ratio between the times since this is better comparable to the calculations performed in this chapter. The square root of the surface Fourier number is the ratio between fluxes as shown in equation 2.14.

$$\sqrt{Fo_s} = \frac{c_b \sqrt{\frac{2D \left(\frac{d \ln A}{dt} \right)}{\pi}}}{\Gamma \left(\frac{d \ln A}{dt} \right)} = \frac{c_b}{\Gamma} \sqrt{\frac{2D}{\pi \left(\frac{d \ln A}{dt} \right)}}$$

Equation 2. 14 Fourier number in the case of convective diffusion.

2.3.7 Methods of calculation of the parameters of the model

Calculations with the model are performed as follows. Values for c_b , Γ_{max} , A_n , k_1 , k_2 , D and $\frac{d \ln A}{dt}$ at $v=0$ are chosen first. It is assumed that $\frac{d \ln A}{dt}$ varies slightly with the distance to the centre corresponding to experimentally obtained velocity profiles. The adsorbed amounts of native and unfolded molecules are obtained from the equations in appendix 2.1 (corresponding to equations 2.3 to 2.5). Beginning from the centre of the surface these equations can be used to calculate the surface concentration of native and unfolded molecules as a function of the distance to the centre. To this end the surface is divided into 100 concentric rings. We then use the surface concentrations of native and unfolded molecules to calculate the surface tension for all rings by the method described in section 2.3.4.

These calculations are performed for a set of values for $\frac{d \ln A}{dt}$ at $r=0$. We then have a relation between surface tension and relative rate of expansion just as can be obtained in the overflowing cylinder (see Chapter 3). In order to match these to experimental data the same calculations are performed for different values of Γ_{max} , A_m , k_1 , k_2 and D . The combinations of parameters are evaluated by calculating the least squares difference of the theoretical and experimental data for the relation between surface tension and relative expansion rate and surface tension and surface concentration. From these calculations we can obtain an estimate for the parameters Γ_{max} , A_m , k_1 , k_2 and D . Since all parameters have a different effect on the relations between surface tension and surface concentration on one hand and surface tension and the relative rate of expansion on the other hand, the uniqueness of the solution is guaranteed. In order to calculate the maximum relative rate of expansion obtained in an overflowing cylinder, the relative expansion rate calculated by the model can be numerically matched to equation 2.12 by adjusting the relative expansion rate so that the mechanical balance expressed by equation 2.12 is satisfied. We do that by matching the calculated surface tension gradient to equation 2.12 by means of adjusting $\frac{d \ln A}{dt}$ at $r=0$ by iteration. This finite element method is equivalent to numerically solving a differential equation for the surface tension as a function of the distance to the centre of the cylinder. We then find the surface tension, the surface tension gradient and the relative rate of expansion that would theoretically be found when we apply these conditions for c_b , Γ_{max} , A_m , k_1 , k_2 and D in the overflowing cylinder.

In order to check the validity of the model, experimental values of a low molecular surfactant were compared to predictions by the model leaving out the unfolding step and assuming the Gibbs equation and the Langmuir equation to apply for the relation between the surface concentration, bulk concentration and surface tension. In this way we can infer if the transport to the surface is predicted well by means of this model. This will show if indeed the transport takes place by means of the proposed mechanism. Subsequently the relation between surface tension and surface concentration and between surface tension and the relative rate of expansion was fitted to the model for one concentration (0.3 g/l) of β -casein by adjusting the

parameters Γ_{max} , A_m , k_1 , k_2 and D . The predictive value could be checked by comparing the values obtained by the model to experimental data. In addition the maximum relative rate of expansion was calculated by comparing the surface tension gradient predicted by means of the model as a function of concentration, with the surface tension gradient that is measured in the overflowing cylinder. In the following section we will discuss if the model indeed has predictive value, meaning that we are able to describe the behaviour of both proteins and surfactants by it.

2.4 Results and discussion.

In the previous sections a simple model was put forward which calculates the behaviour in the overflowing cylinder with respect to the unfolding and adsorption of protein molecules and mechanical properties of the surface. In order to evaluate the model with respect to its predictive capacity the behaviour was modelled for the protein β -casein, and for a surfactant, Tween 20. In order to model Tween 20 the unfolding step was taken out of the model and the adsorption kinetics were changed to Langmuir kinetics. In that case the surface tension must satisfy the Szyskowsky equation which has been adapted to expanding surfaces by Van Voorst Vader (⁵). If the behaviour could be modelled correctly for these different substances it can be assumed that the model can be used to understand both the transport kinetics and the unfolding properties. In figure 2.7 and 2.8 the relation between surface tension and relative rate of expansion and surface concentration and surface tension have been given for experimental and predicted values of β -casein using the method described in section 2.3.7.

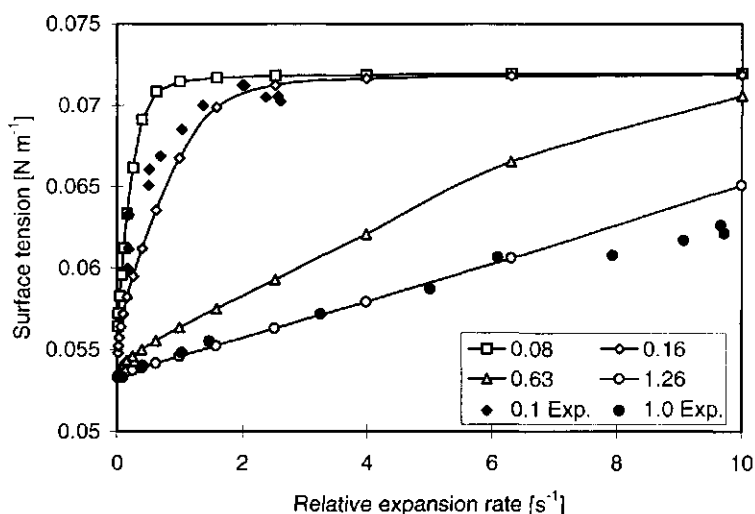


Figure 2. 7 Surface tension as a function of relative rate of expansion for β -casein. open symbols: predictions by the model, closed symbols: Experimental data. Legend indicates bulk concentrations in $[g\ l^{-1}]$ (parameters used are given in appendix 2.2).

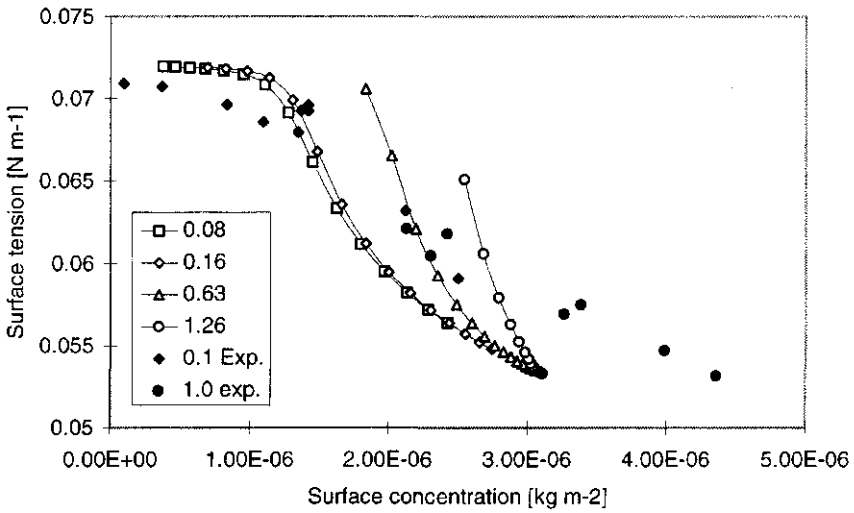


Figure 2. 8 Surface tension as a function of surface concentration for β -casein. Open symbols: predictions by the model, closed symbols: Experimental data. Legend indicates bulk concentrations in $[g\ l^{-1}]$ (parameters used are given in appendix 2.2).

In figure 2.9 predictions and experimental data for the relation between relative rate of expansion and surface tension have been given for Tween 20 as well. The experimental data were obtained by means of a technique which will be described in detail in chapter 3.

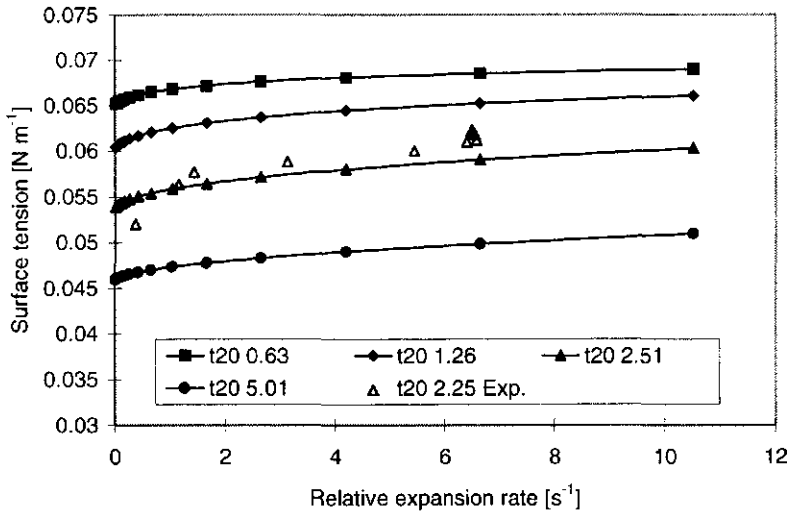


Figure 2. 9 Surface tension as a function of relative rate of expansion for Tween20. closed symbols: predictions by the model, open symbols: Experimental data, Legend indicates bulk concentration of Tween 20 in mM. (parameters used are given in appendix 2.2).

It can be observed that for β -casein the relation between surface tension and relative rate of expansion determined by experiments are fitted better than the relation between surface tension and surface concentration. Part of this can be ascribed to the limited accuracy of the surface concentration data of which the standard deviation is in the order of 0.25 mg m^{-2} . We can conclude from these graphs however that the model is able to predict the trends in the adsorption behaviour for both surface active species which means that the model indeed has the ability to predict data obtained experimentally. This means that it is possible to compare various surface active species with respect to their surface behaviour and trace this behaviour back to the adsorption or unfolding kinetics.

Here we will restrict ourselves to the comparison of four surface active species which perform differently in the overflowing cylinder: Sodium dodecyl sulphate (SDS), Tween 20, β -lactoglobulin and β -casein. These species were first measured by means of the technique described in chapter 3, and subsequently fitted by the model yielding the essential constants for the description by means of the model. In appendix 2.2 the constants used for fitting the data to the model have been given for these substances.

2.4.1 Model calculations: effect of diffusion coefficient and unfolding parameters.

In order to quantify the effect of transport and unfolding on the total behaviour of proteins, model calculations were carried out using the parameters for β -casein as a starting point. The effect of transport only can be modelled by varying the diffusion constant. In figure 2.10 the relation between relative rate of expansion and surface tension has been given for β -casein at a constant concentration of $0.3 \text{ [g l}^{-1}\text{]}$ assuming different diffusion coefficients (varying between 0.13 to 8 times the diffusion coefficient used in the model). It is immediately visible from this graph that surface tension depends strongly on the diffusion coefficient indicating that transport plays an essential role in the variation of surface tension with time scale. In contrast, the relation between surface tension and surface concentration (not shown) was hardly affected by the diffusion coefficient. This is a logical consequence of the fact that the diffusion coefficient has no influence on the processes taking place at the surface.

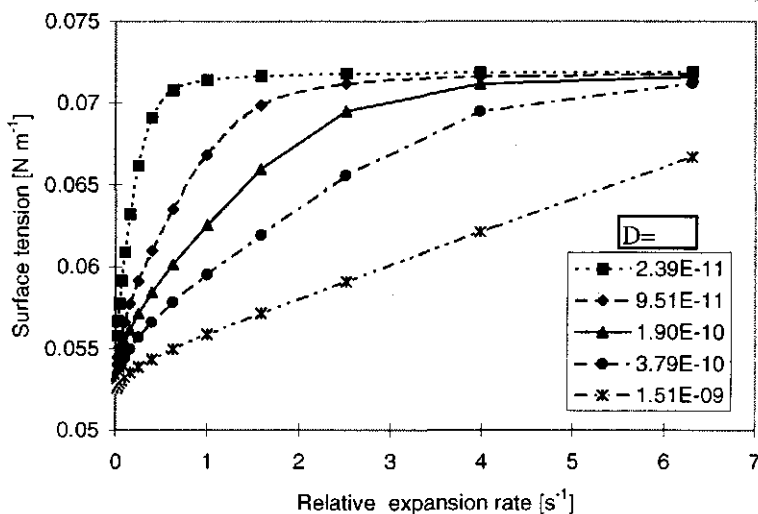


Figure 2.10 Relation between surface tension and relative expansion rate modelled for β -casein $0.3 \text{ [g l}^{-1}\text{]}$. Legend indicates values for diffusion coefficient (other parameters given in appendix 2.2).

In order to quantify the effect of the time scale of the unfolding and refolding, the surface tension as a function of relative rate of expansion was calculated again assuming a concentration of $0.3 \text{ [g l}^{-1}\text{]}$. The rate of unfolding k_1 and refolding k_2 were

multiplied by a factor m , which was varied from 0.13 to 8 (the same as for the diffusion coefficient). It was chosen to multiply both the parameters because in that case the equilibrium situation remains unaffected. The results of this calculation are given in figure 2.11.

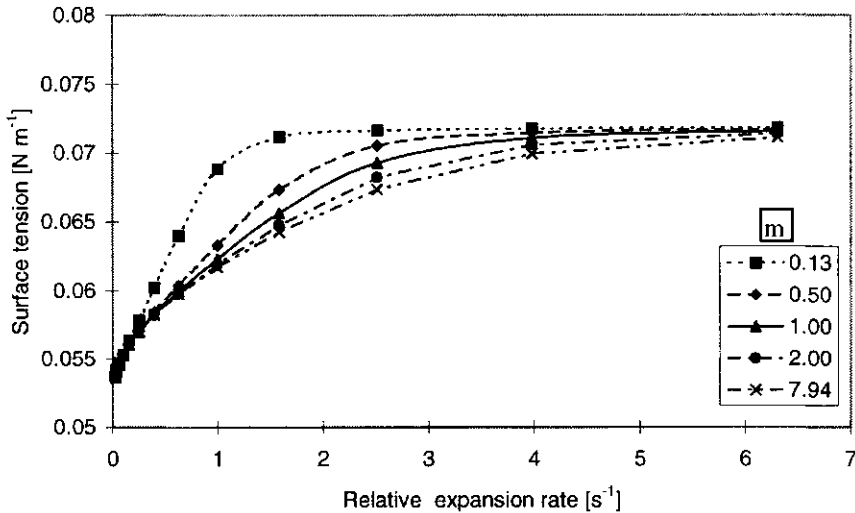


Figure 2. 11 Relation between surface tension and relative expansion rate modelled for β -casein $0.3 \text{ [g l}^{-1}\text{]}$. Legend indicates values for m by which the value k_1 and k_2 have been multiplied (other parameters given in appendix 2.2).

In order to quantify the effect on the relation between surface tension and surface concentration, also this relation was calculated using the same parameters. This relation has been given in figure 2.12.

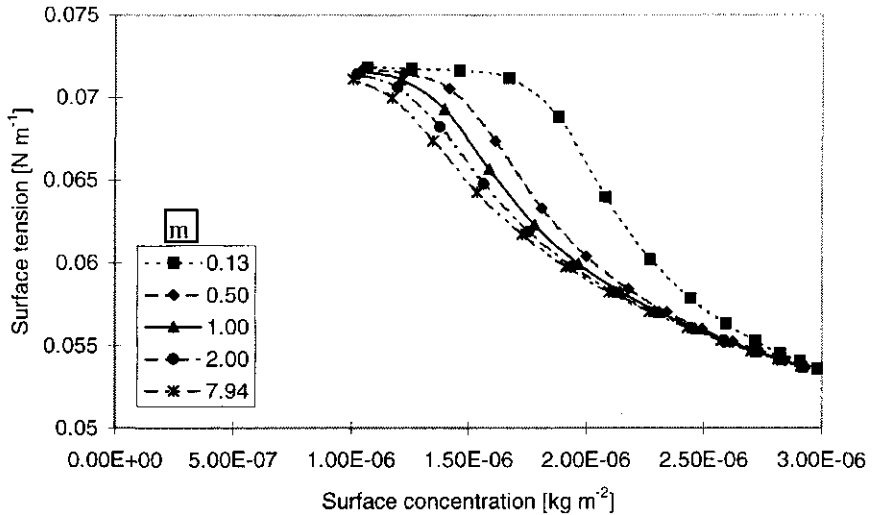


Figure 2.12 Relation between surface tension and surface concentration modelled for β -casein $0.3 \text{ [g l}^{-1}\text{]}$. Legend indicates values for m by which the value k_1 and k_2 have been multiplied (other parameters given in appendix 2.2).

The results in the previous two graphs indicate that the rate of unfolding has a significant effect on the relation between surface tension, surface concentration and relative rate of expansion. The relation between surface tension and relative rate of expansion is not so strongly affected compared to the influence of the diffusion coefficient. The relation between surface concentration and surface tension is affected however. This indicates that under these dynamic conditions, only a certain combination of a diffusion coefficient and unfolding and refolding coefficients leads to a matching description of the experimental data. Hence both transport and unfolding determine the dynamic surface properties of proteins in this model.

2.4.2 Comparison between Tween 20 and SDS

In figure 2.13 the relation between the relative rate of expansion and the surface tension has been given for different concentrations of Tween 20 and SDS.

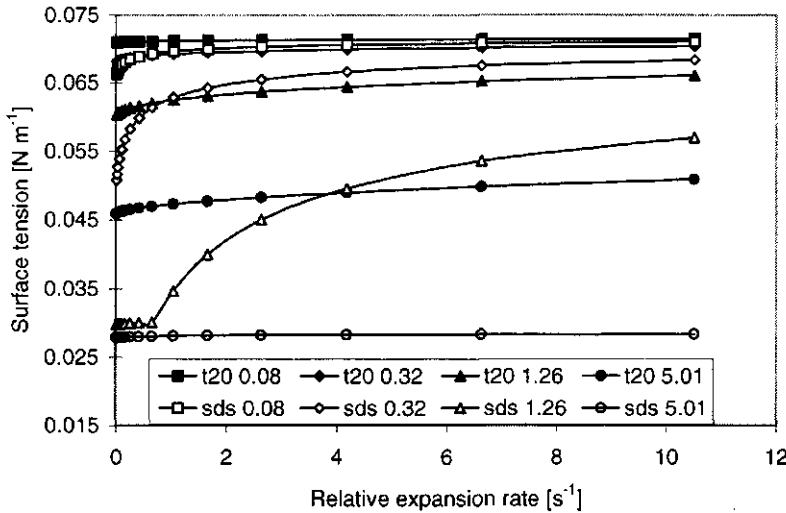


Figure 2.13 Predicted surface tension as a function of relative rate of expansion for Tween 20 and SDS. Closed symbols: Tween 20, open symbols: SDS. Legend indicates concentrations of SDS and Tween 20 in mM.

The difference between these substances is apparent immediately. The surface tension of Tween 20 is much less sensitive to variation in the relative rate of expansion than SDS. This can be explained by the relatively low maximum surface concentration of Tween 20 in comparison to SDS. The characteristic length over which surface active material must be transported to the surface $\frac{\Gamma}{c_b}$ is fairly small for Tween 20 at 1.26 mM this is in the order of $2.6 \cdot 10^{-6}$ m while for SDS this length at the same concentration and is $2 \cdot 10^{-5}$. This means that there is an order of magnitude difference in the length over which transport needs to take place between these two surfactants. With respect to the time the molecules need to be transported to the surface we can

assume that the characteristic time needed is given by $t_c^{\frac{1}{2}} = \frac{\Gamma}{c_b} \sqrt{\frac{1}{\pi D}}$. The

characteristic times for Tween 20 and SDS are 0.0018 and 0.032 seconds respectively, so also a difference of an order of magnitude. This explains that SDS requires more time than Tween 20 to reach equilibrium between bulk and surface. The effect of this difference on the mechanical properties of the surface can be seen in figure 2.14. In this figure the surface tension the square root of the surface Fourier

number and the maximum relative rate of expansion attainable in the overflowing cylinder have been given for both Tween 20 and SDS as a function of concentration of Tween 20. The method by which these calculations are performed are described in 2.3.7.

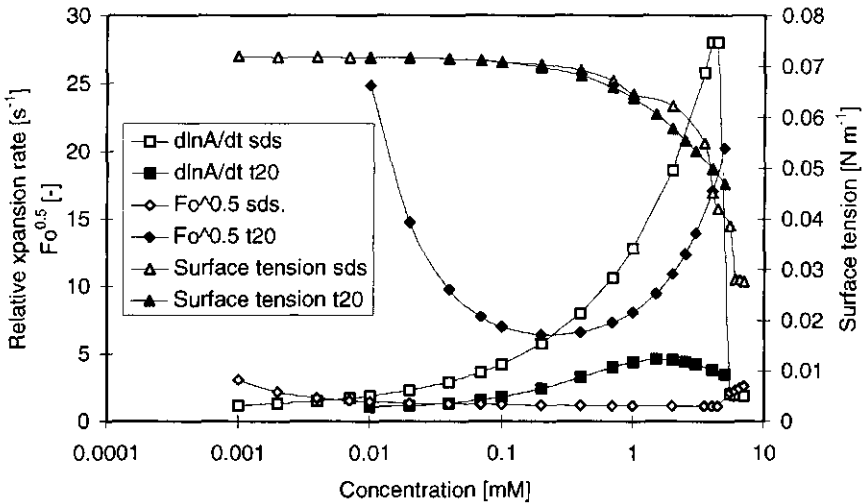


Figure 2. 14 Predicted maximum relative rate of expansion, predicted Square root of surface Fourier number and surface tension as a function of bulk concentration. Tween 20 (t20): closed symbols, SDS: open symbols.

From the square root of the surface Fourier number we can see that in all circumstances the transport is limiting for the surface tension of SDS ($Fo_s^{0.5} \approx 1$) while the transport capability in the overflowing cylinder for Tween 20 is not limiting ($Fo_s^{0.5} \gg 1$). The relative rate of expansion predicted for Tween 20 is much smaller because of this. Hence the diffusion length can be considered to be a decisive factor in the generation of a surface tension gradient for low molecular surfactants. It can be seen that in the case of Tween 20 the relative rate of expansion reaches a maximum just above the concentration at which the square root of the surface Fourier number reaches a minimum. From this it can be inferred that the limitation in transport is necessary to be able to generate a surface tension gradient. At higher concentrations a decrease in the relative rate of expansion can be observed which demonstrates that an unlimited supply of surface active material will depress the ability of a surface to generate a surface tension gradient.

There also appears to be a relation between the first derivative of surface tension to log concentration ($\frac{d\gamma}{d \log c}$) and the relative expansion rate $\frac{d \ln A}{dt}$ both in calculated as in measured data. At the point where θ reaches a maximum $\frac{d\gamma}{d \log c}$ reaches a minimum. This can be explained by the sensitivity of surface tension to both variations in the relative rate of expansion and concentration. This is because under these conditions, the adsorption of additional molecules has a large influence on the surface tension so the sensitivity of surface tension to surface concentration is high. Another striking aspect of these calculations is that for SDS a relative rate of expansion of 27 at a concentration of 4.4 mM is expected in the calculations. In experiments the maximum rate of expansion measured with the overflowing cylinder is in the order of 10 as measured by Bergink (³). The calculations however do not consider the limitations of the overflowing cylinder itself. This maximum expansion rate is due to the gravitational acceleration (g), and it may be that in foaming accelerations higher than 9.81 ms^{-2} are generated causing a higher relative expansion rate. In figure 2.15 the maximum relative rate of expansion at the overflowing cylinder surface has been given as predicted by calculations and determined in experiments with SDS.

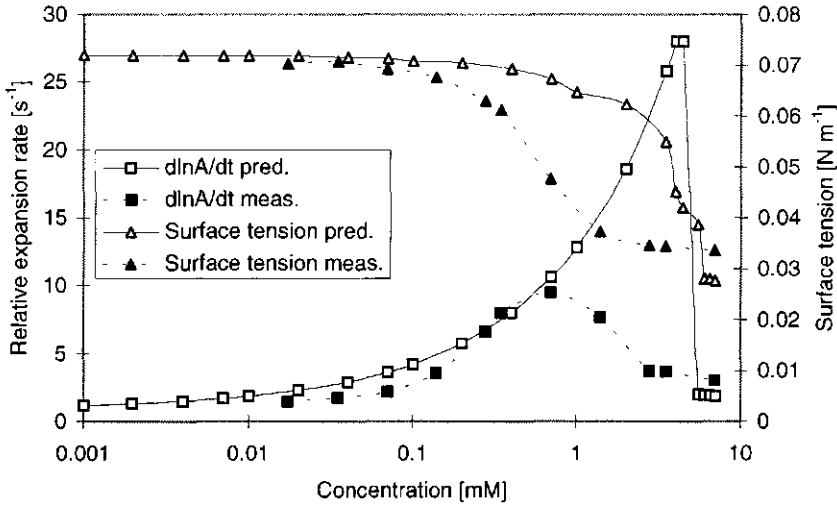


Figure 2. 15 Maximum relative rate of expansion and surface tension as a function of bulk concentration for SDS. Predicted data: open symbols, experimental data: closed symbols.

The relative expansion data are consistent with the predicted values up to a concentration of approximately 1 mM. After this concentration the calculated values show a steep rise while the measured relative expansion rates decrease. This may indicate that the overflowing cylinder itself is limiting the relative rate of expansion. This has consequences for the way the data have to be interpreted with regard to foaming properties. Bergink (³) indicated that there was a relation between foaming properties and the dynamic surface tension for Teepol. This type of surfactant also reached a relative rate of expansion in the order of 10 in the overflowing cylinder. The foamability was also observed to increase after the maximum in the relative rate of expansion was reached. It may well be that in that particular case the overflowing cylinder was the limiting factor for the relative expansion. Hence it may be that the foamability does correlate with the calculated values for these types of surfactants. Den Engelsen (¹⁰) determined the foamability for SDS with the Ross miles test and the shaking test under the same circumstances as in the experiments described here. The critical concentration found in these foaming experiments for SDS was in the order of 2 g/l after which the foamability reached a constant value. The concentration of 4.4 mM corresponds to a concentration of 1.3 g/l. This appears to be in good agreement. The concentration at which a maximum was found in the overflowing

cylinder was 0.7 mM (0.2 g/l). From this it can be inferred that the relative expansion rate measured by means of the overflowing cylinder technique correlates with foamability in this case as long as the maximum relative rate of expansion of the system is not reached. The fact that the foam height does not decrease at higher concentrations is not surprising since the amount of foam produced is a balance between making and breakdown. Breakdown of the foam takes place over time scales that are determined by other properties than the relative expansion rate in the overflowing cylinder. Also a surprising result is that the foamability was demonstrated to correlate with the surface properties in one isolated case.

2.4.2 Comparison between β -casein and β -lactoglobulin

In figure 2.16 the calculated relation between surface tension and relative rate of expansion of different concentrations of β -casein and β -lactoglobulin has been given.

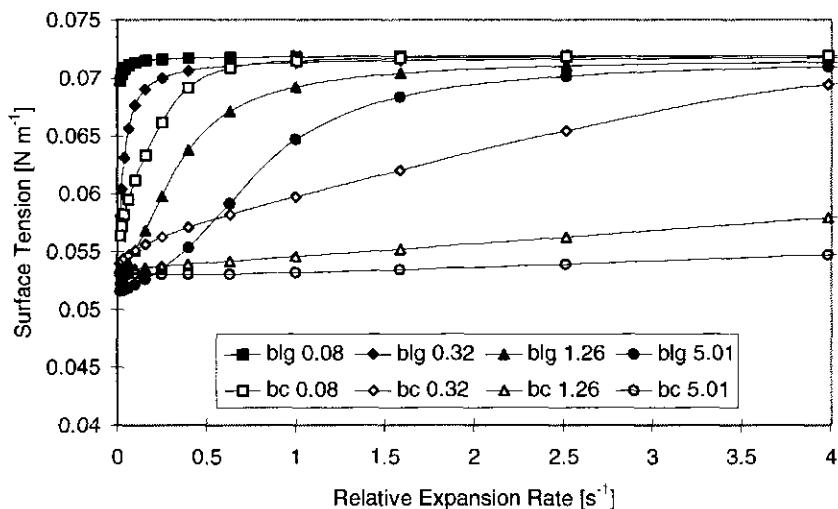


Figure 2. 16 Calculated surface tension as a function of relative rate of expansion for β -lactoglobulin and β -casein. Closed symbols: β -lactoglobulin, open symbols: β -casein. Legend indicates protein concentrations in [g l⁻¹].

Essentially a similar difference as in figure 2.13 can be observed. Although the surface tension is relatively low for high concentrations of β -lactoglobulin, at higher relative rates of expansion the surface tension goes to 72 mN m⁻¹. For β -casein the surface tension can decrease much more at equal concentrations (in g l⁻¹) although the

molecular weight is in the same order of magnitude. This is a consequence of the unfolding behaviour of these proteins since the transport to the surface can be expected to be in the same order of magnitude. The consequence of this on the calculated mechanical behaviour of the surface can be observed in figure 2.17.

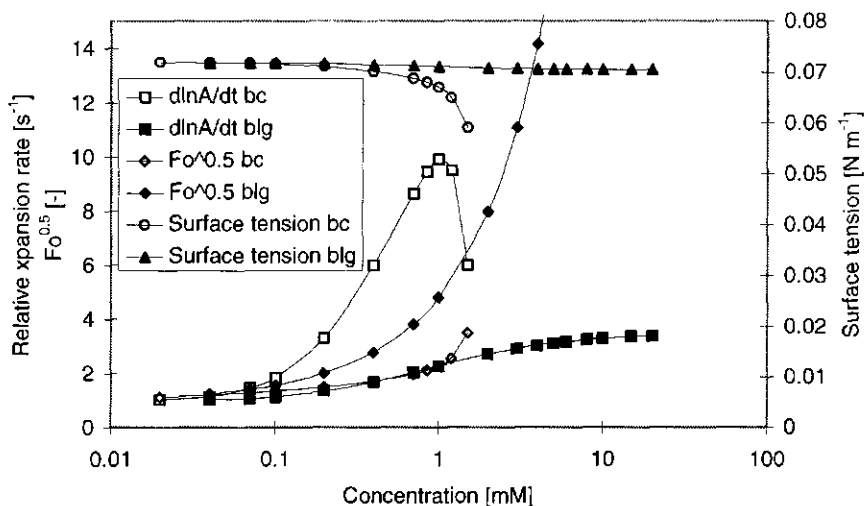


Figure 2. 17 Predicted maximum relative rate of expansion, predicted surface Fourier number and predicted surface tension as a function of bulk concentration. β -lactoglobulin: closed symbols, β -casein: open symbols.

In this figure the relative rate of expansion, the surface Fourier number and the surface tension has been given for β -casein and β -lactoglobulin. Here we can see that β -casein is capable of creating a much larger relative rate of expansion at the surface of the overflowing cylinder. There is a striking correlation between the unfolding constant of the proteins (4 s^{-1} for β -lactoglobulin and 10 s^{-1} for β -casein) and the maximum relative rate of expansion that can be reached in the overflowing cylinder over the whole concentration range. The square root of the surface Fourier number is in the order of 1 for β -casein at low concentrations. This demonstrates that practically all the proteins transported to the surface will adsorb. At higher concentrations (around 1 g l^{-1}) the square root of the Fourier number increases indicating that the transport is no longer limiting the relative expansion rate. In that case the relative rate of expansion is limited by the unfolding rate of the protein. This demonstrates that

with β -casein both the transport to the surface and the unfolding rate can be limiting for the relative expansion rate.

Essentially the same can be observed in the case of β -lactoglobulin. There the square root of the Fourier number can be observed to increase to values far above 1 around concentrations above 0.1 g l^{-1} . In that case the transport is not limiting. Yet the relative rate of expansion does not increase above 4. This tells us that the unfolding of the β -lactoglobulin limits the relative rate of expansion above concentrations above 0.1, so a much lower concentration than found for β -casein. This indicates that the rate of unfolding at the surface of the protein will determine the maximum relative rate of expansion of a surface that can be reached by a protein.

Since the relative expansion rate correlates to the surface tension gradient, the same observations apply for the surface tension gradient. When the behaviour of the proteins and the surfactants are compared we can observe that different mechanisms can limit the generation of surface tension gradients. For Tween 20 it was concluded that the relatively small diffusion length is limiting. In other words the relaxation to equilibrium of Tween 20 is too fast to create a high surface tension gradient. For the proteins however the rate of unfolding determines the maximum surface tension gradient that can be generated.

2.5 Conclusions

In general we can observe that by means of this model it is possible to pinpoint what factors are responsible for a certain behaviour at the surface of an overflowing cylinder both in the presence and the absence of surfactants in the liquid. We have observed that in the presence of surfactants different factors affect the generation of a surface tension gradient in expansion which causes the variations in the relative rates of expansion at the surface of an overflowing cylinder. In the presence of surfactants we can observe that when the relaxation at the surface is fast, indicated by large values of the surface Fourier number, the relative rate of expansion is lower than at lower supply rates of surfactant to the surface. The overflowing cylinder is a good method to measure these variations in surface behaviour although the surface tension gradient that can be generated by the overflowing cylinder can also be limiting (due to the gravitational acceleration) which leads to an underestimation of the maximum relative rate of expansion that can be generated as observed in the case of SDS. This may be the cause of the apparent absence of a correlation between the foaming properties and the behaviour in the overflowing cylinder as described by Bergink-Martens (³). Moreover it has been observed that there can be another cause for limitation of the relative rate of expansion of the overflowing cylinder which is observed in the case of the protein β -lactoglobulin. Here the lower unfolding rate of the protein is the cause of a lower relative rate of expansion. This demonstrates that the model can distinguish between these different causes for a limitation in the relative rate of expansion. This makes the model in combination with the overflowing cylinder technique a powerful tool to understand the exact causes of observed surface behaviour at expanding surfaces.

Appendix 2.1

$$\Gamma_n^n = \frac{A - A \frac{1}{\Gamma_{\max}^n} \frac{\pi r_{n-1}^2 \theta \Gamma_{n-1}^n}{B} + \pi r_{n-1}^2 \theta \Gamma_{n-1}^n + \frac{\pi (r_n^2 - r_{n-1}^2) k_1 \pi r_{n-1}^2 \theta \Gamma_{n-1}^n}{B} + \frac{(\pi (r_n^2 - r_{n-1}^2) k_1)^2}{B}}{A \frac{1}{\Gamma_{\max}^n} \frac{\pi (r_n^2 - r_{n-1}^2) k_1}{B} + B}$$

With $A = \pi (r_n^2 - r_{n-1}^2) c_b \sqrt{2 \frac{d \ln A}{dt} D}$

With $B = \pi r_n^2 \frac{d \ln A}{dt} + \pi (r_n^2 - r_{n-1}^2) k_2$

Appendix 2.1 Expression used for the calculation of Γ_n^n for an arbitrary ringnumber n.

Appendix 2.2 Constants used in the calculations

Properties	values	values	unit
	Tween 20	SDS	
Molar Mass:	1230	288.4	[g mol ⁻¹]
Γ_{\max}	$6 \cdot 10^{-6}$	$3.8 \cdot 10^{-5}$	[mol m ⁻²]
Langmuir Constant	170	120	[mol m ⁻³]
γ_{cmc}	$4 \cdot 10^{-2}$	$3.75 \cdot 10^{-2}$	[N m ⁻¹]
c_{cmc}	$4.5 \cdot 10^{-2}$	$3.2 \cdot 10^{-3}$	[mol m ⁻³]
Diffusion Coefficient	$4 \cdot 10^{-9}$	$2.2 \cdot 10^{-9}$	[m ² s ⁻¹]
$dy/dlnc$	$1.92 \cdot 10^{-3}$	$3.07 \cdot 10^{-3}$	[N m ⁻¹]

Properties of Tween 20 and SDS used for the calculations in the model.

Properties	values	values	unit
	β -casein	β -lactoglobulin	
Molar Mass:	18300	17500	[g mol ⁻¹]
π^* (eqn 2.7)	14.8	18.7	[mN m ⁻¹]
Ω^* (eqn 2.7)	0.59	2.15	[nm ²]
β (eqn 2.7)	25.6	18.9	[mN ⁻¹]
Ω_0 (eqn 2.7)	1.14	0.847	[m ² mg ⁻¹]
Γ_{\max}	$5 \cdot 10^{-6}$	$4.8 \cdot 10^{-6}$	[kg m ⁻²]
Diffusion Coefficient	$2 \cdot 10^{-10}$	$3.2 \cdot 10^{-10}$	[m ² s ⁻¹]
k_1	8.5	4	[s ⁻¹]
k_2	4	6	[s ⁻¹]
A_0	1	2.3	[-]
A_1	1.3	1	[-]

Properties of β -casein and β -lactoglobulin used in the model.

Chapter 3

Adsorption of proteins at liquid interface under continuous steady state dilation: Experiments

3.1 Abstract

The characteristic properties of the overflowing cylinder surface, namely the surface tension, the surface concentration and the relative rate of expansion, are determined by means of respectively the Wilhelmy plate technique, ellipsometry and differential laser Doppler anemometry. This new combination of techniques enables a relatively complete characterization of the dynamic surface properties in terms of unfolding and transport to the surface. These measurements enable us to put the model presented in chapter 2 into perspective. The unfolding rate of different proteins studied is found to increase in the following order lysozyme < BSA < β -lactoglobulin < β -casein. The transport plays a role especially at low concentrations of the proteins.

Also the working mechanism of the overflowing cylinder under the conditions used, is considered in this chapter. It is found that the hydrodynamic properties of the falling film are crucial for the working mechanism of the overflowing cylinder technique. The length of the falling film is demonstrated to be the parameter which determines the potential variation of surface tension over the falling film. The variation of surface tension over the falling film is caused by the viscous drag of the falling liquid at the film surface. With proteins a relatively large part of the drag is transferred in comparison to low molecular surfactants. The difference in behaviour of proteins and low molecular surfactants in this respect can be ascribed to the difference in surface behaviour in both compression and expansion. The compression of a surface gives rise to a relatively low surface tension for proteins due to the slow relaxation of the surface. In expansion the surface tension of proteins is more sensitive to the magnitude of the relative rate of expansion. This leads to a higher surface tension in expansion for proteins than for low molecular surfactants. These results indicate that when a surface is deformed by means of a force parallel to a

surface both the surface properties in compression and expansion play a role of significance.

3.2 Introduction

In the introduction to this thesis presented in chapter 1, the state of the art has been described with respect to the adsorption behaviour of proteins to liquid surfaces. Here, it was concluded that although extensive knowledge exists on the behaviour of adsorbed proteins under static conditions, the literature on surface behaviour of proteins far from equilibrium is less extensive.

In chapter 2 a model has been presented which enables the assessment of the influence of transport and unfolding on the surface properties of adsorbed layers of unfolding protein molecules. In the present chapter, measurements are presented which quantify these properties for a number of different proteins. Experiments presented here use a combination of existing techniques, which enables the determination of both transport properties and unfolding properties. This is done by measuring the surface tension, the surface concentration and the relative rate of expansion at an expanding liquid surface, to which proteins are adsorbing under different conditions of relative expansion rate.

The key technique which makes it possible to study these characteristic surface properties is the overflowing cylinder. This is a fairly straightforward technique in which an expanding surface is created by means of a liquid flow parallel to the surface. In the presence of surface active species this liquid flow causes a hydrodynamic stress which varies over the surface, causing either an acceleration or a deceleration of the surface with respect to the pure liquid.

In order to perform these experiments the overflowing cylinder needs to be operated in a different fashion from that in the experiments of Bergink-Martens (¹). In the experiments described there, the surface properties were determined at the maximum relative rate of expansion only. It is possible however to vary the relative rate of expansion. This provides us with the opportunity to study the surface properties under different conditions of "surface age".

The variation of the expansion rate of the overflowing cylinder is caused by the existence of a surface tension gradient. Bergink Martens et al (¹, ²). demonstrated that the surface tension gradient and the relative rate of expansion are related to each

other in the case that a surfactant solution is present in the overflowing cylinder. In general, the surface tension gradient is necessarily equal to the viscous stress. Since we are also dealing with the situation that the surface is decelerated instead of accelerated with respect to the pure liquid we also need to know the relation between the surface tension gradient and the relative rate of expansion in this situation.

In the falling film in the vicinity of the rim of the cylinder, the surface is expanded due to the falling motion of the liquid. Near the bottom of the falling film, the surface is compressed. In the presence of surface active material this causes a surface tension gradient over the falling film. The magnitude of this surface tension gradient is a measure of the sensitivity of the surface tension of the surfactant solution to expansion and compression of the surface.

This chapter is subdivided into a theoretical and an experimental part. In the theoretical part the hydrodynamics close to the top surface and in the falling film will be covered. These will subsequently be linked to the properties of the surface in terms of surface tension and surface tension gradient. In the experimental part the properties of four different proteins will be quantified in terms of the effectiveness of transport to the surface and the rate of unfolding at the surface when adsorbed.

3.3 Theory for the falling film

3.3.1 Overflowing cylinder

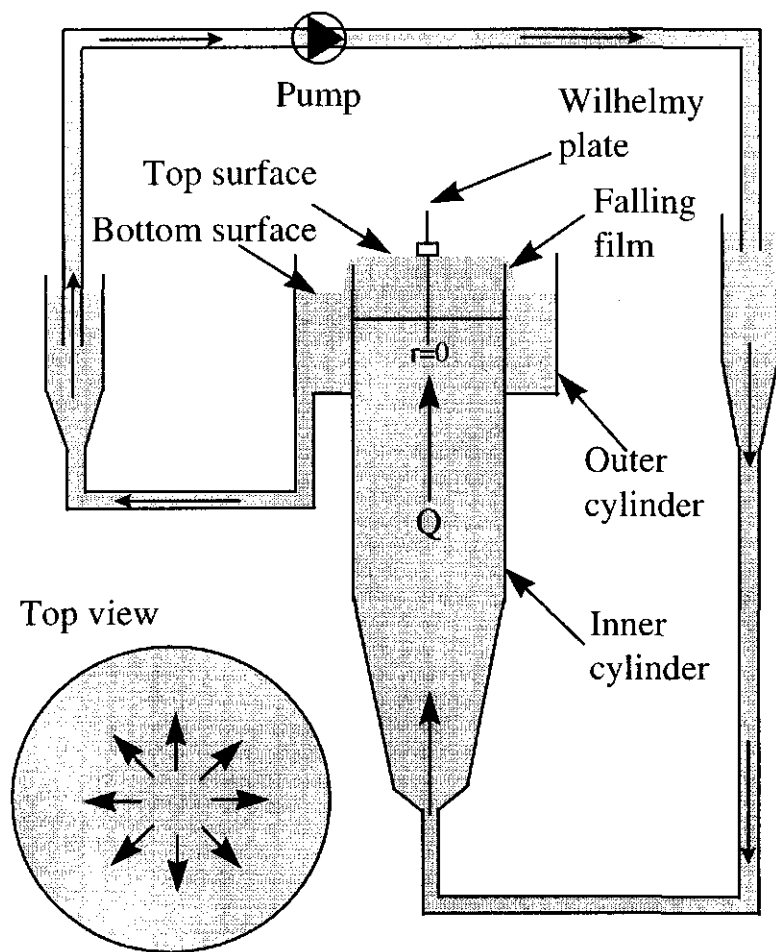
In this section a number of aspects of the operating mechanism of the overflowing cylinder technique will be treated. In section 3.3.2 the overflowing cylinder will be discussed in general terms. In section 3.3.3 the generalized flow profiles of liquid in the overflowing cylinder will be discussed for the case that the surface is accelerated and decelerated with respect to pure water. From these generalized flow profiles the stresses existing at the top surface of the overflowing cylinder can be calculated and also the thickness of the layer influenced by the flow profile can be obtained. In section 3.3.4 the height and the form of the meniscus will be discussed since information is needed about the liquid height profile at the top surface to solve the differential equations associated with the generalized flow profile. In section 3.3.5 the situation at the free falling film will be discussed. The key issue that will be addressed is how the liquid in the falling film influences the working mechanism of

the falling film. In section 3.3.6 the method used to measure surface properties will be discussed in general terms.

3.3.2 General Properties

A schematic representation of the overflowing cylinder is given in Figure 3.1 after Bergink-Martens et al (²), (³), (⁴). Here also the coordinates used throughout this chapter are given. The overflowing cylinder consists of an inner cylinder with thickness in which liquid is pumped up with a constant flow rate Q . The radius of the inner cylinder is indicated with R , the coordinate from the centre of the cylinder is indicated with r . Liquid flows over the rim of the inner cylinder into the space in between the inner and outer cylinder. This space is in hydrostatic contact with a holding vessel. Liquid is pumped out of this vessel into a vessel in contact with the inner cylinder. Due to this constant flow of liquid, a constant hydrostatic pressure difference keeps the flow constant to the flow rate throughout the system.

At the top of the inner cylinder the liquid flows over the rim and along the outside wall of the inner cylinder into the outer cylinder. The level of the liquid in the outer cylinder is at a distance h of the rim of the inner cylinder. This length h is called the falling film length. The vertical coordinate is called z .



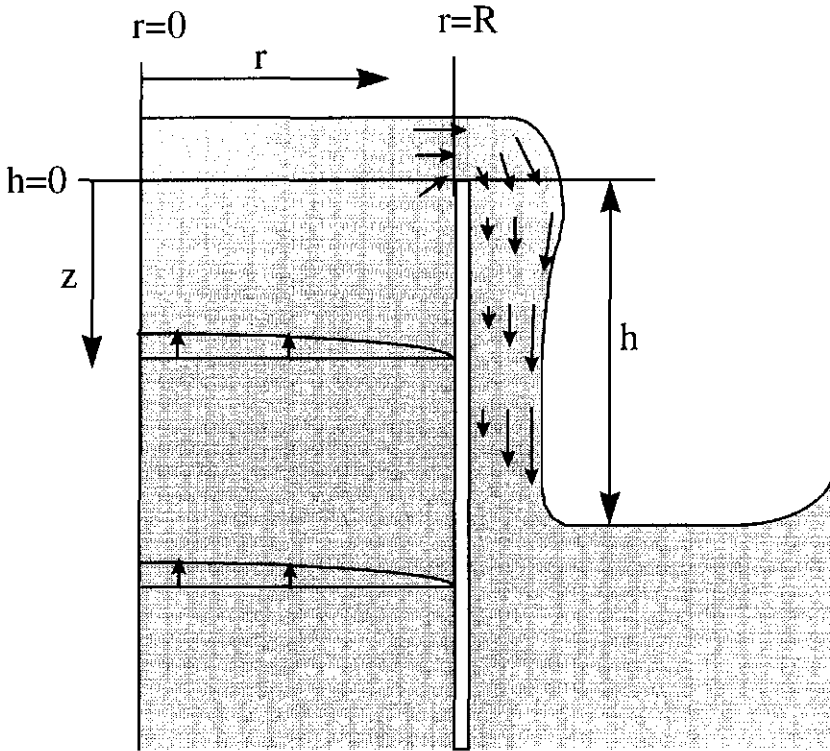


Figure 3. 1 Above a cross section of the overflowing cylinder, below an enlarged cross section of the falling film.

At the outside wall of the inner cylinder, a thin vertical liquid film is exposed to acceleration (falling) due to gravitation. Here the surface is continuously expanded. At the top surface also an expansion is found which is caused by the flow profile at the top surface. When a pure liquid such as water is present, expansion of the surface does not lead to any changes in surface tension. Hence the surface tension remains constant over the whole surface. The radial velocity of the surface is zero at the point where the axis of the cylinder intersects the liquid surface (the stagnation point where $r = 0$ and $z=0$), and increases radially in an approximately linear fashion in the vicinity of this stagnation point. A pure liquid will have a characteristic relative expansion rate $d \ln A / dt$ which depends on the flow rate, the density and the viscosity of the liquid but not on the falling height h (section 3.3.3). In the vicinity of the rim, the surface velocity increases steeply with the distance to the centre.

When a surface active species is present in the liquid, the situation is different. There the falling motion of the falling liquid in the falling film causes a local expansion which causes a surface tension gradient to develop at the free falling film. At the top of the free falling film this results in a higher surface tension than on the horizontal top surface of the overflowing cylinder. This surface tension gradient gives rise to an extra stress at the top surface, which gives rise to an extra increase in the relative rate of expansion.

When the falling film height is small however, it has been found that in the presence of different types of surface active materials, the relative rate of expansion can be lowered to values below that of water at the same falling film height. A characteristic graph showing the relative rate of expansion versus the falling film height has been shown in figure 3.2 for water, a low molecular surfactant and a protein.

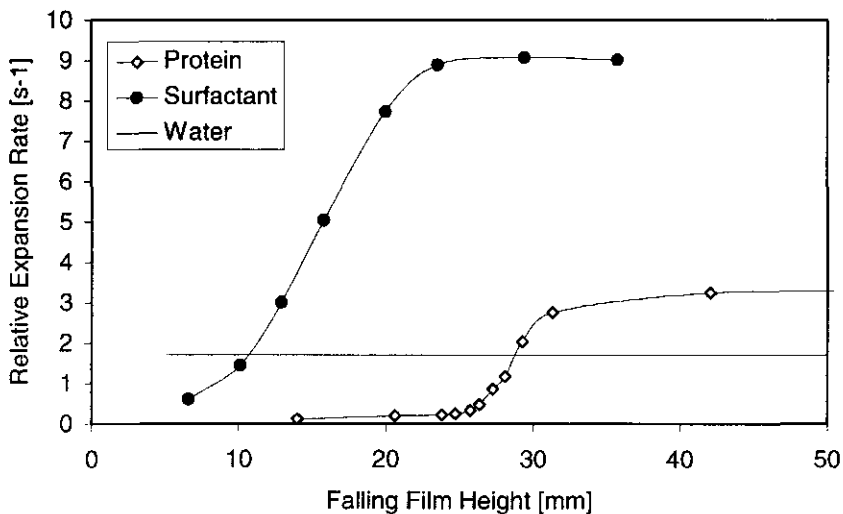


Figure 3.2 Relative rate of expansion as a function of falling film height for: water, a low molecular surfactant and a protein.

From this graph it can be seen that proteins and soaps can impede the motion of the surface, when the falling film height is decreased below a certain critical value. This means that apart from a stress in the direction away from the stagnation point a stress in the opposite direction can be present which causes a decrease in relative rate of expansion. Two possible mechanisms could be the cause of this decrease. The first

possibility is the presence of a surface tension gradient directed from the compressed surface in the space between the inner and the outer cylinder to the top surface. In this case a surface tension gradient exists over the free falling film causing the surface motion to be impeded. The other possibility is that, due to lateral bonds between the proteins, a network is created. This network which builds up from the compressed surface, can extend to the free falling film and the top surface and may impede the motion of the surface. In order to answer this crucial question, the relation between the magnitude of the stress and the relative rate of expansion was investigated in analogy with previous work of Bergink-Martens et. al. ⁽²⁾,⁽³⁾,⁽⁴⁾.

In the case of pure water, the surface expands with a certain characteristic rate of expansion. In this situation no stress is exerted on the surface since the surface tension is constant over the surface. In the case that a shear stress is imposed on the surface, which can only happen if a surfactant is present, this influences the velocity distribution at the surface. The relation between the local stress τ and the velocity gradient at the surface can be written as

$$\tau = \mu \left(\frac{du_x}{dz} \right)_{z=0}$$

Equation 3.1

Here μ means the viscosity of the bulk liquid and u_x is the velocity in the x direction. Three cases can be distinguished, in the operation of the overflowing cylinder. These three cases have been shown in figure 3.3

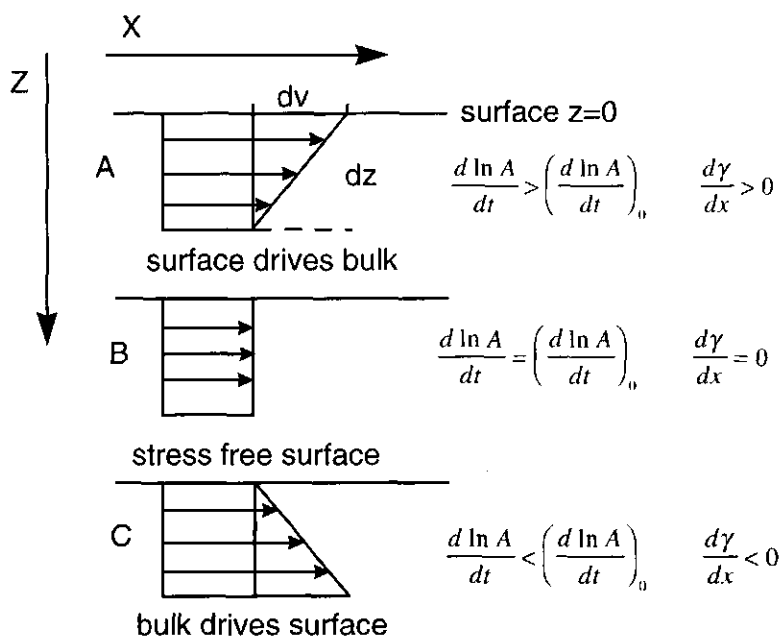


Figure 3. 3 Possible flow profiles at the overflowing cylinder surface.

In the case that the surface is accelerated with respect to pure water the situation is indicated in situation A. In this case the surface tension gradient can be considered to cause the expansion. Hence in this case τ can be considered to be equal to the surface tension gradient as given in equation 3.2. In case B the velocity gradient is zero. In that case there is no difference in velocity between the surface and the bulk phase directly underneath. This is the case for a surface at which no surface active species is adsorbed. In case C a stress of arbitrary origin is present which opposes the stress exerted by the moving liquid. The top surface is decelerated in comparison to the liquid flowing directly underneath. The surface tension gradient at the falling film in this case is negative causing a deceleration of the surface of the free falling film in comparison to the pure liquid.

$$\tau = \frac{d\gamma}{dx}$$

Equation 3. 2

The reason that the overflowing cylinder has been studied before is that the magnitude of the *dynamic surface tension* has been found to correlate with dynamic processes such as the generation of foams. The dynamic surface tension in this case is

defined as the surface tension at maximum relative rate of expansion of the top surface. Looking at figure 3.2 we can observe that different types of surface active substances cause a different behavior at the top surface of the overflowing cylinder. Our aim is to find how the overflowing cylinder operates and how the foaming behavior is correlated to this.

This chapter aims at explaining the different situations that can exist at the surface of an overflowing cylinder depending on the conditions applied. We will distinguish between different aspects of the surface. The mechanical properties expressed as a relation between the relative expansion rate and the stress of the top surface and the falling film will be discussed in sections 3.3.3 to 3.3.5. Mechanical properties are linked to the surface tension gradient and the surface tension over the surface of the overflowing cylinder. In the experimental section characteristic parameters which are measured at the surface of the overflowing cylinder will be presented.

3.3.3 Generalized flow profiles

In previous research Bergink-Martens et. al. (¹) presented a hydrodynamic description of the overflowing cylinder. This is valid in the case the surface is accelerated with respect to the case of the pure solvent. The description developed by Bos (⁵) is based on a numerical solution of the Navier-Stokes equations. These equations quantify the momentum and mass balance of a flowing liquid due to pressure gradients or local stresses. In cylindrical coordinates, these equations can be written as follows.

In equation 3.3, the mass balance has been written, in equation 3.4, the momentum balances in horizontal (coordinate r) and vertical direction (coordinate z) have been given. In these equations v means the velocity, ρ , and p respectively mean density and pressure, ν is the kinematic viscosity μ/ρ , ∇ is the Laplace operator and g is the gravitational acceleration. These equations can be solved by applying appropriate boundary conditions. In this case:

$$\frac{\partial v_r}{\partial r} + \frac{\partial v_z}{\partial z} + \frac{v_r}{r} = 0$$

Equation 3. 3

$$v_r \frac{\partial v_r}{\partial r} + v_z \frac{\partial v_r}{\partial z} = -\frac{1}{\rho} \frac{\partial p}{\partial r} + \frac{\mu}{\rho} \left(\nabla^2 v_r - \frac{v_r}{r^2} \right)$$

$$v_r \frac{\partial v_z}{\partial r} + v_z \frac{\partial v_z}{\partial z} = -\frac{1}{\rho} \frac{\partial p}{\partial r} + \frac{\mu}{\rho} \nabla^2 v_z - g$$

Equation 3. 4

R and D in equation 3.5 means the radius and thickness of the inner cylinder respectively. The first boundary condition tells us that the velocity in the r and z direction is zero at the inner and outer edge of the cylinder wall, the no slip condition. The other boundary condition tells us that in the center of the cylinder the velocity v_r at $z=0$, so at the surface, and the velocity gradient in the whole cylinder in the radial direction are zero.

$$v_r = v_z = 0 \quad \text{at} \quad r = R \wedge r = R + D$$

$$\left(v_r \right)_{r=0} \wedge \left(\frac{\partial v_z}{\partial r} \right)_{r=0} = 0.$$

Equation 3. 5

These equations are solved by assuming a constant of proportionality a between the velocity in the direction of the rim of the cylinder and the cylindrical coordinate r . This means that it is assumed that the velocity increases linearly with r and a is related to $d \ln A / dt$ in the following way:

$$\frac{d \ln A}{dt} = 2a \left[\frac{df(\eta)}{d\eta} \right]$$

Equation 3. 6

In this equation a dimensionless coordinate η is introduced, which can be written as:

$$\eta = z \sqrt{\frac{a\rho}{\mu}}$$

Equation 3. 7

Here, z is the vertical coordinate, a is the constant of proportionality in the velocity distribution and $\mu \rho^{-1}$ is the kinematic viscosity. This parameter η is related to the velocities in the r and z directions by means of a stream function $f(\eta)$ which results in the following equations for v_r and v_z .

$$v_r = a r \frac{df}{d\eta}$$

Equation 3. 8

$$v_z = -2\sqrt{av} \cdot f(\eta)$$

Equation 3. 9

The Navier-Stokes equations can be written in terms of η and by applying the appropriate boundary conditions can be solved for the different circumstances that can exist at the surface. Bergink et. al. (2)(3) demonstrated that in the case the surface is accelerated with respect to pure water (figure 3.3 situation A) the Navier-Stokes equations reduce to:

$$\left[\frac{df(\eta)}{d\eta} \right]^2 - 2f(\eta) \frac{d^2 f(\eta)}{d\eta^2} = \frac{d^3 f(\eta)}{d\eta^3}$$

Equation 3. 10

The Navier-Stokes equations were solved by means of a numerical technique by applying the following boundary conditions:

$$\left[\frac{df(\eta)}{d\eta} \right]_{\eta=0} = 1 \text{ and } f(0) = 0$$

Equation 3. 11

The solution to this equation yield the stream function $f(\eta)$ and its derivatives: $f'(\eta)$ and $f''(\eta)$. Both the stress and the thickness of the layer influenced by the acceleration

of the surface can be calculated by means of these functions. The stress τ exerted at the surface by means of the surface tension gradient can be calculated to be:

$$\tau = \frac{d\gamma}{dr} = -ra\sqrt{a\mu\rho} \left[\frac{d^2 f}{d\eta^2} \right]_{\eta=0}$$

Equation 3. 12

The thickness δ of the boundary layer can be found to be.

$$\delta = \eta_{v,=0} \cdot \frac{\sqrt{2 \frac{\mu}{\rho}}}{\sqrt{2a \left[\frac{df}{d\eta} \right]_{\eta=0}}}$$

Equation 3. 13

In the situation in figure 3.3 c, the surface is decelerated with respect to pure water; in this case a stress τ_c of up to now unknown origin, directed from the rim to the center of the cylinder is present at the surface. This stress partly compensates the pressure gradient caused by the flow of pure liquid and so causing a decrease in the relative rate of expansion. Without going into detail about the origin of this compensating stress, the magnitude of this stress can be calculated. Bos ⁽³⁾ demonstrated that because of the additional stress, an additional term appears in the non-dimensionalised differential equation yielding the following expression:

$$-\left[\frac{df(\eta)}{d\eta} \right]^2 + 2f(\eta) \frac{d^2 f(\eta)}{d\eta^2} + \frac{d^3 f(\eta)}{d\eta^3} = \frac{1}{2a^2 r \rho} \frac{dp}{dr}$$

Equation 3. 14

The left part of the equation can be considered to be a dimensionless constant we will call C, and which represents the addition of the hydrostatic pressure gradient and the unknown compensating stress. Hence the resulting expansion rate of the surface can be considered to be related to the pressure gradient caused by the combined action of the hydrostatic pressure and the unknown compensating stress in the direction of the rim of the cylinder. From previous work ⁽³⁾ we know that the total pressure varies with r as.

$$p \approx C\rho a^2 r^2$$

Equation 3. 15

Here C is an a priori unknown proportionality constant, a is the constant of proportionality of the velocity distribution at the surface (equation 3.6) and r is the distance to the center of the cylinder. As p can be written in terms of the height of the meniscus ($p = \rho g h_m$) h_m can be written as:

$$h_m \approx \frac{Ca^2 r^2}{g}$$

Equation 3. 16

In order for the surface to expand, the pressure needs to decrease with coordinate r . Therefore h_m needs to be higher in the center than at the rim of the cylinder. Since the pressure gradient is the first derivative of pressure to r , by applying equation 3.15, dp/dr can be written as follows.

$$\frac{dp}{dr} = 2C\rho a^2 r$$

Equation 3. 17

Since dp/dr is related to h_m via equations 3.16 and 3.17, C can also be written as a function of h_m as:

$$2C = \frac{2g}{a^2} \frac{h_m}{r^2}$$

Equation 3. 18

If now the variation of the height of the meniscus is determined as a function of r^2 and a^2 , the constant C , which is the right hand term in equation 3.14 can be determined. In that case equation 3.14 can be solved numerically as described by Bos (⁵). The solution again yields the stream function $f(\eta)$ and its derivatives: $f'(\eta)$ and $f''(\eta)$. By means of equations 3.12 and 3.13 respectively the stress τ_d and δ can be calculated from the solutions to this stream function.

These equations provide us with a relation between the stress at the top surface, the flow profile below the surface and the relative rate of expansion in the case the surface is either accelerated or decelerated with respect to a pure liquid.

3.3.4 The height and the form of the meniscus

The height of the meniscus and the variation of the height of the surface provides information about the absolute pressure and pressure variation over the surface respectively via the basic equation $p = \rho g h_m$. Therefore information about the height can also provide us with information about the pressure gradients necessary to cause a certain expansion rate in different circumstances.

The work of Bergink-Martens (²) has shown that the geometry of the surface is influenced by a number of different contributions. The total pressure at the surface can be considered to be caused by three contributions that must be in equilibrium. The hydrostatic pressure p_h given by $\rho g h_m$, the pressure due to the motion of the liquid p_{flow} equal to $\frac{1}{2} \rho v^2$ and the Laplace pressure p_l due to the curvature of the surface. Since the pressure in the cylinder is a constant the Laplace pressure can be written as:

$$p_l = p_h + p_{flow}$$

Equation 3. 19

In this equation p_l is the Laplace pressure, which is determined by the curvature of the surface at the rim of the cylinder. The Laplace pressure can be written as:

$$p_l = \gamma \left(\frac{1}{R_1} + \frac{1}{R_2} \right)$$

Equation 3. 20

Here p_l is the Laplace pressure γ is the surface tension, R_1 and R_2 are the radii of curvature of the surface. Bergink-Martens (¹) found that the height of the meniscus in the center of the cylinder relative to the rim of the cylinder has two contributions. One from the Laplace pressure at the rim, and one from the pressure drop generated by the flow $\Delta h_{m, flow}$:

$$h_{m, dyn} = \frac{\gamma_{dyn}}{\rho g} \left(\frac{1}{R_1} + \frac{1}{R_2} \right) + \Delta h_{m, flow}$$

Equation 3. 21

Here $h_{m\ dyn}$ means the height of the surface at surface tension γ_{dyn} . $\Delta h_{m\ flow}$ was found to be fairly constant for a certain flow rate Bergink-Martens⁽¹⁾. It was found that the radii of curvature remains constant at varying surface tensions. Hence the variation in $h_{m\ dyn}$ is mainly due to variation in the dynamic surface tension.

In figure 3.4 the relation between surface tension and the height of the meniscus above the cylinder has been plotted for two points on the surface for three different surfactant solutions.

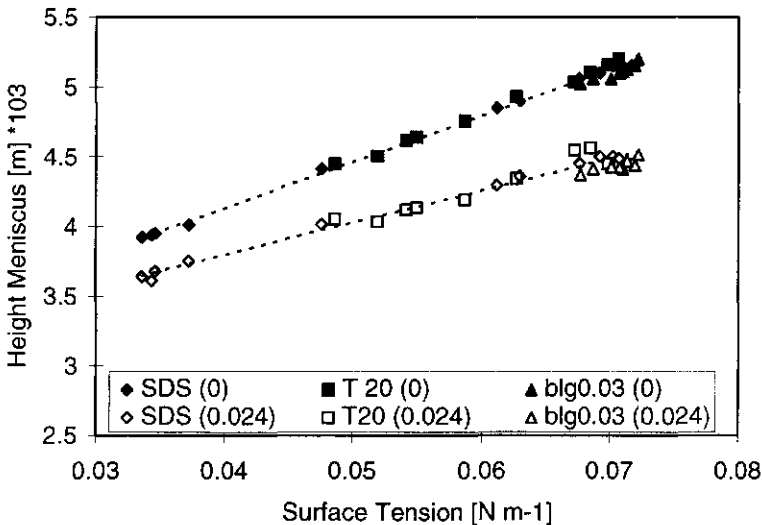


Figure 3. 4 Dynamic surface tension as a function of height of meniscus of the overflowing cylinder surface at radii 0 and 2.4 cm for SDS, Tween 20 and b-lactoglobulin 0.03 g/l.

As has been observed before by Bergink-Martens⁽¹⁾ there is a linear relation within experimental error between these parameters in both situations. Since these data have been obtained by varying length of the falling film the relative rates of expansion at equal surface tensions are different between the three systems considered. Nevertheless the relation between the height of the meniscus and the surface tension is unequivocal which means that the relative rate of expansion has no influence on the height of the meniscus.

In the case of a surface with no stress exerted on it, such as a water surface, the expansion of the surface is caused by the gradient in hydrostatic pressure: In the

center of the cylinder, the meniscus is higher than at the rim. This causes the liquid to flow to the rim of the cylinder. Hence the relative rate of expansion of the surface is due to the acceleration due to gravity.

In the case of the presence of a surface tension gradient, the surface can be accelerated with respect to the pure water surface. The extra stress imposed on the surface, only influences a thin layer on top of the surface. As the flow rate of liquid over the rim of the cylinder remains constant, the effect of the velocity increase, causes the height difference over the surface to become smaller, because part of the work performed by the pressure gradient is taken over by the tangential stress. This tangential stress is caused by the surface tension gradient. This manifests itself in a smaller height gradient over the surface. Hence the surface becomes flatter than the pure water surface.

When the surface is decelerated with respect to the pure water surface, the stress opposes the expansion of the surface. In previous paragraphs it has been demonstrated that this causes an effect in a relatively thick layer below the surface. The viscous stress imposed on the surface by means of the viscous forces of the liquid is canceled partly by the extra stress imposed by the surface layer itself which is caused by surface tension gradients or the presence of a network. This stress also causes the pressure gradient to become lower so that the meniscus flattens with respect to the pure water surface. The velocity of the liquid in the surface layer becomes lower. Concluding it can be observed that in the both cases that the surface is affected by a stress, the surface flattens, which might seem a contradiction. In the case that the surface is accelerated with respect to the pure water surface, the flattening is caused by the increase in velocity while in the case that the surface is decelerated with respect to the pure water surface, the cancellation of stress exerted by viscous forces caused by the liquid results in a lower gradient in height over the surface. The lower surface expansion rate probably has a certain effect on the absolute height since the mean velocity of liquid flowing over the rim is lower. The absolute height of the surface however is mostly determined by the surface tension at the rim. It is difficult to separate these effects from each other so it is not possible to quantify the effect of the decrease in mean velocity on the absolute height.

3.3.5 Correlation between falling height and shear stress at the surface of the falling film

In the overflowing cylinder the top surface is connected to a falling film which is, in turn, connected to the compressed surface present in between the inner and outer cylinder. The surface tensions of these parts of the surface usually differ considerably. Hence the surface tension changes over the length of the film which may affect the motion of the surface of the falling film. Already in figure 3.2 characteristic curves were shown for the dependence of $d\ln A/dt$ on the falling film length. This figure shows that the length of the falling film is a parameter which strongly influences the relative expansion rate of the top surface. Hence understanding the mechanism by which the falling film influences the top surface is useful. Here we are especially interested in the relations between the surface tension, the surface tension gradient and the relative rate of expansion at the surface of the falling film.

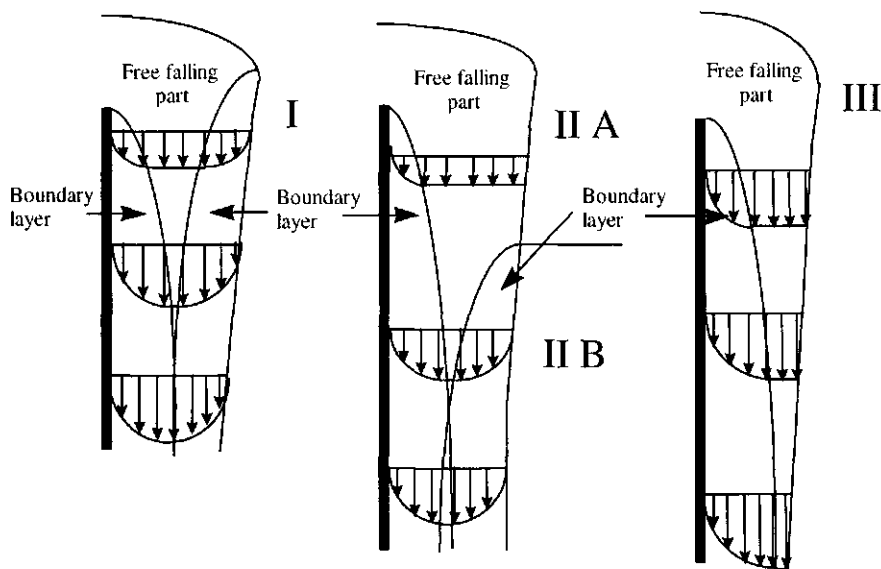


Figure 3.5 Schematic flow profiles at the surface of the falling film of the overflowing cylinder (not to scale): See figure 3.2. I the case for a small falling length, the surface is decelerated, II the case for a large falling length, the top surface is accelerated with respect to water, III the situation for a pure water surface.

Qualitatively we can interpret figure 3.2 as sketched in figure 3.5 Essentially there are three main possibilities (I, II and III).

(I): If the falling length h is small the presence of a surfactant or protein causes the surface in the falling film to decelerate with respect to the pure liquid. The surface tension difference between the top surface and the bottom surface provides a negative (upward) surface tension gradient, which causes a negative relative expansion rate. The surface tension gradient causes the motion at the falling film to be counteracted. Therefore the velocity of the surface is small at the top surface and will be almost 0 at the bottom surface.

In situation II where the film length is large, the expansion rate of the top surface is larger than that of the surface of a pure liquid and it is more complicated since there are two regions IIA and IIB in the falling film (IIA and IIB correspond to expansion and compression respectively). In the top region IIA the relative rate of expansion is positive. The velocity of the surface still increases which happens as a consequence of gravity. Consequently, the surface tension still increases (possibly to the surface tension of the pure solvent). Hence the surface tension gradient is positive as well. At

a certain distance however the velocity reaches its maximum and the situation changes to (IIB). There the surface decelerates and a situation comparable to case I is obtained.

In the case of a pure liquid the situation is as described in III, the surface initially falls down causing an increased expansion rate. During this falling motion, the film thickness becomes smaller and the boundary layer becomes thicker. At a certain point the boundary layer intersects the surface. At that point a half Poiseuille profile is developed.

In figure 3.6 the relative rate of expansion, the surface velocity and the surface tension is indicated schematically for the three cases described in figure 3.5. The coordinate s is the coordinate along the surface. The transition from the top surface to the falling film has been indicated.

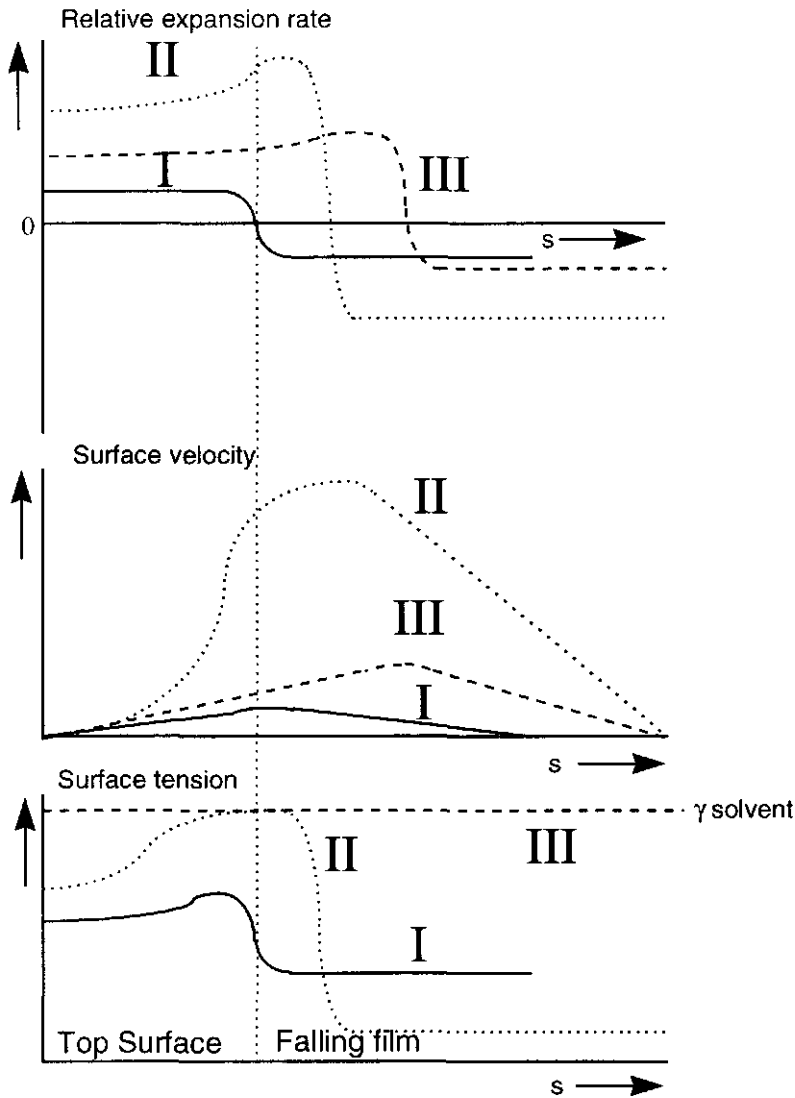


Figure 3. 6 The relative rate of expansion, the surface velocity and the surface tension as function of the coordinate s along the surface for the cases indicated in figure 3.4 ——— situation I, situation II, - - - - -situation III.

Up to now we have qualitatively described the situation in the falling film. Our interest lies in the understanding of how the surface tension affects the surface velocity and the velocity profiles in the falling film. Here three different considerations were looked at: (1) A free falling film, (2) Developing boundary layer velocity profile and (3) Fully developed boundary layer flow (Poiseuille flow).

(1): The falling film at the outside of the overflowing cylinder (fig 3.5 situation IIA and situation III) was compared to a free falling film by Bergink et. al (⁴). The surface of the falling film in the overflowing cylinder is considered to be propelled by a falling motion. In that case the velocity of the surface and the thickness of the falling film is given by:

$$v_0^z = v_0 \left(1 + \frac{2gz}{v_0^2} \right)^{\frac{1}{2}} \quad \delta^0(z) = \frac{\delta_0}{\left(1 + \frac{2gz}{v_0^2} \right)^{\frac{1}{2}}}$$

Equation 3. 22

This causes the surface to expand with an expansion rate $d \ln A / dt$ given in equation 3.23 (⁵).

$$\frac{d \ln A}{dt} = \frac{dv_0^z}{dz} = \sqrt{\frac{2g}{z}}$$

Equation 3. 23

In this equation g is the acceleration due to gravity, z is the length of the free falling film. Bisperink (⁶) gives the relation between the relative expansion rate and the surface tension gradient of a surface expanded in one direction. Modifying this for the situation at the overflowing cylinder leads to:

$$\frac{d\gamma}{dz^*} = \left(\frac{d \ln A}{dt} \right)^{\frac{3}{2}} z^* \sqrt{\mu\rho}$$

Equation 3. 24

With $z^* = z + \frac{\pi R^2}{2\pi R} = z + \frac{R}{2}$ where R is the radius of the overflowing cylinder This expression for z^* comes from the consideration that the top surface is the hinterland of the falling film and should therefore be included into the coordinate z.

(2): In essence the previous equations provide the situation for a free falling film which is hardly affected by the surface tension gradient. In the situation that the surface tension gradient does have an influence, which happens at small film lengths, (fig 3.5 situation I) but also towards the bottom of a long film (fig 3.5 situation IIB),

the situation should be reconsidered. In first approximation it will be assumed that the motion at the free surface is stopped almost completely. Hence $v_z=0$ and

$$\frac{d \ln A}{dt} = 0. \text{ In a later stage we will check if such an approximation is comparable to}$$

the real situation. In the case of a stationary film it can be assumed that a boundary layer builds up at the surface of the free falling film. Due to the falling motion, the liquid in the film is accelerated while the surface remains motionless. If the liquid in the film would be considered to perform a free fall from velocity v_0 at the rim of the cylinder, the velocity at distance z from the rim of the cylinder would be given by v_0^z in equation 3.22

The exact solution Blasius found for a laminar boundary layer for the thickness of the boundary layer δ given in equation 3.25, and the drag coefficient c_f is given in equation 3.26 Daily and Harleman (7)

$$\delta = \frac{5z}{Re_z^{1/2}} \quad \text{and} \quad Re_z = \frac{U_\infty z \rho}{\mu}$$

Equation 3. 25

In this equation Re_z is the Reynolds number for that point in the boundary layer, U_∞ , ρ and μ are respectively the velocity at infinite distance from the boundary layer at equal z , the density and the viscosity. The local drag coefficient in this case is:

$$c_f = \frac{0.664}{Re_z^{1/2}}$$

Equation 3. 26

Generally the shear stress at the surface is given by the following equation Daily and Harleman (7)

$$\tau_0 = c_f \rho \frac{U_\infty^2}{2} = 0.332 \rho \frac{U_\infty^2}{U_\infty^{1/2} z^{1/2}} \left(\frac{\mu}{\rho} \right)^{1/2}$$

Equation 3. 27

When equations 3.22 and 3.25 to 3.27 are combined and assuming the liquid in the film performs a free fall at a distance ∞ , the shear stress at the surface is given by:

$$\tau_0 = 0.332 \sqrt{\rho \mu} \frac{(\sqrt{v_0^2 + 2gz})^{\frac{3}{2}}}{\sqrt{z}}$$

Equation 3. 28

Hence from the combination of these equations it would be expected that a correlation of the falling height with the local stress imposed at the surface of the free falling film would result in a dependency on $\sqrt[3]{z}$. In this approximation it is assumed that a part of the liquid in the film performs a free fall while both surfaces of the falling film are motionless due to the no slip condition at the wall of the cylinder and the surface tension gradient at the other side.

(3): At a certain length however the part of the liquid that performs a free fall is reduced to zero as the volume of liquid influenced by the stagnant surface increases with the distance from the top of the film and also the thickness of the film decreases due to the acceleration due to gravity. In the case that the amount of liquid pumped over the rim of cylinder becomes equal to the amount of liquid flowing through both boundary layers, we can assume that a transition takes place to a complete Poiseuille profile. In this case the amount of liquid flowing through the falling film Q is related to thickness of the free falling film δ as indicated in equation 3.29 Bird Stewart and Lightfoot (⁸). In this case the situation is as described in I and IIB of figure 3.4 with the difference that a Poiseuille profile is a developed form of the boundary layer profile.

$$Q = \frac{2\rho g \left(\frac{1}{2}\delta\right)^3 (2\pi R)}{3\mu}$$

Equation 3. 29

Here ρ g and R are respectively the density, the acceleration due to gravity and the radius of the cylinder, μ and $\frac{1}{2}\delta$ are the viscosity and half the thickness of the falling film. The velocity profile of the film in this case is given by:

$$v_z = \frac{\rho g \left(\frac{1}{2}\delta\right)^2}{2\mu} \left[1 - \left(\frac{x}{\frac{1}{2}\delta}\right)^2 \right]$$

Equation 3. 30

Here x means the coordinate in horizontal direction calculated from the middle of the film. The other parameters are the same as in the previous equation. The stress on either side of the film can be calculated from the first derivative of v_z to x at the surface of the film. In this case:

$$\tau = \mu \left(\frac{dv_z}{dx} \right)_{x=0} = \rho g \frac{1}{2} \delta$$

Equation 3. 31

From equation 3.29 the thickness of the falling film can be calculated if we know Q . In that case also the stresses at the surface can be calculated. If the stresses calculated from equation 3.28 and 3.31 are equal it can be assumed that the falling film can be described by a Poiseuille profile and the stress can be assumed to be constant with respect to the film length and is given by equation 3.31.

Now we have essentially defined the circumstances which can be found at the surface of a falling film at the outside wall of the inner cylinder of the overflowing cylinder. The parameter we will use, to check the assumptions made here, is the surface tension difference between the top of the film and the bottom of the film. This parameter can be calculated by integrating the stress over the length of the falling film, taking in account the velocity of the liquid at the entrance to the falling film, the flow rate of liquid and the radius of the cylinder. Then the surface tension can be calculated as a function of the film height.

The velocity of the liquid at the entrance of the falling film was estimated to be the mean velocity at the rim of the cylinder which can be calculated by dividing the flow rate by the circumference of the cylinder and the film thickness. The flow rate is $0.138 \cdot 10^{-4} \text{ [m}^3 \text{ s}^{-1}\text{]}$. The circumference of the cylinder is 0.173 [m] . The height of the

meniscus at the rim of the cylinder is in the order of 4 mm. Hence the mean velocity at the entrance of the film can be considered to be in the order of $0.02 \text{ [m s}^{-1}\text{]}$. Performing the integration over the film height of equation 3.24 (by first substituting equation 3.23), equation 3.28 and 3.31 gives the surface tension differences for the three different circumstances of a falling film (1), developing boundary layer (2) and developed boundary layer or Poiseuille profile (3). This has been shown in figure 3.7. The values found there will later be compared to measurements performed in the overflowing cylinder (section 3.5.1.2.).

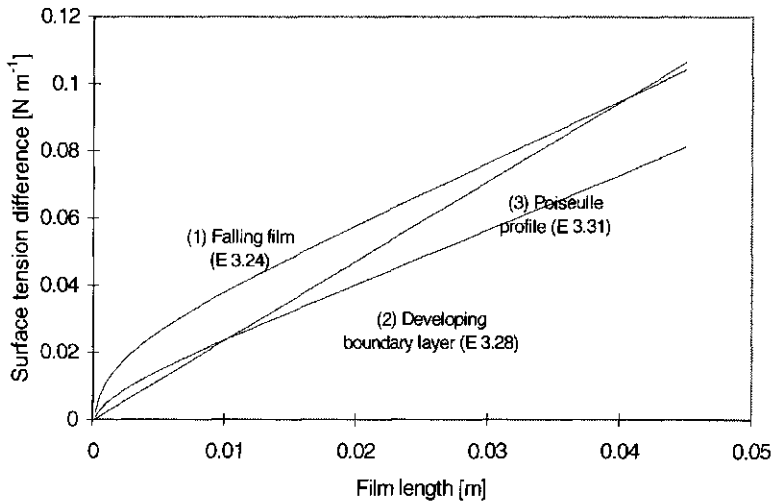


Figure 3. 7 Surface tension difference between $z=0$ and $z=h$ of the film as a function of the film length h in the overflowing cylinder for (1) a free falling film (2) a developing boundary layer and (3) a film in Poiseuille flow. Corresponding equations in text have been given between brackets.

Until now we have considered that the surface tension gradient is the cause of a deceleration of a surface. However there may be another cause for a deceleration of a surface which is the presence of a rigid bulk layer that decelerates the motion of the surface. The presence of such a rigid bulk layer will manifest itself in a deviation from the theory discussed above. In that case the surface tension difference over the falling film will be less than predicted by theory.

3.3.6 Dynamic surface properties

The overflowing cylinder technique provides a method in which dynamic surface properties of surfactant solutions can be studied. Because the surface expands at a constant relative rate of expansion in time, the adsorption of surface active species can be studied under circumstances far from equilibrium. When the surface tension is measured, a relationship can be found between surface tension and relative rate of expansion. This relationship can provide us with information about the total effect of dilation on the surface tension of the surfactant solution, but may not be conclusive with respect to the way for instance proteins are adsorbed to the surface, because there may be a time effect on the relation between the surface tension and surface concentration. Only if we assume that there is a unique relation between surface tension and surface concentration this relationship holds. If there is a situation in which molecules need a certain time to unfold before a decrease in surface tension takes place, this relation does not hold any more because the rate of unfolding is a parameter which may influence the surface tension. In order to perform conclusive experiments, information is needed about the surface concentration as a function of the relative expansion rate as well. If information would be available about surface tension and surface concentration as a function of relative rate of expansion, enough information is available to completely describe the situation existing at the surface. In that situation two sub processes; transport and unfolding can be studied separately. In this chapter dynamic surface properties are studied by means of a newly developed method. With this method the overflowing cylinder technique was combined with ellipsometry, the Wilhelmy plate technique and laser-Doppler anemometry in order to provide the required information on the surface behaviour. This technique enabled the determination of the surface concentration, the surface tension and the relative rate of expansion of an expanding surface in a steady state. With this method enough information was obtained to determine the unfolding parameters k_1 , k_2 , A_{11} and A_{12} described in the previous chapter. Here these properties were studied for four different proteins: β -casein, bovine serum albumin (BSA), β -lactoglobulin and lysozyme. The reason why these proteins have been chosen are because these proteins have been studied extensively by other authors working in the same field, and for their difference in surface behaviour. In table 3.1 a number of characteristic properties are given for these proteins.

Protein	Diffusion coefficient [m ² s ⁻²]	Iso Electric Point	Dimensions (l _x w _x h) Å	Molecular Weight [g mole ⁻¹]
β-Casein	5*10 ⁻¹⁰	5.2		24000
β-Lactoglobulin	1*10 ⁻¹⁰	5.1		18300
BSA	7*10 ⁻¹¹	4.7-4.9	116x27x27	67000
Lysozyme	1*10 ⁻¹⁰	9.2	30x30x45	14500

Table 3. 1: Characteristics of proteins used in experiments, information from various sources.

3.4 Materials and methods

3.4.1 Materials

β-Casein was obtained from Eurial ref.041091, bovine serum albumin, β-lactoglobulin and lysozyme were all obtained from Sigma and were used without further purification. Imidazole, NaCl and HCL were analytical grade and purchased from Merck and used without purification. All experiments were carried out at room temperature 23° C in the presence of 0.075 M Imidazole buffer at pH 6.7.

Solutions were made by adding concentrated solutions of buffer and protein to the liquid in the overflowing cylinder. Before measuring the liquid in the cylinder was pumped at a constant rate of 0.022 l s⁻¹ in order to ensure thorough mixing of the buffer and the protein solution with the liquid in the cylinder.

3.4.2 Methods

In order to measure surface tension, surface concentration, relative rate of expansion and falling height, two identical overflowing cylinder set-ups were used. In one of these devices, the surface tension and surface concentration were measured using the Wilhelmy-plate technique and ellipsometry respectively. In the second setup the falling height, the relative rate of expansion and the surface tension were measured using respectively a screw micrometer, differential laser Doppler anemometry and the Wilhelmy plate technique.

Ellipsometry is a technique which uses the phase shift and the amplitude ratio of parallel and perpendicularly polarized light to quantify the thickness and the

refractive index of an adsorbed layer. Two parameters Ψ and Δ are measured and can be related to the thickness and refractive index of the layer. The relations between these parameters are not straightforward and can only be calculated numerically so a computer program was used to calculate the thickness of the layer and the refractive index of the layer from measured data of Δ and Ψ . The relation between the refractive index and thickness of the adsorbed layer and the adsorbed amount is given in the following equation Benjamins and de Feyter (⁹), Mc Crackin (¹⁰).

$$\Gamma = \frac{h_l (n_l - n_0)}{a}$$

Equation 3. 32

In this equation, Γ means the surface concentration, h_l and n_l respectively mean the thickness and the refractive index of the adsorbed layer, n_0 means the refractive index of the solution and a the refractive index increment of the solution. This equation assumes that the refractive index increment is a constant, which means that the refractive index increases linearly with concentration.

The ellipsometer used for the experiments described in this chapter was an improved version of a commercial DRE-ELX1 ellipsometer obtained from Dr. Riss Ellipsometerbau GMBH, Ratzeburg, Germany. The mechanical alignment system of the incident angle of this ellipsometer was changed in order to obtain a more accurate alignment of the incident angle and a higher degree of flexibility to be able to measure close to the Brewster-angle of the solution. The ellipsometer was mounted on a translation stage in order to enable the alignment of the ellipsometer to the sample surface at the overflowing cylinder.

Measurements on the overflowing cylinder surface were performed as follows. First the incident angle of the ellipsometer with respect to the surface was adjusted so that, the light spot was exactly in the middle of the surface and the angle was sufficiently near to the Brewster angle to ensure that accurate measurements were possible. Prior to the measurements the incident light had been analyzed by the ellipsometer and stored as reference values. Then the height of the surface with respect to the ellipsometer was adjusted by means of a microscrew until maximum intensity on the detector of the ellipsometer was reached. Then a measurement was started which consisted of 50 individual measurements of Δ and Ψ . This was done by means of a

minimum search in intensity measured by a photodiode by means of a rotating polariser propelled by a stepping motor. The measured values were stored and analyzed at a later time by means of a computer program converting ellipsometric data of Δ and Ψ to thickness and refractive index of the adsorbed layer. On the second set-up measurements of surface tension, falling film height and relative rate of expansion were carried out by the Wilhelmy plate technique, screw micrometer and differential laser Doppler anemometry respectively. Laser Doppler anemometry is a technique by which the velocity of a particle in a medium or in this case on a surface, can be measured. This can be done by measuring the difference in frequency of scattered light from a particle from two coherent light beams intersecting on a probe volume. A schematic drawing of the set-up is given in figure 3.8.

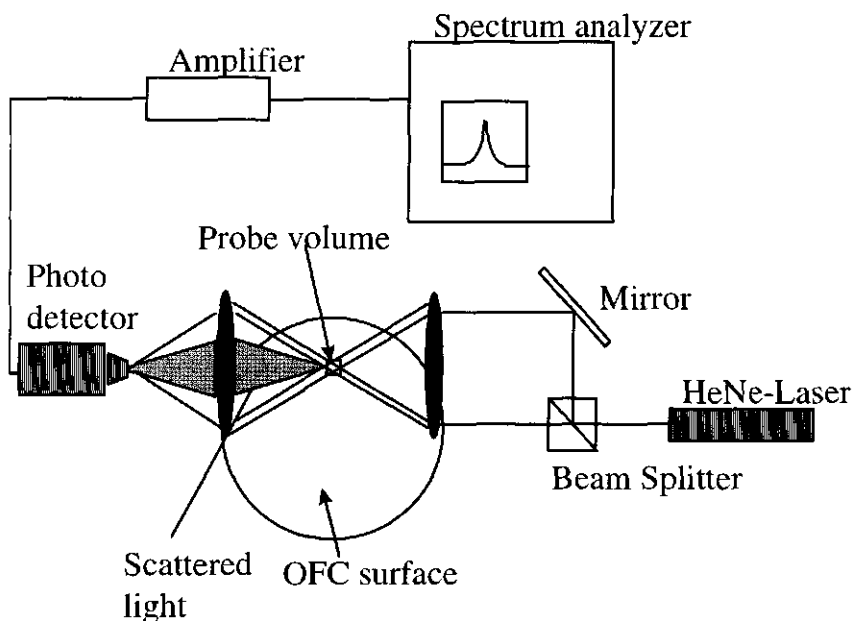


Figure 3. 8 Differential laser Doppler set-up, highly schematic.

Two coherent laser beams incident at the surface are crossed in the probe volume. Particles present on the surface are moving with velocity V_r . During the presence of the particle in the probe volume, light is scattered from the particle and focused on a photomultiplier tube by means of a lens. The light reflected directly from the surface is stopped by means of two beam stops on the lens. Since the Doppler shifts of the

scattered light of the two light beams differs, this causes a fluctuating intensity with a certain frequency to be recorded by the photomultiplier tube. This frequency satisfies the following equation:

$$f_d = \frac{2v_x \sin(\frac{1}{2}\theta)}{\lambda}$$

Equation 3. 33

In this equation, v_x is the velocity of the surface in the probe volume, θ is the angle between the light beams and λ is the wavelength of the light. The signal from the photomultiplier tube is analyzed by means of a frequency analyzer, which measures the Doppler shift f . By means of this Doppler shift, the velocity of the surface can be calculated by means of equation 3.42. A more complete description of this method can be found in (').

3.5 Results and Discussion

3.5.1 Mechanical Characteristics of adsorbed protein layers

In section 3.3 the theoretical considerations underlying the behaviour of the top surface and the falling film of the overflowing cylinder have been discussed. These theoretical considerations were necessary because the overflowing cylinder technique differs from most other techniques used in surface rheology. In chapter 1 it has already been mentioned that in the determination of surface rheological parameters two kinds of techniques are used. Most measurement techniques are techniques in which the surface is deformed in a homogeneous fashion and the response to the deformation is measured in terms of surface tension. The overflowing cylinder differs from these methods because there a liquid flow is applied to a surface and the response of the system is measured in terms of relative rate of expansion, surface tension and surface tension gradient. This causes the surface properties such as surface tension, relative rate of expansion and surface concentration to differ over the surface.

In this section we will compare the theoretical considerations to experiments performed with this technique. In section 3.5.1.1 the mechanical properties of the top surface will be discussed. There the equations given in section 3.3.3 will be solved

and the consequences for the mechanical surface properties will be evaluated. In section 3.5.1.2 the mechanical properties of the falling film will be discussed. There a comparison will be made between the equations derived in section 3.3.5 and experimental data.

3.5.1.1 The relation between deformation and viscous stress at the top surface

In sections 3.3.3 to 3.3.5 the relations between stress and deformation have been discussed for the top surface and the falling film. Here the theory provided in these sections will be applied to the overflowing cylinder. In previous sections it has already been mentioned that two different situations can exist in the overflowing cylinder: The case in which the surface expands more rapidly than in the case of the pure solvent and the case in which the surface is decelerated with respect to the pure solvent. In both cases the surface tension gradient and the viscous stress compensate each other. In the situation that the surface is accelerated Bergink-Martens et. al. (¹), (³) demonstrated that a surface tension gradient is present which accelerates the surface with respect to water. In this chapter and the following chapters such a surface tension gradient will be indicated as a *co-operative* surface tension gradient. In the situation in which the surface is decelerated with respect to water, the origin of the stress is less clear. If a surface tension gradient is present which opposes the expansion of the surface, this will be indicated as an *opposing* surface tension gradient. In the case the stress is caused by a rigidity of the adsorbed layer while the surface tension gradient does not play a significant role, this will be indicated as *surface rigidity*.

In section 3.3.3 expressions for the stream function, the thickness of the layer influenced by the surface and the stress as a function of the relative rate of expansion have been given for the top surface. If the stream function $f(\eta)$ and its derivatives can be obtained these characteristic parameters of the surface are known. For the situation in which the surface is decelerated with respect to water, parameter C (eqn 3.15 to 3.18) needs to be determined experimentally. To this end relations between the square root of the differences in height of the meniscus in the center and at 2.4 cm

from the centre have been plotted as a function of the squared relative rate of expansion in figure 3.9.

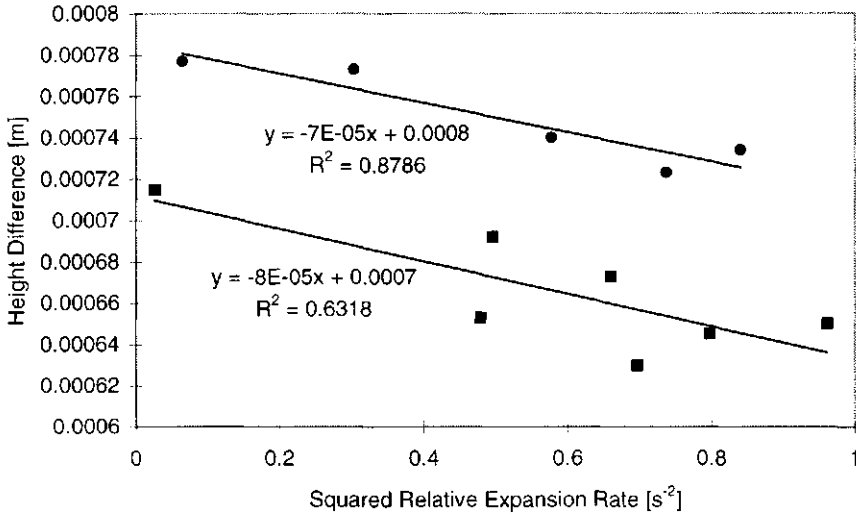


Figure 3.9 Relation between squared relative rate of expansion and difference in height of meniscus of overflowing cylinder between $r=0$ and $r=0.024$ m for two arbitrary systems. $(d \ln A / dt < (d \ln A / dt)_0)$

These values are necessary to obtain the proportionality constant C (equation 3.18) which is needed to solve equation 3.12, Bos (5) derived for the situation in which a stress is which opposes the expansion of the surface. C was determined from the

mean of the slopes which is $\frac{dh}{d\left(\frac{d \ln A}{dt}\right)^2}$ which is a constant that can be inserted in

eqn 3.18 (using 3.6 and 3.11 to relate a to $\frac{d \ln A}{dt}$) yielding a value for C in the order

of magnitude of 10. The large variation in the data is caused by the limited accuracy of the screw micrometer and the errors made in determining the relative rate of expansion. This value was used to obtain an order of magnitude for the stress caused by the surface layer. In figure 3.10 and 3.11 the solutions to the differential equation in the form of the relation between η and the stream function and it's derivatives can

be found. In figure 3.11 also the value for $\frac{dp}{dr}$ following from the value of C

(equation 3.17) has been given.

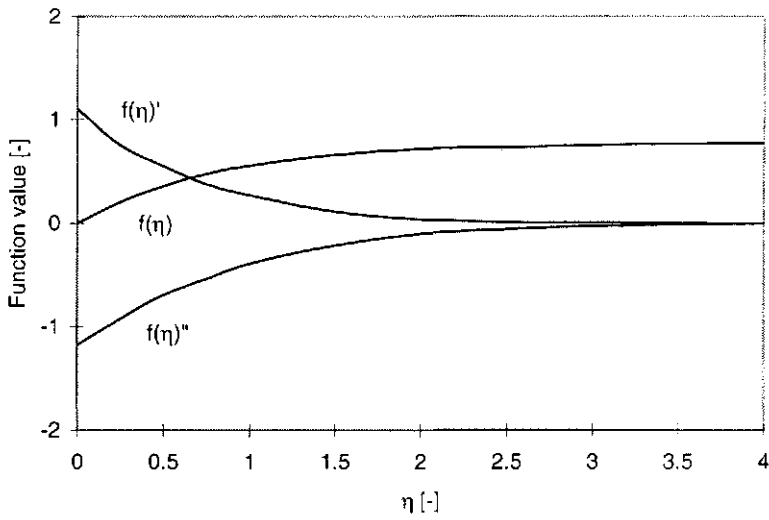


Figure 3. 10 Relation between parameter η and stream function and its derivatives $f(\eta)$, $f'(\eta)$ and $f''(\eta)$ for surface accelerated with respect to water

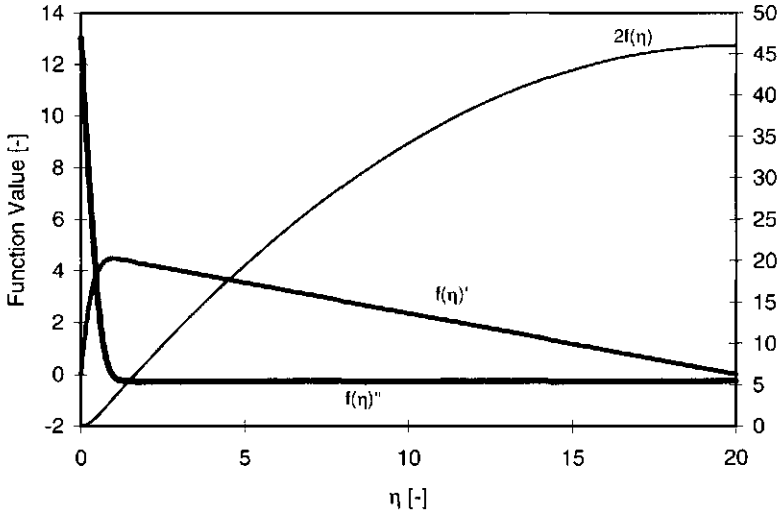


Figure 3. 11Relation between parameter η and stream function and it's derivatives $f(\eta)$, $f'(\eta)$ and $f''(\eta)$ for surface decelerated with respect to water. Arrows indicate the corresponding axis.

An important value in these curves for our purposes is the value of the second derivative at $\eta=0$, we will call S. This value is a proportionality constant between the stress at the surface and the relative expansion rate in eqn. 3.12. These values are respectively -1.17 and 13 for the surface accelerated and decelerated with respect to water and can be obtained from figure 3.10 and 3.11. Therefore (also using eqn. 3.6) equation 3.12 can be rewritten as in equation 3.34

$$\frac{d\gamma}{dr} = -S \frac{1}{2\sqrt{2}} r \sqrt{\eta} \rho \left(\frac{d \ln A}{dt} - \left(\frac{d \ln A}{dt} \right)_{solv} \right)^{\frac{2}{3}}$$

$$S = -1.17 \quad \text{if} \quad \frac{d \ln A}{dt} > \left(\frac{d \ln A}{dt} \right)_{solv}$$

$$S = 13 \quad \text{if} \quad \frac{d \ln A}{dt} < \left(\frac{d \ln A}{dt} \right)_{solv}$$

Equation 3. 34

In this equation S is a dimensionless constant, and $\left(\frac{d \ln A}{dt}\right)_{solv}$ is the relative rate of expansion of the surface in the case a pure solvent is present. This means that the stress associated with the deceleration needs to be about 10 times higher to cause the same change in $d \ln A / dt$ than the stress needed for the acceleration. Another interesting value is the point $\eta_{v_f=0}$ (the value of the stream function at which the velocity in horizontal direction becomes zero) Since $\frac{df}{d\eta}$, the first derivative of the stream function is proportional to v_x , this value can be found by requiring $\frac{df}{d\eta} = 0$.

This provides us with the proportionality constant of the thickness of the layer that is influenced by the flow pattern at the surface. These are 3 and 20 respectively for the surface accelerated and decelerated with respect to water. The equation describing the thickness of the film influenced by the expanding surface is given by equation 3.35.

$$\delta_q = \frac{T \sqrt{2 \frac{\mu}{\rho}}}{\sqrt{\frac{d \ln A}{dt}}}$$

$$T = 3 \quad \text{if} \quad \frac{d \ln A}{dt} > \left(\frac{d \ln A}{dt}\right)_{solv}$$

$$T = 20 \quad \text{if} \quad \frac{d \ln A}{dt} < \left(\frac{d \ln A}{dt}\right)_{solv}$$

Equation 3. 35

In this equation T is a dimensionless constant. This means that the layer that is influenced by the flow pattern at the top of the surface is about 7 times thicker for the decelerated surface than for the accelerated surface. In figure 3.12 the stress necessary to cause a certain expansion rate at the top surface of the overflowing cylinder has been plotted as a function of the expansion rate.

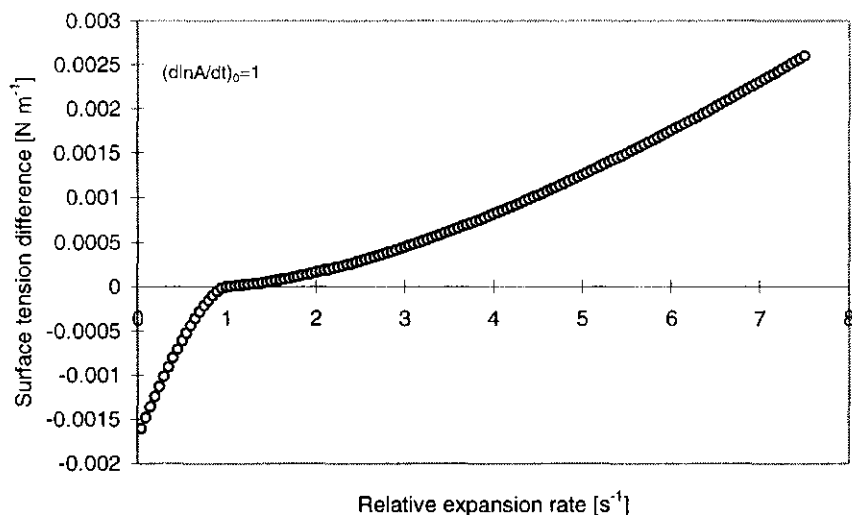


Figure 3.12 Surface tension difference between centre and rim of the cylinder calculated to be necessary to cause a certain relative rate of expansion at the top surface

This graph is a kind of master curve which indicates the surface tension difference needed to generate a certain relative rate of expansion by means of any surface active substance. In the situation that the surface is decelerated with respect to water the surface tension difference that is necessary to cause this deceleration can be seen also. In the case that the surface is decelerated with respect to the water surface it can be seen that a compensating surface tension between the center and the rim of the cylinder in the order of 1.6 mN m^{-2} is needed to reduce the expansion rate of the surface to zero. These values are relatively modest when we compare these to the stresses that can be generated at the surface of the falling film however (see section 3.3.5). This means that the falling film must play a large role in the behaviour of the overflowing cylinder as a whole.

3.5.1.2 Mechanical Properties of the Falling Film

In figure 3.13 the surface tension difference between the top surface and the bottom surface measured at the middle of the top surface and in the middle of the bottom surface has been plotted as a function of $h^{5/4}$ for various systems and various relative rates of expansion of the surface.

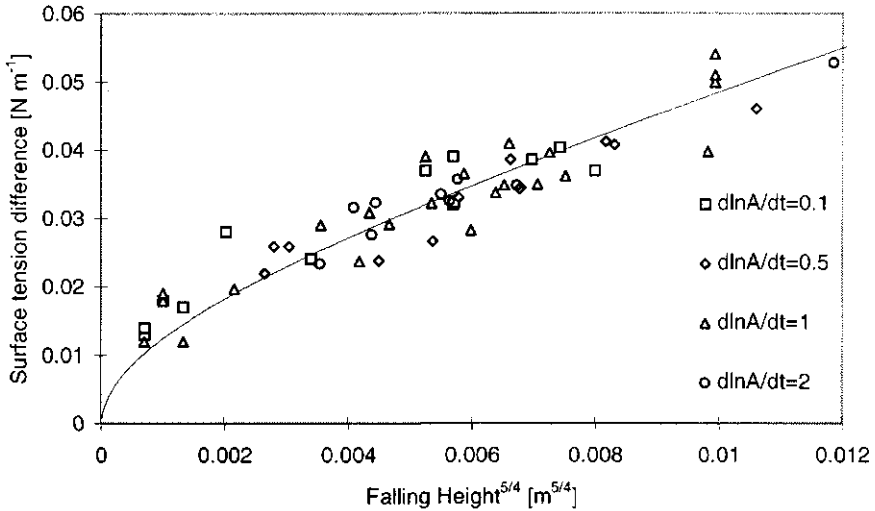


Figure 3.13. Difference in surface tension between the top and bottom surface for various systems as a function of $h^{5/4}$ for different surface active species at different relative rates of expansion. Drawn line is theoretical line obtained using flow profile for developing boundary layer eqn. 3.28.

The different lines in the graph indicate the relations between the surface tension and $h^{5/4}$ for different relative rates of expansion. In this graph the theoretical line already given in figure 3.6 for a developing boundary layer flow has been plotted as well. Points which are high up in this graph indicate that at a certain relative rate of expansion of the top surface, a high surface tension difference is created between the top and bottom of the falling film. In this graph we can see that the surface tension difference is matched almost exactly by the theoretical line.

This means that the liquid film at the outside wall of the overflowing cylinder can be approximated by a stagnant surface at relative rates of expansion of the top surface below 2 s^{-1} . This property can be used to measure the ability of a surface active material to resist the deformation of the surface by means of surface tension gradients. If the relative rate of expansion is measured as a function of film length, the film length at which a finite but small relative rate of expansion is reached at the surface, say 1 s^{-1} , can be converted into a surface tension difference between the top and bottom surface by figure 3.6. This is the surface tension gradient that will be

found between the top and bottom surface. In later chapters we will demonstrate the significance of this value for practical purposes.

The fact that the theoretical line matches so well also tells us that surface tension gradients are responsible for the deceleration of the surface and the action of a network in the case of proteins does not play a significant role unless the network should somehow manifest itself in the surface tension. As it can be expected that the building up of network structure is time dependent also experiments were carried out to investigate this time dependence by first increasing and subsequently decreasing the film length. These experiments showed that there is no significant time dependence in the relation between surface tension difference and film length. Hence by means of this method it is not possible to demonstrate the existence of stagnant bulk layers of proteins.

In order to study this for various types of surface active materials the line for $dnA/dt=1$ has been plotted for various surface active species which are indicated in Figure 3.14.

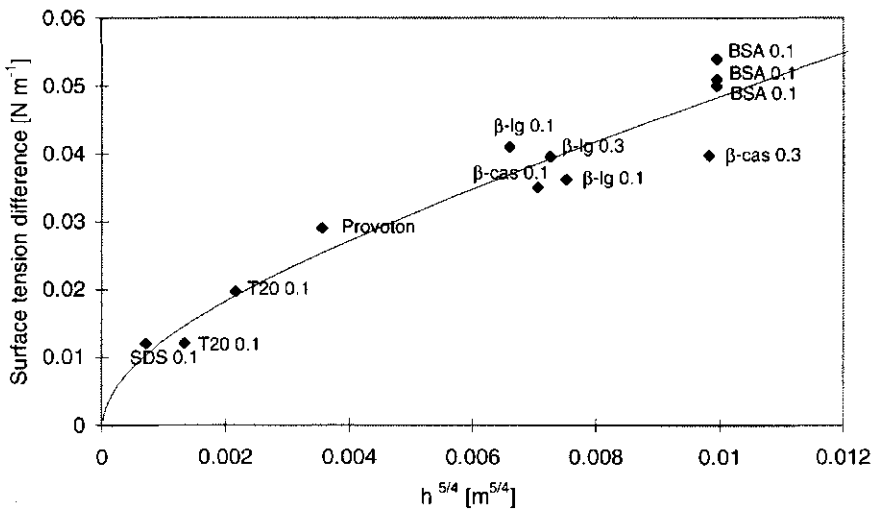


Figure 3. 14 Difference in surface tension between the top and bottom surface for various systems as a function of $h^{5/4}$ for different surface active species plotted with concentrations in $[g l^{-1}]$ at a relative rate of expansion of 1. The different systems have been indicated in the graph.

In this graph it is immediately obvious that the length at which a relative rate of expansion occur for proteins are high up in the graph while these are at the lower end for low molecular surfactants. Apparently this indicates a fundamental difference between proteins and low molecular surfactants. In order to explain this difference in response we need to clarify in more detail why such a behaviour is caused in the first place. In the centre of the top surface and at the end of the bottom surface the velocity of the surface is zero. Nevertheless there is a difference in surface tension. At the top surface and also at the top of the falling film the surface velocity grows with the distance from the centre of the surface. This means that this velocity also has to decrease again over a part of the falling film and the bottom surface. Also we have seen in section 3.5.1.1 that the constant of proportionality between the surface tension gradient and the relative rate of expansion differs by a factor 10 between the situation that the surface tension gradient opposes or promotes the expansion of the surface, due to the difference in the situation at the surface. This means that a surface tension gradient is more successful in promoting expansion than in opposing expansion. In figure 3.15 this has been shown in a schematic way for two different circumstances at the falling film.

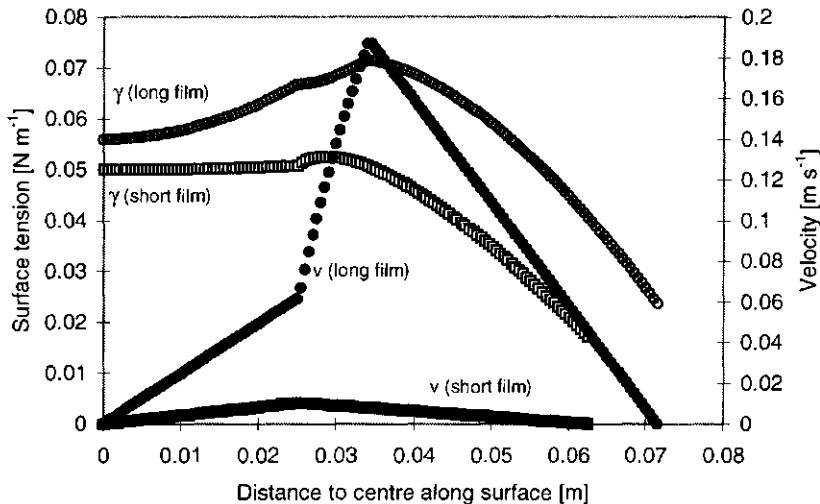


Figure 3. 15 Calculated surface tension and surface velocity as a function of the place at the surface for two different circumstances: small film length \square , large film length \circ . (Surface tension: open symbols, surface velocity: closed symbols.)

This figure illustrates that in the compressed part of the falling film (which is the part in which the surface velocity decreases), the surface tension decrease is much higher than the surface tension increase in the expanded part of the surface. Since the surface tension of the expanding surfaces do not differ too much in Generally it can be said that the surface tension difference between the bottom and the top surface will be dependent on the sensitivity of surface tension to expansion or compression and the conditions applied in the overflowing cylinder. In figure 3.16 the measured surface tension in the expanded and the compressed part of the overflowing cylinder has been given for a number of different surface active substances. BSA, β -lactoglobulin β -casein, Tween 20 and SDS (Sodium dodecyl sulphate) as a function of the relative rate of expansion of the top surface of the overflowing cylinder.

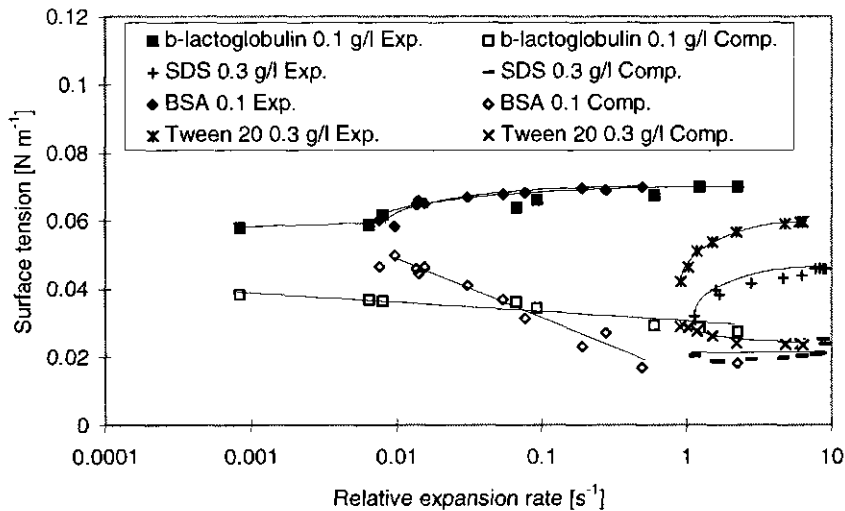


Figure 3. 16 Measured surface tension in the compressed and expanded part of the surface as a function of the relative rate of expansion of the top surface for different surface active species.

From this graph it is immediately clear that the low molecular substances SDS and Tween 20 exhibit a very different behaviour compared to the proteins. The surface tension difference between the compressed and expanded surface depends on the relative rate of expansion for both the proteins and the surfactants. This graph indicates however that the relaxation to surface tensions near equilibrium is in the order of 100 times faster for low molecular surfactants than in the case of proteins.

(the relative rate of expansion that the surface tension in expansion and compression show the tendency to move closer to each other happens at 0.01 s^{-1} for the proteins β -casein and β -lactoglobulin and 1 s^{-1} for the surfactants SDS and Tween 20) It can be seen as well that the surface tension of protein solutions go to a surface tension of 72 mNm^{-1} if the relative rate of expansion is high although these substances seem to be capable of reaching very low surface tensions when compressed which can be ascribed to the ability to accumulate at a compressed surface. Indeed a *stagnant* surface behaviour has been reported in the presence of proteins, Prins et. al.⁽¹¹⁾, Benjamins and van Voorst Vader⁽¹²⁾, Boerboom et. al.⁽¹³⁾, indicating that proteins are capable of resisting motion of the surface while low molecular surfactants are much less capable to resist these deformations. This is most likely caused by the fact that compression of a surface covered with proteins does not lead to an immediate desorption of proteins which can cause the lowering of the surface tension below the equilibrium value whereas the desorption of low molecular surfactants is much faster with low molecular surfactants. Indeed Mac Ritchie⁽¹⁴⁾ has shown that compressing surfaces with adsorbed proteins relax only very slowly to equilibrium.

3.5.2 Surface Properties of proteins

In section 3.5.1 the mechanical properties of the top surface and the falling film were discussed. In this section the surface properties of proteins measured with the overflowing cylinder technique will be discussed. In section 3.5.2.1 measurements of surface tension, surface concentration and relative rate of expansion will be presented on four distinctly different proteins obtained by the technique discussed in section 3.4. In section 3.5.2.2. the parameters obtained by means of the model in chapter 2 will be presented which quantify the relative importance of unfolding and transport of these proteins.

3.5.2.1 Surface properties of proteins: Experiments

In order to illustrate which process causes the major differences among the different proteins, in figure 3.17 the surface tension as a function of relative rate of expansion has been given for all protein solutions with bulk concentrations of 0.3 g/l .

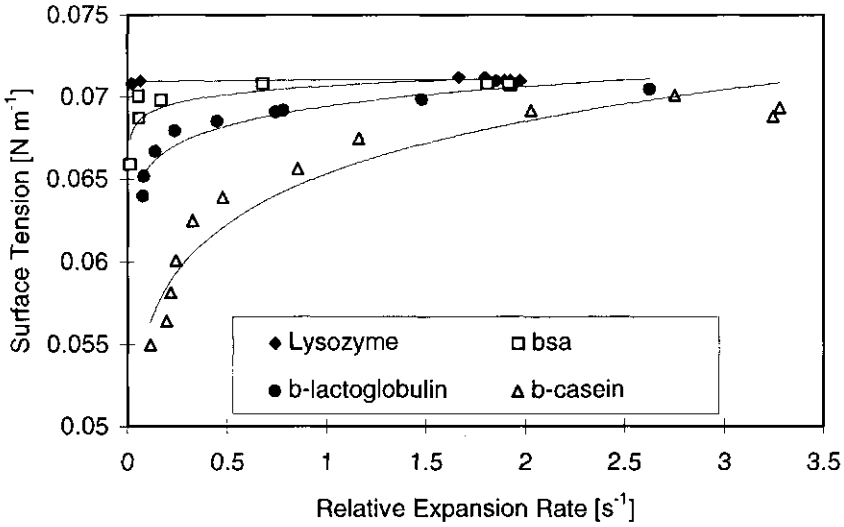


Figure 3. 17 Measured relation between surface tension and relative rate of expansion for different proteins at bulk concentrations of 0.3 g/l.

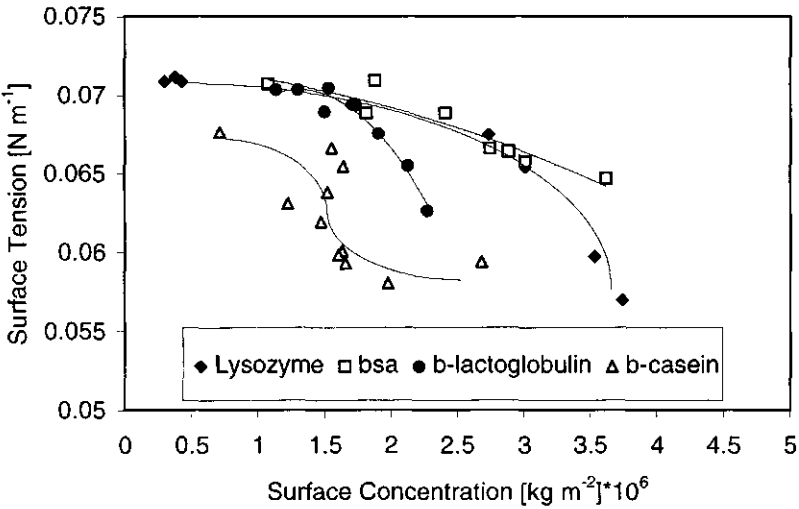


Figure 3. 18 Measured relation between surface tension and surface concentration for different proteins at bulk concentration of 0.3 g/l.

In this figure the differences between the proteins are immediately obvious. The surface tension at equal relative rate of expansion decreases in the following order for the different proteins: lysozyme, BSA, β -lactoglobulin, β -casein. This means that the capability of the proteins to lower the surface tension increases in the same order.

Whether unfolding or transport is responsible for the differences between the different proteins cannot be directly inferred from this figure. In order to clarify this, figure 3.18 presents the corresponding relations between surface concentration and surface tension for the different proteins at the same bulk concentration of 0.3 g/l. From this figure we can observe that β -casein and β -lactoglobulin require relatively low surface concentrations to lower the surface tension under dynamic circumstances and the same bulk concentrations in terms of mass. It is hard to tell directly from these curves if transport to the surface or unfolding is responsible for the difference between these proteins.

In figures 3.19, 3.21, 3.23 and 3.25 measurements of surface tension versus relative rate of expansion have been given for respectively lysozyme, BSA, β -lactoglobulin and β -casein for a number of different concentrations of these proteins. In figures 3.20, 3.22, 3.24 and 3.26 the corresponding measurements of surface tension versus surface concentration have been given for the same proteins.

Essentially the relation between surface tension and the relative rate of expansion show the time dependence of the decrease of the surface tension. The time scale of the experiment can be regarded to be the reciprocal of the relative rate of expansion. All the curves show the same type of behaviour: When the relative rate of expansion decreases the surface tension decreases also. It can be seen however that these proteins are different with respect to the time scale over which a substantial surface tension decrease takes place. Essentially two sub-processes, transport and unfolding, may be responsible for the differences observed.

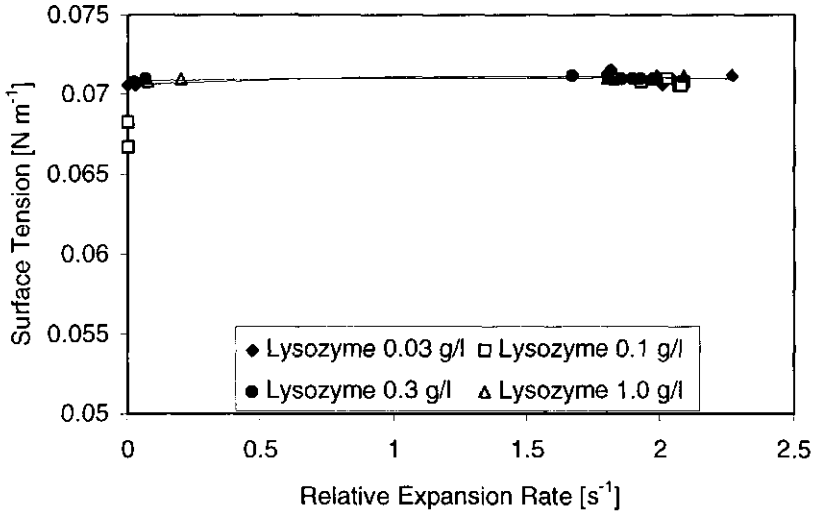


Figure 3. 19 Measured relation between surface tension and relative rate of expansion for lysozyme.

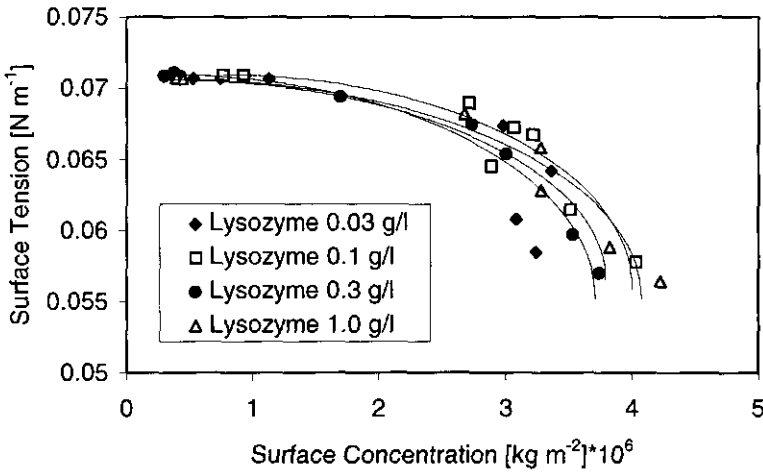


Figure 3. 20 Measured relation between surface tension and surface concentration for lysozyme.

For lysozyme, it can be observed that even at very low relative rates of expansion (below 0.1) the surface concentration belonging to the surface tension at that relative rate of expansion is still low, in comparison to the other proteins shown in the figure 3.20. This suggests that the transport of lysozyme to the surface is slow. In a paper by van Aken and Merks (¹⁵) it has been found also that the surface tension decreases only after a considerable lag time for lysozyme even if the proteins were supplied to the surface by spreading. This was ascribed to the high electrical charge of lysozyme at neutral pH. This causes the lysozyme to unfold very slowly even if the molecules are adsorbed at the surface.

In table 1 the diffusion constants have been given for the different proteins. Since these values are comparable for these proteins this indicates that the diffusion constant cannot be responsible for this difference between the molecules. Hence, there must be another cause for this behavior. Probably, the chance of adsorption of a lysozyme molecule in contact with the surface is low compared with the chance of adsorption of the other molecules. Also the surface tension decrease at surface concentrations above 1.2 mg m^{-2} is low when compared the equilibrium relation between surface tension and surface concentration for lysozyme provided in figure 3.20. Hence also the rate of unfolding is slow.

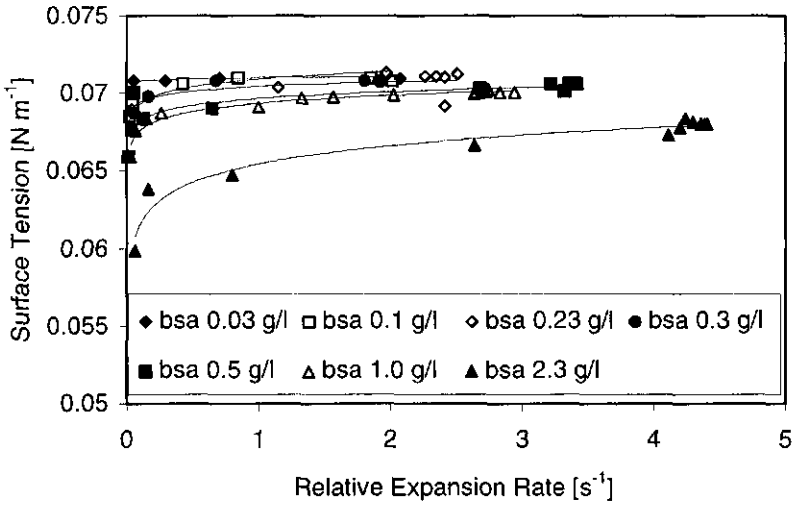


Figure 3. 21 Measured relation between surface tension and relative rate of expansion for BSA.

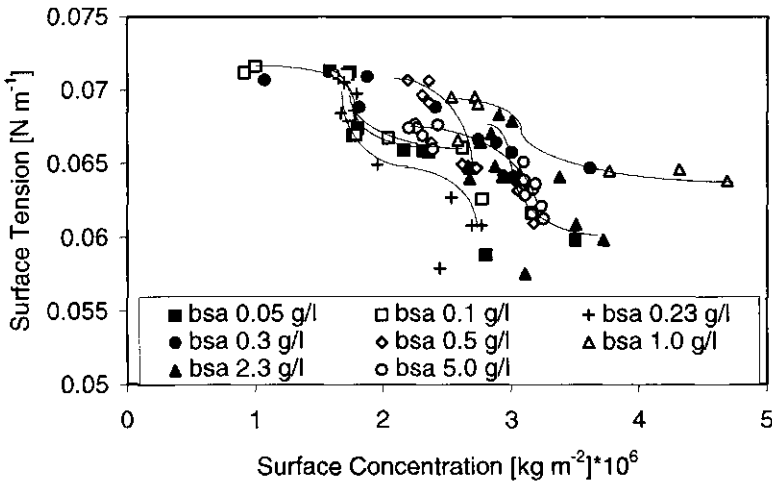


Figure 3. 22 Measured relation between surface tension and surface concentration for BSA

With BSA we can see a stepwise transition in the relation between surface tension and surface concentration in figure 3.22 in contrast to the equilibrium curve which has the shape of a sigmoid (¹⁶). In the relation between relative rate of expansion and

surface tension figure 3.21, the surface tension deviates from the surface tension of pure water only at a relative expansion rate between 0.8 and 0.3 for bulk concentrations below 0.5 g/l of BSA. The corresponding decrease in surface tension in figure 3.22 takes place around a surface concentration of $1.6 \cdot 10^{-6} \text{ kg/m}^2$. From the work of van Aken and Merks (¹⁵) it can be observed that if the BSA molecules would be present in an equilibrium conformation, the surface tension would be around a value of 56 mN m^{-1} . In this case the unfolding would be responsible for the surface tension decrease.

For higher bulk concentrations of BSA of around 0.5 g/l and higher another shape of the relation between surface tension and surface concentration and surface tension and relative rate of expansion can be seen to appear. At these bulk concentrations, the surface concentration is high while the surface tension is also at a relatively high value. This discrepancy in the behaviour between low and high bulk concentrations probably can be explained by assuming that at that concentration the transport to the surface of BSA molecules is so fast that the decrease in surface tension could be caused by hard sphere interactions rather than due to unfolding occurring at the surface. In this situation such a behavior is recognized due to the slow unfolding of BSA in combination with a fast adsorption. This hypothesis is supported by the fact that the relation between surface tension and surface concentration, is similar for high concentrations at surface tensions below 65 mN m^{-1} .

This indicates that in the case of BSA, the unfolding is not the main parameter which limits the surface tension decrease in this situation, because another mechanism is present which can cause a surface tension decrease. The fact that both transport and unfolding may be responsible for the surface behaviour in different ways may also be responsible for the rather low predictability a priori of surface behaviour of some proteins.

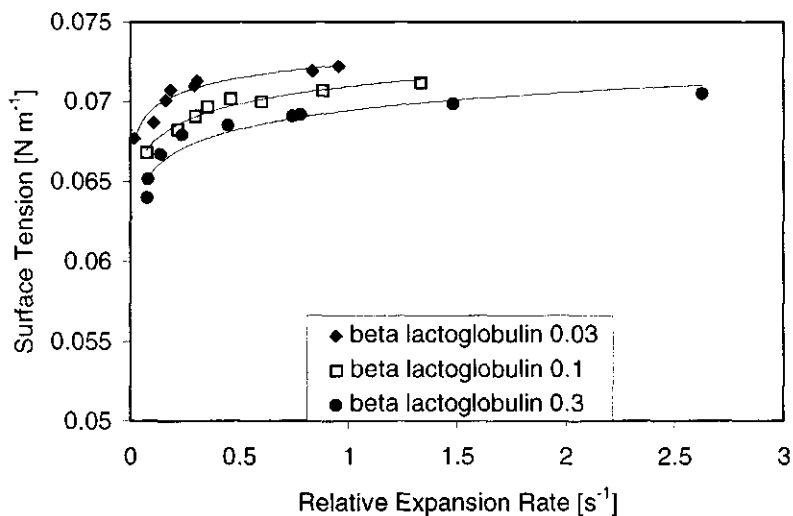


Figure 3. 23 Measured relation between surface tension and relative rate of expansion for β -lactoglobulin.

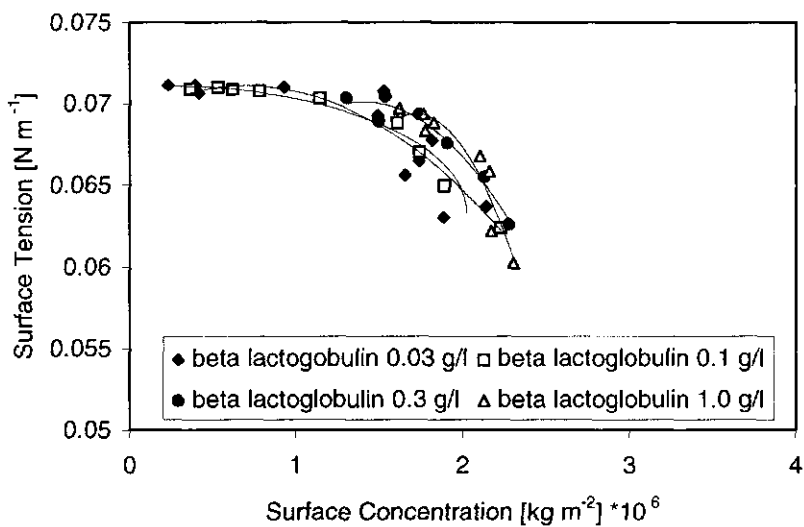


Figure 3. 24 Measured relation between surface tension and surface concentration for β -lactoglobulin.

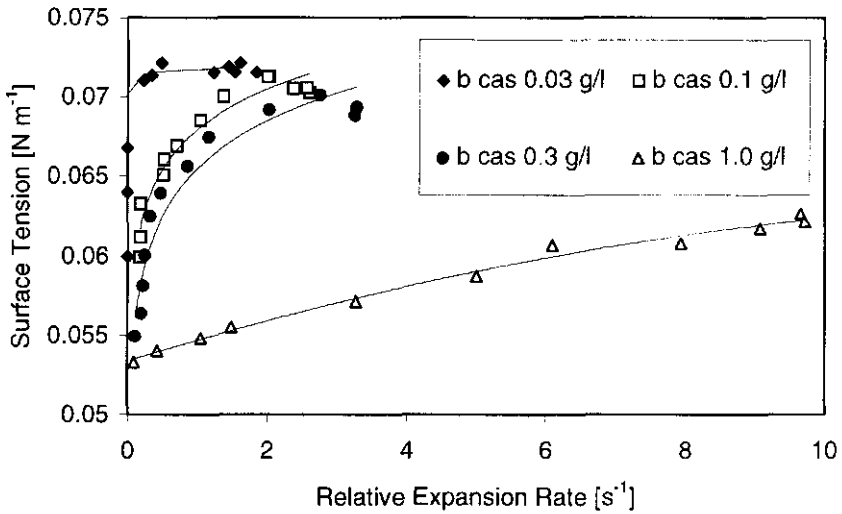


Figure 3. 25 Measured relation between surface tension and relative rate of expansion for β -casein.

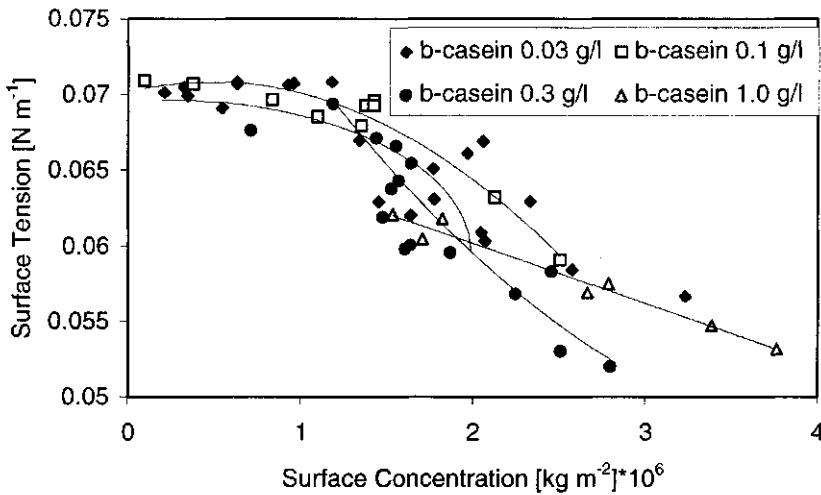


Figure 3. 26 Measured relation between surface tension and surface concentration for β -casein.

β -Lactoglobulin and β -casein are comparable with respect to the relations between surface tension and relative rate of expansion although the maximum relative rate of

expansion is larger for β -casein. The relations between surface concentration and surface tension for these proteins are also comparable, although for β -casein a more S shaped relation is found which is comparable to the situation with BSA. In comparison to lysozyme and BSA, the decrease in surface tension is high even at relatively low surface concentrations of around 2 mg/m^2 . This indicates that during the time scale of the experiment, the unfolding is not limiting the surface tension decrease to any significant degree. This is also the reason the relations between surface tension and surface concentration are similar in all the graphs. Probably the main limiting factor at this bulk concentration, is the transport of proteins to the surface. This is confirmed by figures 3.23 and 3.25. These curves show that the maximum relative rate of expansion for the proteins is around 10 for β -casein and around 4 for β -lactoglobulin. Here the maximum value of the relative rate of expansion at high bulk concentrations can be seen as an indicator of the unfolding constant since the unfolding constant determines the decrease in surface tension in the case the transport is not limiting.

3.5.2.2 Surface properties of proteins: comparison to the model

In order to quantify the different behaviour of the proteins with respect to the unfolding and transport behaviour, in table 3.2 the characteristic constants as determined by the model in chapter 2 have been given.

Here D/D_0 means the ratio between the diffusion coefficient predicted by the model and the theoretical diffusion coefficient. This value provides a parameter which quantifies the chance of a molecule to adsorb when present at the surface. A^u/A^n indicate the increase of specific surface area of the molecule and therefore is a parameter which indirectly describes the geometrical consequences of unfolding on the proteins. K_1 and K_2 respectively indicate the unfolding and refolding rate of the molecules. In chapter 2 the underlying considerations and theory have been discussed.

The ratio of the diffusion coefficients is most pronounced for lysozyme, which means that the rate of adsorption at the surface is quite small in comparison to the transport rate to the surface. Apparently lysozyme is transported to the surface in a much higher rate than it adsorbs at the surface. The most probable explanation already given by van Aken and Merks (¹⁶) is that even a small amount of lysozyme adsorbed at the

surface can hinder the adsorption of more molecules arriving at the surface. The most probable cause is that electrostatic interactions between the molecules causes this inhibition of the adsorption.

The data which quantify the unfolding properties A''/A'' , k_1 and k_2 show that for the proteins studied here there is a significant variation in unfolding properties. When looking at k_1 and k_2 , a variation of two orders of magnitude is observed between lysozyme and β -casein. This means that the rate of unfolding at the surface can vary substantially between the different proteins. This is an indication that the internal stability of the protein molecule can have a significant effect on the rate of unfolding at an aqueous surface.

The geometric influence of unfolding is expressed in A''/A'' . This parameter also differs considerably between the proteins studied here. For β -casein an increase in surface area of the molecules is observed while in the case of β -lactoglobulin, a significant decrease is found. As this parameter indirectly reflects the changes in the molecular structures of proteins as a consequence of the adsorption process, probably the unfolding leads to other consequences with respect to the occupied area per molecule in the case of β -casein then it does in the case of β -lactoglobulin. It may be that due to the unfolding of β -lactoglobulin the unfolding at the surface leads to an increase of intermolecular interactions between the proteins causing the adsorbed protein layer to become more compact. Indeed it has been observed that for instance the surface dilational modulus of β -lactoglobulin is high which is ascribed to intermolecular interactions (¹⁶). With β -casein the unfolding may give rise to an accumulation of trains at the surface which may give rise to the occupation of a larger area per adsorbed molecules.

Protein	D/D ₀	A _u /A _n	k ₁ [s ⁻¹]	k ₂ [s ⁻¹]
			Unfolding	Refolding
β -Casein	0.8	1.67	8.5	4
β -Lactoglobulin	4	0.4	2.5	2.5
BSA	1	6.6	0.13/0.05	0.13/0.05
Lysozyme	100	unknown	<<0.1	unknown

Table 3. 2 Characteristic properties of proteins determined by the model

Since in the previous sections we have observed that the ability of a surface to create a cooperative surface tension gradient is the main mechanism by which a surface can be assumed to cause an enhanced dilation at the surface, the data presented here can be put in perspective. For β -Lactoglobulin and β -casein, the cooperative surface tension gradient can be assumed to be high which is caused by their rapid unfolding, this leads to a relatively fast expansion. For BSA, the same applies but this is probably due not to the rate of unfolding, which is rather slow, but probably because BSA can create a decrease in surface tension because of hard sphere interactions at the surface between the molecules. For this the supply of molecules needs to be high. For Lysozyme, it is not possible to create a large surface tension gradient for two reasons. The first is that the adsorption rate at the surface is very slow, which may be due to electrostatic interactions. The other reason is that the unfolding of lysozyme is very slow, which may be due to the strong internal structure of lysozyme.

More generally speaking this technique in combination with the model enables us to study the unfolding behavior of proteins at interfaces in more detail. The results for the proteins obtained here roughly match our impressions. The future application of this technique could be sought in describing the effects of chemical and physical modification of proteins or studying the effects of pH, temperature concentration and solvent conditions.

3.5.3 Relation between mechanical properties and surface properties

In previous sections both the mechanical properties of the overflowing cylinder surface and the surface properties of a number of proteins have been discussed. It has been stated in section 3.5.1 that the link between surface properties and mechanical properties is that the surface properties influence the mechanical properties because of the relation between the surface tension and the relative rate of expansion. These relations depend strongly on the type of surface active substance. For proteins we have observed that both the sensitivity of surface tension to the relative expansion and compression rate is high. It has been observed also that there is a distinct *difference between the different proteins*. For BSA and in a lesser degree for β -lactoglobulin we have observed that the unfolding rate of the protein limits the decrease of surface tension at higher relative rates of expansion. Nevertheless the surface tension difference between the compressed and expanded surface is generally

high for proteins which can be seen in figure 3.14. This is due to the low surface tension at the compressed surface. We infer that for the mechanical properties of surfaces deformed by means of forces parallel to the surface, all time scales, ranging from the maximum expansion to maximum compression rate, present at the surface together determine the resistance to deformation of the surface. This is a situation different from one in which a surface is subjected to a uniform expansion or compression. There one time scale is the characteristic for the surface.

3.5.3.1 Applicability to foaming behaviour

In the previous paragraphs a detailed study has been presented on the operating mechanism of the overflowing cylinder technique. It has been demonstrated previously (¹⁷) that the behaviour of different solutions in the overflowing cylinder correlates well with foaming behaviour. How can this be understood taking in account that the surface of the overflowing cylinder is at least two orders of magnitude bigger than the surface of a bubble in a foam and the time scale does not necessarily match the deformation rate of the bubbles?

In section 3.3.5 the answer to this question is already given implicitly. There it was demonstrated that the stress that can be imposed on fully immobile surface is much higher in most cases than the stress that is effectively transferred to the surface. The effective part of the stress, which is the part that is indeed transferred, is determined mostly by the properties and the concentration of the surface active species in bulk. In a previous paper, it has been found that the surface tension gradient generated at the overflowing cylinder surface correlates positively with the amount of foam created by alcohol/water solutions (¹⁷). For proteins it has been found that the surface tension depends on two mechanisms: transport and unfolding, and that both mechanisms can play a role, depending on the relevant time scale. If the unfolding of a protein is a fast process, (such as in the case of β -Lactoglobulin and β -casein) this may be beneficial for the creation of foams because the proteins can adsorb and unfold in a relatively short time. However even if the unfolding is relatively slow, like in the case of BSA, at the surface can be responsible for the decrease of surface tension and thus can give rise to surface tension gradients. In this case the supply of proteins to the surface must be high however. In the literature it has been reported that also these proteins have good foaming properties (¹⁸).

In section 3.5.3 an explanation for this foaming behavior has been given. It was concluded that in the case a surface is deformed by means of a parallel force to the surface a wide range of time scales together determine the response of the surface to this force. This means that both the surface properties of the compressed and expanded surface play a significant role. The effective stress that can be transferred to a parallel surface depends on the surface tension difference between expanded and compressed surface. In that case the surface tension difference between the top and the bottom surface of the overflowing cylinder shown in section 3.5.1.2 is characteristic for the surface properties. An obvious question is then: when do forces applied parallel to the surface play a role in foaming. This question will be addressed in chapter 5.

In the case of low molecular surfactants we can observe that generally the surface tension in the compressed surface is close to the equilibrium surface tension indicating that the time scale of relaxation of these species in compression is orders of magnitude faster than those of proteins. Bergink-Martens (¹) found that foam creation by shaking solutions with Teepol, a low molecular surfactant, correlates with the dynamic surface tension. This suggests that the transport of surface material to the surface determines the creation of foams under these circumstances.

3.6 Conclusions

This chapter has a twofold aim. First of all an analysis of the working mechanism of the overflowing cylinder was made and secondly the dynamic surface behavior of both proteins and surfactants were studied using the overflowing cylinder technique in such a way that both the influence of adsorption and unfolding at the surface could be studied separately in the way as was suggested in chapter 2.

The analysis of the working mechanism of the cylinder showed that the falling film is the cause of the surface tension gradients generated anywhere at the overflowing cylinder surface. If surface active material is present in the liquid, the falling liquid within the film drags the surface of the falling film causing a surface tension gradient at the surface. It was found that the boundary layer theory could be used to explain the difference in surface tension between the top and bottom surface of the overflowing cylinder. Hence the overflowing cylinder is a suitable method to impose

a drag force on a surface and can be used to measure the resistance to deformation of a surface.

By means of hydrodynamics the surface of the overflowing cylinder was analyzed in the situation the was decelerated in comparison to water. The situation in which the surface was accelerated with respect to water has already been covered by Bergink-Martens (¹). It was found that a tenfold higher surface tension gradient is needed to decelerate a surface in comparison to an acceleration. Also the layer affected by the surface is seven times thicker in the case a surface is decelerated than for an accelerated surface.

The overflowing cylinder was also used as a device to characterize several types of proteins and low molecular surfactants for their dynamic surface behavior.

Surfactants were generally shown to create relatively small difference in surface tension between the top and bottom surface of the overflowing cylinder. Hence the surface tension gradient over the falling film is not so high. This can be ascribed to the very rapid relaxation to the equilibrium surface tension at the compressed bottom surface of the overflowing cylinder. Also the surface tension of an expanded surface is relatively low. Generally we can say that the relaxation to equilibrium surface tension for low molecular surfactants is higher due to the absence of an unfolding step.

The proteins that were considered were β -casein, β -lactoglobulin, BSA and Lysozyme. It was shown using the model described in chapter 2 that for proteins there is a strong dependence of surface tension on both unfolding and transport. Generally a large difference between the surface tension of the top and bottom surface was found. This means that proteins are capable to create high surface tension gradients. This can be ascribed to the sensitivity of the surface tension to expansion of the surface and also the inability to desorb from a surface which causes a low surface tension in compression.

Generally the adsorption to the surface is rather slow. There are large differences between the different proteins. From the proteins considered, Lysozyme appears to adsorb extremely slow. Also the unfolding at the surface was demonstrated to differ considerably. At least a factor 1000 difference could be found in the unfolding rate of the different proteins. The order from quick to slow of the protein considered was as

follows: β -casein, β -lactoglobulin, BSA, Lysozyme. This is more or less in accordance with the expectations.

Generally we can say that the overflowing cylinder is a suitable device to study dynamic surface behavior in relation to foaming properties as long as the foaming properties are dependent on the ability of the surface active species to create surface tension gradients.

Chapter 4

Modelling the adsorption of binary mixtures of proteins and low molecular surfactants at air/water surfaces.

4.1 Abstract

The adsorption of binary protein surfactant mixtures of β -casein and Tween 20 has been studied making use of a model describing the behaviour of the transport and adsorption of binary mixtures to expanding surfaces and the overflowing cylinder technique in analogy with chapter 2 and chapter 3 for single species. Assuming certain characteristic properties regarding the transport and the unfolding, the model was demonstrated to be capable of predicting the surface properties of binary mixtures of proteins and surfactants. Both the model and the experiments indicate that in the case of expanding surfaces, the transport and unfolding kinetics of proteins play the most dominant role in the surface behaviour. Factors such as the presence of micelles, preferential adsorption of surfactant molecules or aggregation in bulk, which play a large role in equilibrium situations are only of marginal importance in the adsorption under expanding conditions. The model was found to be capable to predict the trends in surface properties of binary mixtures at expanding surfaces. In the case the surface is compressed the low molecular surfactant Tween 20 dictates the surface tension, indicating that preferential adsorption does play a dominant role. Hence the relevant time scale of the deformation of a surface element determines the dominant mechanism and dominant substance, which in turn determines the overall surface properties. In the situation that at a surface more than one time scale plays a role such as surfaces which are deformed by a drag force, different substances may dominate the behaviour at different parts of the surface.

4.2 Introduction

In the production of disperse foods, often more than just one type of surfactant is added to the product. Proteins are used as stabilisers for disperse phases such as

emulsion droplets or foam bubbles. Also, low molecular surfactants such as sucrose esters like Tween 20 are used for this purpose. The reasoning behind the decision to add more than one surfactant is that each species causes a certain specific behaviour which is desirable for a specific purpose. Moreover, the addition of a certain component can be desirable to obtain a specific consistency associated with the end product. Often however, the different types of surfactant added interact in the surface in a way that can be favourable during production but unfavourable for the end product or the other way around. The current state of the art does not enable us to predict whether to expect favourable or unfavourable interactions. If we should be capable to understand, and possibly predict, how the composition of the bulk phase in the presence of more than one surface active species would affect the surface behaviour over different time scales, it is possible to influence the dispersion behaviour more effectively.

4.2.1 Scope of this chapter

In chapter 2 of this thesis it has been demonstrated that by means of a model describing unfolding and transport to the surface the surface behaviour of proteins and low molecular surfactants could be understood under steady state expanding conditions. If we apply the calculation methods used there to study the behaviour of mixtures, information can be obtained about how proteins and surfactants influence each other under expanding surface conditions. Hence, in this chapter the phenomena associated with interactions between proteins and surfactants at expanding air/water interfaces will be studied by means of this model.

In chapter 3 the overflowing cylinder technique was discussed as a method to obtain relevant characteristic properties of surface active species for one component systems. Here the overflowing cylinder technique will be used to study binary mixtures of low molecular surfactants and proteins. The predictions made with the model will be compared to the experiments. These experiments and calculations may help to identify the dominant time scale(s) for sub-processes relevant for the behaviour of for instance a foam bubble. In chapter 5, foaming experiments will be presented with the systems presented in this chapter. These experiments match the data provided in this chapter to foam formation and drainage.

4.2.2 Model

In order to model the behaviour of the mixtures at the expanding surface of the overflowing cylinder we will use the theoretical treatment of the behaviour of single surfactant systems in chapter 2. This provides the basis for the calculation of the mass balance of both species at the surface. The way of reasoning in chapter 2 for the calculation of single species can be summarised as follows. A circularly shaped surface with a stagnation point in the centre expands at a rate increasing slightly with the distance from the centre. This surface is subdivided into an arbitrary number n of concentric rings ($n=100$). Each ring is assumed to have a constant surface concentration and surface tension. Because the surface dilates, surface active material is transported from one ring to another. In addition surface active material is supplied from the bulk solution to the surface by means of convective diffusion. Both these rates depend on the local relative expansion rate. Over each ring a mass balance is constructed for each species. From this mass balance the surface concentration is calculated. By means of this surface concentration, the surface tension is calculated for each ring. Hence, the variation of surface tension over the surface is known and the surface tension gradient can be calculated. In the case of the adsorption of protein, unfolding is included in the model by introducing a time dependent unfolding step at each ring and calculating the mass balance for the native and unfolded molecules. In the calculations it has been assumed that the supply rates of the various species do not depend on the composition; i.e. the species do not interact. This assumption is probably correct if the volume fractions of both species in bulk are small.

4.2.3 Literature

Several studies on the interaction between low molecular surfactants and proteins at aqueous surfaces have been published, but few papers explain the behaviour in a quantitative way.

De Feyter and Benjamins (¹) investigated the competitive adsorption of a large number of surfactants on the one hand with proteins β -casein and β -lactoglobulin on the other under static conditions. It is shown that the affinity of both species, expressed in the lowering of interfacial energy at the surface, and the chain length of the protein both play a role in the competition for available space at the surface. Low molecular surfactants can displace proteins from the surface because of their higher

interfacial energy per unit area occupied at the surface. The time scale by which such a displacement takes place is often unknown, however.

Dijt (²) studied the competitive adsorption of polymers of different types and chain lengths at solid surfaces as a function of time using reflectometry. This study reveals that time scale of rearrangement processes of the polymer, the polymer chain length and affinity of the polymer segments for the surface determine the rate of exchange of polymers at the solid surface. Due to the high affinity of the polymer for the surface and the fact that the polymer is attached to the surface by more than one segment, desorption from the surface is extremely slow in the presence of the polymer only. In the presence of displacers i.e. soap molecules, however the displacement progresses rapidly.

Murray and Dickinson (³) reviewed the surface rheology of various mixtures of proteins and low molecular surfactants in relation to their individual components. In the presence of even a low quantity of low molecular surfactants, the characteristics of the surface change dramatically with respect to the dilational- and shear moduli and the loss tangent. Generally adsorbed layers of low molecular surfactants have a small resistance to deformation and relax rapidly when subjected to a stress. This manifests itself in a low dilational modulus and a small loss angle both in shear and in dilation. Adsorbed layers of proteins generally have a relatively high resistance to deformation and relax very slowly when subjected to stress manifesting itself in a high dilational modulus and a high loss angle. When even low quantities of low molecular surfactants are added to a protein solution, the surface dilational modulus decreases and the loss tangent increases. This is ascribed to the disruption of lateral interactions between the proteins.

Coke et al (⁴) studied mixtures of β -lactoglobulin and Tween 20 with respect to lateral diffusion, thinning of films and drainage. Lateral diffusion of adsorbed layers of β -lactoglobulin increased significantly when Tween 20 was added to the system. The thinning of films under gravity, which was quite slow in the presence of β -lactoglobulin only, increases due to the presence of low molecular surfactants. Also thinning of films is more chaotic resulting in marginal regeneration in the presence of Tween 20. These effects result in a more rapid drainage of foams under gravity. Binding studies indicate that β -lactoglobulin and Tween 20 form complexes in the bulk phase. Apparently these complexes adsorb resulting in disruption of the lateral

interactions between the proteins. The binding of surfactant of β -lactoglobulin may be ascribed to its biological task in milk where β -lactoglobulin acts as a transport molecule for fatty substances Clark et al. (⁵). Mackie et. al. (⁶) concluded that mixtures of β -casein and Tween 20 do not form complexes but act in a more or less additive manner.

4.3 Model of binary adsorption at expanding surfaces under steady state dilation

In this section a description will be given of assumptions used to extend the model described in chapter 2 to the model describing the behaviour of binary mixtures in this chapter.

4.3.1 Adsorption kinetics

It has been established that in static conditions proteins can be displaced from surfaces by means of low molecular surfactants (¹), (²), (³), (⁴). In that case something happens to the relation between bulk concentration and surface concentration of both species due to the presence of another species. How this competition for available space at the surface takes place it is not clear however. Several intricacies concerning the time dependent adsorption of these molecules can play a role. Therefore three possible ways of co-adsorption have been studied here. (i) First, it is possible that the surfactants and the protein compete for space at the surface on the basis of geometrical exclusion. This means that the fraction of the species at the surface adsorbed in binary systems is proportional to the fraction that is not occupied by the other species. So suppose that a fraction of ϕ is occupied by species 1, the fraction of area available for species 2 to adsorb to is $(1-\phi)$. This means that a fraction $(1-\phi)$ of the molecules will adsorb compared to the situation when only species 2 is present. We will call this type of behaviour non-preferential adsorption here. (ii) Secondly it is possible that the adsorption of a low molecular surfactant is not hindered by the presence of proteins. In that case surfactants adsorb uninhibited and proteins adsorb only to the fraction of the area not occupied by surfactants. (iii) Thirdly it is possible

that proteins adsorb preferentially which is the reverse situation of the second situation.

With respect to the calculation of the area of the surface occupied by each species, two ways of calculation the surface area will be used. In the case of non-preferential adsorption, the area fractions occupied by the different species will be calculated as follows: Suppose the surface area to be occupied by three different kinds of molecules: Solvent molecules (o), protein molecules (p) and surfactant molecules (s). Only the fraction of the area occupied by water molecules is accessible to adsorption of either protein or surfactant. Hence we explicitly assume that the adsorption of either species affects the surface area available for adsorption of the other species. The fractions of the surface area occupied by solvent, protein and surfactant are respectively. ϕ_o , ϕ_p and ϕ_s . The maximum surface concentrations of protein and surfactant in the absence of other species are indicated with Γ_p^∞ and Γ_s^∞ , respectively. The surface concentrations of protein and surfactant in the absence of the second species are indicated with: Γ_p^o and Γ_s^o respectively. The resulting actual surface concentrations are indicated with Γ_p and Γ_s . The resulting surface concentrations can be written as function of the surface concentrations in the absence of the other species as follows:

$$\Gamma_p = (1 - \phi_s) \Gamma_p^o \quad \phi_p = \frac{\Gamma_p}{\Gamma_p^\infty}$$

Equation 4. 1

$$\Gamma_s = (1 - \phi_p) \Gamma_s^o \quad \phi_s = \frac{\Gamma_s}{\Gamma_s^\infty}$$

Equation 4. 2

The total fraction available for the three species is 1 so:

$$\phi_o + \phi_s + \phi_p = 1$$

Equation 4. 3

Rearranging and combining these equations leads to the surface fractions of the species to become:

$$\phi_s = \left(\frac{\Gamma_p^\infty}{\Gamma_p^0} - 1 \right) \left(\frac{\Gamma_p^\infty}{\Gamma_p^0} \frac{\Gamma_s^\infty}{\Gamma_s^0} - 1 \right)^{-1} \quad \text{and} \quad \phi_p = \left(\frac{\Gamma_s^\infty}{\Gamma_s^0} - 1 \right) \left(\frac{\Gamma_s^\infty}{\Gamma_s^0} \frac{\Gamma_p^\infty}{\Gamma_p^0} - 1 \right)^{-1}$$

Equation 4. 4

In the case of the surfactant adsorbing preferentially Γ_s can be considered to be equal to Γ_s^0 . The adsorbed amount of protein can then simply be considered to be $(1-\phi_s) \Gamma_p$. Hence this equation tells what effect the effect will be on the adsorbed amount if part of the surface is occupied by another species. The surface tension at such a surface will be covered in the next section.

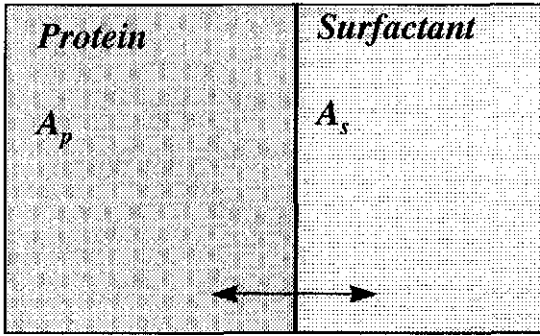
4.3.2 Influence of micelles

With respect to the adsorption of low molecular surfactants also the presence of micelles may influence the flux of the low molecular surfactants to the surface. As has been stated in chapter 2 this may influence the surface properties of the low molecular surfactant. Essentially two situations may exist. (i) The micelles are transported to the surface, in the same rate as the monomers. In this case the existence of micelles does not have any effect of the flux of surfactant to the surface. (ii) The second possibility described by Bijsterbosch (⁷) is that the concentration of monomers in bulk liquid is lowered due to the presence in micelles. In the vicinity of the expanding surface however, these micelles fall apart as a response to the lowering of the surfactant concentration close to the surface. This causes a decrease in the mass flux of surfactant to the surface compared to the situation that all surfactants are present as monomers. When we assume however that the response of the micelles to a lowering of the bulk concentration leads to a fast transfer of molecules from the micelles to the bulk in comparison to the rate of transport, then the rapid adjustment of the micelles to the concentration in the bulk phase of surfactant monomers reduces the distance over which surfactants need to be transported to the surface. Bijsterbosch (⁷) calculated a dimensionless scaling factor for the surfactant flux to the surface for this situation as a function of the concentration of surfactant. Here we will study the situation for the cases that the surfactant is present in micelles which dissociate very

fast and for the case the micelles are transported to the surface by convective diffusion so the influence of the presence of surfactants in micelles is neglected.

4.3.3 The surface tension

In order to calculate the surface tension it is assumed that the molecules do not form complexes which are surface active. The molecules are assumed to interact laterally at the surface, each species having their own influence on the surface tension. This is illustrated in the highly schematic drawing of the situation of figure 4.1. Consider the surface to consist of two separate areas. At area 1 only molecules of type 1 are adsorbed. At area 2 only molecules of type 2 are adsorbed. Suppose there is a barrier between the two separate areas. At a certain position of the barrier the surface tension will become equal. This will be assumed to be the surface tension perceived at the surface in the presence of two adsorbed species. Hence the calculation of the surface tension is performed as follows. We consider the total surface area to be 1, with fractions of A_p and A_s occupied by protein and surfactant respectively. The surface concentrations of protein and surfactant are Γ_p and Γ_s respectively. The surface tensions of the surface area occupied by protein and surfactant are respectively γ_p and γ_s . As there is no interaction between proteins and surfactants, we can assume the surface to consist of two separate compartments one of which is occupied by protein and one of which is occupied by surfactants so A_p and A_s . The partial surface concentrations of protein and surfactant are Γ_p/A_p and Γ_s/A_s . Because these surfaces are in contact with each other, the surface tensions γ_p and γ_s must be equal when mechanical equilibrium is assumed.



Conditions: $\gamma_p = \gamma_s$ and $A_p + A_s = 1$

Figure 4. 1 Illustration for the calculation of surface tension (highly schematic).

For both surfactants we can consider the surface tension to be described by:

$$\gamma = \int_0^{\Gamma} \frac{d\gamma}{d\Gamma} d\Gamma$$

Equation 4. 5

In this equation Γ means the surface concentration of one species confined to its partial surface area. Hence in order to reach equilibrium the following expression needs to be satisfied:

$$\int_0^{\Gamma_p} \frac{d\gamma_p}{d\Gamma_p} d\Gamma_p = \int_0^{\Gamma_s} \frac{d\gamma_s}{d\Gamma_s} d\Gamma_s$$

Equation 4. 6

The boundaries between which this expression needs to be integrated are $\frac{\Gamma_p}{A_p}$ and $\frac{\Gamma_s}{A_s}$.

The calculation of this is elementary when $\frac{d\gamma}{d\Gamma}$ is a constant. In the case of both proteins and surfactants however $\frac{d\gamma}{d\Gamma}$ is not a constant. Therefore the calculation was performed numerically. $\frac{d\gamma}{d\Gamma}$ for the unfolded protein systems were obtained from the model of van Aken ⁽⁸⁾ who presented a model to which the equations of state of proteins could be fitted well (see chapter 2). Also we used the method described in

chapter 2 to calculate the fraction of proteins unfolded at a certain relative rate of expansion. The fraction that is unfolded was assumed to exhibit the behaviour of proteins in equilibrium conditions. The protein molecules not unfolded were assumed to be adsorbed with one segment only and are assumed to play no role of significance in the determination of surface tension and were not included in the calculations for reasons of simplicity.

4.3.4. The surface tension gradient

The surface tension gradient can be calculated from this surface tension variation over the radius of the expanding surface and can be compared to the stress generated by the flow of liquid along the surface. Just as in chapter 2, from this stress a relative surface expansion rate can be calculated which can be matched to the relative expansion rate inserted in the model. This makes it also possible to calculate the maximum relative rate of expansion. (For further information see chapter 2 and chapter 3)

4.3.5 The surface Fourier number

In Chapter 2 the square root of the surface Fourier number has been introduced to study single species systems. In this chapter we will use the same number to quantify if the transport or the unfolding limits the generation of a surface tension gradient. In

$$\sqrt{Fo_s} = \frac{c_b}{\Gamma} \sqrt{\frac{2D}{\pi \theta}}$$

Equation 4. 7

chapter 2 the square root of the surface Fourier number was defined as:

In this equation, c_b means bulk concentration, D is the diffusion coefficient, Γ is surface concentration and θ is the relative rate of expansion. The square root of the surface Fourier number gives the ratio between the potential transport flux, which is the supply rate expressed in the flux of molecules to the surface and the dilution rate of the surface due to the dilation.

For binary systems different values will be found than for single species systems since the square root of the Fourier number will overestimate the potential transport flux since only part of the surface will be accessible for adsorption of one species.

Hence the calculated Fourier numbers will generally be above 1 also in conditions that the transport is limiting for the adsorption of species to the surface. Nevertheless the trends will show under which conditions the transport to the surface is limiting for the adsorption to the surface.

4.4 Materials and Methods

4.4.1 Materials

For the overflowing cylinder experiments described in this chapter all surface active substances were dissolved in imidazole buffer pH 6.7 at an ionic strength of 0.075 M. Imidazole, HCl and NaCl were analytical grade and obtained from Merck and used as received. β -Casein was obtained from Eurial ref. 041091. Tween 20 analytical grade was obtained from Sigma. The proteins and Tween 20 were dissolved by stirring at room temperature for approximately 1 hour and were used immediately after stirring. All substances were used without further purification.

4.4.2 Calculations

In order to calculate the surface concentration, surface tension and surface tension gradient a certain procedure is followed which resembles the procedure in chapter 2. First the surface concentration as a function of the distance to the centre of the surface of both species in the absence of the other species is calculated (by the model described in chapter 2). In order to do this the bulk concentrations of low molecular surfactant and protein, the relative rate of expansion and the variation of the relative rate of expansion over the surface are used as input. For details of this calculation see chapter 2.

Then the surface concentration of both species is calculated in the presence of the other species either under the condition of geometric exclusion or under the condition of preferential adsorption of low molecular surfactants as indicated in equation 4.1 to 4.4.

After that the surface tension is calculated numerically as indicated in equation 4.6. From the surface tension difference over the radius, the surface tension gradient can be calculated. Which can numerically be matched to the relative rate of expansion used as input.

Now we are able to calculate the surface tensions and surface concentration of proteins and surfactants under expanding conditions at an interface under certain assumptions a priori. In order to match the experimental conditions as closely as possible we made use of literature data or our own experimentally determined values for the calculations which were obtained by fitting the single species systems to the model in chapter 2. In enclosure 4.1 the values necessary to model the well know systems β -casein and Tween 20 can be found.

In order to investigate the trends in the competitive adsorption behaviour of proteins and low molecular surfactants, calculations were performed for different bulk concentrations and relative rates of expansion of β -casein and Tween 20. This system was chosen because Tween 20 is a nonionic surfactant so no electrostatic interactions between β -casein and Tween 20 will influence the behaviour. Moreover β -casein and Tween 20 do not form any complexes, contrary to for instance β -lactoglobulin and Tween 20, Mackie et al (⁶). Hence it can be expected that the β -casein/Tween 20 system will exhibit comparatively unbiased behaviour. The challenge is of course to ascribe the different behaviour of these systems to the physical mechanisms determining the competitive adsorption and to obtain a working knowledge of the phenomena observed as a consequence of this competitive adsorption process.

4.4.3 Overflowing cylinder technique.

The experiments were carried out as described in chapter 3 section 3.4.1 For the sake of brevity this will not be repeated here.

4.5 Results and discussion

In order to impart a certain structure in the discussion we will separately discuss several aspects involved in the binary adsorption of proteins and surfactants. In section 4.5.1 the calculated effect of the composition of the bulk phase on surface concentration, surface tension and surface tension gradients and the relative rate of expansion related to it will be discussed. In section 4.5.2 calculated intricacies of the system will be discussed such as the mechanism of competition, influence of the critical micelle concentration and influence of the unfolding rate and the presence of a different type of surfactant. In section 4.5.3 the predictions performed with the model will be compared to experimental data in order to obtain information on the

validity of the assumptions and the predictive value of the model. Also the possible applications of the calculations and the experimental technique for binary systems will be discussed.

4.5.1 General trends of calculations

In this section general trends of one type of system will be discussed to obtain general trends in the adsorption behaviour. The system discussed in the following sections is based on the Tween 20/ β -casein system in which Tween 20 adsorbs preferentially. In this system the critical micelle concentration was accounted for by assuming that the micelles inhibit the adsorption of low molecular surfactants, in the way described by Bijsterbosch (⁷). To study these general trends we chose the following conditions: The concentration of protein was chosen to be 0.3 g l^{-1} unless stated otherwise and the concentration of Tween 20 was varied. We assumed that Tween 20 adsorbs preferentially because in previous studies on competitive adsorption on static surfaces this was found to be the case (¹), (⁴).

4.5.1.1 Calculated Surface Concentration

In figure 4.2 the calculated surface concentrations of β -casein and Tween 20 have been given for different concentrations of surfactant in bulk at a constant concentration of protein as a function of the relative rate of expansion. The conditions stated in 4.5.1 have been assumed to apply.

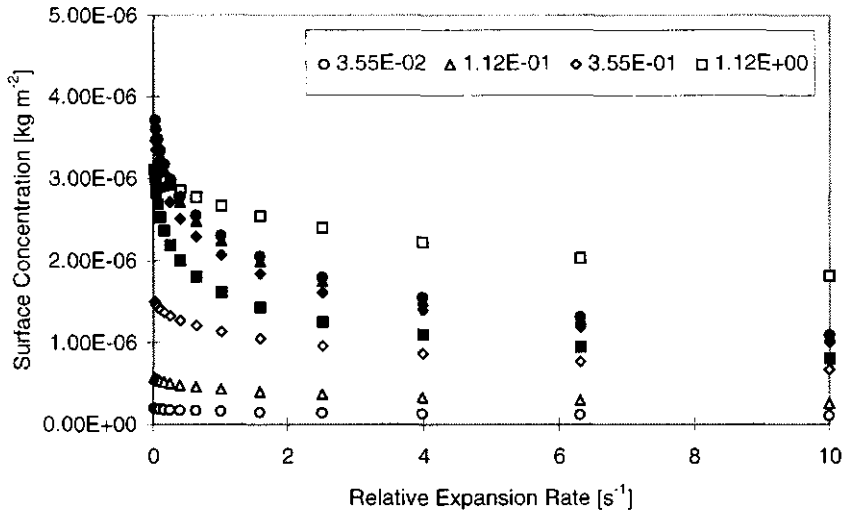


Figure 4. 2 Calculated Surface concentration of protein and surfactant as a function of relative rate of expansion for β -casein/Tween 20 system and 0.3 g/l β -casein system, preferential adsorption of Tween20, no transport of micelles. Open symbols Tween 20, closed symbols β -casein. Legend indicates the bulk concentration of surfactant [mM].

It can be clearly seen that the surface concentration of proteins and surfactants differs considerably with respect to their susceptibility to expansion of the surface. The low molecular surfactant retains more or less the same surface concentration, as a function of the relative expansion rate while the surface concentration of protein differs considerably with relative rate of expansion. This can be explained by the difference in adsorption behaviour of both species. Because of the high affinity character of the adsorption of proteins, the surface concentration mainly depends on the transport to the surface, which limits the surface concentration. The adsorption of low molecular surfactants are assumed to follow Langmuir kinetics. In that case the maximum surface concentration at a certain bulk concentration is both dependent on the concentration of free surfactant molecules in bulk and on the transport of molecules to the surface. Hence for the surfactant the surface concentration depends on the relative rate of expansion only if the expansion rate of the surface is fast enough to deplete the surface partially of the adsorbed surfactant. In chapter 2 it has already been mentioned that the parameter determining the characteristic

transportation length $\frac{\Gamma}{c_b}$ (which is the distance the molecules need to be transported over to create a surface concentration of Γ) together with the diffusion constant determines the sensitivity of the surface concentration to the relative expansion rate. In the case of proteins, $\frac{\Gamma}{c_b}$ is relatively high especially at low concentrations of the protein in bulk, due to the fact that due to the high affinity character of proteins the equilibrium surface concentration remains high irrespective of the bulk concentration. With low molecular surfactants $\frac{\Gamma}{c_b}$ is generally lower because in this case the equilibrium surface concentration depends on the bulk concentration of the surfactant. In figure 4.3 also the calculated fraction of the surface covered by the surfactant has been plotted as a function of the relative rate of expansion under the same circumstances as in figure 4.2.

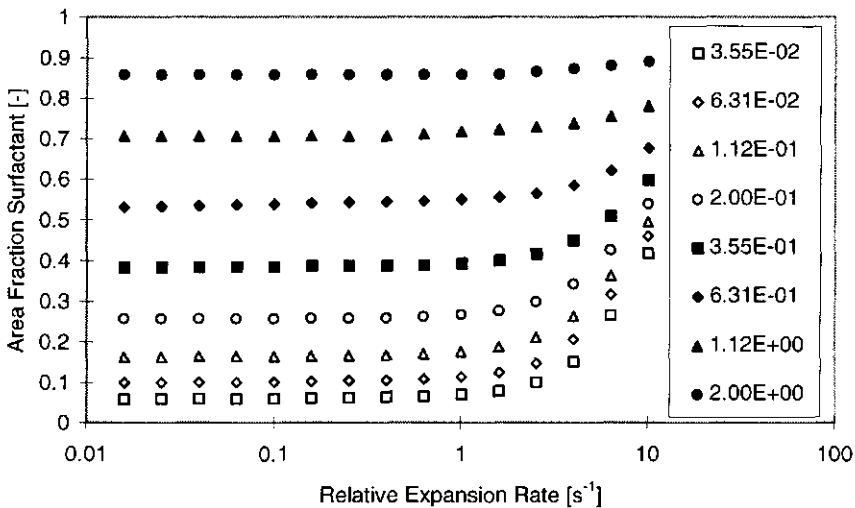


Figure 4.3 Calculated area fraction of surfactant as a function of relative rate of expansion. β -casein/Tween 20 system 0.3 g/l β -casein, preferential adsorption of Tween 20, no transport of micelles. Legend indicates the bulk concentration of Tween 20 in mM.

Here it can be seen that especially for low concentrations of Tween 20 and low relative rates of expansion the amount of protein adsorbed to the surface is high. This may seem somewhat surprising since de Feyter and Benjamins (⁵) demonstrated that

the affinity per occupied unit area and the number of monomers per molecule determines the distribution of molecules between the bulk and the surface. Because of their high affinity per monomer, surfactants are able to displace proteins from air/water interfaces under static conditions. The phenomenon observed here is caused by the effect of time on the adsorption process however. In the case the surface is in equilibrium, the surface concentration is not limited by the flux of molecules to the surface. In this time dependent case however the transport to the surface is generally limiting the adsorption of proteins, while the surface concentration of low molecular surfactant is generally limited due to their Langmuir kinetics. This is not the case for proteins for which the concentration in bulk has hardly any influence on the surface concentration at concentrations considered here. This causes the surface concentration of low molecular surfactants to be limited by the bulk concentration while there is no limit to the adsorption of protein molecules. Especially when the relative expansion rate is small and the surfactant concentration is low, the proteins will occupy a relatively large part of the surface area.

4.5.1.2 Calculated Surface Tension

In figure 4.4 the relations between the calculated surface tension and relative rate of expansion have been given for the same system as considered in figure 4.2 and 4.3 and their individual components in the same concentrations.

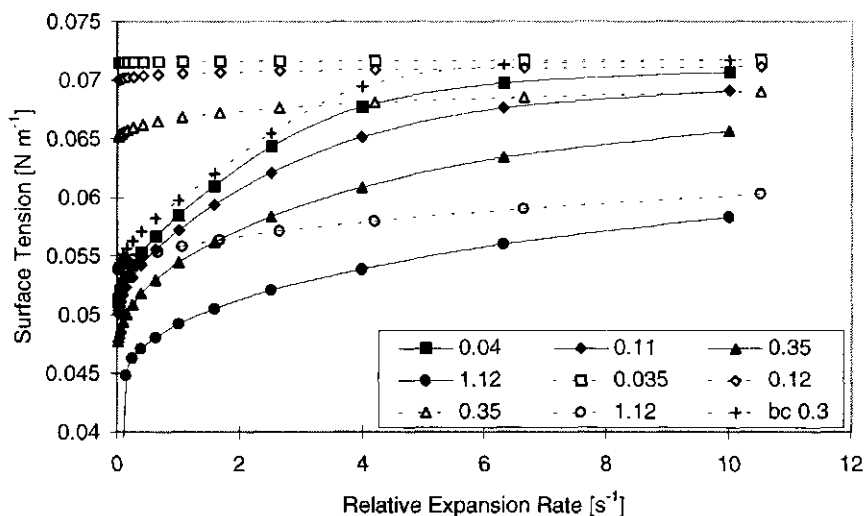


Figure 4.4 Calculated Surface tension as a function of relative rate of expansion for β -casein/Tween 20 system: open symbols, 0.3 g/l β -casein (+) and Tween 20 alone: closed symbols: binary systems preferential adsorption of Tween 20, 0.3 g/l β -casein, no transport of micelles. Legend indicates bulk concentration of Tween 20 in mM.

In this figure the synergy of the co-adsorption between surfactant and protein can be quantified by comparing data belonging to binary systems to those of the individual components. This synergy manifests itself when we compare the surface tension of the individual components and the surface tension of the mixture. We can see that the decrease in surface tension is higher than just the sum of the lowering of the surface tensions of both species individually. The reason for this synergistic behaviour is that the proteins and the surfactants both cover a certain surface area and both species are assumed to cause a similar decrease of surface tension at that specific surface area. The total surface tension decrease depends on their combined ability to lower the surface tension $\frac{d\gamma}{d\Gamma}$. This value varies strongly with Γ for proteins and stays more or less constant for surfactants. If we consider the relation between surface tension and surface concentration for β -casein as given by Graham and Phillips⁽⁹⁾ and van Aken⁽⁸⁾ we find a sharp increase in $\frac{d\gamma}{d\Gamma}$ around a surface concentration of $1.3 \cdot 10^{-6} \text{ kg m}^{-2}$. If the surface concentration at the specific area occupied by proteins is around this

value, the magnitude of the surface tension is very sensitive to even a small increase in surface concentration of either the surfactant or the protein. In figure 4.3 it has already been seen that the fraction of area covered by proteins is highest at lower relative rates of expansion. As both species occupy part of the surface, the surface tension decrease of the mixture depends on the surface tension decrease due to the confinement of each species to part of the surface (see section 4.3.3). Hence when the area occupied by proteins is high, the surface tension depends strongly on the protein behaviour. This is the reason that the surface tension is relatively close to the surface tension of the protein at relative rates of expansion below 0.5 s^{-1} .

4.5.1.3. Calculated Relative rate of expansion

In chapter 2 it was demonstrated that the maximum relative rate of expansion of the surface of the overflowing cylinder could be calculated from the model. In figure 4.5 the results of similar calculations for mixtures of β -casein and Tween 20 have been given in combination with the predicted surface tension.

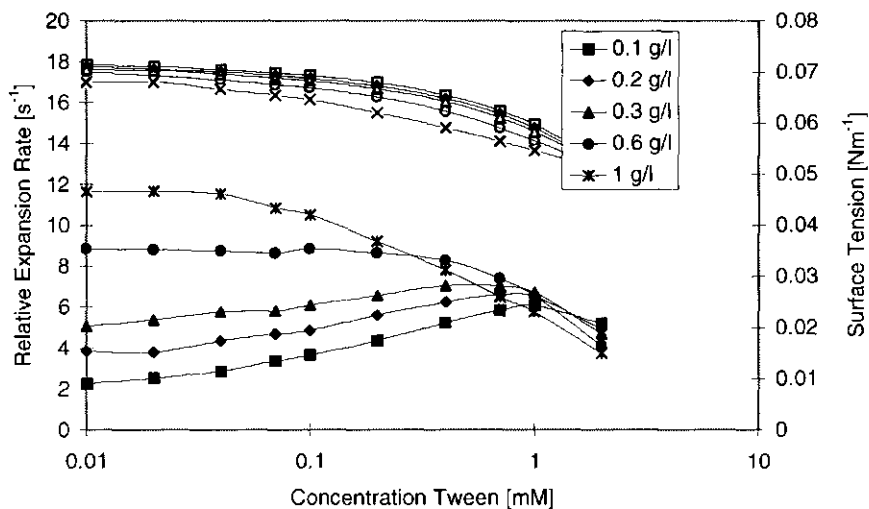


Figure 4.5 Calculated dynamic surface tension (open symbols, right axis) and maximum relative rate of expansion (closed symbols, left axis) as a function of bulk concentration of surfactant for different concentrations of β -casein. Conditions: preferential adsorption of Tween 20, no transport of micelles. Legend indicates bulk concentration of β -casein.

These calculations indicate that the magnitude of the maximum relative rate of expansion in the overflowing cylinder for β -casein/Tween 20 mixtures depends on both the concentrations of β -casein and Tween 20. The existence of a maximum in the relative rate of expansion as a function of bulk concentration has been demonstrated by Bergink (¹⁰) and is ascribed to the dependence of the relative rate of expansion on the transport kinetics to the surface. The shift of the maximum in the relative rate of expansion observed in the figure at different protein concentrations is most likely caused by a gradual shift from protein like behaviour (high concentrations of β -casein) to surfactant like behaviour (low concentrations of β -casein). This means that also in the relative rate of expansion there is a distinct mutual influence of β -casein and Tween 20. This means that the surfactant and protein together determine the relative rate of expansion that can be generated at the surface of the overflowing cylinder.

4.5.1.4 Calculated Surface Fourier number

In figure 4.6 the square root of the surface Fourier number for convective transport ($\sqrt{Fo_s}$) is given as a function of Tween 20 concentration for the same systems as in the previous figure.

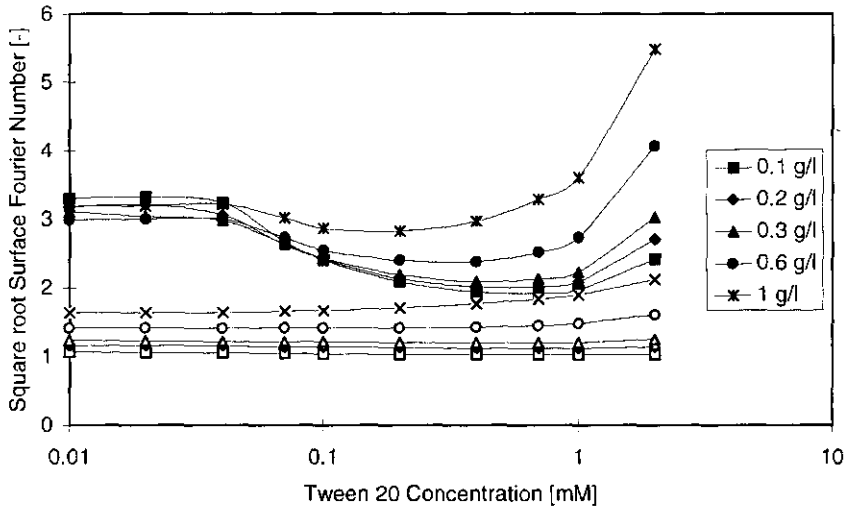


Figure 4. 6 Square root of surface Fourier number for protein and surfactant as a function of bulk concentration of surfactant for different concentrations of β -casein. Conditions: preferential adsorption of Tween 20, no transport of micelles. Closed symbols $\sqrt{Fo_s}$ for Tween 20, open symbols $\sqrt{Fo_s}$ for β -casein. Legend indicates bulk concentration of β -casein in $g\ l^{-1}$.

This number provides interesting information on the potential transport to the surface in comparison to the adsorption to the surface. At low concentrations of surfactant it is found that $\sqrt{Fo_s}$ for the surfactant molecules is considerably above 1, which means that the supply of the Tween 20 molecules is considerably above their rate of dilution at the time scale considered. This is due to the relaxation behaviour of the surfactant. In chapter 2 we already observed that this type of behaviour is due to the small transportation length of Tween 20 to the surface. In this case the relaxation due to the transport is too fast to cause a significant deviation from the surface concentration in equilibrium. The depression of $\sqrt{Fo_s}$ of the surfactant around the intermediate concentrations of surfactant is due to the increase in the relative rate of expansion (given in figure 4.5), which causes a depletion of the surface of both proteins and surfactants. In that case a larger fraction of the molecules supplied is indeed adsorbed. The sharp increase around the concentration at which a maximum in the relative rate of expansion is reached, is caused by both the increase in the transport

flux of surfactant due to the rise in concentration and the decrease in relative expansion rate, which means that the dilution of the surface occurs more slowly. Hence the expansion is no longer able to dilute the surface enough to cause a high surface tension gradient.

The magnitude of $\sqrt{Fo_s}$ for the protein transport is distinctly different from that of the surfactant molecules. Here we observe that this number remains constant and slightly above 1, which is an indication that not the Tween 20 adsorption, but transport limits the adsorption of protein molecules. The small rise in $\sqrt{Fo_s}$ for proteins at higher surfactant concentrations is caused by the same effects as for the low molecular surfactants. This shows that also in the presence of a high concentration of low molecular surfactants the transport limits the adsorption of proteins. The adsorption of low molecular surfactants is limited by the Langmuir kinetics, which indicates that for these molecules the adsorbed amount is not far from the equilibrium value.

4.5.2 Influence of intricacies

Up to now the general trends have been discussed of one specific system in order to explain the trends in the mechanical and surface behaviour of protein/surfactant mixtures. However a number of variations in the model were investigated as well. Here the cause and effect relations for different intricacies in the model have been given in table 4.1.

Cause → Effect on: Surface properties ↓	Mechanism of Competition	Transport of micelles	Low Unfolding rate of protein
relation γ and $d\ln A/dt$	minor	minor	lower γ at $d\ln A/dt \approx K_u$
$d\ln A/dt$ (max)	minor	higher at c_s where $d\ln A/dt$ reaches maximum	higher $d\ln A/dt$ at $d\ln A/dt$ $\approx K_u$
A_p	minor	smaller at c_s where $d\ln A/dt$ reaches maximum	lower

Table 4.1 Influence of different intricacies on different characteristic properties of the expanded surface.

In this table, the different intricacies considered are mentioned in the top row. In the first column, the different relations or parameters are mentioned on which these intricacies might have an effect. These are the relations between the surface tension and the relative rate of expansion (see for instance figure 4.4.), The maximum relative rate of expansion (see for instance figure 4.5) and A_p , the fraction of the area occupied by proteins (see for instance figure 4.3). In the different cells, the qualitative effects on the parameters or relations have been mentioned.

In this table it can be observed that only the transport of micelles and the unfolding behaviour of the protein has an influence on the dynamic surface properties predicted by the model. This effect indicates that it matters whether or not micelles contribute to the transport of molecules to the surface. In the case micelles are transported the maximum relative rate of expansion which can be reached by the expanding surface is higher. The fraction of area occupied by the surfactant is also higher in that case.

In the case the unfolding of the proteins at the surface should be hindered by the presence of surfactants, this will be visible in the vicinity of the relative rate of expansion at which the unfolding constant is equal to the relative rate of expansion because in that case the unfolding is the limiting factor for the depression of surface tension. A higher unfolding constant will cause the relative rate of expansion to be higher in that case. The fraction of area occupied by the proteins will not be altered significantly however.

Essentially the influence of the intricacies discussed in this chapter for the total behaviour are rather limited except for specific circumstances in terms of concentration and relative rate of expansion. This supports the idea that kinetics are *grosso modo* responsible for the behaviour of these systems under expanding conditions.

4.5.3 Experiments

In order to obtain a frame of reference for the model and to obtain information of other characteristic properties of these protein/surfactant mixtures, experiments were performed analogous to the experiments described in chapter 3.

In figure 4.7 and 4.8 the dependence of surface tension on the relative rate of expansion and surface concentration is given for systems with a constant protein concentration of 0.3 g/l β -casein and different concentrations of Tween 20.

Predictions by means of the model are given as well. The conditions that were chosen are: preferential adsorption of the protein and no transport by the surfactant micelles.

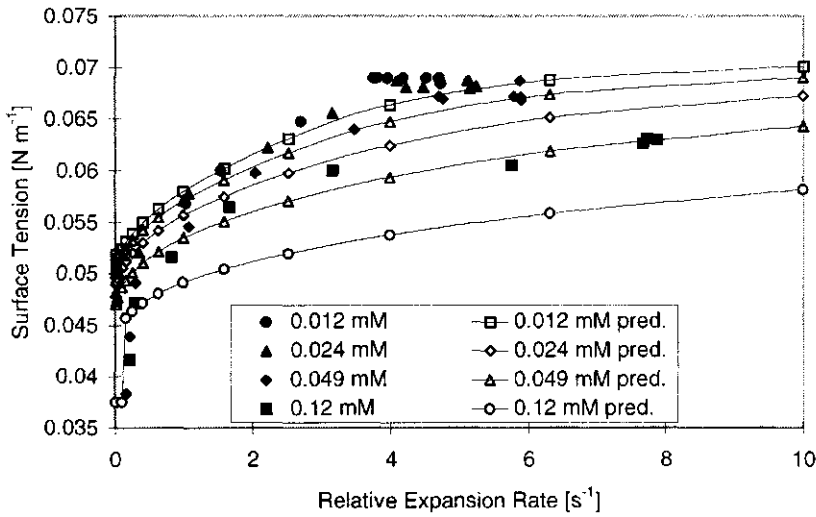


Figure 4. 7 Surface tension as a function of relative rate of expansion for β -casein 0.3 g/l with different concentrations of Tween 20. Comparison between the model and measured data. Predictions: open symbols, Measured data: closed symbols.

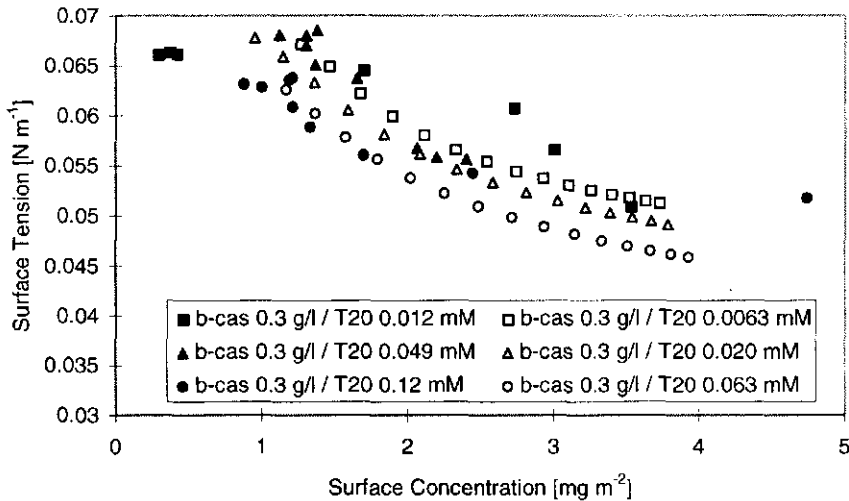


Figure 4. 8 Surface tension as a function of surface concentration. Comparison between predictions by the model and measured data. Open symbols: data predicted by the model closed symbols: measured data.

In figure 4.8 the surface concentration plotted in the figure is the surface concentration of both surfactant and protein based on ellipsometer sensitivity for protein and surfactant. In preliminary experiments it was found that the sensitivity of the ellipsometer for the surface concentration of proteins is in the order of five times higher than the sensitivity for Tween 20 due to the difference in the refractive index increment.

It can be seen in figure 4.7 that at higher relative rates of expansion, there is a good match between theoretical and experimental results. It can be seen that the predicted surface tension corresponds to a Tween 20 concentration that is about a factor of 2 lower. Hence, the model overestimates either the transport, or the synergy of the molecules at the surface. In order to clarify this the bulk concentration of surfactant in the calculations was chosen a factor 2 lower in figure 4.8. Then a good agreement was found between calculated and predicted results. Hence, probably overestimating the transport rate of Tween 20 to the surface is responsible for the deviation found in figure 4.7.

The influence of the choice for preferential adsorption of protein and the transport of micelles to the surface was of marginal importance to the values determined by the model as compared to the experimental error, so it is not possible to conclude which of these mechanisms determines the behaviour. Analogous to the experiments in chapter 3, the relative rate of expansion was measured as a function of the falling height. This can be seen in figure 4.9.

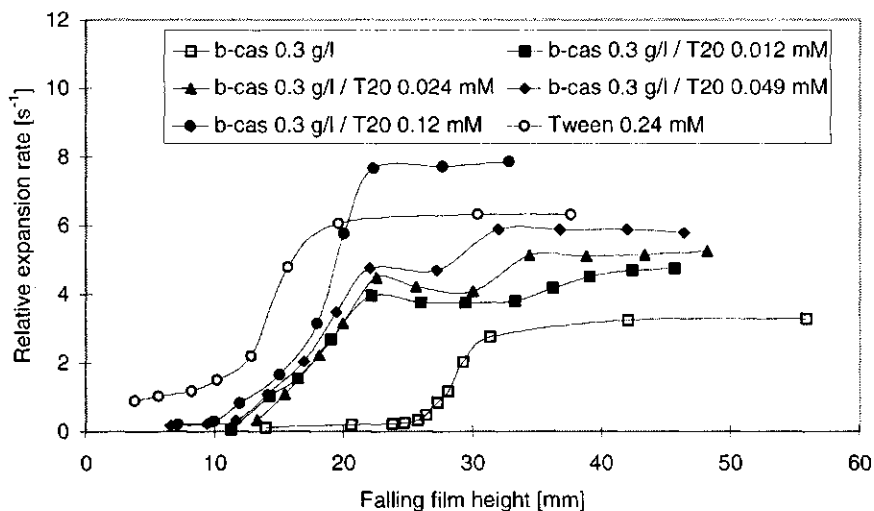


Figure 4.9 Relative rate of expansion as a function of film height in the overflowing cylinder. Different combinations of β -casein and Tween 20.

This relation was demonstrated to be a measure of the surface tension difference between the top and bottom surface in chapter 3. Here we can observe that these relations differ substantially for the Tween 20 containing samples and the pure β -casein sample. From this we can conclude that Tween 20 has a substantial influence on the generation of a surface tension gradient over the falling film in the overflowing cylinder. This can be ascribed to both the behaviour in expansion and the behaviour in compression. The addition of Tween 20 causes the surface tension in expansion to be significantly lower than that for the pure protein and causes the surface tension in the compressed surface to be about equal to the surface tension of Tween 20. This can be seen in figure 4.10. Here the surface tensions in compression and expansion of characteristic systems of β -casein, Tween 20 and a mixture of β -casein and Tween 20 are shown.

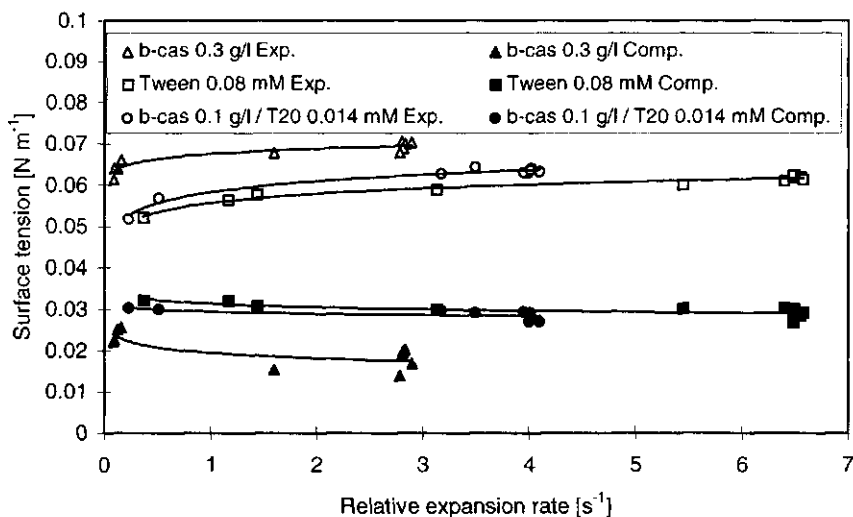


Figure 4.10 Surface tension in compression and in expansion as a function of relative rate of expansion the top surface for Tween 20, β -casein and a mixture of these substances.

Here it can be seen that the behaviour of the protein/surfactant mixtures in the compressed surface closely follows the behaviour of Tween 20. From this we can conclude that in the case of a compressed surface the surfactant plays the most dominant role. As the surface tension at the compressed surface is substantially higher than in the case of β -casein this means that the surfactant must be able to displace proteins from the surface. This means that the desorption kinetics of the β -casein are affected when also Tween 20 is present at the surface. This is in accordance with what De Feyter et al. found for the competition between surfactant and proteins at static surfaces. Also Dijt ⁽⁶⁾ demonstrated that the process of desorption of polymers from solid surfaces is accelerated significantly in the presence of a low molecular surfactant. This means that in the presence of a low molecular surfactant the surface approximates equilibrium much faster than in the case that only proteins are present at the surface.

At the top surface, so under expanding conditions, especially the relative rate of expansion is different between the Tween 20 or the Tween 20/ β -casein mixture. Although the surface tension both in compression and expansion is similar for both systems both in compression and expansion, the relative rate of expansion is lower

for the mixture. The presence of the β -casein contributes to decrease the surface tension but apparently does not contribute to increase the relative expansion rate. This figure generally shows that the surface tension at the top surface is not important for the magnitude of the relative rate of expansion. Hence this figure experimentally confirms the conclusions that can be drawn from figure 4.5.

4.6 Conclusions

In this chapter calculations were carried out on the surface properties of mixtures of proteins and surfactants under dynamic conditions. From these calculations it appears that the properties which determine the equilibrium situation play a minor role compared to the factors affecting the way this equilibrium situation is reached in time such as the transport to the surface and the unfolding rate of the protein molecules. In a simple model describing the competition for the available space at the surface a synergy could be detected in the behaviour of both species at the surface. This synergy manifests itself in a relatively constant maximum relative rate of expansion with different concentrations of both surface active species. In the case of a single surface active species, there is a distinct maximum in the relative expansion rate at a certain concentration. This effect can be ascribed to the different species complementing each other in the creation of surface tension gradients over a range of different concentrations.

It was demonstrated that the calculations predicted the trends observed in experimentally determined data on the same systems. From this we can conclude that also for binary systems of a protein and a surfactant, the kinetics of transport to the surface and the unfolding of proteins play the major role the surface properties of expanded surfaces. In order to understand the total behaviour of a surface deformed by a stress parallel to the surface also information is needed on the behaviour of the compressed surface. In these compressed surfaces it was observed that the low molecular surfactant plays the most dominant role. The behaviour in the compressed surface is probably the source of the difference in behaviour between proteins and protein/surfactant mixtures. A good understanding of the surface behaviour in compression of these mixtures may be the key to a better understanding of the surface rheological properties.

Appendix 4.1

Properties Tween 20	value	unit
Molar Mass:	1230	[g mol ⁻¹]
Γ_{\max}	$6 \cdot 10^{-6}$	[mol m ⁻²]
Langmuir Constant	170	[mol m ⁻³]
γ_{cmc}	$3.75 \cdot 10^{-2}$	[N m ⁻¹]
c_{cmc}	0.045	[mol m ⁻³]
Diffusion Coefficient	$4 \cdot 10^{-9}$	[m ² s ⁻¹]
$d\gamma/d\ln c$	$1.92 \cdot 10^{-3}$	[N m ⁻¹]

Properties of Tween 20 used for the calculations in the model.

Properties β-casein	value	unit
Molar Mass:	18300	[g mol ⁻¹]
Γ_{\max}	$5 \cdot 10^{-6}$	[kg m ⁻²]
Diffusion Coefficient	$2 \cdot 10^{-10}$	[m ² s ⁻¹]
k_1	8.5	[s ⁻¹]
k_2	4	[s ⁻¹]
A_0	1	[-]
A_1	1.3	[-]

Properties of β -casein used in the model.

Chapter 5

Foaming properties of proteins, surfactants and their mixtures in relation to dynamic surface behaviour

5.1 Abstract

In this chapter the relevance of surface properties of proteins and protein/surfactant mixtures for foaming is tested. The surface properties measured in the previous chapters can be expected to correlate to different kinds of foaming properties both during making and storage. In previous chapters we have concentrated on measuring the relation between stress and deformation parallel to the surface. Foaming properties that are likely to be dependent on these properties are the bubble size and the drainage behavior. Here the correlation between these foaming and surface properties was considered.

Foaming experiments were carried out by whipping a certain amount of liquid in a specially constructed setup. Foam creation and drainage experiments were carried out by means of this set-up.

The bubble size was found to decrease with the maximum stress that can be exerted at the bubble interface while the revolution rate of the whisk was shown to have a relatively limited influence on the bubble size. This can be explained if we assume that the transfer of stress limits the breakup of bubbles. An interesting aspect of the relationship found between the bubble size and the maximum stress at the bubble surface is that it applies for different revolution rates of the whisk and different the types of surfactant.

The drainage was also demonstrated to be influenced by the resistance to deformation of the bubble surfaces to shear stresses. In order to obtain information regardless of foam structure and dimensions, the drainage was normalised for the surface area of the foams. It could be shown that film thickness and the normalised drainage rate were related in a characteristic way. The normalised drainage rate at a certain film thickness could be found to correlate to the surface tension difference between the top surface and the bottom surface of the overflowing cylinder at a certain relative expansion, arbitrarily chosen to be 1 s^{-1} . This

supports the hypothesis that the resistance to deformation caused by surface tension gradients is responsible for the resistance against drainage.

It was found that neither of the theoretical models in literature describing the drainage of films or plateau borders considered here, was able to explain the discharge of liquid from the foam in time. This may be due to the structure of the foam not being ideal or to other sub-processes such as coalescence and disproportionation which may also play a role at the same time. It is more likely however that the mechanism that was assumed to be responsible for the drainage in the model does not represent the actual situation in the foam.

5.2 Introduction

In the previous chapters we have concentrated on determining the surface- and mechanical properties of diverse surface active species mainly under conditions of continuous dilation and in the case the surface is subjected to viscous stresses. These chapters have provided some understanding of the influence of transport to and unfolding at macroscopic surfaces and the relation between surface and mechanical properties. Here we will try to correlate these properties to foaming properties. This is difficult because the surface properties are not correlated in a simple way to the properties of the foam such as bubble size distribution or drainage behaviour. Nevertheless such an exercise may provide useful information about the way the surface properties and foaming properties are interrelated.

We are mainly interested in the difference between the foaming properties of different surface active species at different concentrations. Therefore we chose to study various systems of which one would expect significant differences in foaming behaviour. Also, the concentrations of these surfactants was varied. For protein systems we chose β -casein and β -lactoglobulin. These proteins exhibit a totally different viscoelastic behaviour (Williams and Prins (¹, ²), (this thesis, chapter 2): β -lactoglobulin is a protein which is believed to create a tough adsorbed layer when enough surface active material can adsorb at the surface. This results in a high dilational modulus accompanied by a small loss angle, which means that the surface is almost purely elastic. Adsorbed layers of β -casein for a protein have a fairly low dilational modulus and a larger phase angle indicating that the surface is more viscous (¹), (²). From the unfolding experiments we were able to demonstrate that β -casein unfolds about twice as fast as β -lactoglobulin. Both types of protein have good foaming properties, however.

In order to study the behaviour of low molecular weight surfactants we chose the nonionic Tween 20. In addition we chose to study different combinations of the proteins and Tween 20. Clark et al (³), Clark et al (⁴), Dickinson et al (⁵), De Feijter and Benjamins (⁶) studied these different systems by means of different surface rheological techniques. Generally it was concluded that the low molecular surfactant Tween 20 dominates the mechanical behaviour and adsorbs preferentially in equilibrium. Foaming experiments on these systems demonstrated that the drainage behaviour was determined by the presence of low molecular surfactant Wilde (⁷).

In order to measure the performance of a commercial surfactant, we chose a technical foaming agent, Provoton, which is used to create the foam used for the production of foam concrete. Provoton is a hydrolysate of keratin, made by alkaline hydrolysis at elevated temperatures with sodium hydroxide and subsequent neutralisation by means of hydrochloric acid.

Obvious questions are: how do these systems compare to each other when it comes to foaming, and can we understand differences from their dynamic surface behaviour? Hence, we will need to establish what mechanisms in foam creation relate to the mechanical and surface properties studied here. Foaming properties can generally be subdivided into foam generation properties and foam stability. While foam generation depends on the ability to incorporate gas into a liquid, the stability depends on the ability to keep the gas bubbles dispersed in the liquid. These properties may correlate, but in some cases they do not, such as in the case of transient foams created by mixtures of water and alcohols studied by Tuinier et al. (⁸). This means that the surface properties which keep the foam stable are not the same as the surface properties that determine foam creation. In the previous chapters a clear distinction was made between the time scales and whether the surface is deformed by parallel or normal forces. This has been done to distinguish between situations which may exist in either the foam creation process or in a foam in storage. The success of foam creation depends on different properties and circumstances, such as the shear stress, the viscosity and density of the continuous phase and the geometry of the device. Therefore the influence of surface properties may be interrelated with other factors which may make it difficult to distinguish between these different aspects. During storage we can distinguish again between different types of instability such as drainage, disproportionation and coalescence. In this chapter we will mainly discuss drainage properties because these properties depend on the inhibition of viscous flow around a bubble due to the surface properties.

In order to explain the outcome of the experiments we have to be aware of a number of aspects of the production of the foam by means of the whipping method used here. The method comprises the whipping of a certain amount of liquid for a certain amount of time. These aspects are the following:

A: During the foam production the amount of air in the foam varies in time giving rise to varying bulk rheological properties and density temporally in the foam phase. The rheological behaviour of foams has been studied by Kroezen (⁹). It was demonstrated that foams are shear thinning substances. In addition the inhomogeneity of the foam causes wall slip especially at low deformation rates. The rheological behaviour was shown to depend on the density of the foam and the bubble size distribution as well.

B: As the velocity of the foam will not be equal in all parts of the vessel it can be assumed that bubbles are subjected to cycles of comparative rest and strong deformation. Due to this period of comparative rest bubbles may be considered to be more close to equilibrium with the surrounding liquid than during deformation in the vicinity of the stirrer.

C: Due to vigorous stirring action the bubbles are not only split up but coalesce as well. This may affect the bubble size distribution of the foam since bubbles of different sizes may be more or less susceptible to coalescence and break-up.

D: The presence of a certain amount of liquid from which the foam is made also implies that the amount of foam created is limited. The total amount of gas that can be dispersed into the liquid is determined by the bubble size distribution of the foam and the amount of liquid present and is influenced by the type and the amount surfactant present, the whipping speed and the geometry of the mixer. With the amount of gas incorporated into the liquid the rheological properties of the foam change (see point A).

These four points illustrate the degree of complication encountered when studying foaming behaviour by means of the whipping method. Hence, we should be aware of these complicating factors, which makes it difficult to apply theories described in literature to these systems.

5.2.1 Foam Production

Walstra (^{10, 11}) reviewed the literature on the creation of emulsions and foams and concludes that there are essentially two types of flow by which bubbles can be broken up. A laminar and a turbulent region can be distinguished. The relative importance of these is determined by the

energy input, the geometry of the equipment, the flow regime and many other factors. In laminar flow, bubbles are broken up by means of viscous flows around a bubble, either in shear or in plane hyperbolic flow. A critical Weber number can be defined which equals the ratio between viscous stress and Laplace pressure at which a bubble breaks up. Bubbles can also be broken up by means of inertial forces. In that case local pressure variations are responsible for the breakup of bubbles.

Another parameter determining the breakup is the flow condition at the surface of a bubble. This can be laminar or turbulent, depending on the Reynolds number. In table 5.1 the dependence of bubble radii on the properties of the flow conditions and characteristic properties of the liquid has been given and the different regimes have been indicated.

Flow Type: Breakup by means of:	Laminar flow Shear forces	Turbulent flow Shear forces	Turbulent flow Inertial forces
$Re_{\text{flow}} \frac{r\rho v}{\eta}$	<1000	>2000	>2000
$Re_{\text{drop}} \frac{r\rho v}{\eta}$	<1	<1	>1
drop diameter	$\frac{2\gamma We_{\text{crit}}}{\eta_c G}$	$\frac{\gamma}{\epsilon^{\frac{1}{2}} \eta^{\frac{1}{2}}}$	$\frac{\gamma^{\frac{3}{5}}}{\epsilon^{\frac{2}{5}} \rho^{\frac{1}{5}}}$

Table 5.1 drop diameter caused by different flow and droplet breakup types:

Walstra and Smulders (¹⁰) symbols in list of symbols.

5.2.2 Drainage of foams

Chesters (¹²) reviewed the literature regarding the stability of liquid/liquid dispersions. He distinguishes between three cases: immobile interfaces, partially mobile interfaces and fully mobile interfaces. The drainage is described in terms of the thinning of films. In this chapter we consider not only the thinning of films between bubbles but also the flow of liquid through the plateau borders. A number of models have been described in literature which consider both drainage through plateau borders and drainage through foam films Narsimhan (¹³) Gururaj (¹⁴). Generally, these two types of drainage have different time scales, which depend on the liquid holdup of the foam. In general, the process of drainage can be assumed

to proceed as follows. First, the initially thick films drain rapidly into the plateau borders of the foam. When the film thins, however the drainage is slowed down by the resistance to deformation of the bubble surfaces which hinders the flow from the films. This of course depends on the rigidity of the films in the foam. After this the plateau borders contribute most to the total drainage and the thickness of the films decreases only marginally in comparison to the plateau borders.

For our purpose a distinct drawback of these models is that the surface properties are not linked to the composition of the surfactant solution. The resistance to drainage is generally assumed to be a function of surface tension or a surface dilational viscosity. However it can be seen that proteins for instance usually have a strong resistance to drainage which would not be expected in terms of these models. Our purpose is to obtain an understanding on the surface properties that may explain the stability against drainage of foams created from various surface active species. Hence, only an unequivocal relation between the rate of drainage and the surface properties described in the previous chapters, for various different systems, would prove that this approach is correct.

Hence here we will try to correlate the surface properties obtained by measurements in the overflowing cylinder to the drainage behaviour by normalising the drainage rate to surface areas of the foams. This accounts for the systematic differences in bubble size and volume fraction of liquid. It should also make it more easy to distinguish between the various regimes in the drainage process.

The most logical parameter to which the rate of drainage should correlate is the difference in surface tension between the top and bottom surface of the overflowing cylinder at a certain relative rate of expansion of the top surface, as drainage will cause a lateral motion of the surface. In chapter 1 it was suggested that in that case the surface tension difference between the compressed and expanded surface would give the resistance to deformation in terms of stress.

In table 5.2 the discharge rate from the foam films into the plateau borders and the discharge from the plateau borders has been given for the different regimes.

Drainage type	Film thickness
Immobile interfaces (no flattening)	$h = h_0 e^{-\frac{t}{t_{ch}}}, \quad t_{ch} = \frac{3\pi \mu^c r^2}{2F}$
Immobile interfaces (flattening)	$\frac{1}{h^2} - \frac{1}{h_0^2} \approx \frac{16\pi \gamma^2 t}{3\mu^c r^2 F}$
Partially mobile interfaces	$\frac{1}{h} - \frac{1}{h_0} \approx \left(\frac{2\pi \gamma}{r}\right)^{\frac{3}{2}} \frac{2t}{\pi \mu^d \sqrt{F}}$
Fully mobile interfaces	$h = h_0 e^{-\frac{t}{t_{ch}}}, \quad t_{ch} = \frac{3\mu^c r}{2\gamma}$
Plateau border drainage	$\frac{1}{a_p} = 0.0125 \frac{c_s \rho t}{\mu^d}$ in Narsimhan (¹³)

Table 5. 2 Drainage in various circumstances, Chesters (¹²), symbols in list of symbols.

5.3 Materials and methods

5.3.1 Materials

For the foaming experiments described in this chapter all surface active substances apart from Provoton were dissolved in imidazole buffer pH 6.7 at an ionic strength of 0.075 M.

Imidazole, HCl and NaCl were analytical grade and obtained from Merck and used as received.

β -Casein was obtained from Eurial ref. 041091. Lyophilized β -Lactoglobulin was obtained from Sigma (lot 100h8185). Tween 20 analytical grade was obtained from Sigma.

The proteins and Tween were dissolved by stirring at room temperature for approximately 1 hour and were stored overnight at 4 °C. All substances were used without further purification.

Provoton was kindly made available by Voorbij prefab beton, Wilnis, The Netherlands.

Provoton is a brown viscous liquid containing approximately 30 % hydrolysed protein and 13% NaCl by weight. SDS-page electrophoresis shows that Provoton contains two major high molecular fractions at 17 kD and 60 kD along with low molecular protein fragments below 5kD.

The solutions with Provoton were made by dissolving the material in distilled water and stirring for 5 minutes. The solutions were used immediately after stirring.

5.3.2 Methods

The foaming experiments were carried out as follows. Foams were made in the device depicted in figure 5.1. Liquid was poured in the holding vessel (1) and stirred for 180 seconds. Just before stopping the stirring, a sample of 0.2 ml was taken from the foam and inserted into a cuvet filled with the original liquid. Using a CCD camera fitted onto a microscope several frames of the bubbles were collected in the first minutes after the sample was taken. These frames were analyzed by means of image analysis yielding the bubble size distribution of the foam. Directly after taking the sample the motor was switched off and the height of the foam in the holding vessel was recorded. Then the holding vessel was taken out and placed above a balance and the tap (2) was opened enabling liquid to flow out of the vessel through the sintered plate (3). The weight of the liquid which flowed from the foam was recorded at equal intervals of time. These experiments were repeated for a number of different revolution rates of the whisk and for the different systems.

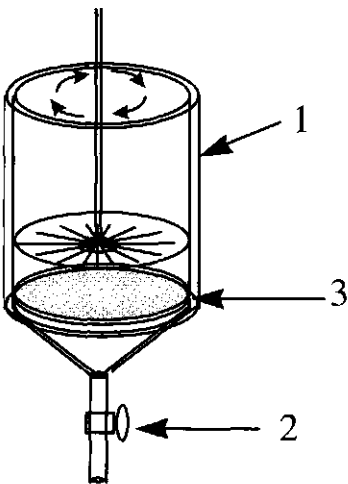


Figure 5.1 Foaming setup used in the experiments

5.4 Results and Discussion

5.4.1 Foam Formation

In figure 5.2 and 5.3 the amount of foam and the volume/area mean bubble radius of a foam created by whipping 200 ml of Provoton and β -lactoglobulin solutions varying in concentration have been plotted as a function of the revolution rate of the whisk.

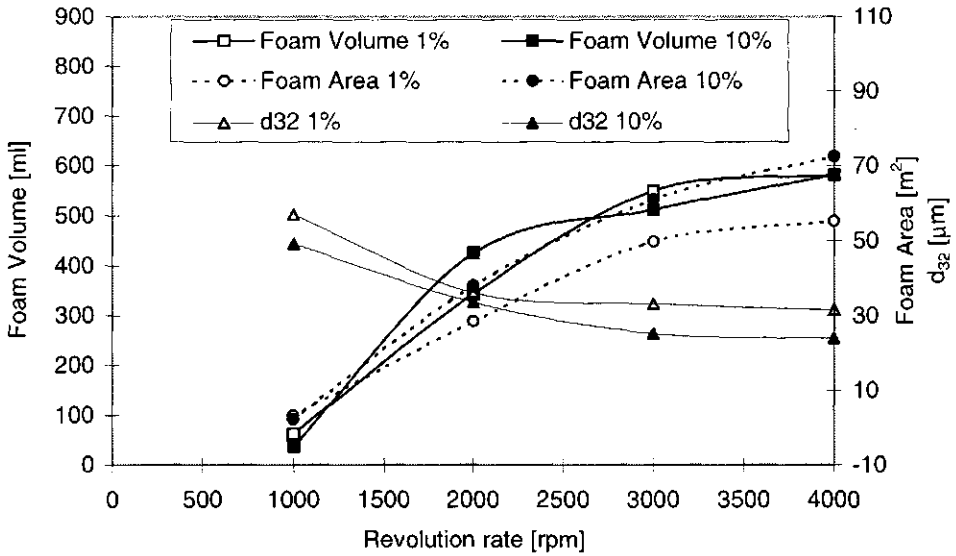


Figure 5. 2 Foam volume, foam area and volume surface mean diameter as a function of revolution rate of the stirrer for Proviton solutions at 1% and 10% by mass.

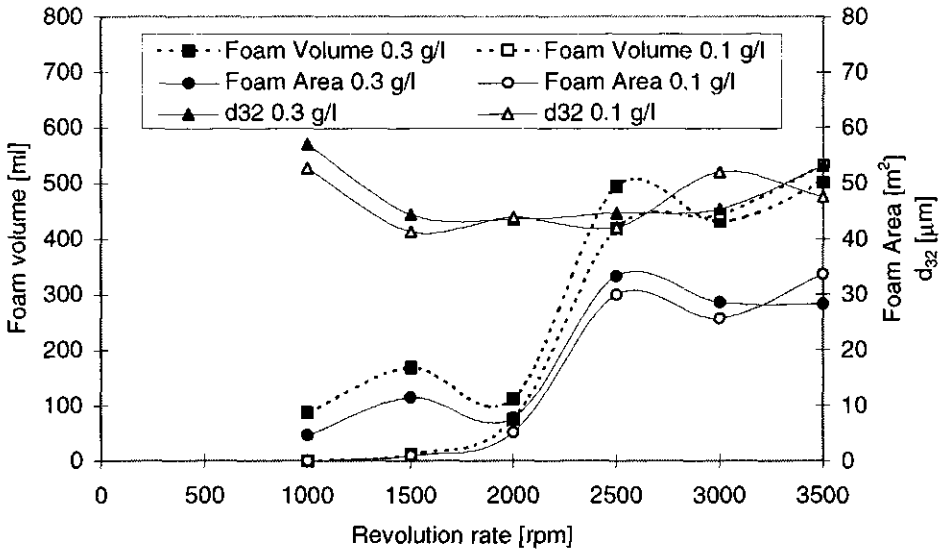


Figure 5. 3 Foam volume, foam area and volume surface mean diameter as a function of revolution rate of the stirrer for β-lactoglobulin 0.1 g/l and 0.3 g/l

From the results in the previous graphs a distinct dependence of concentration and rate of revolution of the whisk can be observed. The amount of foam created can be observed to be relatively insensitive to variations in these concentrations but increases with the revolution rate of the whisk. In contrast we can observe a relative insensitivity of the bubble size to the revolution rate of the whisk while in that case the concentration of the surfactant plays a significant role.

The amount of foam created can be assumed to depend on the creation of a vortex. During the experiment it can be observed that air is sucked in at the centre of the whisk and is dispersed in the foam. The creation of a vortex will depend on inertial effects and therefore will depend on the rheological properties, the density of the foam and the rate of revolution of the whisk. Hence hydrodynamics will mainly be responsible for the amount of foam that is created so for the foam height.

The radii of the bubbles in the foam have been fitted to the equations in table 5.1 In all cases, the calculated decrease of the bubble size is overestimated compared to the situation observed in the foam. This may be due to the relation between the rheological properties and the amount of bubbles in the foam. The calculations are based on the situation in an emulsion where a constant amount of dispersed phase is present which is low compared to the situations in foams. In the case of a foam the amount of dispersed phase does not remain constant but varies with stirrer velocity. Since we do not know the relation between the apparent viscosity and the composition of the foam it is not possible to relate these data directly to theory.

Bergink Martens⁽¹⁵⁾ was able to relate the dynamic surface tension to foaming properties. There may be a relation between the Laplace pressure and the bubble size if the break-up of a bubble is resisted by the Laplace pressure. Here we take the dynamic surface tension as the surface tension at the bubble surface. In that case the Laplace pressure is given by equation 5.1.

$$\Delta p_l = \frac{2\gamma_{dyn}}{r_b}$$

Equation 5.1

This can be calculated using the dynamic surface tension data given in earlier chapters and the bubble radii from the previous graphs. There indeed appears to be a relation between the

Laplace pressure and the bubble size. This has been given in figure 5.4 for all systems studied at revolution rates of 3000, 3500 and 4000. If the bubble radius would be dependent on the Laplace pressure, the stirrer is assumed to create a pressure variation in the liquid causing the break-up of bubbles. In that case we assume that bubbles are broken up by forces acting perpendicular to the surface.

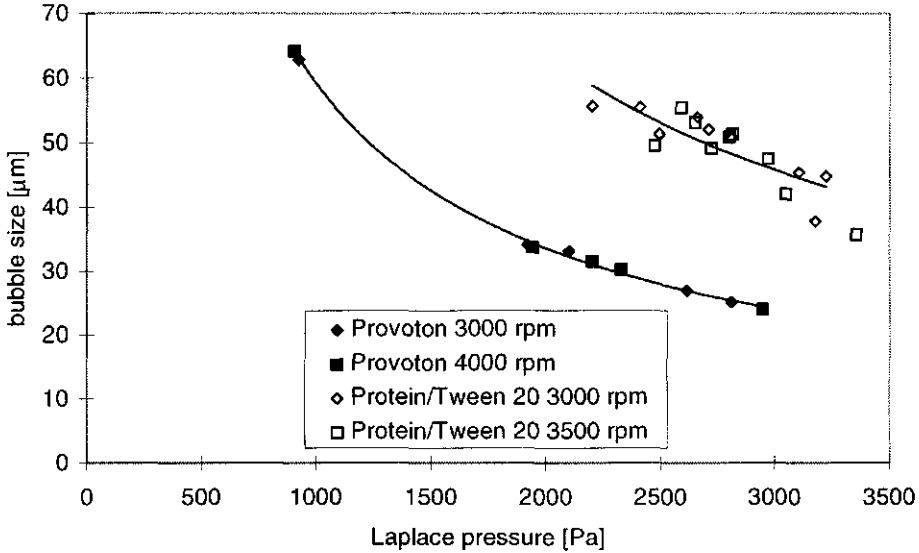


Figure 5.4 Relation between Laplace pressure and d_{32} for Provoton, β -casein/Tween 20 and β -lactoglobulin/Tween 20 systems.

In contrast to what we assumed this figure shows that a higher Laplace pressure correlates to a smaller bubble size. This would mean that a higher surface tension in the expanded surface leads to smaller bubbles. If the Laplace pressure would be an indication of the resistance to bubble breakup we would expect the opposite however. From this figure we can also see that there is a separate relation for the Provoton and the protein/Tween 20 system. Hence the relation appears to be equivocal since there are two distinct lines corresponding to two different systems. This would mean that there would be a system dependent systematic difference.

As the ultimate aim is to obtain a generic relation instead of a specific relation the break-up of bubbles due to viscous forces was also considered. If the difference between the surface

tensions in expansion and compression is divided by the radius of a bubble: $\frac{\gamma_{exp.} - \gamma_{comp.}}{r}$ we

obtain an expression for the mean stress over a surface. If there would be a generic relation between this stress and the bubble size, it would mean that the break up of bubbles takes place by means of a shear stress imposed by the liquid. This relation has been given in figure 5.5.

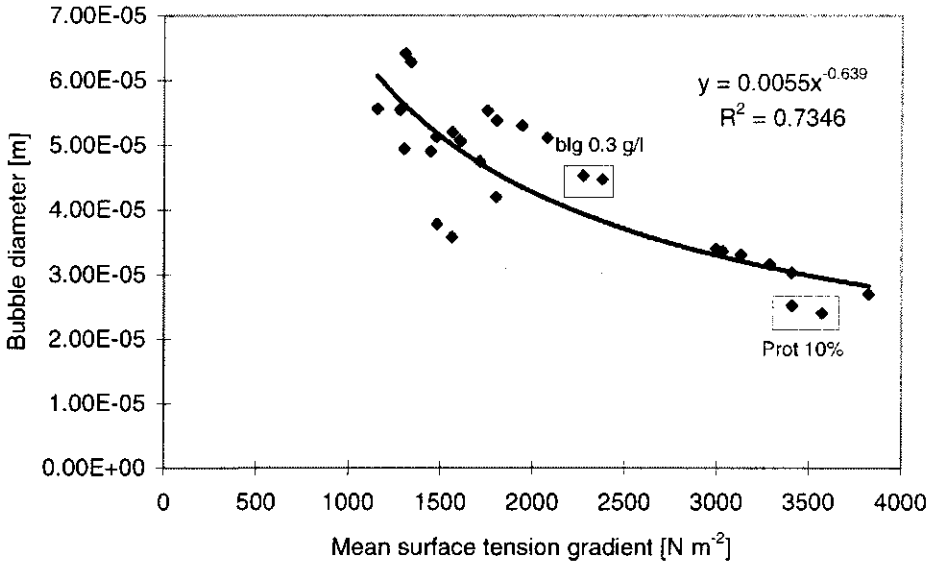


Figure 5. 5 relation between the mean surface tension gradient and the mean bubble size for Provoton, β -casein/ Tween 20 and β -lactoglobulin/Tween 20 systems. Provoton 10% by mass and β -lactoglobulin 0.3 g/l have been indicated for stirring rates 3000 and 4000 rpm.

The surface tension values have been determined using the overflowing cylinder technique and have been shown in chapter 4 already. Considering that the systems studied here differ considerably and the conditions differ also, this relation is surprisingly good. As this relation is generic instead of specific we can assume that indeed this mean stress correlates to the bubble size. Also this relation suggests a negative correlation between the maximum surface tension gradient and the bubble size, indicating that a higher resistance to deformation leads to smaller bubbles. Hence this relation changes the perception of the process that is responsible for the breakup of bubbles near the stirrer. The validity of the relation between the maximum stress at the bubble surface and the bubble size would mean that the stress that can be imposed at a bubble surface is determined by the surface properties of the bubble surface and not by conditions such as stirrer speed that are externally applied.

There may be another explanation for this behaviour. If the coalescence rate would increase due to a higher stirrer speed it would mean that the bubble size would be affected also by coalescence. This should be visible in the bubble size distribution. Since larger bubbles are less stable against coalescence a high rate of coalescence would cause the bubble size distribution to become bimodal. In figure 5.6 and 5.7 the bubble size distributions have been given for respectively 10 % Provoton and 0.3 g/l β -lactoglobulin at different revolution rates of the stirrer.

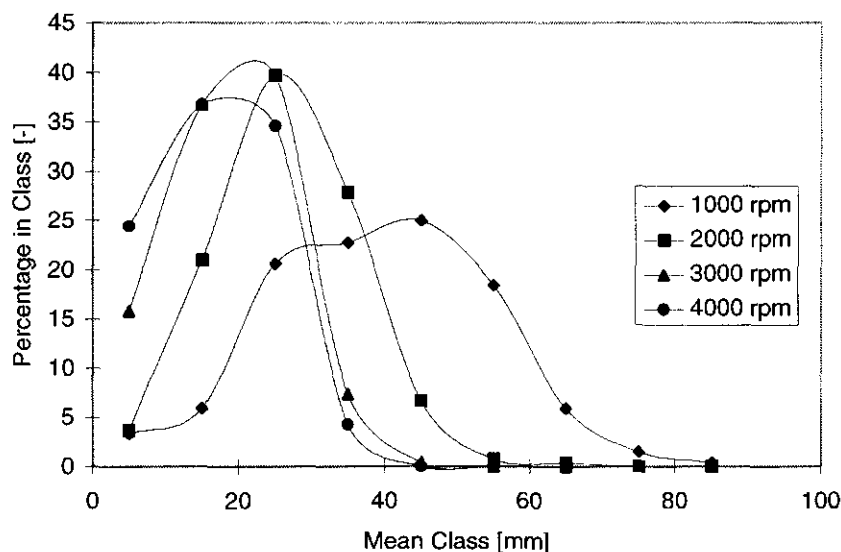


Figure 5. 6 Bubble size distribution for 10% provoton at different rates of revolution of the stirrer.

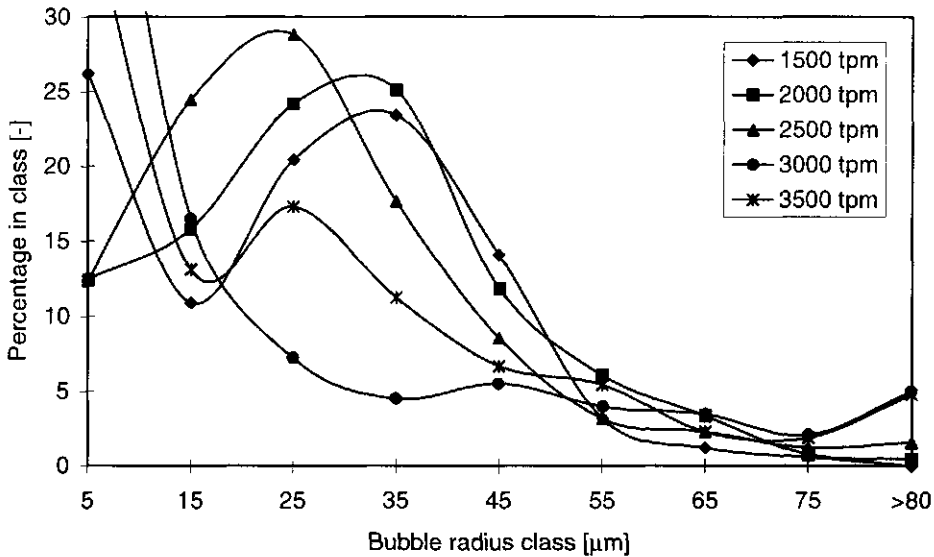


Figure 5.7 Bubble size distribution for 0.3 g/l β -lactoglobulin at different rates of revolution of the stirrer.

From these graphs we can see that the bubble size distribution for Provoton and β -lactoglobulin are different. Provoton has a rather slim distribution at higher revolution rates compared to β -lactoglobulin.

For β -lactoglobulin we can see that the fraction of bubbles above 45 μm at higher rates of revolution of the stirrer is finite. Such a wide bubble size distribution would indeed point into the direction of an increased rate of coalescence for β -lactoglobulin. With Provoton this is not the case. In figure 5.5 the points corresponding to β -lactoglobulin and Provoton 10% have been indicated. All points are relatively near the line which indicates presence of larger bubbles does not significantly influence the general trend.

The overflowing cylinder appears to be a suitable method to study relationships between deformation rate and surface properties parallel to the surface. These properties have been shown to correlate to bubble break-up. This may be somewhat surprising since the expansion rate that is generated at the surface in the break-up process is generally expected to be some orders of magnitude higher than those found in the overflowing cylinder. If we consider however that the maximum stress at the surface limits the "grip" of the liquid flow around the bubble on the bubble surface this correlation could be motivated. In that case the following

mechanism could play a role. Due to the liquid flow around the bubble the surface is expanded in one place and compressed at another, this leads to a net force driving the two ends of the bubble apart which is opposed by the Laplace pressure. If the bubble has reached a certain geometry, it will become unstable leading to breakup. The surface tension difference that can be generated between the expanded and compressed surface is a measure of how effective the viscous stress can be transferred to the bubble. Hence if this surface tension difference is high, smaller bubbles can be created by means of this mechanism.

5.4.2 Drainage behaviour

The systems in this chapter have been chosen in order to facilitate the interpretation of the behaviour within one type of surfactant in different concentrations and between classes of different surfactants. The type of surfactants that has been varied in concentration is Provoton. This type of surfactant has been chosen because we are interested in the performance of protein hydrolysates in comparison to the behaviour of low molecular surfactants and a proteins.

In chapter 4 the competitive adsorption of Tween 20 and β -casein has been studied. Tween 20 appeared to have a large effect on the surface behaviour. Hence also mixtures of Tween 20 and β -casein and β -lactoglobulin were studied.

The interpretation of the drainage behaviour is complicated by the fact that the bubble size distributions and the foam heights are not equal for the systems studied here. Hence the drainage needs to be normalised for these properties in order to quantify the differences between the systems. Here the mean film thickness was chosen to be the normalised parameter. This thickness can be calculated as follows. Consider the total area of the foam. This can be calculated from the mean bubble size by means of equation 5.2

$$A_j = \frac{V_{fg}}{\frac{4}{3}\pi r_{(32)}^3} 4\pi r_{(32)}^2 = \frac{V_{fg}}{\frac{1}{3}r_{(32)}}$$

Equation 5. 2

Then the mean film thickness h_f will simply be

$$h_f = \frac{1}{2} \frac{V_{fl}}{A_f} = \frac{1}{6} \frac{V_{fl} F_{(32)}}{V_{fs}}$$

Equation 5.3

In these equations A_f is the total surface area of the foam, V_{fg} and V_{fl} are respectively the volume of gas and the volume of liquid in the foam. By using these expressions the total area of the bubbles is accounted for in the drainage behavior. This makes it possible to compare foams with more or less equal foam heights, since a different foam height will affect the length over which the drainage takes place. In figure 5.8 the film thickness of foams made at 3000 rpm has been plotted as a function of the time for the different Provoton systems studied.

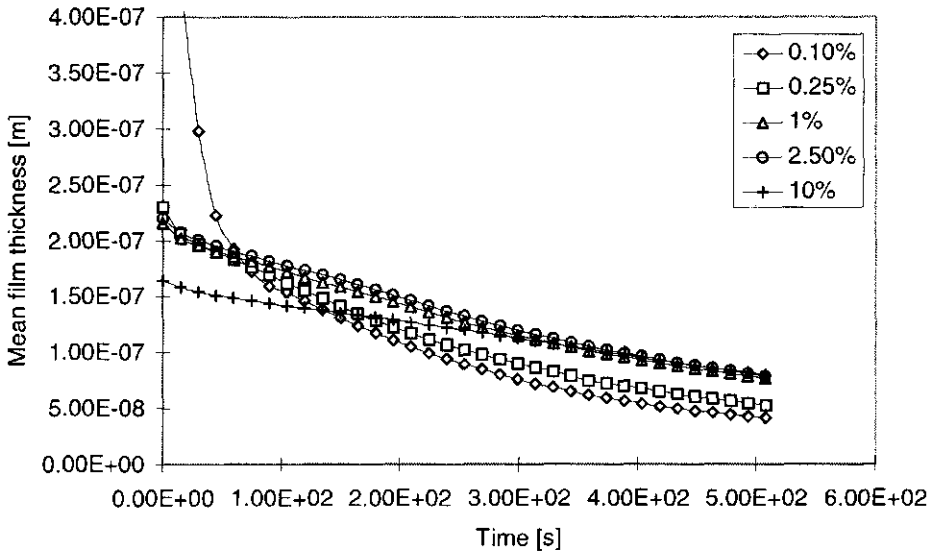


Figure 5.8 Relation between the mean film thickness calculated by equation 5.3 and the time of drainage for Provoton in different concentrations for foams made at a stirrer speed of 3000 rpm.

We can clearly see that there is a significant difference between the different concentrations. First of all the film thickness at the start is large for the foams of low concentrations. This means that when we would like to compare the drainage of the foams at equal film thickness we will have to do that at different times after the creation of the foams.

As theory predicts there are two regimes that can be distinguished in the curves. In the initial phase of the drainage we can observe a relatively quick thinning (a high normalised discharge rate). In this region the film thickness of the lower concentrations are highest because of the larger bubble size and the lower amount of gas dispersed in the foam. This causes the foam to drain faster at lower concentrations. At a certain time the curves of the higher and lower concentrations cross. At that time, the mean film thickness becomes lower for the lower concentrations.

In order to compare the different systems with respect to their drainage behaviour the discharge rate has been normalised to be the first derivative of the film thickness with respect

to time $\frac{\Delta h}{\Delta t}$. In figure 5.9 the discharge rate of the Provoton foams made at 3000 rpm has

been plotted as a function of the film thickness. This makes it possible to quantify the discharge rate at more or less equal conditions in the foam.

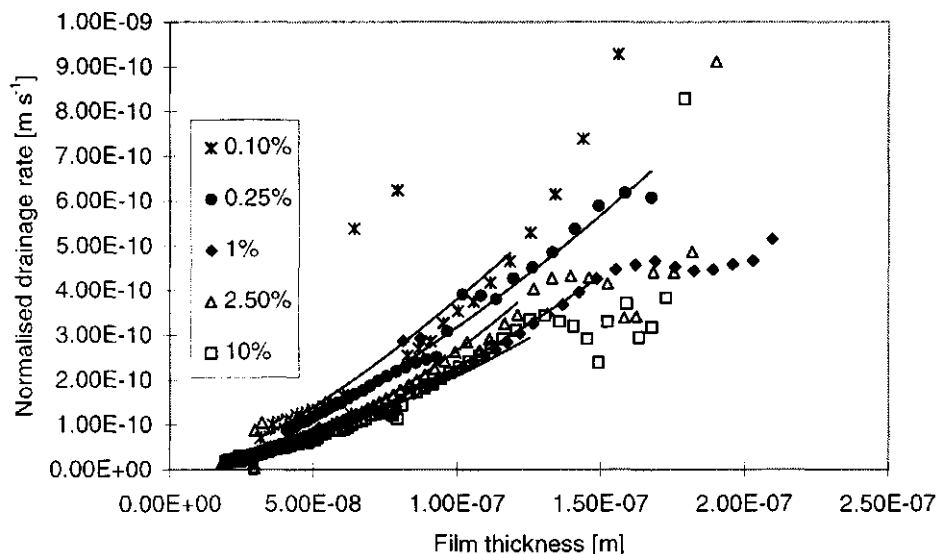


Figure 5. 9 Relation between the normalised drainage rate and the film thickness for different concentrations of Provoton for foams made at a revolution rate of 3000 rpm.

In this figure we can observe a shoulder in the curve for higher concentrations of Provoton around a film thickness of $0.15 \mu\text{m}$. This shoulder corresponds to the end of the initial drainage phase. In this phase of the drainage, the drainage rate is high and decreases until at a

certain point the drainage becomes more or less constant and even shows an increase. This initial region may be the transition from a bubbly foam to a polyhedral foam. After this phase the drainage rate decreases gradually with film thickness. This would theoretically correspond to drainage through the plateau borders. In this phase the discharge rate is related to the film thickness and also the liquid fraction in the foam by a power of approximately 1.5 which was determined from the curves.

In literature it was demonstrated however that the discharge from a foam is related to the squared fraction of liquid in the foam. This discrepancy from theory could be caused by at least two reasons. First of all there is a bubble size distribution rather than just one bubble size which may influence the drainage considerably, in addition other sub-processes such as coalescence and disproportionation occurring in the foams during the drainage process may influence the drainage as well. Hence it is difficult to conclude from these results which mechanism is responsible for the drainage.

Nevertheless we can observe a significant difference between the rates of drainage between the different types of surface active species. As we are interested in the influence of surface properties on drainage, in figure 5.10 the discharge rate at a film thickness of $1 \cdot 10^{-7}$ m has been plotted as a function of the surface tension difference between the top and the bottom of the overflowing cylinder at a relative expansion rate of 1 s^{-1} .

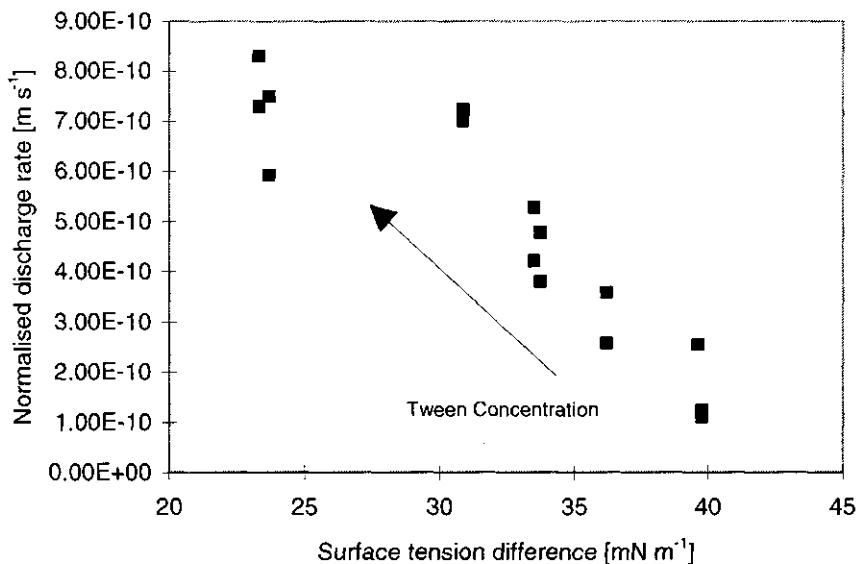


Figure 5. 10 Normalised drainage rate at a mean film thickness of $1 \cdot 10^{-7}$ m as a function of the surface tension difference between the top and bottom surface of the overflowing cylinder at an expansion rate of 1 s^{-1} . Systems considered β -casein/Tween 20 and β -lactoglobulin/Tween 20.

In this figure we can see that a distinct relation between these parameters exists. Over an increase in surface tension difference of 10 mN m^{-1} the normalised drainage rate decreases by approximately an order of magnitude. It should be noted that the thickness of the film and the expansion rate have been taken rather arbitrarily and merely serve to illustrate this relation. The systems in which a considerable amount of Tween 20 is present are in the top left corner of the graph indicating that these systems have little or no resistance to drainage. In the overflowing cylinder it has been observed that the surfaces of systems in which a substantial amount of Tween 20 is present are mobile while the other systems are not. This graph suggests that there might be a mobile/immobile transition around a surface tension difference of 30 mN m^{-1} as from that point on we see a decrease in the normalised drainage rate. With this in mind the explanation of the instability due to drainage of foams of these systems is straightforward. In expansion both the action of the low molecular surfactant and the protein lowers the surface tension. In the compressed surface, Tween 20 adsorbs preferentially causing the protein to desorb from the surface and keeps the surface tension high (in the order of the surface tension in equilibrium) and keeps the surface mobile so the discharge from the films but also from the plateau borders proceeds quick in comparison to the other systems in

the graph. In the case of pure proteins, the surface tension is rather high in the expanded part of the surface but can drop to very low values in the compressed part of the surface. Hence the drainage rate and the surface tension difference between the top and bottom surface of the overflowing cylinder at an expansion rate of 1 s^{-1} correlate with each other. It should be noted that the expansion rate of 1 s^{-1} has been taken rather arbitrarily. Of course the expansion rates at surfaces in the foam will not be equal if there is a significant difference between the drainage rates. Considering this the correlation is still remarkably unequivocal.

Considering this relation we should realise that both the surface tension in compression and the surface tension in expansion play a significant role in the stability against drainage. This means that more than just one time scale determines the behaviour of the surface. This consideration may also apply to other intricacies observed in foaming properties of proteins as these are the substances that are influenced most by properties of the compressed surface as the surface tension is very low while for low molecular surfactants the surface tension remains more or less around the equilibrium value. A condition for these relations to apply is that the surface must be deformed by a force parallel to the surface. It may be that the large stability to coalescence of proteins is in fact due to the resistance in lateral direction of the surface caused by surface tension gradients.

In Chapter 1 a classification has been made to create a certain order in the way surfaces can be assumed to be deformed in the several sub-processes occurring in foams. From this subdivision we can see that spreading and coalescence may also be influenced by forces imposed parallel to the interface. Spreading is caused by the generation of surface tension gradients. Coalescence may depend on the resistance of a surface to lateral deformation because the flow of liquid in a film can be inhibited by a high surface tension gradient. This can cause the films to become thin after a longer period of time, causing the probability of coalescence to be lower.

5.5 Conclusions

In this chapter various aspects of foam making and foam drainage of various systems were studied. The main aim was to obtain relations between the properties measured by means of the overflowing cylinder technique and characteristic properties of foam formation and

stability to drainage. Since we were interested in generic correlations, systems were chosen that could be considered to be very different in both foaming and surface behaviour. The foam creation process is known to consist of the incorporation of air into the foam and a subsequent breakup to smaller bubbles. For the systems investigated it was found that the incorporation of air into the liquid only depended on the revolution rate of the whisk and can be assumed to be completely hydrodynamically driven. The bubble size did not correlate to the theories currently in use for predicting the bubble size. It could be shown however that the mean bubble size could be correlated to the maximum amount of stress that can be transferred to a surface as determined by the overflowing cylinder technique. This indicates that the limitation to breakup of bubbles can be considered to be a surface property rather than a parameter that can be influenced by simply increasing the intensity of the stirring. It also indicates that in creating foams compressed surfaces do play a significant role. In literature the properties of surfaces in compression have not been studied in great detail hence more information on these properties may provide useful information

In order to correlate the drainage properties to the surface properties the drainage was normalised to the film thickness in order to obtain comparable data for the drainage process between the different foams created. These were shown to differ considerably between the different systems studied which could be ascribed to surface properties in terms of the difference in surface tension between the top and bottom liquid surface as observed in the overflowing cylinder device.

This leads to the conclusion that the surface properties of both compressed and expanded surfaces are relevant for the breakup and drainage occurring in foams. This may not only be true for the processes of foam formation and drainage but could also apply to other destabilising mechanisms which are driven by forces acting parallel to the surface such as coalescence.

Appendix 5.1 List of symbols

a_p	Cross sectional area of Plateau border	[m]
c_v	Inverse dimensionless surface viscosity	[-]
F	Force	[N]
G	Shear rate	[s ⁻¹]
h	Film Thickness	[m]
r	Radius bubble	[m] (break-up equations)
r	Film radius	[m] (drainage equations)
t	Time	[s]
t_{cb}	Characteristic time	[s]
v	Velocity	[m s ⁻¹]
We	Weber Number	[-]
ϵ	Energy density	[Ns ⁻¹ m ⁻²]
γ	Surface tension	[Nm ⁻¹]
η	Viscosity	[Nsm ⁻²] (breakup equations)
μ	Viscosity	[Nsm ⁻²] (drainage equations)
ρ	Density	[kg m ⁻³]

Superscripts

c	Continuous phase
d	Disperse phase

Chapter 6

General discussion and conclusions

6.1 Introduction

In chapter 1 the aim of this thesis was described as: obtaining an understanding on the foaming properties of protein hydrolysates. In first approximation it was considered that the behaviour of protein hydrolysates could be approximated by a mixture of proteins and low molecular surfactants. Since we only know little about the dynamic adsorption processes of protein, the approach chosen here was to fill in a number of gaps in our understanding of the foaming process, especially for protein like substances. In order to do so the relations between surface properties, mechanical properties of the surface and foaming properties need to be understood. In the analysis of the problem we also came across the fact that deformations of surface by forces applied parallel to the interface has received little to no attention in the past while these deformations may play a large role in foaming properties. In addition time scales of unfolding of proteins at interfaces are largely unknown while these may also play a large role in the foaming properties of proteins. These subjects can be assumed to be relevant for the interpretation of foaming properties of protein like foaming agents.

In this chapter we will ask ourselves the following question: Has this work brought us any closer to the understanding of foaming in general and especially the foaming performance of protein hydrolysates? In order to answer this question, first we will highlight the most important findings. After that we will extrapolate these findings to their practical implications for foaming in general and using this basis, come to a hypothesis regarding the behaviour of protein hydrolysates.

6.2 Important findings

In the creation and stability of foams we can distinguish between various sub-processes that play a role. In order to make a foam it is essential that a large bubble can be broken up into smaller bubbles. In foam breakdown we can distinguish between various mechanisms that ultimately cause the breakdown of the foam such as drainage, disproportionation and coalescence of bubbles. In order to understand the foaming process we have to take these

sub-processes into account. In order to understand the rate at which these sub-processes take place in relation to the surface properties we need to mimic the conditions as closely as possible in the equipment we use to characterise the surface properties.

All these sub-processes can be considered to act over certain characteristic time scales which in turn depend strongly on the surface properties of the functional substance that causes the foaming behaviour. As time scales play such an important role, the surface properties have to be considered as a function of time scale as well. The time dependence of the surface properties are determined by the adsorption rate to the surface and for macromolecular surfactants also the time required to unfold at the surface.

Another important aspect of these sub-mechanisms which is often forgotten is that the surface is deformed in a certain manner, characteristic for the sub-process. In chapter 1 a distinction was made in the way surfaces can be deformed. We made a distinction in the direction with respect to the surface in which a force can be applied (tangential or normal). It could be demonstrated that if a force is applied parallel to the surface this leads to a inhomogeneous deformation of the surface, meaning that the surface properties such as surface tension, surface concentration and relative expansion rate vary over the surface. In the case of a homogeneous deformation which takes place in the case a pressure is applied on a bubble, the surface properties remain constant over the surface. Hence we could make a division of the sub-mechanisms determining foaming properties on the basis of these different types of deformation.

6.2.1 Foaming properties

In chapter 5 we concluded that the resistance to deformation of a surface parallel to the surface is important for the rate of drainage and the bubble size which can be generated at a constant rate of revolutions of a stirrer. This resistance to deformation is caused by a gradient in surface tension over the surface which originates from the response of a surface to a viscous flow parallel to the surface. If the resistance to this type of deformation increases, the drainage rate decreases. This can be ascribed to a decreased mobility of the surface around a bubble which inhibits the flow of liquid around it.

Surprisingly it was found also that a higher resistance to deformation parallel to the surface causes smaller bubbles to be formed during stirring. This can be ascribed to the following mechanism. When a bubble is broken up by means of shear, the bubble becomes unstable at a

certain critical ellipsoidal shape of the bubble. In order for the bubble to attain such a geometry the Laplace pressure causing the bubble to maintain its circular shape must be overcome. This can be achieved by the drag caused by the liquid motion around the bubble. This drag force must somehow be transferred from the bulk liquid to the surface. One way by which the drag force of the liquid can be applied is by means of a shear stress at the surface of the bubble. As a response to the drag force the surface is expanded at a certain place and compressed at another. This means that there is a net force driving the two ends of a bubble apart and causing it to assume an ellipsoidal shape. An important issue here is how effective the drag force can be applied at the surface and what stress needs to be transferred for the bubble to break. When the resistance to the viscous drag is high, this means that the drag is transferred effectively to the surface which means that the bubble is exposed to a larger stress causing it to be deformed to a larger extent. This leads to a larger degree of instability of bubbles with an equal radius exposed to the same flow profile around the bubble which will ultimately lead to smaller bubbles.

Hence an important issue is how the transfer of the viscous drag can be manipulated. In the last chapter it was found that in that respect, the type and the concentration of surface active species is an important factor.

An important a priori consideration was that the time scale plays a significant role in the behaviour of the surface. When a uniform expansion or compression is considered, the relative expansion rate defines the life time of the surface. This time scale can be compared to time scales of, for instance, disproportionation. However, in the situation that the surface is deformed by a force parallel to the surface we find a *range* of relative expansion rates over the surface. Hence, in this situation we cannot define a single time scale.

6.2.2 Mechanical properties of surfaces

With the overflowing cylinder it has been demonstrated that there is a certain limit to the mean surface tension gradient that can be generated at the surface of a certain solution of surface active material. In the overflowing cylinder this can be determined by measuring the surface tension difference between the compressed and the expanded surface at maximum relative rate of expansion of the expanded surface at fixed settings of the overflowing cylinder. This mean gradient varies from system to system. E.g. proteins can generate a higher surface tension difference between the expanded and compressed part of the surface

than low molecular surfactants under the same conditions. Hence, the shear stress that can be transferred to the surface by the viscous flow along the surface is dependent on the type of surface active species present. The fact that the maximum shear stress (σ_{\max}) that can be generated in an overflowing cylinder correlates with the size of the bubbles generated in a whipping process demonstrates that σ_{\max} is a measure of the driving force of bubble splitting under the conditions studied here. This indicates that forces that work parallel to the surface are possibly more important for the creation of foams than presumed.

6.2.3 Influence of transport and unfolding for dynamic surface properties

The difference between the surface properties of proteins, surfactants and mixtures of these surface active species have also been determined using the overflowing cylinder technique. Especially proteins have received considerable attention in this research, since these substances are the raw materials of protein hydrolysates and may have properties comparable in some cases. It was considered that the unfolding of proteins at interfaces may be a rate determining step in the adsorption process. By means of experiments with the overflowing cylinder, and using a simple model, the rates of attachment and unfolding could be determined separately. It was found that in expansion the unfolding can indeed be a rate determining step in the adsorption process. This depends on conditions of concentration and unfolding rate at the surface.

Generally speaking, the unfolding rate of the protein plays a significant role in the magnitude of the surface tension in expansion provided the relative expansion rate is comparable to the unfolding rate of the protein. In that case, the decrease of surface tension due to unfolding of proteins at a surface element of the surface is balanced by the increase of surface tension caused by the dilution of molecules due to the expansion of the surface. This situation generally occurs at higher concentrations of the protein. The unfolding behaviour of proteins determines for a large part the behaviour at expanding surfaces at higher concentrations which are generally relevant to the industrial practice.

An important conclusion is also that the rate of unfolding of proteins may differ over several orders of magnitude. It was found that β -casein and β -lactoglobulin unfold in 0.1 and 0.25 seconds respectively whereas Lysozyme does not unfold to any degree in 100 seconds. The conclusion was that the conformational stability of proteins is important for the rate of

unfolding at the surface. In addition a certain adsorption barrier was found for Lysozyme. This corroborates the observation of van Aken and Merks (¹).

As it has been found that also the situation in the compressed part of the surface is important for the foaming properties, the unfolding rates of proteins could not be simply related to the foaming properties. Hence, also the situation in the compressed part of the overflowing cylinder was studied by measuring the surface tension. It was found that in compression the surface tension of protein solutions is relatively low. When an adsorbed layer of proteins is compressed, the adsorbed proteins desorb very slowly from the surface because desorption comprises the refolding and diffusion away from the interface, both of which are slow processes

The relatively low value of the surface tension in compression and the relatively high value of the surface tension in expansion enables proteins to generate a high surface tension gradient when exposed to drag forces parallel to the surface.

With experiments and calculations on low molecular weight surfactants it was found that these substances adsorb rather quickly due to the absence of a time consuming unfolding step and a smaller diffusion length. In expansion this tends to keep the surface tension relatively close to the equilibrium value. In compression essentially the same consideration applies. The desorption of low molecular surfactants from a compressed surface is rapid due the absence of a refolding step. This causes the surface tension in compression to be relatively close to the equilibrium value as well.

Hence interesting systems to study are mixtures of surfactants and proteins. Here the system β -casein/Tween 20 was studied. In this situation two species are present at the surface. In static conditions it has been found by others that the low molecular surfactant is able to displace proteins from the interface due to the higher binding energy of low molecular surfactants per unit area.

At expanding interfaces, proteins and surfactants were found to adsorb in a more or less additive manner. The decrease of surface tension at the expanded surface is higher than the added decrease of surface tension of both species individually. This can be attributed to the fact that both species occupy a certain area at the surface causing the effective surface concentration of both species to be higher.

In compression we find a surface tension which is close to the equilibrium surface tension of the low molecular surfactant however. This surface tension is generally higher than the surface tension of the compressed protein surface. Hence, the protein apparently does not play a role of significance at the compressed surface.

These observations can be explained by considering the time scales in terms of the relative rate of expansion or compression of the surfaces. In the expanded surface, the supply to the surface or the rate of unfolding are limiting the decrease of surface tension. In that situation proteins are capable of adsorbing to the surface along with low molecular surfactants because the surface is not fully occupied and the surface tension is relatively high.

In the situation the surface is compressed, proteins desorb preferentially. This can be assumed to be caused by the relatively high adsorption energy per unit area of low molecular surfactants. In this situation the desorption of proteins proceeds more quickly than when just proteins are present at the surface. Essentially the same mechanism has been encountered for the displacement of polymers by low molecular surfactants at solid surfaces as observed by Dijt (²).

6.3 Significance for practical situations

What do these conclusions and observations tell us about the way we need to interpret surface properties to explain the effect on foaming properties? First of all, we can say that the subdivision into forces applied parallel or perpendicular to the surface has been found to be beneficial for the understanding of foaming properties. From this subdivision we can understand in what situation we have to consider surface tension gradients as driving forces for a process and in what situation we have to consider dilational moduli or surface dilational viscosities instead.

As we have devoted most of the attention in this thesis to deformations of surfaces by parallel forces we can now attempt to make predictions of the consequences of the presence of a certain surface active species for drainage, creaming, and bubble break up by means of shear forces since these processes can be assumed to depend on the resistance to forces acting parallel to the surface.

6.3.1 Resistance to creaming and drainage of foams

Drainage and creaming are both processes which can be inhibited strongly if the resistance to deformation parallel to the surface is large. In the previous chapters we have seen that this resistance depends on the type of surface active species. In general we can say that adsorbed layers of proteins can generate a high surface tension gradient, even at low deformation rates of the surface. If we consider figure 6.1 which indicates the surface tension in the compressed and expanded surface of the overflowing cylinder as a function of the relative expansion rate for (i) a protein, (ii) a surfactant (iii) a mixture of a surfactant and a protein and (iv) Provoton (a protein hydrolysate) we can see that even at low expansion rates, the difference between the surface tension in expansion and compression remains high, while for the mixture of protein and low molecular surfactant this difference quickly decreases around expansion rates around 1.

We now consider the following example to illustrate the significance of these findings: Suppose the potential viscous drag caused by the liquid flow around a bubble would be enough to create a surface tension difference of a certain magnitude between the top and the bottom of a creaming bubble. In figure 6.1 we can see that a certain surface tension difference corresponds to a certain relative rate of expansion which is lower for proteins than it is for low molecular surfactants.

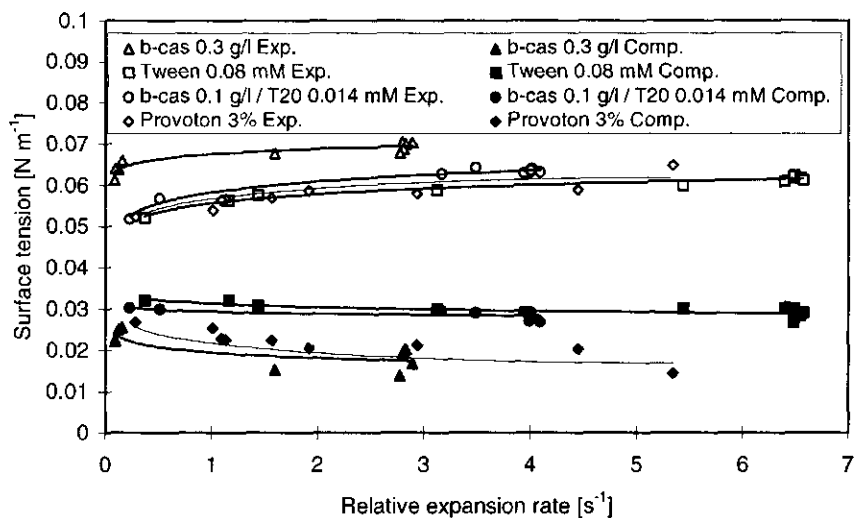


Figure 6.1 relation between surface tension in compression and expansion as a function of the relative expansion rate of the top surface in the overflowing cylinder for different substances.

This means that in the case that low molecular surfactants are present, the expansion rate of the top surface will be much higher. Hence the surface will be much more mobile than the corresponding protein surface. This will cause the drainage rate to be much higher in the case of low molecular surfactants, since the rate of flow of liquid through a film between two bubbles is much higher. It can be seen also that mixtures of proteins and surfactants will compare best to low molecular surfactants in this respect. Indeed we see a higher drainage rate for low molecular surfactants and mixtures of low molecular surfactants and proteins compared to proteins alone. Hence, from these measurements we can understand the difference in drainage rate of foams made by different types of surface active species.

6.3.2 Bubble break up by viscous forces

In the case of break-up of bubbles by means of viscous forces we have observed that the maximum surface tension difference between the compressed surface and the expanded surface of the overflowing cylinder is correlated negatively to the bubble size. Hence a high surface tension difference gives smaller bubbles. This has been explained by the fact that the transfer of stress is determined by the surface tension difference that can be generated between the expanded and the compressed part of the bubble surface if we assume that the

potential stress that maximally can be generated is not limiting. In figure 6.1 we can see that of all species, proteins can generate the highest surface tension difference, although the relative expansion rate is generally lower than that for some low molecular surfactants and mixtures of proteins and surfactants. Hence, from these experiments it should be possible to estimate the magnitude of the mean bubble size created by whipping, for different types of surface active species.

The relative rate of expansion at which this maximum in surface tension difference is reached merely tells us to what degree the surfaces tends to yield to the viscous drag imposed. Hence, essentially the relative rate of expansion merely indicates the mobility of the surface in this case and can be seen as the mechanism by which the surface tension difference is created at the bubble surface.

Can we now also understand what the optimal concentration for the creation of small bubbles will be of various surfactants on the basis of these findings? Since this has not been explored in detail we shall have to make an educated guess. Because it has been established that a high surface tension difference between the expanded and compressed surface at the maximum expansion rate is apparently the main factor that determines the bubble size, the smallest bubbles will be obtained at the concentration when this value reaches a maximum. Here we assume that bubble break-up will occur by a gradual deformation of the bubble to the point of instability. For proteins the surface tension in expansion in most cases will reach 72 mN m^{-1} at the maximum relative rate of expansion. Only in the case that the relative rate of expansion is smaller than the unfolding rate of the proteins and the concentration is high, the surface tension will deviate significantly from 72 mN m^{-1} as in the case of β -casein at higher concentrations. Hence, the surface tension at the expanded surface will generally not play any role of significance in the magnitude of the bubble size. Therefore the surface tension in compression will play the most important role in most cases. The surface tension in compression of proteins will depend on two mechanisms, which are: (i) the rate of desorption, (ii) the supply from the expanded surface. The supply to the compressed surface will be high in situations where also the relative rate of expansion of the expanded surface is high and the surface concentration of especially unfolded proteins is high. Increasing the concentration of protein will most probably lead to a maximum in the relative rate of expansion as has been calculated in chapter 2. In that case the supply to the compressed surface will most probably reach a maximum causing the surface tension in the compressed

part of the surface to be lowest. Hence, the optimal concentration to create small bubbles will probably be in the order of the concentration at which the maximum in the relative rate of expansion is reached. The rate of desorption of proteins from compressed surfaces has not been explored in this thesis so no information is available on this subject. MacRitchie (³), however, concluded that the rate of desorption of proteins depends strongly on the molecular weight of the protein. Large molecules tend to desorb more slowly than smaller molecules. Hence a high molecular weight would probably cause a lower surface tension in compression. The surface tension in compression will probably not be very dependent on the protein concentration, and the relative rate of expansion of the surface since the desorption of the protein is so low that the surface concentration will be very high regardless of the supply

In the case that low molecular weight surfactants are present in the surface of a bubble which is broken up by means of viscous forces, we find that in compression the surface tension is close to the surface tension in equilibrium since the desorption proceeds quickly. Hence, the surface gradient that can be created will depend mostly on the increase in surface tension due to expansion. Bergink Martens (⁴) found a maximum in the surface tension difference between the expanded and the equilibrium surface tension when the concentration of surfactant in solution was increased. This would indicate that there would be an optimal concentration for surfactants to obtain small bubbles. This has indeed been found in the calculations performed in chapter 2 but was not confirmed in experiments. The explanation of this optimum is that in that situation the sensitivity of the surface tension to the relative rate of expansion reaches a maximum. Below this maximum, the generation of surface tension gradients is inhibited due to a lower supply of surface active molecules to the surface. Above this maximum, the supply is too high to deplete the surface fast enough from surface active material by the expansion of the surface.

This opens a rather unforeseen prospect to use the model presented in chapter 2. Since the model can be used to estimate the concentration at which the maximum relative rate of expansion is reached, this opens the opportunity to calculate the optimal concentration for the creation of small bubbles since at this concentration the surface tension difference between a compressed and expanded surface will reach a maximum. It is not sure however if the amount of small bubbles will indeed decrease if the concentration is increased since this was not

explored in this thesis. Nevertheless it could help to calculate a minimum concentration at which optimal foaming can be achieved.

Bergink-Martens (⁴) also established that there is a relation between the amount of foam created by shaking and the dynamic surface tension. It has been found that in contrast to low molecular surfactants proteins do not reach low surface tensions in expansion. If this relation should apply for various types of surfactant we would be able to understand why foam creation with proteins is difficult whereas with proteins small bubbles are created. This would mean that the creation of small bubbles would be caused by a different process than the creation of larger bubbles. Since we found in the experiments that the theories on bubble formation did not match the bubble sizes found, we can assume that these will generally apply for the larger bubbles created in the foams. In these theories indeed the surface tension in expansion does play a role of significance according to Walstra and Smulders (⁵). Of course the influence on the two processes amount of foam and small bubble size, will depend on circumstances like type of foaming device, amount of energy dissipated, type of surface active species present and concentration.

6.4 Foaming properties of protein hydrolysates

If we now extrapolate these findings to the foaming properties of protein hydrolysates we can understand why these substances can be very effective in the creation and stabilisation of foams. Protein hydrolysates can be considered to consist of chains of amino acids of different molecular size of which the primary, secondary and tertiary structure has been disrupted by the hydrolysis. The adsorption of the hydrolysates at expanding surfaces will proceed quickly in comparison to proteins since the molecules are smaller and possibly do not require a time consuming unfolding step as in the case of native globular proteins. In addition the distribution of molecular weights will promote the transport of enough surface active material. The surface tension in expansion will be less sensitive to the relative rate of expansion than proteins and will therefore be below 72 mN m^{-1} . This would explain why formation of larger bubbles in a foam will be more easy with protein hydrolysates compared to proteins.

It can be assumed that in the case of hydrolysates, the larger molecules will adsorb preferentially because the monomeric energy of adsorption is similar for the molecules. In

that case it has been demonstrated by Dijt (²) that larger molecules adsorb preferentially at solid surfaces. In contrast in mixtures of surfactants and protein molecules are displaced by low molecular surfactants. Hence, as a function of time scale it may well be that there is a shift in the molecular size of the adsorbed molecules towards a higher molecular weight at longer times. In a compressed surface this will cause the larger molecules to dominate over the lower molecular weight fractions. This will cause the surface tension in the compressed surface to be significantly lower than the surface tension in equilibrium because the desorption from the surface is slow since both the rearrangements at the surface and the diffusion from the surface are slow processes for these large molecules. This will cause the surface tension between the expanded and compressed surface to be high. We found that in this situation also smaller bubbles can be created which would lead to a smaller bubble size in the foam.

As we have seen in chapter 5, the rate of drainage depends on the surface tension difference between the compressed and the expanded surface of the overflowing cylinder. From Figure 6.1 we can see that for Provoton this difference is comparable to that for proteins. Hence, the drainage of these substances will be relatively slow in comparison to low molecular surfactants.

Hence, the Provoton hydrolysate more or less combines the advantages of a low molecular surfactant with the advantages of a protein with respect to adsorption and foaming behaviour, which explains the good foaming properties of this foaming agent.

If we consider the model system chosen to mimic the competitive adsorption of low molecular surfactants and high molecular surfactants namely, β -casein/Tween 20 we can observe that in practical situations this will not compare with protein hydrolysates due to the fact that Tween 20 has the tendency to drive the high molecular weight β -casein out of the surface in compression. This causes the surface tension in compression to be close to the equilibrium surface tension of Tween 20 in a compressed surface. This will cause the formation of large bubbles due to a low surface tension in expansion but will inhibit the creation of smaller bubbles. Also, drainage will be fast due to the high mobility of the surface. In general we can conclude that the combination of a low molecular surface active species having a high affinity for the surface with a protein is not effective for the improvement of foaming properties.

Summary

The research described in this thesis covers a number of aspects of the relation between surface properties and foaming properties of proteins, low molecular surfactants and mixtures thereof. This work is the result of a question of the industrial partners if it is possible to understand the foaming properties of protein hydrolysates. As there are many aspects of the surface properties that can be responsible for the foaming behaviour a number of problems were defined by which we can obtain a better understanding of the relation between surface properties and foam formation and stability in relation to the type of surface active substance.

In this thesis an important question a priori has been: How can we understand the foaming properties from the properties of the surface active species. We presumed that the molecular properties cannot be translated forthwith to foaming properties but that a number of translation steps are necessary. First of all the molecular properties need to be translated into surface properties which manifest themselves in mechanical properties of surfaces and films. In addition there is a relation between these mechanical properties and the foaming properties.

An important consideration a priori was that the way in which the surface is deformed is important for finding the relevant relation between the mechanical properties and the foaming properties. Here we made a distinction in two types of deformation being deformations caused by forces applied parallel and perpendicular to the surface.

A force that is applied perpendicular to the surface (pressure) generally leads to a homogeneous deformation of the surface. The properties of the surface change with time or time scale but at the surface there are no differences with respect to surface tension, surface concentration or relative rate of expansion. Forces applied perpendicular to the surface generally lead solely to enlargement or reduction in surface area. Forces applied parallel to the surface (shear forces) can also lead to enlargement or reduction in surface area. These forces are generally due to viscous friction with the surface. In addition to a change in surface area these forces also cause a redistribution of surface active material over the surface. Hence the surface concentration, the surface tension as well as the relative rate of expansion vary over

the surface. This leads to a surface tension gradient that is necessarily equal to the viscous drag at the surface.

It is striking that in literature only homogeneous deformations are studied in detail. This fact can be attributed to the difficult experimental accessibility of surfaces subjected to shear forces. Nevertheless shear forces may play a role in the foaming properties such as in drainage and bubble break-up. An important part of this thesis will be devoted to the relation between viscous friction and surface motion.

A device which enables the quantification of the relation between viscous drag and motion of the surface in relation to the surface properties is the overflowing cylinder. This device consists of an inner cylinder surrounded by an outer cylinder with a larger diameter. In this inner cylinder liquid is pumped up which flows over the rim into the space between the inner and outer cylinder. At the top surface we find a continuously expanding surface of which the relative expansion rate remains approximately constant over the surface in the vicinity of the centre of the cylinder. The expansion rate of the surface can be influenced by changing the length of the falling film. Hence within certain limits the expansion rate at the top surface can be varied. If we consider the falling film at the leading edge of the inner cylinder the falling motion of the liquid in the film causes the deformation of the surface parallel to the surface. If we would be able to measure the properties of the falling film we could learn how the surface properties vary with distance. However the surface of the falling film is experimentally not accessible. Therefore in this thesis the changes in surface properties of the falling film have been studied by measuring the surface tension of the top and bottom surface at a fixed place. This provides a reasonable measure of the surface tension difference over the falling film of the overflowing cylinder.

In order to interpret this difference, the conditions at the falling film have been approximated by means of simple hydrodynamic theory. From this approximation we could conclude that there is a relation between the relative expansion rate, the length of the falling film and the surface tension difference. The surface of the falling film is propelled by the falling motion of the liquid which causes a surface tension gradient at the surface as a consequence of the viscous drag. If we compare the calculations with experimental data we can find that this approach is in agreement with the

experiments. Hence the difference in surface tension over the falling film can be considered to be a measure of the resistance to deformation of the surface to forces applied parallel to the surface.

The surface tension gradients which could be generated by means of different surface active species appeared to differ significantly from each other. Especially the difference between low molecular surfactants and proteins could be shown to be large. This can be ascribed to the sensitivity of the surface tension of these substances to expansion and compression of the surface. Adsorbed layers of proteins have a high surface tension in expansion. This can be explained by the time required for unfolding at a surface of these substances. In compression low surface tensions are found for proteins due to the slow desorption of proteins. The surface tension of low molecular surfactants is less sensitive to compression and expansion. In expansion the relatively short diffusion length causes the surface tension to deviate much less from the equilibrium surface tension. In compression these substances desorb easily causing the surface tension to be close to the equilibrium surface tension as well. Hence the surface tension gradient that can be generated by proteins is much larger than for low molecular surfactants. If mixtures of low molecular surfactants and proteins (Tween 20 and β -casein) are considered it is found that in expansion the surface tension is influenced by both species. In compression however the surface tension is around the equilibrium surface tension of the low molecular surfactant. From this we can conclude that the low molecular surfactant determines the surface tension in compression. Most probably there the affinity of the surface active substance for the surface is important which causes the preferential desorption of proteins. This means that the surfaces of these mixtures have a low resistance to deformation by forces applied parallel to the surface.

Unfolding behaviour of proteins at interfaces

The most important class of surface active substances which have been studied in this thesis are proteins due to the similarities in structure and properties with protein hydrolysates. Proteins consist of 20 different amino acids which vary in residual group. Despite the similarity in the basic structure of these substances the difference

in foaming properties between proteins is large. In literature this difference in foaming properties is ascribed to the difference in unfolding rate during adsorption at air/water interfaces of these polymers. There are no reliable data on the unfolding rate of proteins however. The overflowing cylinder technique can be used to determine the unfolding rates of proteins since the top surface is in a steady state while the relative expansion rate is finite. The relative expansion rate can be seen as a characteristic time scale of the surface.

In order to measure the unfolding rate of the proteins, at the top surface, the surface tension, the relative rate of expansion and the surface concentration were determined using the Wilhelmy plate technique, laser Doppler anemometry and ellipsometry respectively. With these three parameters the surface can be characterised completely. The reasoning behind the characterisation is as follows: If proteins need time for the unfolding at an interface, the relative expansion rate determines the mean degree of unfolding of the proteins at the interface. As a function of the relative rate of expansion and at equal adsorbed amounts the surface tension will vary due to a difference in the mean degree of unfolding.

If we would know the surface tension and surface concentration for different bulk concentrations as a function of the relative rate of unfolding then we would be able to establish the influence of the unfolding rate of the protein on the surface tension. Since this is difficult to determine on the basis of the raw data, a simple model was used to express this influence of unfolding in an unfolding and a refolding parameter. In this model the transport to and the unfolding at the top surface of an overflowing cylinder has been described. The unfolding and refolding has been described by means of a first order reaction. In essence we assume that the degree of unfolding can be seen as an average over many stages of unfolding over a large number of molecules. By dividing the interface into a large number of concentric rings and by carrying out the calculations for the transport and unfolding for each concentric ring the surface properties can be calculated as a function of the distance to the centre. By varying the relative rate of expansion as a function of the distance to the centre in the same way as takes place at the top surface of the overflowing cylinder also the surface tension gradient can be determined. Since there is a fixed relation between the surface tension gradient and the maximum relative rate of expansion, the maximum relative rate of expansion can be determined by means of iteration.

In this thesis the unfolding behaviour of the proteins: β -casein, β -lactoglobulin, BSA and lysozyme has been determined experimentally. In literature these proteins have been characterised well with respect to adsorption and unfolding behaviour. The unfolding rates of these proteins differ several orders of magnitude. β -Casein and β -lactoglobulin were shown to unfold most rapid. The characteristic time scales of unfolding of these proteins is in the order of a tenth for β -casein to a few tenths for β -lactoglobulin. Lysozyme hardly unfolds within the time scale of the experiment which indicates that the unfolding takes more than 100 seconds. The model was shown not to apply for BSA since the change in surface tension proceeds in two steps. Nevertheless it could be calculated that the unfolding of BSA takes place in a time scale in the order of 20 seconds.

The model and the overflowing cylinder technique have also been applied to mixtures of proteins and low molecular surfactants. The system β -casein/Tween 20 was chosen because in this system no complications are known such as aggregation in the bulk phase, or electrostatic interactions at the surface. At expanding interfaces these systems were shown to behave in a more or less additive manner. The surface tension of the mixture appeared to be lower than the addition of the decrease in surface tension of each species individually. This can be attributed to the fact that both species occupy part of the space at the interface. In static conditions it was found in literature that low molecular surfactants can displace proteins from the interface. This difference in behaviour is caused by the fact that in expansion the surface tension is controlled mainly by transport to and unfolding at the surface while in equilibrium time scale is irrelevant and the affinity of the substances to the surface determines the behaviour. Despite certain deviations the measured properties were indicated to be consistent with the calculations by the model. Higher order effects such as the presence of the surfactants in micelles and preferential adsorption were shown to have little effect of these mixtures at expanding surfaces.

Foam formation and foam stability

in order to quantify the experimental values and techniques of this research for practical situations, foaming experiments have been performed for a number of relevant systems. In these experiments, the bubble size and the drainage rate of the foams have been determined. Subsequently the results of these experiments were related to mechanical surface properties.

The experiments indicated that the surface tension difference over the falling film in the overflowing cylinder correlated with the bubble size and the rate of drainage. For the formation of foam this means that not only the amount of energy supplied is important for the bubble size but that also characteristic properties of the surface being the maximal viscous drag that can be transferred is important for the break-up of foam bubbles. The explanation that can be given for this is that the shear stress generated at the surface provides the deformation that leads to an unstable shape of the bubbles which finally leads to break-up. Surface active species that enable the generation of a high shear stress therefore promote the generation of small bubbles.

In addition it was demonstrated that there is a relation between drainage and viscous friction at the bubble surface. The rate of drainage expressed in the decrease of the characteristic film thickness decreases when a higher surface tension difference between top and bottom surface in the overflowing cylinder is present at a rather arbitrarily chosen relative rate of expansion of 1 s^{-1} .

In chapter 6 the foaming properties of protein hydrolysates were discussed. The most important reason that protein hydrolysates have good foaming properties is that in these systems the low molecular components do not displace high molecular components. This causes the surface tension difference between a compressed and expanded surface to be high. This supports the creation of small bubbles and the resistance to drainage. It is possible that the good foamability of protein hydrolysates compared to proteins is caused by the lower surface tension in equilibrium.

In general it can be said that surface tension gradients play a larger role in foam formation and foam stability than the attention in literature would suggest. More attention for the properties which determine the resistance against deformation of

surfaces parallel to the surface would lead to a better insight in the reasons why different surface active substances exhibit different foaming behaviour.

Samenvatting

Het onderzoek dat in dit proefschrift beschreven is besteedt aandacht aan een aantal aspecten van de relatie tussen oppervlakteeigenschappen en schuimeigenschappen van eiwitten, laagmoleculaire surfactants en mengsels daarvan. Dit werk is tot stand gekomen naar aanleiding van een vraag van de industriële partners of het mogelijk is om het schuimgedrag van eiwithydrolysaten te begrijpen. Aangezien er vele aspecten in het oppervlakgedrag aan te wijzen zijn die verantwoordelijk (kunnen) zijn voor het schuimgedrag zijn een aantal probleemstellingen gedefinieerd waarmee een beter beeld kan worden opgebouwd van de relatie tussen oppervlakte-eigenschappen en schuimvorming en stabiliteit in relatie tot het type oppervlakte-actieve stof.

In dit proefschrift is dus a priori een belangrijke vraag geweest: Hoe kunnen we uit de eigenschappen van de oppervlakteactieve stof, de schuimeigenschappen begrijpen. We zijn ervan uitgegaan dat de moleculaire eigenschappen niet zonder meer vertaald kunnen worden in schuimeigenschappen maar dat daar een aantal vertaaltappen voor nodig zijn. Allereerst zullen de moleculaire eigenschappen vertaald moeten worden in oppervlakte-eigenschappen die zich vervolgens weer in mechanische eigenschappen van oppervlakken en films manifesteren. Daarnaast bestaat er een relatie tussen deze mechanische eigenschappen en de schuimeigenschappen.

Een belangrijke constatering vooraf was dat de manier waarop het oppervlak vervormd wordt belangrijk is voor het vinden van de juiste correlaties tussen de mechanische eigenschappen en de schuimeigenschappen. Hier hebben we twee soorten deformaties onderscheiden namelijk deformaties die veroorzaakt worden door krachten loodrecht op het grensvlak en deformaties veroorzaakt door krachten parallel aan het grensvlak. De relatie tussen kracht en vervorming zullen in beide gevallen verschillen vanwege de invloed op het grensvlak.

Een kracht die loodrecht op het grensvlak (druk) wordt aangebracht leidt in het algemeen tot een homogene deformatie van het grensvlak. De eigenschappen van het grensvlak veranderen met de tijd of de tijdschaal maar over het grensvlak bestaan geen verschillen met betrekking tot oppervlaktetenspanning, relatieve expansiesnelheid of belading. In het algemeen leidt een homogene deformatie slechts tot vergroting of verkleining van het grensvlak. Krachten die parallel aan het grensvlak worden

aangebracht worden in het algemeen veroorzaakt door viskeuze wrijving van vloeistoffen met het oppervlak. Naast een oppervlaktevergroting of verkleining vindt daarnaast ook een herverdeling van oppervlakteactief materiaal over het grensvlak plaats. Als gevolg hiervan variëren de belading, de oppervlaktespanning en de expansiesnelheid over het grensvlak. Dit leidt tot een oppervlaktespanningsgradiënt die noodzakelijkerwijs gelijk is aan de viskeuze wrijving aan het grensvlak ter plaatse.

Opvallend is dat de literatuur eigenlijk alleen aan de eerste manier van deformatie aandacht besteedt. Dit kan geweten worden aan de problematische experimentele toegankelijkheid van oppervlakken die aan afschuifkrachten worden blootgesteld. Toch kunnen afschuifkrachten aan oppervlakken belangrijk zijn voor verschillende sub-processen die in schuim een rol spelen zoals drainage en schuimvorming. Een belangrijk onderdeel van dit proefschrift gaat dan ook over de relatie tussen viskeuze wrijving en beweging van het oppervlak.

Een apparaat waarmee de relatie tussen viskeuze wrijving en oppervlaktebeweging bestudeerd kunnen worden in relatie tot oppervlakteeigenschappen is de overlopende cilinder. Dit apparaat bestaat uit een binnencilinder die omgeven is door een grotere concentrische buitencilinder. In de binnencilinder wordt vloeistof omhoog gepompt die over de rand van de binnencilinder in de ruimte tussen de binnen- en buitencilinder stroomt. Aan het topoppervlak vinden we een continu expanderend oppervlak waarvan de relatieve expansiesnelheid ongeveer constant blijft in de buurt van het centrum van de overlopende cilinder. De expansiesnelheid van dit oppervlak kan worden beïnvloed door de lengte van de vallende film te variëren. Binnen zekere grenzen kunnen dus de omstandigheden aan het grensvlak worden gevarieerd.

Als we de vallende film aan de rand van de binnencilinder beschouwen treffen we daar een situatie aan waarbij door de valbeweging van de vloeistof in de film het oppervlak parallel aan het oppervlak wordt gedeformeerd. Als we dus de eigenschappen aan de vallende film zouden kunnen meten zouden we daaruit kunnen leren hoe de oppervlakteeigenschappen variëren met de afstand. Het oppervlak van de vallende film is experimenteel echter moeilijk toegankelijk. Daarom is in dit proefschrift de verandering van de oppervlakteeigenschappen over de vallende film bestudeerd door aan het topoppervlak en het benedenoppervlak op een vaste plaats de

oppervlaktespanning te meten. Hiermee kan een redelijke indruk verkregen worden ten aanzien van het oppervlaktespanningsverschil over de vallende film van de overlopende cilinder.

Om dit verschil in oppervlaktespanning te interpreteren zijn allereerst de omstandigheden in en aan de vallende film met een stagnerend oppervlak benaderd met behulp van een eenvoudige hydrodynamische beschouwing. Uit deze beschouwing kon worden geconcludeerd dat er een relatie bestaat tussen de relatieve expansienelheid, de lengte van de vallende film en het oppervlaktespanningsverschil. Het oppervlak van de vallende film wordt aangedreven door de valbeweging van de vloeistof die door viskeuze wrijving aan het grensvlak een oppervlaktespanningsgradient creeërt. Uit een vergelijking van deze beschouwing met experimenten kon worden geconcludeert dat de beschouwing in grote lijnen juist is. Het verschil in oppervlaktespanning over de vallende film kan dus gezien worden als een maat voor de weerstand tegen vervorming van het oppervlak tegen krachten parallel aan het grensvlak.

De oppervlaktespanningsgradienten die door verschillende oppervlakeactieve stoffen konden worden opgewekt bleken significant van elkaar te verschillen. Met name laagmoleculaire surfactants en eiwitten bleken een groot verschil te vertonen. Dit is te wijten aan de gevoeligheid van de oppervlaktespanning van deze stoffen voor expansie en compressie van het grensvlak. Geadsorbeerde eiwitlagen blijken in expansie een hoge oppervlaktespanning te hebben. Dit kan worden verklaard doordat de ontvouwing van eiwitmoleculen aan een gransvlak tijd kost. In compressie worden daarentegen lage waarden gevonden voor de oppervlaktespanning omdat de eiwitmoleculen moeilijk desorberen. De oppervlaktespanning van laagmoleculaire surfactants zijn veel minder gevoelig voor compressie en expansie. In expansie zorgt de relatief korte diffusielengte ervoor dat de afwijking van de evenwichtsoppervlaktespanning relatief klein is. In compressie desorberen laagmoleculaire surfactants gemakkelijk zodat ook daar een oppervlaktespanning gevonden wordt die relatief niet veel van de evenwichtsoppervlaktespanning afwijkt. Het opgewekte oppervlaktespanningsverschil tussen het top en bodemoppervlak is voor eiwitten dan ook veel hoger dan voor laagmoleculaire surfactants. Ten aanzien

van mengsels van surfactants en eiwitten werd gevonden dat in expansie de oppervlaktespanning door beide soorten surfactants wordt bepaald. In compressie echter ligt de oppervlaktespanning rond de evenwichtswaarde van de laagmoleculaire surfactant. Hieruit kunnen we concluderen dat de laagmoleculaire surfactant het gedrag in compressie bepaalt. Hoogst waarschijnlijk is daar de affiniteit van de oppervlakteactieve stof belangrijk en desorberen de eiwitten preferent. Dit betekent dat de oppervlakken van deze mengsels een lage weerstand tegen deformatie door afschuifkrachten hebben.

Ontvouwingsgedrag van eiwitten aan grensvlakken

De belangrijkste klasse van oppervlakteactieve stoffen die in dit proefschrift zijn bestudeerd zijn eiwitten vanwege de overeenkomsten in structuur en eigenschappen met eiwithydrolysaten. Eiwitten zijn opgebouwd uit 20 verschillende aminozuren die verschillen in restgroep. Ondanks de vergelijkbaarheid in de basisstructuur van deze stoffen is het verschil in schuimeigenschappen binnen deze groep groot. In de literatuur wordt het verschil in schuimvormingseigenschappen onder andere toegeschreven aan het verschil in ontvouwingssnelheid tijdens adsorptie aan gas/vloeistofgrensvlakken van deze polymeren. Er bestaan echter geen betrouwbare gegevens op dit gebied. Een goede mogelijkheid om de ontvouwingssnelheid aan het grensvlak te kwantificeren is de overlopende cilindertechniek. Het boven oppervlak van de overlopende cilinder bevindt zich namelijk in een steady state terwijl het toch expandeert met een eindige relatieve expansiesnelheid. De relatieve expansiesnelheid kan worden gezien als de karakteristieke tijdschaal van het oppervlak.

Aan het topoppervlak van de overlopende cilinder werden voor de bepaling van de ontvouwingssnelheid; de oppervlaktespanning, de relatieve expansiesnelheid en de oppervlakteconcentratie van het eiwit bepaald door middel van respectievelijk de wilhelmy plaat techniek, laser doppler anemometrie, en elipsometrie. Met deze drie parameters kan het oppervlak compleet gekarakteriseerd worden. De redenering achter deze karakterisering is de volgende. Als eiwitten tijd nodig hebben voor de ontvouwing aan het grensvlak bepaalt de relatieve expansiesnelheid de gemiddelde mate van ontvouwing van de eiwitten. Als functie van de relatieve expansiesnelheid en bij een gelijke hoeveelheid geadsorbeerd materiaal zal toch de

oppervlaktespanning variëren als gevolg van een verschil in de gemiddelde ontvouwing van de eiwitten.

Als we nu voor verschillende concentraties van een eiwit de oppervlaktespanning en de oppervlakteconcentratie als functie van de relatieve expansiesnelheid weten, dan kunnen we nagaan hoe groot de invloed van de ontvouwingssnelheid van het eiwit op de oppervlaktespanning is. Aangezien dit niet gemakkelijk te kwantificeren is, is een eenvoudig model gebruikt om deze invloed van ontvouwing in een ontvouwings- en hervouwingsparameter uit te kunnen drukken. In dit model is het transport naar en de ontvouwing aan het grensvlak van een overlopende cilinder beschreven. De ontvouwing en hervouwing aan het grensvlak is beschreven als een eerste orde reactie. In feite gaan we er hierbij vanuit dat de mate van ontvouwing als een middeling kan worden opgevat over zeer veel stadia van ontvouwing over een groot aantal moleculen. Door het oppervlak in de berekening te verdelen in een groot aantal concentrische ringen en de berekening voor het transport en ontvouwing voor elke concentrische ring uit te voeren kunnen de oppervlakteeigenschappen als functie van de afstand tot het midden worden berekend. Door nu de relatieve expansiesnelheid te variëren met de afstand tot het centrum zoals in de overlopende cilinder plaatsvindt kan ook de oppervlaktespanningsgradient worden bepaald. Aangezien er een vaste relatie is tussen de oppervlaktespanningsgradient en de maximale relatieve expansiesnelheid kan door middel van iteratie de relatie tussen bulkconcentratie en de maximale relatieve expansiesnelheid worden bepaald.

In dit proefschrift is het ontvouwingsgedrag van de eiwitten: β -caseïne, β -lactoglobuline, BSA en lysozym experimenteel bepaald. Van deze eiwitten is in de literatuur qua adsorptie en oppervlaktedrag veel bekend. De verschillen met betrekking tot ontvouwingsgedrag bedragen tussen deze eiwitten een aantal ordes van grootte. β -caseïne en β -lactoglobuline bleken het snelste te ontvouwen. De karakteristieke tijdschaal van ontvouwing van deze eiwitten is in de orde van een tiende voor β -caseïne tot enkele tienden van seconden voor β -lactoglobuline. Lysozym bleek nauwelijks te ontvouwen binnen de tijdschaal van de meting hetgeen aantoont dat de ontvouwing langer duurt dan 100 seconden. BSA bleek niet aan het model te voldoen omdat de verandering van de oppervlaktespanning in twee stappen

verloopt. De ontvouwing van BSA verloopt over een tijdschaal in de orde van 20 seconden.

Het model en de overlopende cilindertechniek zijn ook toegepast op mengsels van eiwitten en surfactants. Hierbij is voor het systeem β -caseïne/Tween 20 gekozen omdat zich in dit systeem voor zover bekend geen complicaties vertoont zoals aggregatie in de bulkfase of electrostatische interacties aan het grensvlak. Aan expanderende grensvlakken bleken deze systemen zich min of meer aanvullend te gedragen. De oppervlaktespanning van het mengsel bleek lager te zijn dan elk van de systemen afzonderlijk. Dit kan worden geweten aan het feit dat beide stoffen een gedeelte van de ruimte aan het grensvlak innemen zodat de effectieve belading hoger is dan in de aanwezigheid van slechts één type surfactant. In statische omstandigheden werd in de literatuur waargenomen dat laagmoleculaire surfactants eiwitten van het grensvlak kunnen verdringen. Dit verschil wordt veroorzaakt doordat in expansie de oppervlakte-eigenschappen grotendeels door transport en ontvouwing worden bepaald terwijl in evenwicht de tijdschaal minder van belang is en de affiniteit van de stoffen tot het grensvlak daar maatgevend is. Ondanks een zekere afwijking bleken de gemeten eigenschappen van het grensvlak consistent met het model. Hogere orde effecten als de aanwezigheid van surfactants in micellen en preferentiële adsorptie bleken weinig invloed te hebben op het gedrag van deze mengsels aan expanderende oppervlakken.

Schuimvorming en schuimstabiliteit

on de relevantie van de experimentele waarden en technieken van dit onderzoek voor de praktijk te kwantificeren zijn met een aantal relevante systemen ook schuimexperimenten uitgevoerd waarbij drainage en de bellengrootteverdeling van de schuimen bepaald is. Deze experimenten zijn vervolgens gerelateerd aan de mechanische oppervlakteeigenschappen. Uit de experimenten bleek dat het oppervlaktespanningsverschil over de vallende film in de overlopende cilinder goed correleerde met de grootte van de bellen in het schuim en de drainagesnelheid. Voor de vorming van schuim kon daarmee worden aangetoond dat niet alleen de de input van energie door de roerder van belang is voor de belgrootte maar dat ook de

kenmerken van het grensvlak uitgedrukt in de maximale viskeuze wrijving die kan worden overgebracht van belang is voor het opbreken van de schuimbellen. De verklaring die daarvoor kan worden gegeven is dat de schuifspanning die aan het grensvlak kan worden opgewekt voor de deformatie van de bel zorgt waardoor deze een instabiele vorm aanneemt en opbreekt. Stoffen die zorgen dat een hoge schuifspanning kan worden opgewekt aan het grensvlak bevorderen daardoor het ontstaan van kleine bellen.

Tevens kon een relatie tussen drainage en de viskeuze wrijving worden aangetoond. De drainagesnelheid uitgedrukt in de afname van de karakteristieke filmdikte neemt af bij een groter oppervlakte spannings verschil tussen topoppervlak en beneden oppervlak van de overlopende cilinder bij een arbitrair gekozen relatieve expansiesnelheid van 1 s^{-1} .

In hoofdstuk 6 is nader ingegaan op de schuimeigenschappen van eiwithydrolysaten. De belangrijkste reden dat eiwithydrolysaten goede schuimstoffen zijn is dat in deze systemen de laagmoleculaire componenten in eiwithydrolysaten de hoogmoleculaire componenten niet verdringen van het grensvlak. Dit zorgt ervoor dat het oppervlaktspanningsverschil tussen compressie en expansie groot is. Dit bevordert het ontstaan van kleine bellen en de weerstand tegen drainage. Het is mogelijk dat de goede verschuimbaarheid van eiwithydrolysaten in vergelijking met eiwitten veroorzaakt wordt door de lagere oppervlaktspanning in expansie.

In het algemeen kan worden gesteld dat oppervlaktspanningsgradienten een grotere rol spelen in schuimvorming en schuimstabiliteit dan de aandacht ervoor in de literatuur doet vermoeden. Meer aandacht voor de eigenschappen die de weerstand bepalen tegen vervorming van grensvlakken parallel aan het oppervlak zou dan ook meer inzicht kunnen bieden in de redenen waarom verschillende oppervlakteactieve stoffen een verschillend schuimgedrag vertonen

References

Chapter 1

- ¹ Tuinier, R., Bisperink, C.G.J., van den Berg, C., Prins, A., Transient foaming behaviour of aqueous alcohol solutions as related to their dilational surface properties, *Journal of Colloid and Interface Science*, 179 (1996) p. 327-334.
- ² Lyklema Fundamentals of Interface and Colloid Science Part III, Academic press, In press.
- ³ Chang, C., Frances, E.I., Adsorption dynamics of surfactants at the air/water interface: a critical review of mathematical models, data and mechanisms., *Colloids and Surfaces A*, 100 (1995), p. 1-45.
- ⁴ Lucassen-Reynders, E.H., Anionic surfactants: Physical Chemistry of surfactant action, Marcel Dekker Inc., New York (1981).
- ⁵ De Feyter, J.A., Benjamins, J., Adsorption of PVA at the Air-water interface: I Applicability of the Gibbs adsorption equation, *Journal of Colloid and Interface Science*, 81 (1981) p. 91-107.
- ⁶ Benjamins, J., de Feyter, J.A., Evans, M.T.A., Graham, D.E., Phillips, M.C., *Faraday Discussions Chem. Soc., Dynamic and Static Properties of Proteins Adsorbed at the Air/Water Interface* 59 (1975) p. 218-229.
- ⁷ Graham, D.E., Phillips, M.C., *Journal of colloid and Interface Science, Proteins at Liquid Interfaces II. Adsorption Isotherms*, 70 (1979) p. 415-425.
- ⁸ De Feyter, J.A., and Benjamins, J., *Adsorption Kinetics of Proteins at the Air-Water Interface in Food Emulsions and Foams* Ed: E. Dickinson. Royal Society of Chemistry, London, (1987).
- ⁹ Hunter, J.R., Kilpatrick, P.K., Carbonell, R.G. *Journal of Colloid and Interface Science, Lysozyme Adsorption at the Air/Water Interface*, 137 (1990), p. 462-482.
- ¹⁰ Hunter, J.R., Kilpatrick, P.K., Carbonell, R.G. *Journal of Colloid and Interface Science, β -casein Adsorption at the Air/Water Interface*, 142 (1991), p. 429-447.
- ¹¹ Walstra, P., *Emulsion Stability In: Encyclopaedia of emulsion technology volume 4*, Marcel Dekker Inc. New York (1996) p. 1-61.
- ¹² Norde, W., Adsorption of proteins from solution at the solid-liquid interface, *Advances in Colloid and Interface Science* 25 (1986) p. 276-340.
- ¹³ De Feyter, J.A., Benjamins, J., Soft Particle model of Compact Macromolecules at Interfaces, *Journal of Colloid and Interface Science*. 90 (1982) p. 289-292.
- ¹⁴ Van Aken, G.A., A phenomenological model for the dynamic interfacial behaviour of adsorbed protein layers, in: *Food Macromolecules and Colloids*, Eds. Dickinson, E., Lorient, D., Royal Society of Chemistry, Cambridge (1995).
- ¹⁵ Douillard, R., Daoud, M., Lefebvre, J., Minier, C., Lacannu, G., Coutret, J., State Equation of β -casein at the air/water interface, *Journal of Colloid and Interface science*, 163 (1994) p. 277-288.
- ¹⁶ Douillard, R., Applicability of polymer theories to the thermodynamics of proteins at the air/water interface: example of β -lactoglobulin, *Colloids and Surfaces B: Biointerfaces* 1 (1993) p. 333-340.
- ¹⁷ Eaglesham, A., Herrington, T.M., Penfold, J., a neutron reflectivity study of a spread monolayer of bovine serum albumin, *Colloids and Surfaces*, 65 (1992) p. 9-16.

- ¹⁸ Atkinson, P.J., Dickinson, E., Horne, D.S., Richardson, R.M., in: *Food Macromolecules and Colloids*, Eds: Dickinson, E., Lorient, D., Royal Society of Chemistry, Cambridge, (1995) p. 77-.
- ¹⁹ Atkinson, P.J., Dickinson, E., Horne, D.S., Richardson, R.M., Neutron Reflectivity of adsorbed β -Casein and β -lactoglobulin at the Air/Water Interface, *Journal of the Chemical Society: Faraday Transactions*, 91 (1995) p. 2847-2854.
- ²⁰ Atkinson, P.J., Dickinson, E., Horne, D.S., Leermakers, F.A.M., Richardson, R.M., Theoretical and experimental investigations of adsorbed protein structure at a fluid interface, *Ber. Bunsen-Ges.* 100 (6) (1996) p. 994-998.
- ²¹ Brinkhof, R., Protein adsorption at static and expanding air/water interfaces studied by neutron reflectometry, IRI report 132-98-02, Delft (1998).
- ²² Leaver, J., Dalgliesh, D.G., The topography of bovine β -casein at an oil water interface as determined from the kinetics of trypsin-catalysed hydrolysis, *Biochimica et Biophysica Acta*, 1041 (1990) p. 217-222.
- ²³ Norde, W., Favier, J.P., Structure of adsorbed and desorbed proteins, *Colloids and Surfaces* 64 (1992) p. 87-93.
- ²⁴ Gunning, A.P., Wilde, P.J., Clark, D.C., Morris, V.J., Parker, M.L., Gunning, P.A., Atomic Force Microscopy of Interfacial Protein Films, *Journal of Colloid and Interface Science*, 183 (1996) p. 600-602.
- ²⁵ De Feijter, J.A., Benjamins, J., Tamboer, M., Adsorption displacement of proteins by surfactants in oil in water emulsions, *Colloids and Surfaces*, 27 (1987) p. 243-266.
- ²⁶ Coke, M., Wilde, P.J., Russell, E.J., Clark, D.C., The influence of surface composition on the stability of foams formed from protein surfactant mixtures, *Journal of Colloid and Interface Science*, 138 (1990) p. 489-503.
- ²⁷ Clark, D.C., Husband, F., Wilde, P.J., Cornec, M., Evidence of extraneous surfactant adsorption altering adsorbed layer properties of β -lactoglobulin, *Journal of the Chemical Society: Faraday Transactions*, 91 (1995) p. 1991-1996.
- ²⁸ Westerbeek, J.M.M., Prins, A., Function of α -tending emulsifiers and proteins in whipable emulsions, In: *Microemulsions and Emulsions in Foods*, Eds: El-Nokaly, M., Cornell, D., ACS Symposium series No. 448, (1991) p. 146-160.
- ²⁹ Clark, d.C., Smith, L., Wilson, D.R., A spectroscopic study of the conformational properties of foamed bovine serum albumin, *Journal of Colloid and Interface Science*, 121 (1988) p. 136-147.
- ³⁰ Walstra, P., De Roos, A, Proteins at air-water and oil-water interfaces: static and dynamic aspects, *Food reviews international*, 9, 4 (1993) p. 503-525.
- ³¹ Ward, A.F.H., Tordai, L., Time dependence of boundary tensions of solutions I the role of diffusion in time effects, *Journal of Chemical Physics*, 14 (1946) p. 453-461.
- ³² Van Voorst Vader, F., Erkens, Th. F., van den Tempel, M., Measurement of dilational surface properties, *Transactions Faraday Society*, 60 (1964) p. 1170-1177.
- ³³ MacRitchie, F., *Chemistry at Interfaces*, Academic Press Inc. San Diego (1990) p.165-167.
- ³⁴ MacRitchie, F., Desorption of Protein Monolayers, *Journal of Colloid and Interface Science*, 61 (1977) p.223-226.
- ³⁵ Mac Ritchie, F., Equilibrium adsorption of proteins, *Journal of Colloid and Interface Science*, 32 (1970) p. 55-61.
- ³⁶ Van Kalsbeek, H.K.A.I., Thesis in preparation, Wageningen University
- ³⁷ Fisher, L.R., Mitchell, E.E., Parker, N.S., A critical role for interfacial compression and coagulation in the stabilization of emulsions by proteins 119 (1987) p. 592-594.

- ³⁸ MacRitchie, F., Desorption of proteins from the air/water interface, *Journal of Colloid and Interface Science*, 105 (1985) p. 119-123.
- ³⁹ Benjamins, J., Van Voorst Vader, F., The determination of the surface shear properties of adsorbed protein layers, *Colloids and Surfaces*, 65 (1992) p. 161-174.
- ⁴⁰ Krägel, J., Siegel, S., Miller, R., Born, M., Schano, K.-H., Measurement of interfacial shear rheological properties: an automated apparatus, *Colloids and Surfaces A*, 91 (1994) p. 169-180.
- ⁴¹ Krägel, J., Siegel, S., Miller, R., Surface shear rheological studies of protein adsorption layers, *Progr. Colloid Polym. Sci.*, 97 (1994) p. 183-187.
- ⁴² Graham, D.E., Phillips, M.C., Proteins at Liquid Interfaces IV. Dilational Properties, *Journal of Colloid and Interface Science*, 76 (1980) p. 227-239.
- ⁴³ Kokelaar, J.J., Prins, A., de Gee, M., New method for measuring the surface dilational modulus of a liquid, *Journal of Colloid and Interface Science*, 146 (1991) p. 507-511.
- ⁴⁴ Bergink-Martens, D.J.M., *Interface Dilation: The overflowing cylinder technique*, Ph.D. Thesis Wageningen Agricultural University, (1994).
- ⁴⁵ Joos, P., De Keyser, The overflowing funnel as a method for measuring surface dilational surface properties, *Levich Birthday Conference*, Madrid (1980).
- ⁴⁶ Rillaerts, E., Joos, P., Measurement of the dynamic surface tension and the surface dilational viscosity of adsorbed mixed monolayers, *Journal of Colloid and Interface Science*, 88 (1982) p. 1-7.
- ⁴⁷ Dickinson, E., Rolfe, S.E., Dalglish, D.G., Surface shear viscometry as a probe of protein-protein interactions in mixed milk protein films adsorbed at the oil-water interface, *Int. J. Biol. Macromol.*, 12 (1990) p.189-194.
- ⁴⁸ Benjamins, J., Cagna, A., Lucassen-Reynders, E.H., *Viscoelastic properties of triacylglycerol/water interfaces covered by proteins*, *Colloids and Surfaces, A*, 114 (1996) p.245-254.
- ⁴⁹ Murray, B.S., Dickinson, E., *Interfacial rheology and the dynamic properties of adsorbed films of food proteins and surfactants*, *Food Science and Technology International*, 2 (1996) p. 131-145.
- ⁵⁰ Yalakshimi, Y., Ozanne, L., Langevin, D., *Viscoelasticity of surfactant monolayers*, *Journal of Colloid and Interface Science*, 170 (1995) p. 358-366.
- ⁵¹ Lucassen Reijnders, E.H., *Interfacial viscoelasticity in emulsions and foams*, *Food Structure*, 12 (1993) p. 1-12.
- ⁵² Serrien, G., Joos, P., *Dynamic surface properties of aqueous sodium dioctyl sulfosuccinate solutions*, *Journal of Colloid and Interface Science*, 139 (1990) p. 149-159.
- ⁵³ Williams, A., Prins, A., *Comparison of the dilational behaviour of adsorbed milk proteins air-water and oil-water interfaces*, *Colloids and Surfaces A*, 114 (1996) p. 267-275.
- ⁵⁴ Serrien, G., Geeraerts, G., Ghosh, L., Joos, P., *Dynamic surface properties of adsorbed protein solutions: BSA, Casein and buttermilk*, *Colloids and Surfaces* (1992) p. 219-233.
- ⁵⁵ Chen, J., Dickinson, E., Iveson, G., *Interfacial interactions, competitive adsorption and emulsion stability*, *Food Structure*, 12 (1993) p. 135-146.
- ⁵⁶ Chen, J., Dickinson, E., *Surface shear viscosity and protein-surfactant interactions in mixed protein films adsorbed at the oil/water interface*, *Food Hydrocolloids*, 9 (1995) p. 35-42.
- ⁵⁷ Krägel, J., Wüstneck, R., Clark, D.C., Wilde, P., Miller, R., *Dynamic surface tension and surface shear rheology studies of mixed β -lactoglobulin/Tween 20 systems*, *Colloids and Surfaces A*, 98 (1995) p. 127-135.
- ⁵⁸ Wilde, P.J., Clark, D.C., *The competitive displacement of β -lactoglobulin by tween 20 from oil/water and air/water interfaces*, *Journal of Colloid and Interface Science*, 155 (1993) p. 48-54.

- ⁵⁹ Clark, D.C., Wilde, P.J., Bergink-Martens, D.J.M., Kokelaar, A.J.J., Prins, A., Surface dilational behaviour of a mixture of aqueous β -lactoglobulin and Tween 20 solutions, In: Food Colloids, Eds. Dickinson, E., Walstra, P., Royal Society of Chemistry, Cambridge (1993) p. 354-364.
- ⁶⁰ Bergink-Martens, D.J.M., Bos, H.J., Prins, A., Schulte, B.C., Surface dilation and fluid dynamical behaviour of newtonian liquids in an overflowing cylinder I Pure liquids, *Journal of Colloid and Interface Science*, 138 (1990) p. 1-9.
- ⁶¹ Bergink-Martens, D.J.M., Bos, H.J., Prins, A., Surface dilation and fluid dynamical behaviour of newtonian liquids in an overflowing cylinder II Surfactant solutions, *Journal of Colloid and Interface Science*, 165 (1994) p. 221-228.
- ⁶² Van Aken, G.A., Merks, M.T.E., Adsorption of soluble proteins to dilating surfaces, *Colloids and Surfaces*, 114 (1996) p. 221-226.
- ⁶³ Chen, J., Dickinson, E., Surface shear viscosity and protein-surfactant interactions in mixed protein films adsorbed at the oil-water interface, *Food Hydrocolloids*, 9 (1995) p. 35-42.
- ⁶⁴ Dickinson, E., Rolfe, S.E., Dalgliesh, D.G., Surface shear viscometry as a probe of protein-protein interactions in mixed milk protein films adsorbed at the oil-water interface, *International Journal of Biological macromolecules* 12 (1990) p. 189-194.
- ⁶⁵ MacRitchie, F., *Chemistry at Interfaces*, Academic Press Inc. San Diego (1990) p.156-183.
- ⁶⁶ Prins, A., *Principles of Foam Stability*, In: *Avances in Food Emulsions and Foams*. Eds: Dickinson, E. Stainsby, G., Elsevier Applied Science, (1988), p. 91-100.
- ⁶⁷ Bird, R.B., Stewart, W.E., Lightfoot, E.N., *Transport Phenomena*, Wiley, New York (1960).
- ⁶⁸ Walstra, P., *Formation of Emulsions*, in: *Encyclopaedia of Emulsion Technology*; volume 1, Ed: Becher, P. Marcel Dekker, New York (1983)
- ⁶⁹ Williams, A., Janssen, J.J.M., Prins, A., Behaviour of droplets in simple shear flow in the presence of a protein emulsifier, *Colloids and Surfaces A*, 125 (1997) p. 189-200.
- ⁷⁰ de Bruijn, R.A., Tipstreaming of drops in simple shear flows, *Chemical Engineering Science*, 48 (1993), p. 277-284.
- ⁷¹ Taisne, L., Walstra, P., Cabane, B., Transfer of oil between emulsion droplets, *Journal of Colloid and Interface science*, 184 (2) (1996), p. 378-390.
- ⁷² Prins, A., Dynamic surface properties and foaming behaviour of aqueous surfactant solutions, In *Foams*, Ed: Akers, R.J., Academic Press Inc., London (1976). P. 51-60.
- ⁷³ Zuidberg, A.F., *Physics of foam formation on a solid surface in carbonated liquids*, PhD. Thesis, Wageningen Agricultural University, (1997).
- ⁷⁴ Malhotra, A.K., Wasan, D.T. Effects of surfactant adsorption desorption kinetics and interfacial rheological properties on the rate of drainage of foam and emulsion films, *Chemical Engineering Communications*, 55 (1987) p. 95-128.
- ⁷⁵ Narsimhan, G., A model for unsteady state drainage of a static foam, *Journal of Food Engineering*, 14 (1991) p. 139-165.
- ⁷⁶ Bhakta, A., Ruckenstein, E., Foams and concentrated emulsions: Dynamics and "phase" behaviour, *Langmuir*, 11 (1995) p. 4642-4652.
- ⁷⁷ Chesters, A.K., The modelling of coalescence processes in fluid-liquid dispersions. A review of current understanding, *Trans I ChemE part A* 69 (1991) p. 259-270.
- ⁷⁸ Exerowa, D., Kashchiev, D., Platikanov, D., Stability and permeability of amphiphile bilayers, *Advances in Colloid and Interface Science* 40 (1992) p. 201-256.
- ⁷⁹ Baets, P.J.M., Stein, H.N., Influence of surfactant type and concentration on the drainage of liquid films, *Langmuir*, 8 (1992) p. 3099-3101.

- ⁸⁰ Prins, A., Arcuri, C., van den Tempel, M., Elasticity of thin liquid films, *Journal of Colloid and Interface Science*, 24 (1967) p. 84-90.
- ⁸¹ Aronson, A.S., Bergeron, V., Fagan, M.E., Radke, C.J., The influence of disjoining pressure on foam stability and flow in porous media, *Colloids and Surfaces A*, 83 (1994) p.109-120.
- ⁸² Ronteltap, A.D., Beer foam physics, Ph.D. Thesis, Wageningen Agricultural University, (1989)
- ⁸³ Ronteltap, A.D., Damsté, B.R., De Gee, M., Prins, A., The role of surface viscosity in gas diffusion in aqueous foams. I. Theoretical, *Colloids and Surfaces*, 47 (1990) p.269-283.
- ⁸⁴ Ronteltap, A.D., Damsté, B.R., De Gee, M., Prins, A., The role of surface viscosity in gas diffusion in aqueous foams. II. Experimental, *Colloids and Surfaces*, 47 (1990) p.285-298.
- ⁸⁵ Monsalve, A., Schechter, R.S., The stability of foams: Dependence of observation on the bubble size distribution, *Journal of Colloid and Interface Science* 97 (1984) p. 327-335.
- ⁸⁶ Walstra, P. The role of proteins in the stabilisation of emulsions, in: *Gums and stabilisers for the food industry 4*, Eds, Phillips, G.O., Williams, P.A., Wedlock, D.J., IRL-Press, Oxford (1988).
- ⁸⁷ Tadros, T.F., Vincent, B., in: *Encyclopaedia of Emulsion Technology*; volume 1, Ed: Becher, P. Marcel Dekker, New York (1983).
- ⁸⁸ Clark, D.C., Coke, M., Mackie, A.R., Pinder, A.C., Wilson, D.R., Molecular diffusion and thickness measurements of protein stabilised films, *Journal of Colloid and Interface Science*, 138 (1990) p. 207-219.
- ⁸⁹ Bisperink, C.G.J., The influence of spreading particles on the stability of thin liquid films, Ph.D. Thesis, Wageningen Agricultural University, (1997)
- ⁹⁰ Prins, A. Foam stability as affected by the presence of small spreading particles, In: *Surfactants in solution*; volume 10 Ed: Mittal, K.L., Plenum Press, New York, (1989).

Chapter 2

- ¹ Bergink-Martens, D.J.M., Interface Dilation: The overflowing cylinder technique, Ph.D. Thesis Wageningen Agricultural University, (1994).
- ² Serrien, G., Geeraerts, G., Ghosh, L., Joos, P., Dynamic surface properties of adsorbed protein solutions: BSA, Casein and buttermilk, *Colloids and Surfaces* (1992) p. 219-233.
- ³ Damadoran, S., Song, K.B., Diffusion and energy barrier controlled adsorption at the air-water interface, in *Interactions of food proteins*, ACS symposium series nr: 454, Eds. Parris, N., Barford, R., (1991).
- ⁴ Bergink-Martens, D.J.M., Bos, H.J., Prins, A., Surface dilation and fluid dynamical behaviour of newtonian liquids in an overflowing cylinder II Surfactant solutions, *Journal of Colloid and Interface Science*, 165 (1994) p. 221-228.
- ⁵ Van Voorst Vader, F., Erkens, Th. F., van den Tempel, M., Measurement of dilational surface properties, *Transactions Faraday Society*, 60 (1964) p. 1170-1177.
- ⁶ Helfand, E., Frisch, H.L., Lebowitz, J.L., Theory of the Two- and One-Dimensional Rigid Sphere Fluids, *Journal Chem. Physics*, 34 (1961) p. 1037-1042
- ⁷ Van Aken, G.A., A phenomenological model for the dynamic interfacial behaviour of adsorbed protein layers, in: *Food macromolecules and colloids*, Eds: Dickinson, E., Lorient, D, Royal society of chemistry, Conference proceedings, Cambridge (1995) p. 43-49.
- ⁸ Bergink-Martens, D.J.M., Bos, H.J., Prins, A., Schulte, B.C., Surface dilation and fluid dynamical behaviour of newtonian liquids in an overflowing cylinder I Pure liquids, *Journal of Colloid and Interface Science*, 138 (1990) p. 1-9.

⁹ Prins, A., Bergink-Martens, D.J.M. in *Food Colloids and Polymers: Stability and Mechanical Properties*, (Eds.) Dickinson, E., Walstra, P., Royal Society of Chemistry, Cambridge, (1993), p. 291-300.

¹⁰ den Engelsen, C.W., *Structure, properties, and behaviour of three-phase foam*, Thesis, Twente University, (1996).

Chapter 3

¹ Bergink-Martens, D.J.M., *Interface Dilation: The overflowing cylinder technique*, Ph.D. thesis, Agricultural University Wageningen, (1993).

² Bergink-Martens, D.J.M., Bos, H.J., Prins, A., *Surface dilation and fluid-Dynamical behaviour of Newtonian liquids in an overflowing cylinder: II Surfactant Solutions*, *Journal of Colloid and Interface science*, 165 (1994) p. 221-228.

³ Bergink-Martens, D.J.M., Bos, H.J., Prins, A., Schulte, B.C., *Surface dilation and fluid-dynamical behaviour of Newtonian liquids in an overflowing cylinder: I Pure liquids*, *Journal of Colloid and Interface science*, 138 (1990) p. 1-11.

⁴ Bergink-Martens, D.J.M., Bisperink, C.G.J., Bos, H.J., Prins, A., Zuidberg, A.F., *Surface dilational behaviour of surfactant solutions: A comparison between the overflowing cylinder and the free falling film technique*, *Colloids and Surfaces*, vol. 65 (1992) p. 191-199.

⁵ Bos, H.J., *Personal communication* (1996).

⁶ Bisperink, C.G.J., *The influence of spreading particles on the stability of thin liquid films*, Thesis, Wageningen Agricultural University (1997).

⁷ Daily, J.W., Harleman, D.F.R. *Fluid Dynamics*, Addison Wesley, Reading Massachusetts, (1966).

⁸ Bird, R.B., Stewart, W.E., Lightfoot, E.N., *Transport Phenomena*, Wiley, New York (1960).

⁹ Benjamins, J., de Feyter, J.A., *Ellipsometry as a tool to study the adsorption behaviour of synthetic and biopolymers at the air/water interface*, *Biopolymers* 17 (1978) p. 1759-1772.

¹⁰ McCrackin, F.L., Passaglia, E., Stromberg, R.R., Steinberg, H.L., *Measurement of the thickness and refractive index of very thin films and optical properties of surfaces by ellipsometry*, *Nat. bur. Standards, A. Physics and Chemistry*, vol. 67A, no. 4 (1963) p. 363-377.

¹¹ Prins, A. Jochems, A.P.M., van Kalsbeek, H.K.A.I., Boerboom, F.J.G., Wijnen, M.E., Williams, A. *Skin formation on liquid surfaces under non equilibrium conditions*, *Progr. Colloid Polym. Sci.* vol. 100, (1996), p. 321-327.

¹² Benjamins, J. van Voorst Vader, F. *The determination of the surface shear properties of adsorbed protein layers*, *Colloids and Surfaces*, vol. 65, (1992), p. 161-174.

¹³ Boerboom, F.J.G., de Groot-Mostert, A.E.A., van Vliet, T. Prins, A., *Bulk and surface rheological properties of adsorbed proteins: A comparison*, *Netherlands Milk and Dairy Journal*, vol. 50, (1996), p. 183-197.

¹⁴ Mac Ritchie, F., *desorption of protein monolayers*, *Journal of Colloid and Interface Science*, 61 (1977) p. 223-226.

¹⁵ Van Aken, G.A., Merks, M.T.E. *Adsorption of soluble proteins to dilating surfaces*, *Colloids and Surfaces A*. vol. 114, (1996) p. 221-226.

¹⁶ Williams, A., Janssen, J.J.M., Prins, A., *Behaviour of droplets in simple shear flow in the presence of a protein emulsifier*, *Colloids and Surfaces A*, 125 (1997) p. 189-200.

¹⁷ Tuinier, R., Bisperink, C.G.J., van den Berg, C., Prins, A., Transient foaming behaviour of aqueous alcohol solutions related to their surface dilational properties, *Journal of Colloid and Interface Science*, 179 (1996) p. 327-334.

¹⁸ Kim, S.H., Kinsella, J.E., Surface activity of proteins: relationships between surface pressure development, viscoelasticity of interfacial films and foam stability of Bovine Serum Albumin, *Journal of Food Science*, 50 (1985) p.1526-1531.

Chapter 4

¹ De Feijter, J.A., Benjamins, J., Tamboer, M., Adsorption displacement of proteins by surfactants in oil in water emulsions, *Colloids and Surfaces*, 27 (1987) p. 243-266.

² Dijt J.C., *Kinetics of polymer adsorption, desorption and exchange*, Thesis Wageningen Agricultural University (1993).

³ Murray, B.S., Dickinson, E., Interfacial rheology and the dynamic properties of adsorbed films of food proteins and surfactants, *Food Science and Technology International*, 2 (1996) p. 131-145.

⁴ Coke, M., Wilde, P.J., Russell, E.J., Clark, D.C., The influence of surface composition on the stability of foams formed from protein surfactant mixtures, *Journal of Colloid and Interface Science*, 138 (1990) p. 489-503.

⁵ Clark D.C., Husband, F., Wilde, P.J., Cornec, M., Miller, R., Krägel, J., Wüstneck, R., Evidence of extraneous surfactant altering adsorbed layer properties of β -lactoglobulin. *J. Chem. Soc. Faraday Trans.* 91 (1995) p. 1991-1995.

⁶ Mackie, A.R., Nativel, S., Wilson, D.R., Ladha, S., Clark, D.C., Process-Induced changes in molecular structure that alter adsorbed layer properties in oil-in-water emulsions stabilised by β -casein/tween20 mixtures, *J. Sci, Food Agric.* 70 (1996) p. 413-421.

⁷ Bijsterbosch, H.D., *Copolymer adsorption and the effect on colloidal stability*, PhD thesis, Wageningen Agricultural University (1998).

⁸ Van Aken, G.A., A phenomenological model for the dynamic interfacial behaviour of adsorbed protein layers, in: *Food macromolecules and colloids*, Eds: Dickinson, E., Lorient, D, Royal society of chemistry, Conference proceedings, Cambridge (1995) p. 43-49.

⁹ Graham, D.E., Phillips, M.C., Proteins at liquid interfaces, II adsorption isotherms, *Journal of Colloid and Interface Science*, 70 (1979) p.415-425.

¹⁰ Bergink-Martens, D.J.M., *Interface Dilation: The overflowing cylinder technique*, Ph. D. Thesis, Wageningen Agricultural University, (1994).

Chapter 5

¹ Williams, A., Prins, A., Comparison of the dilational behaviour of adsorbed milk proteins air-water and oil-water interfaces, *Colloids and Surfaces A*, 114 (1996) p. 267-275.

² Boerboom, F.J.G., A.E.A., de Groot-Mostert, Prins, A., van Vliet, T., Bulk and surface rheological behaviour of aqueous protein solutions. A comparison, *Netherlands milk & dairy journal* 50 (1996) p. 183-198.

³ Clark, D.C., Wilde, P.J., Bergink-Martens, D.J.M., Kokelaar, A.J.J., Prins, A., Surface dilational behaviour of a mixture of aqueous β -lactoglobulin and Tween 20 solutions. In: *Food Colloids*, Eds. Dickinson, E., Walstra, P., Royal Society of Chemistry, Cambridge (1993) p. 354-364.

- ⁴ Clark, D.C., Coke, M., Mackie, A.R., Pinder, A.C., Wilson, D.R., Molecular diffusion and thickness measurements of protein stabilised films, *Journal of Colloid and Interface Science*, 138 (1990) p. 207-219.
- ⁵ Murray, B.S., Dickinson, E., Interfacial rheology and the dynamic properties of adsorbed films of food proteins and surfactants, *Food Science and Technology International*, 2 (1996) p. 131-145.
- ⁶ De Feijter, J.A., Benjamins, J., Tamboer, M., Adsorption displacement of proteins by surfactants in oil in water emulsions, *Colloids and Surfaces*, 27 (1987) p. 243-266.
- ⁷ Wilde, P.J., Foam measurement by the microconductivity technique: An assessment of its sensitivity to interfacial and environmental factors, *Journal of Colloid and Interface Science* 178 (1996) p. 733-739.
- ⁸ Tuinier, R., Bisperink, C.G.J., van den Berg, C., Prins, A., Transient foaming behaviour of aqueous alcohol solutions as related to their dilational surface properties, *Journal of Colloid and Interface Science*, 179 (1996) p. 327-334.
- ⁹ Kroezen, A.B.J., Groot Wassink, J., Bubble Size distribution and energy dissipation in foam mixers, *JSDC*, 103 (1987) p. 386-394.
- ¹⁰ Walstra, P., Smulders, I., Making emulsions and foams: An overview, In: *Proteins, Lipids and Polysaccharides*, Eds: Dickinson, E., Bergenstahl, B., Royal society of chemistry, Cambridge (1997) p. 367-381.
- ¹¹ Walstra, P., Emulsion stability, in *Encyclopedia of emulsion technology*, Volume 4, Ed: Becher, P., (1996) p.1-61.
- ¹² Chesters, A.K., The modelling of coalescence processes in fluid-liquid dispersions. A review of current understanding, *Trans I ChemE part A* 69 (1991) p. 259-270.
- ¹³ Narsimhan, G., A model for the unsteady state drainage of a static foam, *Journal of food engineering*, 14 (1991) p. 139-165.
- ¹⁴ Gururaj, M., Kumar, R., Ghandi, K.S., A network model of static foam drainage, *Langmuir*, 1995, p. 1381-1391.
- ¹⁵ Bergink-Martens, D.J.M., Interface Dilatation: The overflowing cylinder technique, Ph.D. Thesis Wageningen Agricultural University, (1994).

Chapter 6

- ¹ Van Aken, G.A., Merks, M.T.E., Adsorption of soluble proteins to dilating surfaces, *Colloids and Surfaces*, 114 (1996) p. 221-226.
- ² Dijt, J.C., Kinetics of polymer adsorption, desorption and exchange, Wageningen Agricultural University, Ph.D. Thesis (1993)
- ³ MacRitchie, F., Desorption of Protein Monolayers, *Journal of Colloid and Interface Science*, 61 (1977) p.223-226.
- ⁴ Bergink-Martens, D.J.M., Interface Dilatation: The overflowing cylinder technique, Ph.D. Thesis Wageningen Agricultural University, (1994).
- ⁵ Walstra, P., Smulders, I., Making emulsions and foams: An overview, In: *Proteins, Lipids and Polysaccharides*, Eds: Dickinson, E., Bergenstahl, B., Royal society of chemistry, Cambridge (1997) p. 367-381.

Nawoord

Aan het einde van dit proefschrift wil een aantal mensen bedanken die op welke wijze dan ook hebben bijgedragen aan het tot stand komen van dit proefschrift of die van deze tijd een memorabele tijd hebben gemaakt.

Ik wil beginnen met professor Prins. Door uw enthousiasme voor het vak en uw manier dit over te brengen ben ik aan dit onderzoek begonnen. Door uw capaciteiten als coach en uw talent het goede in mij boven te brengen heb ik daar ook nooit spijt van gehad. Met name de discussies op wetenschappelijk gebied (uren en uren) zullen mij altijd bijblijven vanwege de creativiteit en het enthousiasme waarmee u met het vak bezig bent.

Martien jouw kennis en jouw talent verbanden te herkennen hebben mij altijd geholpen het plaatje in het goede perspectief te krijgen. Daarnaast kon ik erop vertrouwen dat als jij mijn rekenarij bekeek je altijd de vinger kon leggen op de zere plek.

Hans Bos, ook jij hebt me geholpen door mij als absolute leek een rudimentair begrip te geven van de hydrodynamica. Niet gemakkelijk volgens mij maar je hebt hiermee een onmisbare bijdrage geleverd aan het begrip van het stagnerende oppervlak aan de vallende film.

Jan Blaakmeer, Simon van Dijk en Willen Norde bedankt voor de begeleiding die jullie me tijdens mijn promotietijd hebben gegeven. Ik hoop dat dit onderzoek naar schuimbeton een stap in de goede richting gebracht heeft en jullie helpt om richting te geven aan eventueel verder onderzoek.

Karin, Rudolf en Jan-Willem jullie hebben allemaal jullie rol gespeeld in het ophelderen van het schuimgedrag en de rol van cement in schuimbeton. Hoofdstuk 5 is grotendeels jullie werk geweest. Bedankt voor de positieve bijdrage!

Kamergenoten, rokersclub, Prinsclub, AIOreisgroepjes, en alle andere collega's van GLF en Fysko bedankt voor de steun, de koffie, de gezelligheid en de discussies over het vakgebied en over alle zinnige en onzinnige onderwerpen. Kortom de gezelligheid zowel op het lab als in de kroeg. Mede door jullie was het naast een leerzame ook een heel leuke tijd.

Paranimfen Henri en Antien, jullie hebben beide heel dichtbij gestaan gedurende mijn tijd in Wageningen en jullie hebben alle fases kunnen volgen in het totstandkomen ervan. Bedankt voor de steun naast het spreekgestoelte maar vooral ook daarvoor.

Pap en mam, dit is ook een beetje jullie boekje. Zonder jullie steun, ook in het verleden, had dit boekje er nooit gelegen. Bedankt voor de bagage die ik mee heb gekregen, ik heb het bij het schrijven van dit boek hard nodig gehad.

Wanda en Suzanne, geen kwaai buien meer over dat vervelende proefschrift dat af moet. Niet avonden achter elkaar meer achter die computer zitten voor de zoveelste correctieronde. Bedankt voor jullie begrip, steun en liefde maar ook omdat jullie me soms achter de computer vandaan sleurden om iets leuks te doen. Gelukkig is het eindelijk af en heeft pappa weer tijd om zonder schuldgevoel leuke dingen te ondernemen.

Frank

Curriculum Vitae

Frank Boerboom werd geboren op 19 mei 1966 te Nijmegen. In 1986 behaalde hij het VWO eindexamen aan de Thorbecke Scholengemeenschap in Zwolle begon met de studie levensmiddelentechnologie aan de Landbouuniversiteit. Onderdeel van deze studie was een stageperiode aan Clarkson University in Potsdam NY en afstudeervakken proceskunde en levensmiddelen natuurkunde. Hij studeerde in 1992 af en begon in september 1992 aan een haalbaarheidsonderzoeks naar schuimstoffen voor schuimbeton. In januari 1994 begon hij met een promotieonderzoek naar de relatie tussen grensvlakeigenschappen en schuimeigenschappen van eiwitten in relatie met schuimstoffen voor schuimbeton. Sinds januari 1998 is hij als scientist fysische chemie werkzaam bij de afdeling CS-R&D van Avebe in Foxhol.